Fall 2014

Multidimensional Approach to Comparative Avian Visual Systems

Bret Alan Moore
Purdue University

Graduate School Form 30
(Revised 08/14)

PURDUE UNIVERSITY
GRADUATE SCHOOL
Thesis/Dissertation Acceptance

This is to certify that the thesis/dissertation prepared

By Bret Alan Moore

Entitled
A MULTIDIMENSIONAL APPROACH TO COMPARATIVE AVIAN VISUAL SYSTEMS

For the degree of Doctor of Philosophy

Is approved by the final examining committee:

Esteban Fernandez-Juricic

Yuk Fai Leung

Jeffrey R. Lucas

Wendy Townsend

To the best of my knowledge and as understood by the student in the Thesis/Dissertation Agreement, Publication Delay, and Certification/Disclaimer (Graduate School Form 32), this thesis/dissertation adheres to the provisions of Purdue University's "Policy on Integrity in Research" and the use of copyrighted material.

Esteban Fernandez-Juricic

Approved by Major Professor(s): _____

_____

Approved by: Richard J. Kuhn 12/02/2014

Head of the Department Graduate Program Date

A MULTIDIMENSIONAL APPROACH TO COMPARATIVE AVIAN VISUAL SYSTEMS

A Dissertation

Submitted to the Faculty

of

Purdue University

by

Bret Alan Moore

In Partial Fulfillment of the

Requirements for the Degree

of

Doctor of Philosophy

December 2014

Purdue University

West Lafayette, Indiana

To my Father, from whom I have been given the freedom, resources, and intellectual ability to professionally explore His design through science, whereby my every attempt to further understand it's beauty continually unveils with joyful reverence the wonder of his creation, and that the existence of every living creature is nothing less than a gracious gift to His children, a most perfect design. It is with honor I can present this work to Him and the public in hopes that it displays to His people even a touch of the true splendor of His craftsmanship and brings Him, and only Him, glory.

ACKNOWLEDGEMENTS

My parents, Mike and Tina Moore, are deserving of my foremost acknowledgement for their love and support throughout my childhood and my time as a student. They and the rest of my family have continued to encourage and guide me throughout my life, and I wouldn't be presenting this dissertation today without them.

I am also especially grateful for my advisor, Esteban Fernandez-Juricic, for his guidance since the day I, as an undergraduate, stumbled into his new and unpacked office upon his arrival at Purdue University. After helping me grow intellectually in science, he has provided me with much freedom as a graduate student to pursue multiple projects aside from this dissertation, and willingly found or provided support for many of my ideas. His patience with me as I simultaneously pursued a Doctor of Veterinary Medicine degree was generous, especially considering his tendency for productiveness and his up-beat nature. I look forward to a long-term collaboration and friendship.

Gina Rupp needs to be given a raise, or be nationally recognized, for the incredible amount of time and effort she put in to get me through the process of pursuing dual-degrees. I'm sure my complications caused her many headaches, but she always gladly smiled and worked to ensure my graduation from this department would be timely and would even happen at all. Thank you Gina for everything, you are a doll!

As my committee, Jeff Lucas, Yuk Fai Leung, and Wendy Townsend have played a role in providing diverse perspectives that would have been overlooked in my original plan of study, and overall have helped shape my project to what is presented here. They have pushed me to achieve my goals in all aspects of my career, and I thank them for their support.

The Department of Biological Sciences has provided me with financial support during my first year as well as tuition support during following years. Duke University also funded Chapters 2 and 3 of my research, and it would not have been possible without

their help. Thank you also to Duke University and NESCent for funding my research, as well as the intellectual support and friendship of the members of our working group: Meg Hall, Chris Heesey, Ellis Loew, Shaun Collin, Jason Kamilar, Erik Warrant, Olaf Bininda-Emonds, Sonke Johnson, Tom Lisney, Kara Yopak, Saul Nava, Nathan Dominy, and Gillian Moritz.

The lab of Jeff Lucas, as well as other members of my lab, deserves much thanks for continually editing papers presented by Esteban and I at our weekly lab meetings. These comments have surely helped progress manuscripts and studies along, and the differing viewpoints obtained have been helpful in many aspects of my growth as a researcher. The companionship of this great group of young (and some old) scientists has made my graduate work even more enjoyable. Luke Tyrrell, it was a pleasure working with you on more side-projects than are good for any person, and I look forward to continuing our strong collaboration and friendship in the future, birds or no birds.

Many undergraduate students have given time to help me with this project, and they must me recognized. Alexandra Osbourne, Ryan Cross, Amanda Mark, Jen Hanchar, Steven Ison, Skyler King, Tony Fleming, Jacquelyn Lynch, Jihyun Han, Sailun You, Amanda Elmore, and Jordan Young gave much time working with retinal physiology and morphology. Megan Doppler is at the forefront of this group, and she enjoyed it so much she decided to stay for both a masters in the lab. Jon Gritzer, Brianna Burry, and Melissa Hoover spent much time with the behavioral and video analysis portion of my project. Katherine Kapernaros assisted me for countless hours during data collection in multiple areas of my project. Finally Pete Perno, Amanda Elmore, and most of all Diana Pita helped me with the often frustrating task of measuring visual fields in birds. Diana has helped in ways unimaginable, and has been a joy to work with, which will continue as she is currently a graduate student in the lab.

My special thanks are extended to my family at Lynn Hall for all their support as I pursued dual-degrees. For their contributions in various aspects of my research, decision-making, and intellectual support, I especially would like to recognize Paul Snyder, Andrea Kerr, Nolie Parnell, Kathy Salisbury, Wendy Townsend, Sandy Taylor, Jim Weisman, Joanne Messick, Peg Miller, Evelyn and Kevin Kazacos, and Laurent Coeutil.

Finally, the completion of my dissertation was only possible with the support of my friends and family. Each of them has given more than they know, and their companionship will never be undervalued. Despite my occasional lack of availability, they have stuck by me and helped me out of even the worst of ruts. Thank you Audrey Moore, Jeremy Cartagena, Andrew and Katie McClain, Caleb and the VanDeman band of brothers, Britney Beckner, Rachel Heintz, Ava Nowak, David Zimmer, Megan McGlothin, Ashley Bernacchi, Max Parkansky, Dimple Patel, Daniel Thomasey, Heather Giacone, Renae Davis, Jackie Mundrawala, Amanda Schoolkraft, Mindy Anderson, Erin Nonos, Erin Martin, and, Katie Bennett, and the rest of my amazing classmates of Purdue D.V.M. 2015.

TABLE OF CONTENTS

Page

Page

Page

Page

LIST OF FIGURES

Figure Page

LIST OF TABLES

ABSTRACT

Moore, Bret Alan. Ph.D., Purdue University, December 2014. A Multidimensional Approach to Comparative Avian Visual Systems. Major Professor: Esteban Fernandez-Juricic.

Since the birth of visual ecology, comparative studies on how birds see their world have been limited to a small number of species and tended to focus on a single visual trait. This approach has constrained our ability to understand the diversity and evolution of the avian visual system. The goal of this dissertation was to characterize multiple visual dimensions on bird groups that are highly speciouse (e.g., Passeriformes), and test some hypotheses and predictions, using modern comparative tools, on the relationship between different visual traits and their association with visual information sampling behaviors. First, I developed a novel method for characterizing quantitatively the retinal topography (e.g., variation in cell density across the retina) of different bird species in a standardized manner. Second, using this method, I established that retinal configuration has converged particularly in terrestrial vertebrates into three types of retinal specializations: fovea, area, and visual streak, with the highest, intermediate, and lowest peak and peripheral ganglion cell densities, respectively. The implication is that foveate species may have more enhanced visual centers in the brain than non-foveate vertebrates. Third, forest passerines that form multi-species flocks and belong to an insectivore niche differ in their visual system configuration, which appeared associated to behavioral specializations to enhance foraging opportunities: species that searched for food at steep angles had relatively wide binocular fields with a high degree of eye movement right *above* their short bills, whereas species that searched for food at shallower angles had narrower binocular fields with a high degree of eye movement *below* their bills. Eye movement allows these species to move their fovea around to visually search for food in the complex forest environment. Fourth, I studied the visual system configuration of nine species of closely related

emberizid sparrows, which appear to maximize binocular vision, even seeing their bill tips, to enhance food detection and handling. Additionally, species with more visual coverage had higher visual acuity, which may compensate for their larger blind spots above their foveae, enhancing predator detection. Overall, the visual configuration of these passive prey foragers is substantially different from previously studied avian groups (e.g., sit-and-wait and tactile foragers). Finally, I studied the visual system configuration and visual exploratory behavior of 29 North American bird species across 14 Families. I found that species with a wider blind spot in the visual field (pecten) tended to move their heads at a higher rate probably to compensate for the lack of visual information. Additionally, species with a more pronounced difference in cell density between the fovea and the retinal periphery tended to have a higher degree of eye movement likely to enhance their ability to move their fovea around to gather high quality information. Overall, the avian visual system seems to have specializations to enhance both foraging and anti-predator behaviors that differ greatly between species probably to adjust to specific environmental conditions.

CHAPTER 1. PROJECT OVERVIEW

1.1 The Classic View on Visual Ecology

Since the early 1940s when the field of visual ecology was introduced it has remained loosely defined (Martin 2012). Perhaps it is because the amount of information animals must gather to determine their environmental interactions and communication is so large. Another possibility is that as humans, we have struggled to avoid viewing the sensory systems of other species in a way that is not like our own, and thus misguided ideas of how animals gather information from their environment has been difficult to avoid. Similarly, how animals perceive their environment remains very much a mystery, as we are unfamiliar with the sensory and cognitive processes that follow uptake of sensory information in the brain. In any case, the ideas and hypotheses put forth thus far have been widely sporadic (Endler et al. 2005; Cronin 2008; Martin 2012).

Visual ecology, since it was introduced by Walls (1942) with *The Vertebrate Eye and its Adaptive Radiations*, has improved our understanding of how a few visual components across many different species may contribute to information gathering. A good example is the information gathered on the density of retinal cells across the retina (represented with retinal topographic maps), as elucidated in the Retinal Topography Maps Database (http://retinalmaps.com.au/; Collin 2008). Topographic maps have been used to study regions of high retinal ganglion cell density (i.e. retinal specializations) since the late 1800s (Chievitz 1891; Slonaker 1897; Walls 1942; Meyer 1977; Collin 1999). The three most widely recognized types of retinal specializations (i.e. fovea, area, and visual streak) have been found in 238 species of vertebrates (Table 1). On a given species, retinal specializations can vary in number (1-4, Table 1) and can occur singly or in combination (e.g., fovea and area, fovea and visual streak, area and streak, etc., Table 1). This degree of inter-specific variability in retinal configuration suggests that there can

be different information gathering strategies across phylogenetically close (Fernández-Juricic et al. 2011b, Moore et al. in review, b) as well as phylogetically distant (Whiteside 1967; Wallman & Pettigrew 1985; Haque & Dickman 2005, Moore et al. 2013) taxa. However, little has been done to elucidate whether this diversity in the type and number of retinal specializations is conserved phylogenetically, let alone how it relates to other visual traits (e.g., visual field configuration, degree of eye movement, etc).

Table 1.1 Number of vertebrate species with different type, number, and combination of retinal specializations determined from retinal topographic maps, which are quantitative accounts of the variation in retinal ganglion cell density across the retina. Data taken from the Retinal Topography Maps Database: http://retinalmaps.com.au/.

Retina specializations	No. species	Amphibians	Birds	Fish	Mammals	Reptiles
Fovea	34	0	18	6	9	1
2 Foveae	7	0	7	0	0	0
Fovea and Area	6	0	3	3	0	0
Area	63	1	20	19	21	2
2 Areae	19	0	2	10	7	0
3 Areae	6	0	0	6	0	0
4 Areae	2	0	0	2	0	0
Fovea and Streak	4	0	2	1	0	1
Area and Streak	37	0	5	13	18	1
2 Areae and Streak	10	0	0	6	4	0
Streak	48	1	17	11	16	3
Area and 2 Streaks	2	0	0	0	2	0
2 Streaks	1	0	0	0	1	0

A common approach in the past was to gather information about a single or small number of species at a time. Large comparative analyses have not yet been widely performed, yet may help us better define general principles about the visual field configuration in vertebrates (Martin 2012, 2014). This is certainly in part due to how well described certain visual traits are across in some species but not in others. For example, we know about color vision in some species (e.g.,Budgerigar *Melpsittacus undulattus* and zebra finch *Taeniopygia guttata*, Bowmaker et al., 1997; Blue tit *Parus caeruleus* and blackbird *Turdus merula*, Hart et al. 2000), but not other visual components (e.g. characteristics of retinal specializations) have been described. In other others, generally a single visual component is studied at a time, which also largely contributes to the spotty nature of our knowledge of only select visual components of certain species. By examining multiple visual traits at a time, we can address the interplay between these visual traits, and determine specializations of the visual system for different ecological conditions (Lythgoe 1979). Overall, we have at our fingertips some amount of comparative information, but have not yet been able to perform comparative analyses on multiple visual properties across multiple species.

The visual system of birds provides us with an excellent opportunity to tackle some of these questions, as avian visual systems are quite diverse in many different visual traits (e.g. retinal organization, Meyer 1977, Hughes 1977, Moore et al. 2012, 2013, Table 1; visual fields, Martin 2007, 2012). Studying this diversity in a phylogenetic context may help us understand divergence of visual traits. For comparative analyses, birds are also good model systems because they exhibit differences in behavior and habitat preference (Martin 2014). Among avian families, Passeriformes are by far the most numerous, consisting of over 50% of the nearly 10,000 birds species on our planet, yet relatively few accounts of their visual dimensions have been described (Martin 2014). Therefore, I will focus on Passeriformes, but also include species from other orders.

1.2 Components of Vision

As the visual system is very complex, consisting of many facets that can influence information gathering in many ways, one must selectively pick certain traits to study that will enable us to test specific hypotheses and predictions. For this project, I chose to focus on three primary components associated with visually guided behaviors. These components are: the variation in cell density across the retina, the position and type of the retinal specialization, and the configuration of the visual field.

The retina is a complex, multilayered neural tissue at the back of the eye upon which an image of the visual surroundings is formed. From a functional perspective, the retina gathers visual information (e.g., food, predators, mates) that is essential for an organism to interact with its environment successfully (Collin, 1999). From an evolutionary perspective, the retina has been shaped according to the visual needs of different species, giving rise to a wide diversity of retinal configurations across vertebrates (Walls 1942; Hughes 1977). This diversity is represented in the different types, numbers, and locations of retinal cells distributed heterogeneously across the retina.

In the retina, rods and cones transform light energy into electrical signals to form a neural image (Collin, 1999). The density of these photoreceptors limits the amount of visual information the *eye* can take in. Through synaptic connections to horizontal and bipolar cells, this visual information ultimately falls on the retinal ganglion cells (RGCs), whose axons come together to form the optic nerve and carry the electrical signal to the visual brain centers (McIlwain, 1996). The density of RGCs limits the amount of information sent to the brain, therefore by studying the distribution across the retina we can obtain a good proxy for the amount of visual information that the brain is receiving.

The density of retinal ganglion cells across the retina is non-homogenous, with some regions having greater cell density than others. Areas of high RGC density increase the visual resolution in the sector of the visual field to which they project (see Fig. 1) (Meyer, 1977). Retinal specializations (e.g. *area*, fovea, visual streak) are these regions with high RGC density, with more closely spaced cells that results in increased image

sampling and visual resolution. The implication is that because retinal specializations occupy a small proportion of the retina, they provide a small area of the visual field with high acuity.

Characterizing variations in the density of RGCs across the retina of different species is relevant from a functional perspective because we can determine the type and position of retinal specializations (Fig. 2), and thus establish the sectors of the visual space that are relevant for information gathering in species with different ecological requirements and phylogenetic histories. With these two pieces of information, we can make testable predictions about scanning strategies (e.g., eye and head movement rates; see below). This assumes that the position of the retinal specialization(s) has adaptive value in terms of gathering information of fitness relevance (e.g., seeking food, avoiding predators, finding mates, etc.) under certain ecological conditions (e.g., open vs. closed habitats). For instance, the koala has a ventrotemporal retinal specialization that projects above its nose where most of the food items (e.g., eucalyptus leaves) are found when hanging from trees (Schmid et al. 1992).

The historical way retinal topography has been described, although quite beneficial to our knowledge-base of retinal organization, has made it very challenging to perform comparative analyses. In my second chapter, I took advantage of the large amount of information that has been described thus far regarding retinal topography, and developed a method by which topographic maps could be quantified and analyzed from a comparative standpoint. The method provides us with a way to quantitatively describe the retinal specialization in terms of its position, type, and number across the retina. Having this standardized set of data for describing retinal organization will enable us to perform further comparative analyses, and would open up the possibilities to address specific questions regarding how they may influence behavior. Therefore, in my third chapter, I used the quantitative data gathered from the new method, and performed a comparative analysis on the retinal specializations of 80 aquatic and terrestrial vertebrates from published topographic maps, and in-so-doing showed implications toward visual search and fixation, as well as some examples of convergent evolution in retinal configuration (Moore et al. in review, b).

The final visual trait I chose to examine is the configuration of the visual field, which is the extent around the head that can be visualized, and thus represents the extent around the head from which animals can gather visual information. Visual field configuration across species is quite diverse (Martin 2012), as different animals have very different ecologies in which they must interact. As a result, different regions of the visual field (e.g. binocular, monocular, blind areas) may be important for different reasons and therefore lead to different visual behaviors. For example, binocular vision may aid in stereopsis (Julesz 1978; Changizi & Shimojo 2008), visualization of the bill tip in birds (Martin 2009; Troscianko et al. 2012; Moore et al. 2013), and increasing short-field contrast discrimination (Heesy 2009), all of which may be beneficial for and driven by foraging ecology (Martin & Katzir 1999). The need to detect predators or conspecifics earlier may lead to a reduction in the width of the blind area (Martin 1984, 2007; Guiellemain et al. 2002). Overall, the visual field configuration likely influences scanning behavior as discussed above in retinal organization, and by studying these visual traits together we may be able to determine their individual effect on scanning behavior and information gathering.

1.3 Visual Scanning

The functional implications of the previously described three visual properties may have an impact on visual behaviors. Notably, visual scanning (also known as vigilance) is the process by which animals change the position of their head and/or eyes to gather information from the surrounding space (Elgar 1989; Treves 2000; Bednekoff & Lima 2002; Beauchamp 2003). For visually-oriented organisms, scanning is an important source of visual information about food, predators, conspecifics, etc. to make decisions that can influence fitness (e.g., detect a predator early to escape successfully).

Scanning has generally been measured as the amount of time or rate individuals spent in body postures that enhance the visibility of the surroundings (Elgar 1989; Treves 2000). In mammals and birds, scanning has been associated with head-up body postures

(Fernández-Juricic et al. 2004; Caro 2005). The quality of visual information while animals are in these vigilance postures depends on the position of the eyes in the skull, the configuration of the visual field, and ultimately the position of the retinal specialization (Fernández-Juricic, 2012).

The orientation of the eyes in the within the orbit (e.g., eyes positioned more frontally or laterally) influences the three-dimensional space around the head over which visual information is gathered. At a given eye position in the skull, the projection of both retinas into the visual space will determine the configuration of the visual field (Fig. 1). For instance, the projections of both retinas towards the nasal direction will determine the width of the binocular field (i.e., monocular right and left visual fields overlapping). The projections of the retinas towards the temporal direction will determine the extent of the right and left lateral visual fields towards the rear of the head (Fig. 1). As previously discussed, areas with a *high density* of photoreceptors and retinal ganglion cells (retinal specializations) (Walls 1942; Meyer 1977) provide high visual resolution of the portion of the visual field to which they project (Collin 1999; Fig. 1). Retinal areas with lower density of photoreceptors and ganglion cells (e.g., retinal periphery) provide relatively lower levels of visual resolution (Meyer 1977; Hughes 1977; Fig. 1). Ultimately, animals rely primarily on their retinal specializations (rather than the whole retina) to examine objects with high visual resolution, and consequently obtain *high* quality information (i.e., overt visual attention, Bisley 2011).

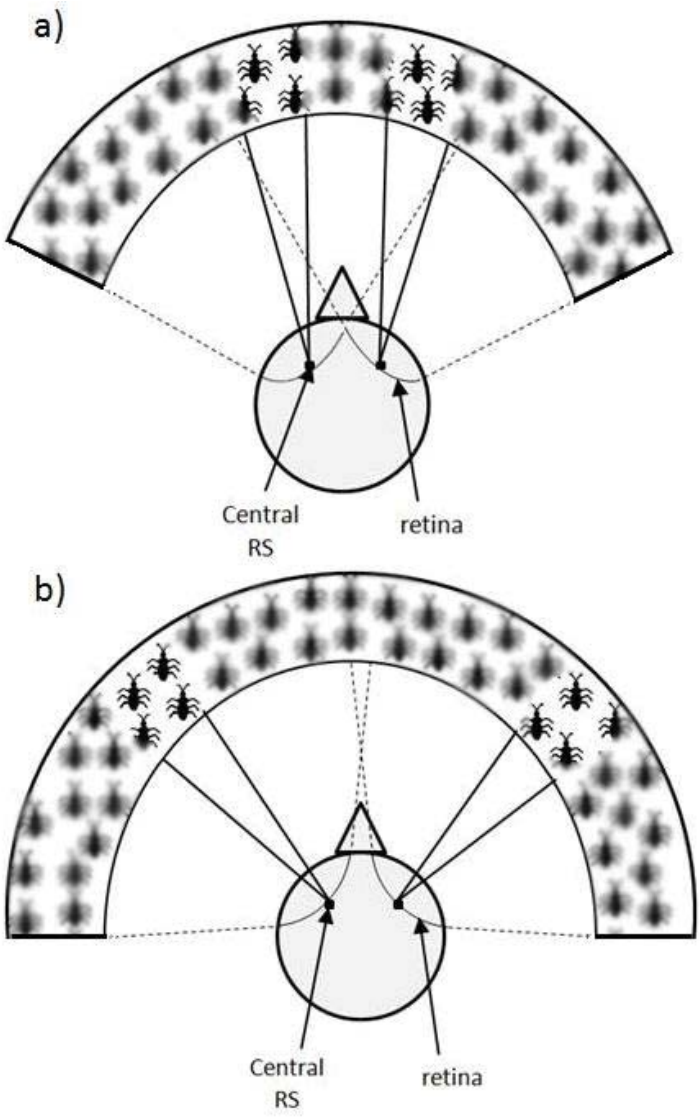

Fig 1.1 Schematic representation on the projection of the right and left retinas into the visual space, which determines the extent of the visual field in species with eyes placed (a) more frontally and (b) more laterally. The figure also shows the projection of centrally located retinal specializations (RS) into the visual field, which provide higher visual resolution than the rest of the retina.

The relative size of the projection of the retinal specialization into the visual field is small compared to the projection of the whole retina. Therefore, animals need to reposition their eyes and heads to enable them to gather the high quality information that retinal specializations provide (Lemeignan et al. 1992; Dawkins & Woodington 2000; Dawkins 2002; Moinard et al. 2005). The rates of eye and head movements have been proposed to be used as proxies of scanning strategies (Fernández-Juricic, 2012). Eye and head movement rates should be different depending on the particular visual task at hand. For instance, in a visual search task, where no objects of interest (e.g., predators, food) are present in visual space, eye and head movement rates are expected to be high (Fernández-Juricic et al. 2011a, b), because animals quickly scan different portions of the visual space with the retinal specialization (Dunlap & Mowrer 1930; Friedman 1975). In a visual search task, visual scanning includes two different major components: fast saccadic eye and/or head movements combined with short periods of visual fixation (Land 1999a, b). However, in a visual tracking task, eye and head movement rates are expected to be lower compared to a visual search task because individuals are visually fixated on a specific object (fixation, Land 1999a, b). Animals switch from visual search to visual tracking using different types of eye (Martinez-Conde & Macknik 2008) and head (Kral 2003) movements.

The variability in the type and number of retinal specializations is expected to influence the proportional area of the visual field with high resolution, which can lead to differences in scanning behavior between species. However, the literature has rarely addressed how retinal morphology can affect scanning strategies (but see Collin 1999), particularly from a comparative perspective. This is an important gap that prevents us from making refined predictions as to how animals with different visual systems gather high quality information in different contexts (e.g., micro-habitats with different levels of predation risk). This has implications for how animals allocate attention to different tasks (e.g., foraging vs. anti-predator behavior), and consequently decision-making.

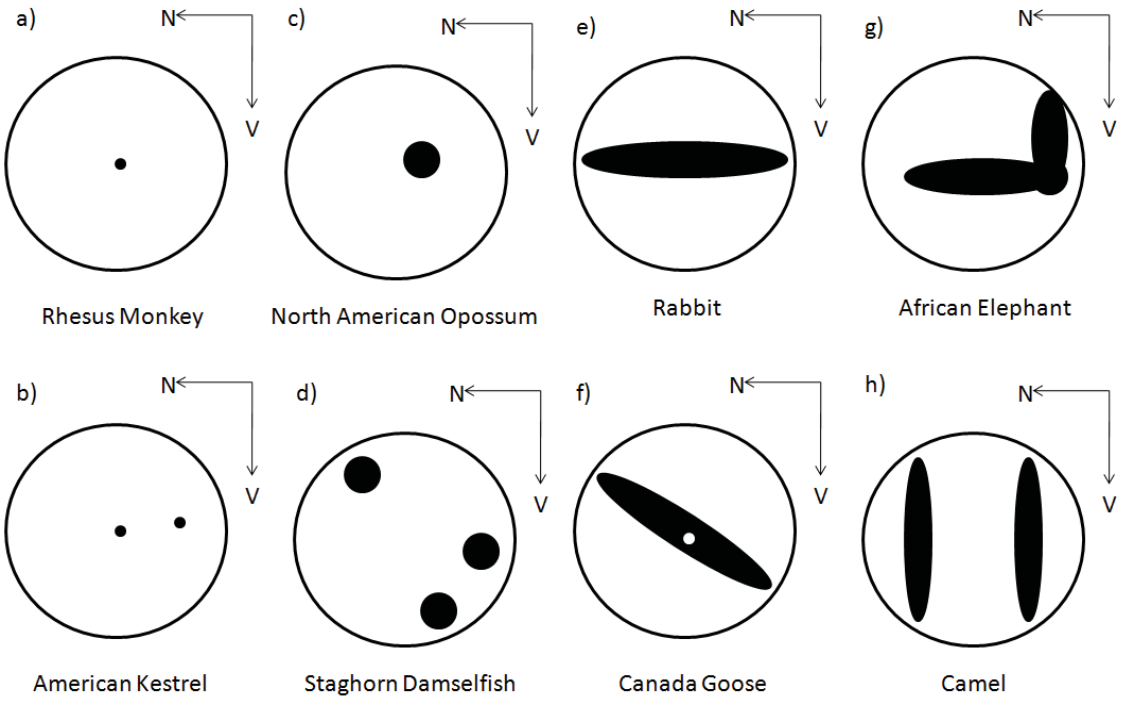

Fig 1.2 Schematic representation showing the variability in the type, position, and number of retinal specializations (fovea, area, visual streak) in different vertebrate species. The figure also portrays the proportional area of the retina that each retinal specialization occupies based on (a) the upper 50% retinal ganglion cell density in the area and visual streak, and (b) the edge of the retinal invagination in the fovea. Examples include: (a) single fovea (central) of the rhesus monkey *Macaca mulatta* (Kim et al. 1996), (b) two foveae (central and temporal) of the American kestrel *Falco sparverius* (Inzunza et al. 1991), (c) single area (dorso-temporal) of the North American Opossum *Didelphis virginiana* (Kolb & Wang 1985), (d) triple area (naso-temporal, temporal, and ventro-temporal) of the staghorn damselfish *Amblyglyphidodon curacao* (Collin & Pettigrew 1988), (e) horizontal streak of the rabbit *Oryctolagus sp.* (Provis 1979), (f) inflected streak and fovea (white dot) of Canada goose *Branta Canadensis* (Fernandez-Juricic et al. 2011c), (g) horizontal and vertical streak of the African elephant *Loxodonta Africana* (Stone & Halasz 1989), and (h) double vertical streaks of the dromedary camel *Camelus dromedaries* (Harman et al. 2001).

1.4 Conclusions

It is clear at this point that there is great diversity among visual systems and visual performance across vertebrates, and many hypotheses have been proposed on the role of different visual properties in guiding behavior (Walls, 1942; Hughes 1977; Moore et al. 2012; Martin 2009, 2012, 2014). However, the selection pressures resulting in these differences are widely unknown. This has limited our understanding of how animals visually gather information from their environment, and has slowed our progress of mapping the evolution of the vertebrate eye. In my dissertation I address some key questions in visual ecology from a comparative standpoint that will help address these limitations. How are different visual components related, and how do they contribute to visual information gathering and visually guided behaviors? What visual traits play an important role in scanning behavior, and together work to aid in the gathering of high quality information in different situations? What is the role of specific visual traits in the various ecological aspects of 1) a particular species and 2) birds in general?

Although the studies in this dissertation take a major leap into a new approach to studying how animals visually gather information, there are still limitations in what can be done at the current time. A good illustration is to examine my focus on retinal ganglion cells. This approach is definitely valid considering their role in visual information transfer to the brain and their role in visual acuity, and the tested relationships between ganglion cell topography and other visual parameters enables us to better interpret the process of visual information gathering. However, we are aware that looking at 'ganglion cells', or any other single aspect concerning vision, is a rather simplistic approach when considering the full complexity of the visual system. For example, there are many different types of ganglion cells that likely have distinct functions based on their different morphologic and physiology characteristics (Carcieri et al. 2003). Differences in types of retinal ganglion cells have included anatomic features (e.g. soma size and dendritic branching characteristics; Boycott and Wassle 1974, Rockhill et al. 2002, Sun et al. 2002), depth (Roska and Werblin 2001, Rockhill et al. 2002, Dacey et al. 2003), synaptic connections (Calkins et al. 1998), projection (Vaney et

al. 1981), autocorrelation function (DeVries and Baylor 1997), and aspects of selectivity (e.g. directional, orientation; Amthor 1989, Cleland and Levick 1974). Ganglion cells have also been shown to have phototransducing capabilities (Berson 2007). Similarly, visual acuity is dependent on much more than eye size and retinal ganglion cell concentration (e.g. cortical processing, lens focusing ability, corneal factors, photoreceptor contributions, etc.). It would of course be ideal to consider each type of retinal ganglion cell, or every factor that we know to contribute in visual acuity, in the following studies to explore their relationships with other visual parameters, but currently the literature hasn't reached a point for that type of comparative analysis and it is beyond the scope of this dissertation.

The goal of this dissertation is three-fold: 1) develop novel ways to collect and analyze comparative information on the visual system of birds, 2) characterize multiple visual dimensions on bird groups that are highly speciouse (e.g, Passeriformes), and 3) test some hypotheses and predictions, using modern comparative tools, on the association between different visual traits and between visual traits and some behaviors.

In my second chapter, I have developed a method by which we can better use the large amount of information we currently have on retinal topography for comparative analysis by quantifying the type, number, and position of retinal specializations (Moore et al. 2012). In my third chapter, I have ran a comparative analysis using this method to understand the patterns of retinal configuration across vertebrates, which have some implications for visual search behaviors (Moore et al., in review, b). In my third chapter, I examined the visual systems in a group of forest-dwelling species that form heterospecific flocks yet have different visual ecologies (Moore et al. 2013). In my fourth chapter, I studied the visual systems in a group of nine closely related species of emberizid sparrow to examine the variation and similarities in their visual traits despite close phylogenetic relatedness (Moore et al. in review, a). Finally, in my fifth chapter, I tested hypotheses about the relationship between retinal configuration and behavior in a group of 29 species across 14 families (Moore et al. in review, c).

1.5 Literature Cited

Amthor FR, Takahashi ES, Oyster CW (1989). Morphologies of rabbit retinal ganglion cells with complex receptive fields. *Journal of Comparative Neurology* 280: 97–121

Beauchamp G (2003). Group-size effects on vigilance: a search for mechanisms. *Behavioural Processes* 63:141–145

Bednekoff PA & Lima SL (2002). Why are scanning patterns so variable? An overlooked question in the study of anti-predator vigilance. *Journal of Avian Biology* 33:143–149

Berson DM (2007). Phototransduction in ganglion-cell photoreceptors. *European Journal of Physiology* 454:849-855.

Bisley JW (2011). The neural basis of visual attention. *Journal of Physiology* 589:49-57

Bowmaker JK, Heath LA, Wilkie SE, Hunt DM (1997). Visual pigments and oil droplets from six classes of photoreceptor in the retinas of birds. *Vision Research* 37:2183-2194

Boycott BB & Wassle H (1974). The morphological types of ganglion cells of the domestic cat's retina. *Journal of Physiology* 240: 397–419

Calkins DJ, Tsukamoto Y, Sterling P (1998). Microcircuitry and mosaic of a blue-yellow ganglion cell in the primate retina. *Journal of Neuroscience* 18: 3375–3385

Carcieri SM, Jacobs AL, Nirenberg S (2003). Classification of retinal ganglion cells: A statistical approach. *Journal of Neurophysiology* 90:1704-1713.

Caro T (2005). *Antipredator defenses in birds and mammals*. The University of Chicago Press, Chicago.

Changizi MA & Shimojo S (2008). A functional explanation for the effects of visual exposure on preference. *Perception* 37:1510-1519.

Chievitz JH (1891). Ueber das Vorkommen der area centralis retinae in den höheren Wirbetierklassen. *Record Anatomy Entwichlingsgesch Supplement* 139:311-334.

Cleland BG & Levick WR (1974). Brisk and sluggish concentrically organized ganglion cells in the cat's retina. *Journal of Physiology* 240: 421–456

Collin SP & Pettigrew JD (1988). Retinal topography in reef teleosts I. Some species with well developed areae but poorly developed streaks. *Brain Behavior and Evolution* 31:269-282.

Collin SP (1999). Behavioural ecology and retinal cell topography. In: *Adaptive Mechanisms in the Ecology of Vision* (Ed. by S. Archer, M.B. Djamgoz, E. Loew, J.C. Partridge & S. Vallerga, pp 509-535. Kluwer Academic Publishers, Dordrecht.

Collin SP (2008). A web-based archive for topographic maps of retinal cell distribution in vertebrates. *Clinical and Experimental Optometry* 91:85-95.

Cronin TW (2008). Visual ecology. In: basbaum AI, Kaneko A, Shepherd GM, Westheimer G (eds). *The senses. A comprehensive reference*, Vision I, vol. 1. Elsevier, Amsterdam, pp 211-245.

Dacey DM, Peterson BB, Robinson FR, Gamlin P (2003). Fireworks in the primate retina: in vitro photodynamics reveals diverse LGN-projecting ganglion cell types. *Neuron* 37: 15–27

Dawkins MS & Woodington A (2000). Pattern recognition and active vision in chickens. *Nature* 403:652-655.

Dawkins MS (2002). What are birds looking at? Head movements and eye use in chickens. *Animal Behaviour* 63:991-998.

DeVries SH & Baylor DA (1997). Mosaic arrangement of ganglion cell receptive fields in rabbit retina. *Journal of Neurophysiology* 78: 2048–2060

Dolan T & Fernández-Juricic E (2010). Retinal ganglion cell topography of five species of ground foraging birds. *Brain Behavior and Evolution* 75:111-121.

Dunlap K & Mowrer OH (1930). Head movements and eye functions of birds. *Journal of Comparative Psychology* 11:99-112.

Elgar MA (1989). Predator vigilance and group size in mammals and birds: a critical review of empirical evidence. *Biological Review of the Cambridge Philosophical Sociey* 64:13–33.

Endler J, Westcott DA, Madden JR, Robson T (2005). Animal visual systems and the evolution of color patterns: sensory processing illuminates signal evolution. *Evolution* 59:1795-1818.

Felsenstein J (1985). Phylogenies and the comparative method. *American Naturalist* 125:1-15.

Fernandez-Juricic E, O'Rourke CT, Pitlik T (2010). Visual coverage and scanning behavior in two corvid species: American crow and Western scrub jay. *Journal of Comparative Physiology A* 196:879-888.

Fernandez-Juricic E (2012). Sensory basis of vigilance behavior in birds: Synthesis and future prospects. *Behavioral Processes* 89:143-152.

Fernández-Juricic E, Beauchamp G, Treminio R, Hoover M (2011a). Making heads turn: association between head movements during vigilance and perceived predation risk in brown-headed cowbird flocks. *Animal Behaviour* 82:573-577.

Fernández-Juricic E, Erichsen JT, Kacelnik A (2004). Visual perception and social foraging in birds. *Trends in Ecology and Evolution* 19:25-31.

Fernández-Juricic E, Gall MD, Dolan T, O'Rourke C, Thomas S, Lynch JR (2011b). Visual systems and vigilance behaviour of two ground-foraging avian prey species: white-crowned sparrows and California towhees. *Animal Behaviour* 81:705-713.

Fernández-Juricic E, Moore BA, Doppler M, Freeman J, Blackwell BF, Lima SL, DeVault TL (2011). Testing the terrain hypothesis: Canada geese see their world laterally and obliquely. *Brain Behavior and Evolution* 77:147-158.

Freckleton RP, Harvey PH, Pagel M (2002). Phylogenetic analysis and comparative data: a test and review of evidence. *American Naturalist* 160:712-726.

Friedman MB (1975). How birds use their eyes. In: Wright, P., Caryl, P., Vowles, D.M. (Eds.). *Neural and Endocrine Aspects of Behavior in Birds.* Elsevier, Amsterdam, pp. 182-204.

Friedman MB (1975). How birds use their eyes. In: *Neural and endocrine aspects of behavior in birds* (Ed. by P. Wright, P. Caryl, & D.M. Vowles), pp. 182-204. Elsevier, Amsterdam.

Gaffney MF & W Hodos (2003). The visual acuity and refractive state of the American kestrel (*Falco sparverius*). *Vision Research* 43(19):2052-2059.

Garland Jr T, Bennet AF, Rezende EL (2005). Phylogenetic approaches in comparative physiology. *Journal of Experimental Biology* 208:3015-3035.

Guillemain M, Martin GR, Fritz H (2002). Feeding methods, visual fields, and vigilance in dabbling ducks (Anatidae). *Functional Ecology* 16:522-529.

Haque A & Dickman JD (2005). Vestibular gaze stabilization: different behavioral strategies for arboreal and terrestrial avians. *Journal of Neurophysiology* 93:1165-1173.

Harman A, Dan J, Ahmat A, Macuda T, Johnston K, Timney B (2001). The retinal ganglion cell layer and visual acuity of the camel. *Brain Behavior and Evolution* 58:15-27.

Hart NS, Partridge JC, Cuthill IC, Bennett ATD (2000). Visual pigments, oil droplets, ocular media, and cone photoreceptor distribution in two species of passerine bird: the blue tit (*Parus caeruleus L.)* and the blackbird *(Turdus merula L.)*. *Journal of Comparative Physiology A* 186:375-387.

Harvey PH & Pagel MD (1991). The comparative method in evolutionary biology. Oxford, UK: Oxford University Press.

Heesy CP (2009). Seeing in stereo: The ecology and evolution of primate binocular vision and stereopsis. *Evolutionary Anthropology* 18:21-35

Hughes A (1977). The topography of vision in mammals of contrasting life style: comparative optics and retinal organization. In: *The visual system in vertebrates* (Ed. by F. Crescitelli), pp. 615-756. New York: Springer-Verlag.

Inzunza O, Bravo H, Smith RL (1989). Foveal regions of bird retinas correlate with the aster of the inner nuclear layer. *Anatomical Record* 223:342-346.

Inzunza O, Bravo H, Smith RL, Angel M (1991). Topography and morphology of retinal ganglion cells in falconiforms - A study on predatory and carrion-eating birds. *Anatomical Record* 229:271-277.

Julesz B (1978). Global stereopsis: Cooperative phenomena in stereoscopic depth perception. In: *Handbook of Physiology, Vol. VIII, Perception*. (Ed. by R. Held, HW, Leibowitz, and H. Teuber, pp. 215-256. Springer, Berlin).

Kim CBY, Tom BW, Spear PD (1996). Effects of aging on densities, numbers, and sizes of retinal ganglion cells in rhesus monkey. *Neurobiololgy of Aging* 17:431-438.

Kolb H & H Wang (1985). The distribution of photoreceptors, dopaminergic amacrine cells and ganglion cells in the retina of the North American Opossum (*Didelphis virginiana*). *Vision Research* 25(9):1207-1221.

Kral K (2003). Behavioural-analytical studies of the role of head movements in depth perception in insects, birds and mammals. *Behavioural Processes* 64:1-12.

Land MF (1999a). Motion and vision: why animals move their eyes. *Journal of Comparative Physiology A* 185:341-352.

Land MF (1999b). The roles of head movement in the search and capture strategy of a tern (Aves, Laridae). *Journal of Comparative Physiology A* 184:265-272.

Lemeignan M, Sansonetti A, Gioanni H (1992). Spontaneous saccades under different visual conditions in the pigeon. *NeuroReport* 3:17-20.

Lythgoe JN (1979). The ecology of vision. Oxford, UK: Clarendon Press.

Martin GR (1984). The visual fields of the tawny owl, *Strix aluco L*. *Vision Research* 24:1739–1751

Martin GR (2007). Visual fields and their functions in birds. *Journal of Ornithology* 148:S547-S562.

Martin GR (2012). Through birds' eyes: insights into avian sensory ecology. *Journal of Ornithology* 153(Suppl 1):S23-S48.

Martin GR (2014). The subtlety of simple eyes: the tuning of visual fields to perceptual challenges in birds. *Philosophical Transactions of the Royal Society B* 369:20130040.

Martin GR & Katzir G (1999). Visual field in short-ted eagles Circaetus gallicus and the function of binocularity in birds. *Brain Behavior and Evolution* 53:55-66.

Martin GR, Jarrett N, Williams M (2007). Visual fields in blue ducks *Hymenolaimus malacorhynchos* and pink-eared ducks *Malacorhynchus membranaceus*: visual and tactil foraging. *Ibis* 149:112–120.

Martin G (2007). Visual fields and their functions in birds. *Journal of Ornithology* 148:547-562.

Martin GR (2009). What is binocular vision for? A birds*'* eye view. *Journal of Vision* 9:1–19.

Martinez-Conde S & Macknik SL (2008). Fixational eye movements across vertebrates: comparative dynamics, physiology, and perception. *Journal of Vision* 8:1-16.

McIlwain JT (1996). An introduction to the biology of vision. Cambridge University Press, New York.

Meyer DBC (1977). The avian eye and its adaptations. In: *The visual system of vertebrates; handbook of sensory physiology* (Ed. by F. Crescitelli), pp. 549-612. Springer, New York, vol VII/5.

Moinard C, Rutherford KMD, Statham P, Green PR (2005). Visual fixation of a landing perch by chickens. *Experimental Brian Research* 162:165-171.

Moore BA, Kamilar JM, Collin SP, Bininda-Emonds ORP, Dominy NJ, Hall MI, Heesy CP, Johnsen S, Lisney TJ, Loew ER, Moritz G, Nava SS, Warrant E, Yopak KE, Fernández-Juricic E (2012). A novel method for comparative analysis of retinal specialization traits from topographic maps. *Journal of Vision* 12:1-24.

Moore BA, Kamilar JM, Collin SP, Bininda-Emonds ORP, Dominy NJ, Hall MI, Heesy CP, Johnson S, Lisney TJ, Loew ER, Moritz G, Nava SS, Warrant E, Yopak KE, Fernandez-Juricic E. Are all vertebrate retinas configured the same? Implications for the evolution of acute vision. In review, b

Moore BA, M Doppler, JE Young, E Fernandez-Juricic (2013). Interspecific differences in the visual system and scanning behavior in three forest passerines that form heterospecific flocks. *Journal of Comparative Physiolpgy A* 199:263-277.

Moore BA, Tyrrell L, Pita D, Fernandez-Juricic E. Vision in Emberizid sparrow: more than meets the eye. In review, a.

Moore BA, Tyrrell L, Pita D, Fernandez-Juricic E. Vision in 29 species of North American birds: a comparative approach. In review, c

Provis (1979). The distribution and size of ganglion cells in the retina of the pigmented rabbit: A qualitative analysis. *Journal of Comparative Neurology* 185:121-138.

Rockhill RL, Daly FJ, MacNeil MA, Brown SP, Masland R (2002). The diversity of ganglion cells in the mammalian retina. *Journal of Neuroscience* 22:3831–3843

Roska B & Werblin F (2001). Vertical interactions across ten parallel, stacked representations in the mammalian retina. *Nature* 410:583–587

Ross CF (2004). The tarsier fovea: functionless vestige or nocturnal adaptation? In, C.F. Ross and R.F. Kay, eds., Anthropoid Origins: New Visions. New York: Kluwer Academic/ Plenum Publishers. pp. 477-537.

Schmid KL, Schmid LM, Wildsoet CF, Pettigrew JD (1992). Retinal topography in the koala (*Phascolarctos cinereus*). *Brain Behavior and Evolution* 39:8-16.

Slonaker, J.R. 1897. A comparative study of the area of acute vision in vertebrates. *Journal of Morphology* 13:445-494.

Stone and Halasz (1989). Topography of the retina in the elephant loxodonta africana. *Brain Behavior and Evolution* 34:84-95.

Sun W, Li N, He S (2002). Large-scale morphological survey of mouse retinal ganglion cells. *Journal of Comparative Neurology* 451:115–126

Treves A (2000). Theory and method in studies of vigilance and aggression. *Animal Behaviour* 60:711–722.

Troscianko J, Bayern AMPV, Chappell J, Rutz C, Martin GR (2012). Extreme binocular vision and a straight bill facilitate tool use in New Caledonian crows. *Nature Communications* 3:1110.

Vaney DI, Peichl L, Wassle H, Illing RB (1981). Almost all ganglion cells in the rabbit retina project to the superior colliculus. *Brain Research* 212:447–453

Wallman J & Pettigrew JD (1985). Conjugate and disjunctive saccades in two avian species with contrasting oculomotor strategies. *J Neurosci* 5:1418-1428.

Walls GL (1942). The Vertebrate Eye and Its Adaptive Radiation. Cranbrook Institute of Science, Michigan.

Whiteside TCD (1967). The head movement of walking birds. *Journal of Physiology* 188:31-32.

CHAPTER 2: A NOVEL METHOD FOR COMPARATIVE ANALYSIS OF RETINAL SPECIALIZATION TRAITS FROM TOPOGRAPHIC MAPS

This chapter has already been published as:

Moore BA, Kamilar JM, Collin SP, Bininda-Emonds ORP, Dominy NJ, Hall MI, Heesy CP, Johnsen S, Lisney TJ, Loew ER, Moritz G, Nava SS, Warrant EF, Yopak KE, Fernandez-Juricic E (2012). A novel method for comparative analysis of retinal specialization traits from topographic maps. *Journal of Vision* 12(12):1-24.

2.1 Abstract

Vertebrates possess different types of retinal specializations that vary in number, size, shape, and position in the retina. This diversity in retinal configuration has been revealed through topographic maps, which show variations in neuron density across the retina. Although topographic maps of about 300 vertebrates are available, there is no method for characterizing retinal traits quantitatively. Our goal is to present a novel method to standardize information on the position of the retinal specializations and changes in retinal ganglion cell (retinal ganglion cell) density across the retina from published topographic maps. We measured the position of the retinal specialization using two Cartesian coordinates and the gradient in cell density by sampling ganglion cell density values along four axes (nasal, temporal, ventral, and dorsal). Using this information, along with the peak and lowest retinal ganglion cell densities, we conducted discriminant function analyses (DFAs) to establish if this method is sensitive to distinguish three common types of retinal specializations (fovea, area, and visual streak). The discrimination ability of the model was higher when considering terrestrial (78%–80%

correct classification) and aquatic (77%–86% correct classification) species separately than together. Our method can be used in the future to test specific hypotheses on the differences in retinal morphology between retinal specializations and the association between retinal morphology and behavioral and ecological traits using comparative methods controlling for phylogenetic effects.

2.2 Introduction

The vertebrate retina is a thin layer of neural tissue lining the back of the eye that samples visual information from the environment before it reaches the visual centers of the brain. Photoreceptor cells are responsible for absorbing light energy or photons and transforming these into electrical signals that pass through a series of interneurons (bipolar, amacrine, and horizontal cells) before reaching the retinal ganglion cells, whose axons form the optic nerve. The optic nerve is organized so that retinotopic information processed at the level of the retina is carried to specific regions of the central nervous system (McIlwain, 1996). The density of photoreceptors and retinal ganglion cells is not homogeneous across the retina (e.g. Walls, 1942; Hughes, 1977; Wagner et al., 1998; Bozzano & Collin, 2000; Schiviz et al., 2008). Regions of the retina with a higher density of photoreceptors and retinal ganglion cells are known as retinal specializations (Walls, 1942; Meyer, 1977). These specializations provide higher spatial resolving power in discrete regions of the visual field (Collin, 1999). Therefore, animals possessing these zones of acute vision rely on them to obtain high quality information about their environment.

Across vertebrates, different types of retinal specializations have been identified, such as foveae, areae, and visual streaks, each varying in number, size, shape, and position in the retina (Walls, 1942; Hughes, 1977; Collin, 1999; Collin & Shand, 2003). A fovea is a pitted invagination of retinal tissue with a high density of photoreceptors and surrounded by high densities of retinal ganglion cells, where the inner retinal layers are displaced and the elongated photoreceptors attain their highest level of cell packing. The

fovea is considered to mediate the highest spatial resolving power of all retinal specializations (Inzunza et al., 1989; Ross, 2004). An area is a concentric increase in ganglion cell or photoreceptor density, but without any obvious retinal displacement of the retinal layers. A visual streak is a band-like area extending horizontally across the retina allowing higher spatial sampling of a panoramic visual field. Each species possesses a species-specific arrangement of retinal specializations, which appears to be under selective pressure by virtue of its ecological niche, ambient light conditions, and habitat complexity (Collin, 1999).

Studying the distribution of neurons across the retina, or retinal topography, of a given species can help us understand how organisms visually perceive their environment, which ultimately affects their behavior (e.g., Temple et al., 2010; Fernández-Juricic et al., 2011a). For instance, among falconiform birds, predatory species, such as the chilean eagle Buteo fuscenses australis and the sparrow hawk Falco sparverius, have been shown to possess both central and temporal foveae, whereas the carrion-eating species, such as the chimango caracara Milvago chimango, condor Vultur gryphus, and black vulture Coragyps atratus, all have a single central fovea (Inzunza et al., 1991). The differences in the location of the retinal specializations in these species may be related to foraging strategies: predatory species are involved in more visually demanding tasks than carrion-eating species, which could account for the presence of the second foveae (Inzunza et al., 1991).

The comparative assessment of the diversity in retinal topography has important implications for better understanding the adaptations of the vertebrate visual system to different environmental conditions. This is particularly relevant given the large number of species whose retinal topography has been examined. Collin (2008) collated published topographic maps and released a public archive (see http://www.retinalmaps.com.au/) with over 300 species of vertebrates and over 1,000 maps. Despite some studies characterizing cell density gradients across the retina (e.g., Wässle et al., 1989; Wässle & Boycott, 1991), at present there is no single standard method for measuring retinal specialization traits quantitatively, such as type, position, and changes in cell density from the retinal periphery to the center of different retinal specializations. Such a

capability would harness the power of such a large comparative resource and allow us to test more challenging hypotheses regarding the evolution of vision across vertebrate taxa.

The aim of this study is to present a novel method to quantify the position of the retinal specialization and the concomitant changes in cell density across the retina. Additionally, we determined whether traits obtained by this method (retinal specialization position, cell density gradients) in combination with other retinal traits (peak and lowest ganglion cell densities) would be sensitive enough to distinguish among three common types of retinal specializations (fovea, area, visual streak) in terrestrial and aquatic vertebrates. The methodological procedures presented in this study will have wide applicability in a comparative context by allowing us to standardize the measurement of retinal features from already published topographic maps in species with different eye size, orbit position in the skull, and overall retinal cell density.

2.3 Methods

We used published topographic maps of the retinal ganglion cell layer instead of the photoreceptor layer because they are more readily available in the literature. The original data consisted of counts of retinal ganglion cells in different regions of the retina that were used to build the topographic maps. Most of the maps used in this study are available in the retinal topographic map database: http://www.retinalmaps.com.au/ (Collin, 2008). We used topographic maps from 88 species of vertebrates (Chondrichthyes, 6; Actinopterygii, 25; Amphibia, 1; "Reptilia", 2; Aves, 21; Mammalia, 33; Appendix 1). Within Mammalia, we did not use the published topographic maps of the human retina (Curcio & Allen, 1990; Harman et al., 2000), because the presentation of these maps did not meet some of our criteria (see below for details); such as, not having the scales available, reconstructing the retina based on wholemounts, etc. In the text, we used the common names of the species, but scientific names are available in Appendix 1. We classified species as aquatic if part of their life cycle relied on water for

foraging and/or breeding purposes. Otherwise, species were considered terrestrial (Appendix 1).

We chose topographic maps that provided the orientation and scale of the retina with easily distinguished and properly labeled iso-density lines. We classified retinal specializations into three categories (fovea, area, visual streak) based on the descriptions and topographic maps presented in the original published papers and some specific criteria (details in Appendix 2). In a limited number of studies, more than one map per species was available, and we chose the one the authors deemed as the most representative. The topographic map of each species was taken as the unit upon which we made measurements on different retinal traits (see below).

From the topographic maps (see example in Figure 1a), we quantified eight traits: (1-2) position of the retinal specialization with two coordinates, (3-6) changes in ganglion cell density from the retinal periphery to the center of the retinal specialization (cell density gradient) in four different regions of the retina (nasal, temporal, dorsal, ventral), (7) peak retinal ganglion cell density, and (8) lowest retinal ganglion cell density. The position of the retinal specialization is relevant to establish the projection of the area with the highest spatial resolving power into the visual field (Collin, 1999). For instance, in a species with laterally-placed eyes, a temporal retinal specialization will project into the binocular visual field. The ganglion cell density gradient from the retinal periphery to the center of the retinal specialization varies substantially between species (e.g., Dolan & Fernández-Juricic 2010). This cell density gradient is a proxy for how improved spatial resolving power provided by the retinal specialization is compared to the retinal periphery (Fernández-Juricic et al. 2011b). For instance, species with a steep cell density gradient are expected to rely more on the retinal specialization for visualizing objects, which could in turn affect patterns of visual search and visual fixation (Fernández-Juricic et al. 2011b). Finally, the highest and lowest retinal ganglion cell densities are proxies for the maximum and minimum levels, respectively, of spatial resolving power within the retina. The peak retinal ganglion cell density has been used in the calculation of the upper levels of visual acuity in some species (Hughes, 1977; Pettigrew et al., 1988; Collin & Pettigrew, 1989; Boire et al., 2001; Dolan & Fernández-Juricic 2010).

2.3.1 Position of the retinal specialization

We first establish the location of the center of the retinal specialization in the topographic map. For a fovea, given its relatively small size, the position was generally marked in the topographic map as a point. The fovea can be identified from a wholemounted retina as a circular pit on the retinal tissue. However, the area and the visual streak occupy a relatively larger spatial extent than the fovea (Walls, 1937). Therefore, we determined the center of either type of retinal specialization as the point with the highest cell density identified in each published topographic map. If this point was not reported, we marked it as the middle point within the highest cell density range, because the highest cell density is usually located at the center of the upper density range in most maps (Collin, 2008).

To quantify the position of the retinal specialization, we used a Cartesian coordinate system (see also Mastronade et al., 1984). Because the outer edges of the retina are removed in a non-uniform fashion during the retinal wholemounting process (Stone, 1981; Ullmann et al. 2012; Figure 1a), we fitted a circle over the retina by eye, based on two criteria: the circle encompassed as much of the retina as possible and the gaps between the circle and the periphery of the retina were minimized (Figure 1b). Once the circle was fitted over the retina, we determined the center of the circle as the intersection of any two diameters, which were traced with Autocad 2010 (http://usa.autodesk.com/autocad/).

From the center of the retina, we then measured the angle of the retinal specialization (in degrees, Θ). The nasal part of the retina was considered as 0° for both right and left eyes, which allowed us to standardize measurements across species irrespective of the eye used to generate the topographic map. We then established 90° as dorsal, 180° as temporal, and 270° as ventral (Figure 1b). The angle of the retinal specialization was measured in relation to the nasal direction (Figure 1c). We measured the relative distance from the center of the retina to the center of the retinal specialization. We first drew a line from the center point of the retina to the retinal specialization (Figure 1d) and measured this distance with the 'aligned measurement' tool in Autocad 2010 (http://usa.autodesk.com/autocad/) (Figure 1d). We divided this distance by the radius of the circle to obtain a standardized distance (Figure 1d), which varied from 0 to 1.

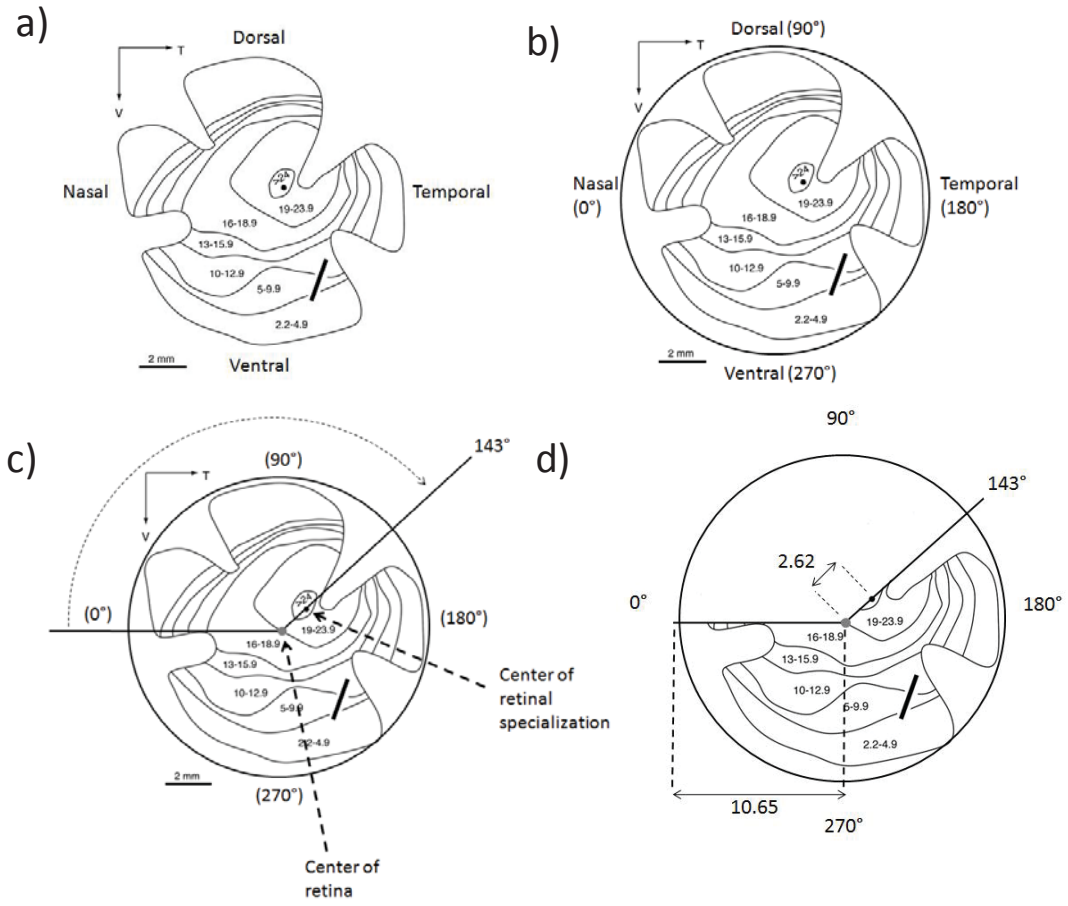

Fig 2.1 (a) Topographic map of the retinal ganglion cell distribution of the California Towhee Pipilo crissalis (Fernández-Juricic et al., 2011a). Shown are iso-density lines (connecting areas of the retina with the same cell density). (b) Circle fitting of the edges of the retina. (c) Angle between the center of the retinal specialization and the nasal axis of the retina. The gray dot represents the center of the retina and the black dot, the center of the retinal specialization. (d) Distance from the center of the retina to the center of the retinal specialization (2.62). This distance is divided by the radius of the circle (10.65) to obtain a standardized distance of the retinal specialization to the center of the retina (0.25).

We converted the angle of the retinal specialization (Θ) and its distance to the center of the retina (r) into Cartesian coordinates, which are both linear (x and y) and can be any positive or negative number (Figure 2). We used (r)cosΘ to obtain the x-coordinate, and (r)sinΘ to obtain the y-coordinate. Cartesian coordinates consist of two linear positive and/or negative values; thus, a right and left retina will provide different x-coordinate values since the eye is flipped around the y-axis. To maintain consistency, we made right eyes the standard, inversing the sign of the x-coordinate for left eyes. Using Cartesian coordinates assumes that the wholemounting process was done similarly across studies to produce the topographic maps. However, this is unlikely to be the case, which could introduce a certain degree of error in our measurements (see more details in the Discussion).

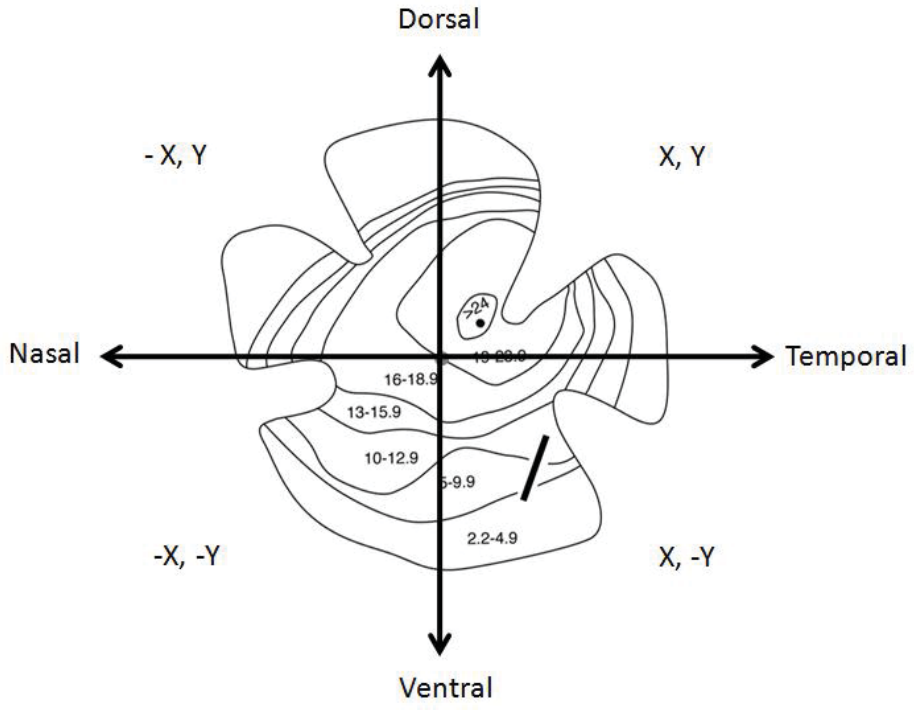

Fig 2.2 Cartesian coordinates to establish the position of the retinal specialization in the retina. The coordinates consist of two linear distances (X and Y coordinates) of both positive and negative values, depending on whether the position of the specialization is on the dorsal, ventral, nasal and temporal sides of the retina.

2.3.2 Cell density gradient across the retina

Topographic maps provide a visual representation of variations in cell density across the retina using lines (iso-density lines or contours, Figure 1a) that connect areas of the retina with similar density (Stone, 1981; Ullmann et al. 2012). We used these iso-density lines and the regions in the retina they delimit to establish changes in cell density from the retinal periphery to the retinal specialization. We used the center of the retinal specialization (see above) as a reference point to draw four vectors across the retina in the nasal, dorsal, temporal, and ventral directions using Microsoft Powerpoint © (Figure 3a). Using Image J (http://rsbweb.nih.gov/ij/), we scaled the topographic map based on the scale provided in the original publication. Along each of the four vectors (dorsal, temporal, ventral, nasal), we marked the points where iso-density lines would intersect with each vector (Figure 3a). In some topographic maps, the vectors would lie on a radial cut of the retina (originally made to flatten the retina onto the slide during the wholemounting procedure). In these instances, we projected the iso-density line into the void space from each direction taking into consideration the normal curvature of the retina.

We set sampling points along two pairs of vectors (nasal-temporal, dorsal-ventral, Figure 3a, b). Along each pair of vectors, we established 21 evenly spaced sampling points (Figure 3b shows an example with the nasal-temporal vector), with the first and the last sampling point marking the edges of the retina, yielding 20 evenly spaced intervals (Figure 3b, 4d). At each of the 21 sampling points, the average density of retinal ganglion cells was recorded by determining which iso-density lines each sampling point fell into (i.e., between which iso-density lines; Figure 4a-f).

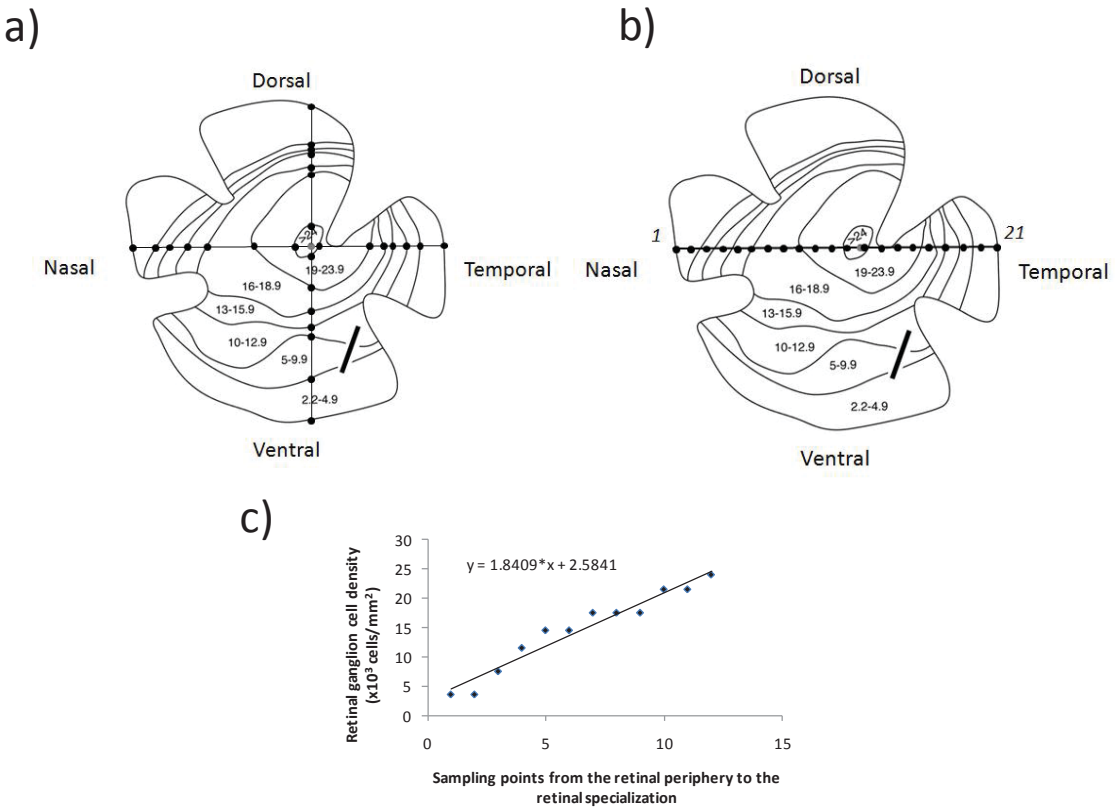

Fig 2.3 (a) Example of the cell density points at the intersection of the iso-density lines along the nasal-temporal and dorsal-ventral vectors crossing the center of the retinal specialization. Notice that the line extends into the radial cuts of the retina (see text for details). (b) Example of the 21 cell density sampling points along the nasal - temporal vector, which divided the sampling line into 20 even spaces. At each point, we measured the mean cell density value that it fell in. (c) Example of plot of the mean cell density in each sampling point from the temporal periphery of the retina to the center of the retinal specialization. We fitted a line and used its slope as the rate of change in cell density from the retinal periphery to the retinal specialization.

First, we measured the distance (mm) between iso-density lines along a given vector (nasal-temporal, dorsal-ventral; Figure 4b). Second, we measured the cumulative distance (mm) at each iso-density line (Figure 4c). Third, we determined the distance (mm) between each sampling point along the vector by multiplying the total length of the vector (e.g., 12.28 mm in Figure 4) by 0.05 (e.g., 0.614 mm in Figure 4) to establish 21 sampling points that were equidistant to each other (Figure 4d). Fourth, we calculated the cumulative distances across sampling points along a given vector (Figure 4e). Fifth, if the cumulative distance up to a particular sampling point was smaller than the cumulative distance up to the iso-density line with the next higher cell density value, we established the mean retinal ganglion cell density for that particular sampling point to be the averaged density between the upper and lower cell density ranges bounded by the iso-density lines that the sampling point fell into (Figure 4f). For instance, in Figure 4, the cumulative distance up to sampling point #3 is 1.228 mm (Figure 4e), which is smaller than the cumulative distance up to the proceeding iso-density line #4, 1.841 mm, with a higher cell density value (Figure 4e). Therefore, the final cell density value obtained for sampling plot #3 was estimated to be 7,500 cells/mm^2 (i.e., average of the cell density range 5,000-9,900 cells/mm^2; Figure 4f). We followed the same procedure to estimate the cell densities of all other sampling points, which were used for the calculation of the slope.

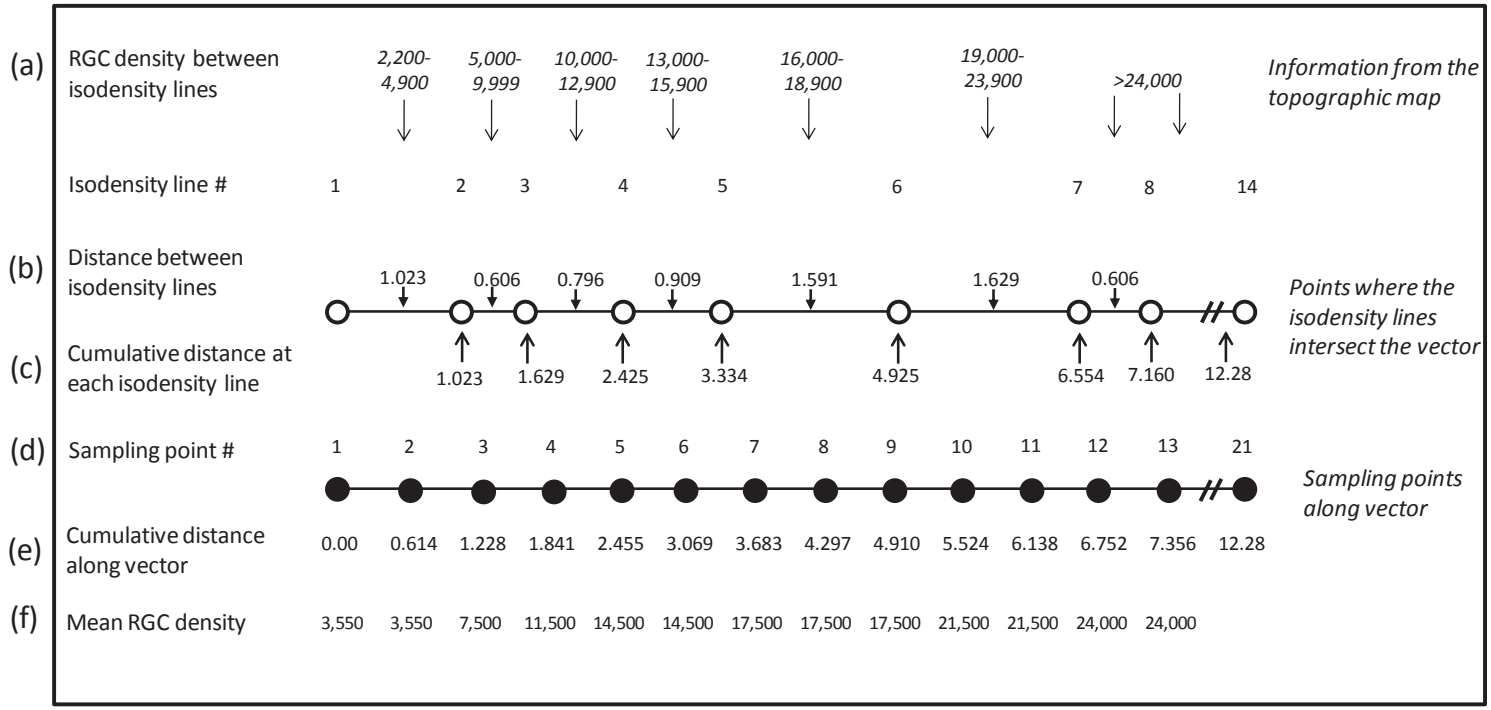

Fig 2.4 Example of how to determine the mean cell density for each of the 21 sampling points. Shown are the first 13 sampling points for the sake of clarity. Distances were scaled to mm to fit the scale provided in the topographic maps. Open circles represent the iso-density lines, and solid circles are the evenly spaced sampling points. The mean retinal ganglion cell (RGC) density is an average of the RGC range between two iso-density lines. The edges of the retina are marked with sampling point 1 (0.00mm) and 21 (12.28mm). Sampling point 13 is the point that falls along the vector prior to crossing over the peak of the retinal specialization. See explanation of the different steps (a-f) in text.

The number of sampling points (21) along a given vector allowed us to capture the high diversity in iso-density line configurations present in the published topographic maps used in this study. We tried using fewer sampling points, but missed changes in iso-density categories in some of the topographic maps. In some cases, some of the 21 sampling points did not fall within the peak density range of the retinal specialization. To determine whether or not this caused a significant change in our slope estimates, we increased the number of sampling points to include the cell density range of the retinal specialization, and recalculated the slope. We found that these two measurements were highly correlated (nasal, $r = 0.99$, $P < 0.001$; temporal, $r = 0.96$, $P < 0.001$; dorsal, $r = 0.99$, $P < 0.001$; ventral, $r = 0.99$, $P < 0.001$). Consequently, we decided to use the 21 sampling points to be consistent across all topographic maps.

In some cases, the author(s) did not include the retinal ganglion cell density for the outer perimeter of the retina on the topographic map. For these maps, when a sampling point fell into the peripheral cell density range, we established that the cell density would be half of the density of the first iso-density line shown nearest the periphery, based on patterns observed in maps that included this piece of information. For instance, if the first peripheral iso-density value was 500 cells/mm^2, a sampling point falling into this range would have a ganglion cell density value of 250 cells/mm^2. After the retinal ganglion cell density values had been recorded for all 21 points on the pairs of vectors (nasal-temporal, dorsal-ventral), we split them into four separate vectors (nasal, temporal, ventral, and dorsal). We then plotted the mean retinal ganglion cell density values at each sampling point and fitted the changes in cell density across the retina with (1) a linear and (2) a non-linear function (2nd order polynomial). From the linear fitting, we used the slope of that line as a proxy for the gradient in cell density change from the retinal periphery to the retinal specialization (example in Figure 3c). From the non-linear fitting, we used the coefficients of the first and second order polynomials as the proxies for the gradient in cell density change. We also ran the analyses with a 3rd order polynomial (data not shown; results available from the corresponding author), but the fit

was even worse than the linear and 2nd order polynomial. We took this dual approach (linear and non-linear) in the cell density gradient characterization since some of the gradients deviated from linearity.

For instance, in some topographic maps (pigmented rabbit, black bream, painted flutemouth, spookfish, staghorn damselfish), we could only get two different cell density values on a specific retinal direction (e.g., a plateau followed by a sudden increase in cell density) because of the low number of isodensity categories or because the retinal specialization was too close to the edge of the retina, reducing the number of sampling points on that specific direction of the retina. For the linear approach, we fitted the data with a Multivariate Adaptive Regression Splines analysis, which yielded a weighted slope based on slopes from lines fitted to different parts of the relationship based on differences in the coefficient of determination (Statsoft, 2011). The slope values obtained from the Multivariate Adaptive Regression Splines analysis were similar to those obtained through linear regression fitting. Therefore, we decided to use the latter so that the slope values were comparable across species. Using a similar procedure for all taxa is particularly important for the application of our method in comparative analyses. Finally, the gradient in cell density change in the nasal regions of the great kiskadee, coral cod, carangid fish, small dogfish, and softskin smoothhead, showed a pattern of increasing-decreasing-increasing cell density from the retinal periphery to the center of the retinal specialization. To determine if the slopes of cell density change on a single retinal direction of these species would bias the conclusions of the linear approach, we re-ran our statistical analysis classifying retinal specializations based on the studied traits (Discriminant Function Analysis, see below) excluding these species, but the overall classification scores were very similar to the analysis including these species (available from the corresponding author upon request). We therefore included these five species in the linear approach analyses to assess the discrimination ability of the model based on the wide range of retinal topographic configurations.

2.3.3 Peak and lowest cell density

From the original publications and the topographic maps, we obtained the peak retinal ganglion cell density. The lowest cell density was obtained from the topographic maps as the cell density at the periphery of the retina. In some cases, the cell density at the periphery was not available. We then established the cell density as half of the density of the first iso-density line reported in the topographic map (see below).

2.3.4 Statistical analysis

The analysis included measurements from 26 fovea, 35 visual streaks, and 33 areae. Six species were represented twice in our dataset (Appendix 1) due to the presence of two retinal specializations in different regions of their retinas: Chilean eagle and American kestrel (central and temporal foveae), and rock pigeon, great kiskadee, and rusty-marginated flycatcher (central fovea and area temporalis), and harlequin tuskfish (streak and area). We decided to include the second retinal specialization from each of these species due to the different morphologies within each retina (e.g., the central retinal specialization had a higher cell density than the temporal one) and to determine if our method could tell the two types of specializations apart on a given species. However, we acknowledge that this introduced a bias by having two data points from each of these six species. We justified this on the basis that this study focuses on presenting a novel method rather than analyzing retinal configurations from a comparative perspective controlling for the effects of phylogenetic relatedness.

We used a discriminant function analysis (DFA) to distinguish among the three types of retinal specializations (fovea, area, visual streak), including the eight retinal traits studied. DFA generates a combination of linear parameters to maximize the probability of correctly assigning cases (e.g., topographic maps) to specific categories (e.g., type of retinal specialization; Quinn & Keough, 2002). We used Wilks' Lambda as the test statistic, which was then used to estimate an F statistic and P-value. Given that some of the traits we measured had a high degree of correlation (>0.70; peak retinal ganglion cell density and nasal, dorsal, and ventral gradient in cell density), we used a forward stepwise selection method to enter the traits in the model. This model selection

procedure enhanced the classification score of the DFA in comparison to standard selection procedures forcing all traits into the model. In the DFA, we used a-priori classification probabilities that were proportional to group sizes (Statsoft, 2011). We used the standardized discriminant function coefficients to interpret the contributions of each retinal trait to the roots of the canonical analysis, which is part of the DFA. We first ran the DFA model pooling terrestrial and aquatic species together, and then considered them separately due to potential differences in retinal configuration (Mass & Supin, 2007). We ran two sets of DFA models, one for the linear and one for the non-linear approach for quantifying cell density gradients. For the DFA using the linear approach for quantifying cell density gradients, we included the following parameters: peak RGC density, lowest RGC density, x-coordinate position, y-coordinate position, and nasal, temporal, dorsal and ventral slopes. For the DFA using the non-linear approach for quantifying cell density gradients, we had two slope coefficients (1^{st} and 2^{nd} order polynomials) in each of the four retinal directions. Because these coefficients are not independent of each other, we ran a Principal Component Analysis (PCA) to combine the two coefficients into a single factor before running the DFA models. Thus, for the DFA using the non-linear approach for quantifying cell densities, we included the following parameters: peak RGC density, lowest RGC density, x-coordinate position, y-coordinate position, nasal PCA factor, temporal PCA factor, dorsal PCA factor, and ventral PCA factor. Therefore, the DFA models using the linear and non-linear approaches for quantifying cell density gradients included the same number of parameters.

2.4 Results

We obtained measurements on all the retinal traits from 94 topographic maps belonging to 88 species of vertebrates (Table 1). Based on the coefficients of variation, position in the x- and y-coordinates showed the highest degree of variability between species; whereas peak retinal ganglion cell density and nasal gradient in cell density, the lowest (Table 1). Different taxa were represented in the extreme values of the traits measured.

The minimum values of the lowest and highest retinal ganglion cell density and cell density gradient in all regions of the retina were represented by mammals, and the minimum values of the x- and y- coordinate were represented by cartilaginous and ray-finned fishes (Actinopterygii and Chondrichthyes; Table 1). The maximum values of lowest and peak retinal ganglion cell density, nasal, temporal, and ventral gradients in cell density were represented by birds, whereas the maximum values of the dorsal gradient in cell density and x- and y-coordinates were represented by ray-finned fish (Actinopterygii; Table 1).

Table 2.1 Descriptive statistics on the different retinal traits measured from the topographic maps of 88 species of vertebrates (see text for details). Values within parentheses are coefficients of variation. SD, standard deviation; Min., minimum value; Max., maximum value; RGC, retinal ganglion cell density.

	Mean ± SD	Min.	Species with min.	Max.	Species with max.
Lowest RGC density	2,340.1 ± 276.7 (116)	10	Western gray kangaroo	12,000	Brown-headed cowbird
Peak RGC density	21,684.9 ± 1947.8 (88)	220	Koala	65,000	American kestrel
Nasal slope	1.05 ± 0.12 (111)	0.007	African elephant	5.77	Rusty-marginated Flycatcher
Temporal slope	2.59 ± 0.37 (140)	0.015	Koala	20.00	Painted flute mouth
Dorsal slope	1.55 ± 0.21 (132)	0.004	Koala	10.50	Rock pigeon
Ventral slope	1.51 ± 0.18 (116)	0.021	Western gray kangaroo	10.00	Staghorn damselfish
x-coordinate	0.01 ± 0.04 (2686)	-0.761	Shovel nosed ray	0.81	Painted flute mouth
y-Coordinate	-0.03 ± 0.02 (710)	-0.809	Spookfish	0.64	Black bream

Considering all species, the DFA with a linear approach for quantifying cell density gradients selected five factors out of the eight: nasal and dorsal gradients in cell density, lowest retinal ganglion cell density, and x- and y-coordinate positions of the retinal specialization. With these factors, the DFA significantly discriminated among the three retinal specializations ($F_{10, 174} = 6.37$, $P < 0.001$). This DFA correctly classified 65.96% of the retinal specializations to the correct type. The visual streak (28 out of 35, 80%) and the fovea (16 out of 26, 61.54%) had the highest classification scores, whereas the area (18 out of 33, 54.55%) had the lowest. The DFA with a non-linear approach for quantifying cell density gradients selected six factors that yielded a significant discrimination among retinal specializations ($F_{12, 172} = 5.24$, $P < 0.001$): nasal, dorsal, and ventral PCA factors representing the gradients in cell density, lowest retinal ganglion cell density, and x- and y-coordinate positions of the retinal specialization. The DFA with a non-linear approach for quantifying cell density gradients correctly classified 67.02% of the retinal specializations to the correct type. The visual streak (30 out of 35, 85.71%) had the highest classification scores, followed by the fovea (15 out of 26, 57.69%) and the area (18 out of 33, 54.55%). Models with both approaches (linear and non-linear) for quantifying cell density gradients performed at similar levels.

We found that sorting species out into terrestrial vs. aquatic increased the overall classification scores of the DFA models. Considering terrestrial species, five factors were selected by the DFA with a linear approach for quantifying cell density gradients to discriminate significantly among the retinal specializations ($F_{10, 104} = 11.18$, $P < 0.001$): peak and lowest retinal ganglion cell densities, temporal gradient in cell density, x- and y-coordinate positions of the retinal specialization. This DFA model increased the overall classification score of the 59 topographic maps of terrestrial species to 77.97%. The visual streak (23 out of 24, 95.83%) and the fovea (20 out of 22, 90.91%) had the highest classification scores, whereas the area (3 out of 13, 23.08%), the lowest. In nine mammal species, the area was misclassified as a visual streak (Table 2). The DFA with a non-linear approach for quantifying cell density gradients also discriminated significantly among retinal specializations ($F_{12, 102} = 9.11$, $P < 0.001$), including six factors: peak and lowest retinal ganglion cell densities, x- and y-coordinate positions of the retinal

specialization, and dorsal and temporal PCA factors representing the gradients in cell density. The overall classification score of this DFA was 79.66%, with the visual streak (23 out of 24, 95.83%) and the fovea (20 out of 22, 90.91%) having the highest scores, and the area the lowest (4 out of 13, 30.77%). In eight mammal species the visual streak was misclassified (Table 2). Models with both approaches (linear and non-linear) for quantifying cell density gradients performed at similar levels.

Table 2.2 Topographic maps of terrestrial vertebrates that were misclassified by the Discriminant Function Analyses considering different retinal traits (see text for details). Two approaches were used (linear and non-linear) to quantify cell density gradients. Scientific names are presented in Appendix 1.

Species common name	Type of RS	Misclassified using the linear approach as	Misclassified using the non-linear approach as
Peafowl	area	fovea	fovea
Mouse lemur	area	visual streak	visual streak
Tree kangaroo	area	visual streak	visual streak
North American opossum	area	visual streak	visual streak
Three-toed sloth	area	visual streak	N/A
Golden hamster	area	visual streak	visual streak
Ferret	area	visual streak	visual streak
Galago	area	visual streak	visual streak
Koala	area	visual streak	visual streak
Hooded rat	area	visual streak	visual streak
Anubis baboon	fovea	visual streak	area
Owl monkey	fovea	visual streak	visual streak
Beagle	visual streak	area	area

The plots of the first and second canonical axis scores (roots 1 and 2 in Figure 5) of the terrestrial species for both the linear and non-linear approaches for quantifying cell density gradients show that there is little overlap between the fovea and the visual streak (Figure 5a, b), which were discriminated mostly along the first canonical axis scores (root 1). Based on the factors with the higher loadings on the canonical axes, species with a fovea showed higher peak and lowest retinal ganglion cell density, whereas species with a visual streak showed a shallower temporal gradient in cell density. The area had intermediate values along root 1 (Figure 5a, b). With respect to the second canonical axis scores (root 2 in Figure 5), a slightly larger number of species with foveae and visual streaks had their retinal specialization located in the dorsal and temporal areas of the retina (Figure 5a, b). The main difference between the linear and non-linear approaches for quantifying cell density gradients was the bottom-left corner of the plot of the canonical axis scores. In the linear approach for quantifying cell density gradients, this sector corresponded to species exhibiting shallow temporal gradients in cell density between the retinal periphery and the retinal specialization (Fig. 5a); whereas in the non-linear approach, this sector corresponded to species with more nasal and ventral retinal specializations (Fig. 5b). Overall, the area overlapped more with the visual streak than with the fovea (Figure 5).

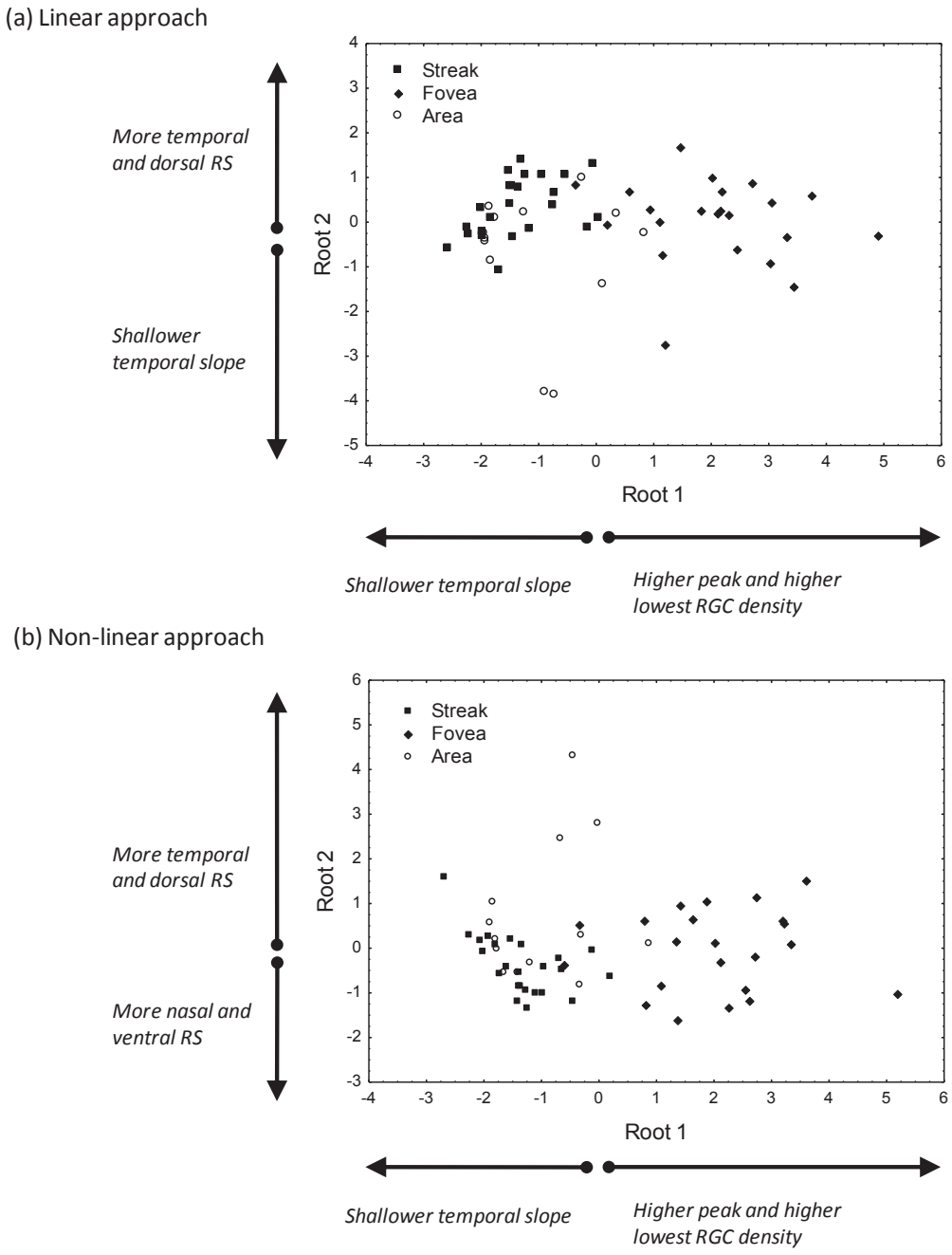

Fig 2.5 Scatterplot of the discriminant functions (canonical axis scores) showing the discrimination of the three types of retinal specializations (fovea, area, and visual streak) for terrestrial vertebrates. We used two approaches, (a) linear and (b) non-linear, to quantify cell density gradients (details in the text). Only two canonical axis scores were computed in each case.

When considering only the aquatic species, seven factors were selected by the DFA with the linear approach for quantifying cell density gradients to discriminate significantly among the retinal specializations ($F_{14, 52} = 3.06$, $P = 0.002$): x- and y-coordinate positions of the retinal specialization, peak and lowest retinal ganglion cell densities, and temporal, nasal and dorsal gradients in cell density. This DFA model assigned 85.71% of the topographic maps to the correct type of retinal specialization (Appendix 2). The area had the highest classification scores (18 out of 20, 90%), whereas the visual streak (9 out of 11, 81.82%) and the fovea (3 out of 4, 75%) had the lowest classification scores. In this DFA model, the most common misclassifications were visual streaks that were sorted as areae in two fish species (Table 3). The DFA model with the non-linear approach for quantifying cell density gradients discriminated significantly among the three retinal specializations ($F_{12, 54} = 9.11$, $P < 0.001$). This model included six factors: peak and lowest retinal ganglion cell densities, x- and y-coordinate positions of the retinal specialization, and dorsal and temporal PCA factors representing the gradients in cell density from the retinal periphery to the retinal specialization. The model classified correctly 77.14% of the cases. The area had the highest classification score (17 out of 20, 85%), followed by the visual streak (8 out of 11, 72.73%) and the fovea (2 out of 4, 50%). The visual streak and the area were commonly misclassified in five fish species (Table 3). The DFA model with a linear approach for quantifying cell density gradients for aquatic vertebrates performed better than the model with the non-linear approach.

Table 2.3 Topographic maps of aquatic vertebrates that were misclassified by the Discriminant Function Analyses considering different retinal traits (see text for details). Two approaches were used (linear and non-linear) to quantify cell density gradients. Scientific names are presented in Appendix 1.

Species common name	Type of RS	Misclassified using the linear approach as	Misclassified using the non-linear approach as
Florida garfish	visual streak	area	area
Lemon Shark	visual streak	area	area
Harp Seal	area	visual streak	visual streak
Coral cod	area	fovea	N/A
Searsid	fovea	area	N/A
Bigfin pearleye	area	N/A	visual streak
Creek chub	area	N/A	visual streak
Harlequin tusk fish	visual streak	N/A	area
Legless searsid	fovea	N/A	area
Searsid	fovea	N/A	visual streak

The plot of the first and second canonical axis scores (roots 1 and 2 in Figure 6) of the aquatic species shows a clear segregation among the fovea, area, and visual streak in the linear and non-linear approaches for quantifying cell density gradients (Figure 6), particularly along the first canonical axis (root 1 in Figure 6). Based on the factors with the higher loadings on the canonical axes, foveae had higher peak and minimum retinal ganglion cell densities and steeper temporal slopes. Visual streaks had shallower temporal gradients in cell density, higher peak retinal ganglion cell densities, and the center of the fovea was placed more nasally and temporally. Finally, areae showed intermediate values between these extremes (Figure 6a, b). The factors associated with the canonical axes were different between the models with the linear and non-linear approaches for quantifying cell density gradients (Figure 6).

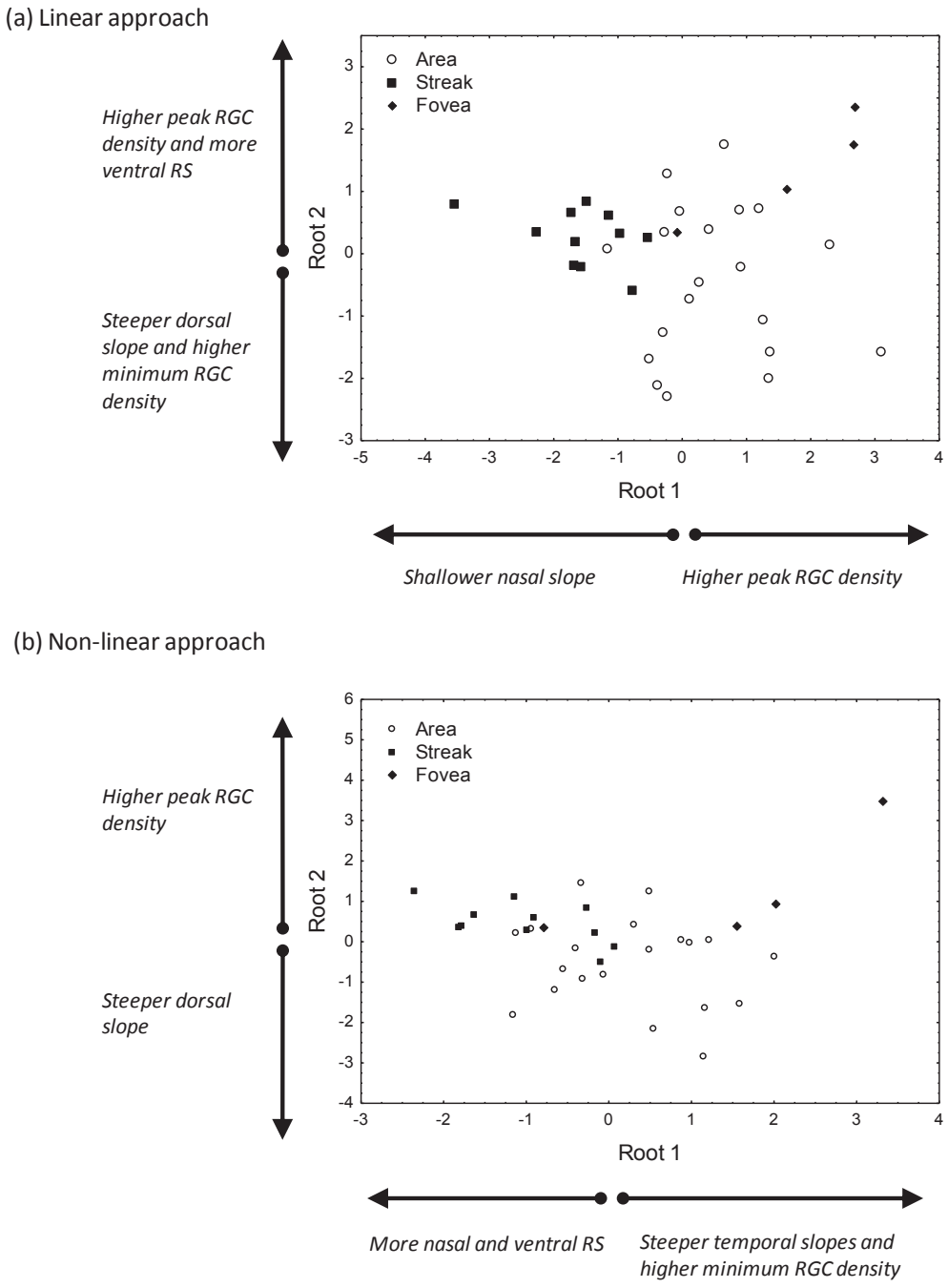

Fig 2.6 Scatterplot of the discriminant functions (canonical axis scores) showing the discrimination of the three types of retinal specializations (fovea, area, and visual streak) for aquatic vertebrates. We used two approaches, (a) linear and (b) non-linear, to quantify cell density gradients (details in the text). Only two canonical axis scores were computed in each case.

Both DFA model approaches yielded classification functions for each type of retinal specialization considering terrestrial and aquatic species (Appendix 3). These functions can be used in the future for the calculation of classification scores for species not used in this analysis to further test the classification ability of the model.

2.5 Discussion

We presented a novel method to characterize retinal traits based on topographic maps of the retinal ganglion cell layer. This method estimates the position of the retinal specialization and the gradient in cell density from the retinal periphery towards the retinal specialization in four axes relevant to the visual ecology of the animal. This information was complemented with the peak and lowest ganglion cell densities available from the topographic maps. Our method provides a quantitative way of evaluating changes in retinal specialization traits across species to test in the future different visual ecology hypotheses. We found that our method is sensitive to identifying among common types of retinal specializations in terrestrial and aquatic mammals (fovea, area, visual streak), which have been generally distinguished on the basis of size and cross-sections of the area with the highest cell density in the retina (Walls, 1942; Hughes, 1977; Collin, 1999). Furthermore, our method can be used to identify retinal topographies that would support different types of retinal specializations on the same retina.

Traditionally, the position of a retinal specialization has been characterized in discrete categories, such as dorsal, ventronasal, central, etc. (Walls, 1942; Meyer, 1977; Hughes, 1977). However, this categorization prevents us from making quantitative estimations that can be used to compare the position of the retinal specialization across species living in different visual environments. Quantitative estimates can allow us to determine more accurately the specific position in the visual field that the retinal specialization projects to, which has important behavioral implications (e.g., foraging, Collin, 1999; anti-predator behavior, Fernández-Juricic, 2012; predator-prey interactions, Cronin, 2005). Our method estimates the position of retinal specializations using a

Cartesian system that takes into consideration the angle of the retinal specialization in relation to the nasal direction as well as the distance between the retinal specialization and the center of the retina. For instance, we found that in terrestrial vertebrates, the fovea and visual streak are located more dorsally and temporally, whereas in aquatic vertebrates the fovea appears to be more ventrally placed. These trends can be tested in future studies using comparative methods controlling for phylogenetic effects.

Our index of the steepness of the gradient in cell density can offer insight into the degree of spatial resolving power provided by the retinal specialization in relation to that of the retinal periphery (Whiteside, 1967; Dolan & Fernández-Juricic 2010). We found a trend that suggests that foveae have steeper gradients (and thus a more pronounced change in spatial resolving power) from the retinal specialization to the retinal periphery and higher peak ganglion cell density in relation to areae and visual streaks. Future comparative studies should assess whether animals with a steep decline in visual resolution towards the retinal periphery rely more heavily upon the retinal specialization for visualizing objects (Fernández-Juricic et al. 2011a).

We used linear and non-linear approaches for quantifying cell density gradients, which overall performed similarly. However, both approaches were less successful in discriminating among the three retinal specializations when we combined terrestrial and aquatic species than when these groups were considered separately. This could be related to variations in the retinal configuration beyond the known differences in eye characteristics between terrestrial and aquatic vertebrates (Dral, 1972; Mass & Supin, 2007). Compared to terrestrial species, aquatic species appear to have higher densities and larger retinal ganglion cells (Mass & Supin, 2010), higher densities of amacrine and neuroglial cells (Mass & Supin, 2000), lower numbers of cone photoreceptors (Peichl et al., 2001), and a higher maximum number of retinal specializations per retina (Collin, 1999). Many of these differences are also taxa-specific (Collin, 1999). The implication is that future comparative studies on retinal topography should assess terrestrial and aquatic species separately.

In terrestrial species, the DFA provided good discrimination (above 90%) for foveae and visual streaks, but lower discrimination for areae. On the contrary, in aquatic

species, the linear DFA in particular discriminated areae better than foveae and visual streaks. One potential factor is that the retinal specialization with the lower discrimination in either model was the one with the lowest sample size. Additionally, in terrestrial species areae were generally misclassified as visual streaks, whereas in aquatic species visual streaks were generally misclassified as areae. In three of the terrestrial mammals with a misclassified area (golden hamster, ferret, hooded rat), the topographic maps showed an area where the lower cell density isolines were slightly elongated, which is sometimes referred in the literature as a "weak" visual streak (e.g., Collin & Pettigrew, 1988a, b), although it does not meet the morphological criteria we used for visual streaks (Appendix 2). Finally, some of the author's original classifications included two types of retinal specializations overlapping (e.g., area and visual streak). We chose one based on specific criteria (Appendix 2) for the discriminant function analysis. However, the lower classification success of some topographic maps suggests that some observed retinal specializations may be intermediate between two different types. Our method has the potential to quantify this degree of variability.

One trait that could facilitate the discrimination of an area from a visual streak in the future is the spatial extent of the retinal specialization. It is assumed that areae are smaller than visual streaks (Hughes, 1977; Collin, 1999). Although the spatial limits of foveae are easier to distinguish morphologically from the wholemounted retina (e.g., the width of the foveal pit), the same does not apply to areae and visual streaks. For instance, the area is defined as an enlargement of the thickness of the retina; however, there is no established criterion to determine where the enlargement begins in a cross-section, let alone in a topographic map. The same is true for the visual streak, as the density thresholds that bound the band of high cell density (hence, spatial resolving power) across the retina are yet to be established. Our method actually identified species that can be used to better understand the morphological differences between areae and visual streaks by comparing the aforementioned retinal traits in species that were correctly as well as incorrectly classified. Future work addressing the spatial limits of retinal specializations (e.g., expressed as the percentage of the peak retinal ganglion cell density) could improve the classification success of models such as the one used in this study.

Our method has some shortcomings. First, measuring the position of the center of the retinal specialization and the ganglion cell density gradient assumes that cell density increases from the periphery towards a single point of peak density in the retina. Consequently, our method is not applicable to the retinal specialization termed radial anisotropy, which is a concentric increase in ganglion cell density towards the periphery of the retina (Dunlop & Beazley, 1981). Determining the center of this retinal specialization is therefore not feasible using our method. Although the radial anisotropy has been reported in species such as the South African clawed frog Xenopus laevis (Dunlop & Beazley, 1984), the sawtoothed eel Serrivomer beani (Collin & Partridge, 1996), and Bonapart's spiny eel Notacanthus bonapartei (Wagner et al., 1998), it is not very common in vertebrates and is primarily reported in studies that have included amacrine cells within the ganglion cell layer, which may account for the higher cell density in the periphery. Second, our method is at the mercy of the publishing authors having oriented the wholemount correctly with regard to the nasal, dorsal, ventral and temporal poles, and the assumption that the shrinkage of the wholemount during processing is low (Stone, 1981, Ullmann et al., 2012). Third, our method assumes that the cells counted are all retinal ganglion cells, which in some cases are difficult to distinguish from other cell types (e.g., amacrine cells; Hughes, 1977; Freeman & Tancred, 1978; Hayes & Holden, 1983; Pettigrew et al., 1988).

Despite these limitations, we believe our novel method can be applied to characterize retinal morphology by standardizing the measurement of retinal traits (retinal specialization position, cell gradient, etc.) from published topographic maps in a wide range of vertebrate taxa. However, when working with taxa with a lower degree of variability in the studied retinal traits, the method can be slightly adjusted. For instance, there are some species with foveae (humans, primates) in which the retinal ganglion cell density increases gradually from the retinal periphery to the center of the retina, and then cell density sharply increases towards the fovea and eventually decreases to almost zero at the very center of the fovea. For these species, increasing the number of sampling points in the perifoveal and foveal areas may provide a better characterization of the

gradients in cell density. In these cases, the non-linear approach for quantifying cell density gradients (even including 3rd order polynomials) may fit the data better.

Although we did not test any specific hypothesis, the retinal traits measured can be used in combination with phylogenetic methods (e.g., Harvey & Pagel, 1991; Nunn & Barton, 2001; Garland et al., 2005), to answer questions about the association between retinal morphology and behavioral, ecological, and life-history traits (e.g., Hall & Ross, 2007; Heesy et al., 2011), which can shed light onto the evolution of the vertebrate visual system. Additionally, our method can be used to establish how different retinal specializations vary in position, ganglion cell density, and cell density gradients in taxa/species with different visual demands and that inhabit a diversity of ecological niches. Finally, the retinal traits measured can be used to distinguish between different types of retinal specializations. This may be particularly important for rare, threatened, or endangered species, for example, where the availability of additional retinal material to use for further analysis (such as sectioning the retina in order to confirm the presence or absence of a fovea) is limited due to logistic or ethical considerations.

2.7 Literature Cited

Boire D, Dufour JS, Theoret H, Ptito M (2001). Quantatative analysis of the retinal ganglion cell layer in the ostrich, Struthio Camelus. *Brain Behavior and Evolution* 58:343-355.

Bozzano A & Collin SP (2000). Retinal ganglion cell topography in Elasmobranches. *Brain Behavior and Evolution* 55:191-208.

Collin SP & Pettigrew JD (1988a). Retinal topography in reef teleosts: I. Some species with well-developed areae but poorly-developed streaks. *Brain Behavior and Evolution* 31:269-282.

Collin SP & Pettigrew JD (1988b). Retinal topography in reef teleosts: II. Some species with prominent horizontal streaks and high-density areae. *Brain Behavior and Evolution* 31:283-295.

Collin SP & Pettigrew JD (1989). Quantitative comparison of the limits in visual spatial resolution set by the ganglion cell layer in 12 species of reef teleosts. *Brain Behavior and Evolution* 34:184-192.

Collin SP & Partridge JC (1996). Fish vision: retinal specialization in the eyes of deep-sea teleosts. *Journal of Fish Biology* 49 (Supplement A):157-174.

Collin SP & Shand J (2003). Retinal sampling and the visual field in fishes. In: *Sensory Processing in Aquatic Environment.* (eds. S. P. Collin and N. J. Marshall). (Springer-Verlag, New York. pp. 139-169).

Collin SP (1999). Behavioural ecology and retinal cell topography. In: S Archer, MB Djamgoz, E Loew, JC Partridge & S Vallerga. *Adaptive Mechanisms in the Ecology of Vision.* Pp 509-535. (Kluwer Academic Publishers, Dordrecht).

Collin SP (2008). A web-based archive for topographic maps of retinal cell distribution in vertebrates. *Clinical and Experimental Optometry* 91:85-95.

Cronin TW (2005). The visual ecology of predator-prey interactions. In: P Barbosa & I Castellanos. *Ecology of predator-prey Interactions*, pp. 105–138. Oxford University Press, Oxford.

Curcio CA & Allen KA (1990). Topography of ganglion cells in human retina. *Journal of Comparative Neurology* 300:5-25.

Dral AGD (1972). Aquatic and aerial vision in bottlenose dolphin. *Netherlands Journal of Sea Research* 5:510-513.

Dolan T & Fernández-Juricic E (2010). Retinal ganglion cell topography of five species of ground foraging birds. *Brain Behavior and Evolution* 75:111-121.

Dunlop SA & Beazley LD (1981). Changing retinal ganglion cell distribution in the frog Heleioporus eyrei. *Journal of Comparative Neurology* 202:221-236.

Dunlop SA & Beazely LD (1984). A Morphometric Study Of The Retinal Ganglion Cell Layer And Optic Nerve From Metamophosis In *Xenopus laevis*. *Vision Research* 24(5):417-427.

Fernández-Juricic E (2012). Sensory basis of vigilance behavior in birds: synthesis and future prospects. *Behavioural Processes* 89:143-152.

Fernández-Juricic E, Gall MD, Dolan T, O'Rourke C, Thomas S, Lynch JR (2011a). Visual systems and vigilance behaviour of two ground-foraging avian prey species: white-crowned sparrows and California towhees. *Animal Behaviour* 81:705-713.

Fernández-Juricic E, Moore BA, Doppler M, Freeman J, Blackwell BF, Lima SL, DeVault TL (2011b). Testing the terrain hypothesis: Canada geese see their world laterally and obliquely. *Brain Behavior and Evolution* 77:147-158.

Freeman B & Tancred E (1978). The number and distribution of ganglion cells in the retina of the brush-tailed possum, *Trichosurus vulpecula*. *Journal of Comparative Neurology* 177:557–567.

Garland Jr. T, Bennett Jr. AF, Rezende EL (2005). Phylogenetic approaches in comparative physiology. *Journal of Experimental Biology* 208:3015-3035

Hall MI & Ross CF (2007). Eye shape and activity pattern in birds. *Journal of Zoology* 271:437-333.

Harman A, Abrahams B, Moore S, Hoskins R (2000). Neuronal density in the human retinal ganglion cell layer from 16-77 years. *Anatomical Record* 260:124-131.

Hart NS, Partridge JC, Cuthill IC (2000). Retinal asymmetry in birds. *Current Biology* 10:115-117.

Harvey PH & Pagel MD (1991). The Comparative Method in Evolutionary Biology. Oxford Series in Ecology & Evolution, Oxford University Press.

Hayes BP & Holden AL (1983). The distribution of displaced ganglion cells in the retina of the pigeon. *Experimental Brain Research* 49:181–188.

Heesy CP, Kamilar JM, Willms J (2011). Retinogeniculostriate pathway components only scale with orbit convergence in primates and not other mammals. *Brain Behavior and Evolution* 77:105–115.

Hughes A (1977). The topography of vision in mammals of contrasting life style: comparative optics and retinal organization. In Crescitelli, F. (ed): *The visual system in vertebrates*. New York: Springer-Verlag, pp 615–756.

Inzunza O, Bravo H, Smith RL (1989). Foveal regions of bird retinas correlate with the aster of the inner nuclear layer. *Anatomical Record* 223(3):342-346.

Inzunza O, Bravo H, Smith RL, Angel M (1991). Topography and morphology of retinal ganglion-cells in Falconiforms: A study on predatory and carrion-eating birds. *Anatomical Record* 229(2):271-277.

Mass AM & Supin AY (2000). Ganglion cells density and retinal resolution in the sea otter, *Enhydra lutris*. *Brain Behavior and Evolution* 55:111-119.

Mass AM & Supin AY (2007). Adaptive features of aquatic mammals' eye. *Anatomical Record* 290:701-715.

Mass AM & Supin AY (2010). Retinal ganglion cell layer of the caspian seal *Pusa caspica*: topography and localization of the high-resolution area. *Brain Behavior and Evolution* 76:144-153.

Mastronade DN, Thibeault MA, Dubin MW (1984). Non-uniform postnatal-growth of the cat retina. *Journal of Comparative Neurology* 228:598-608.

McIlwain JT (1996). An introduction to the biology of vision. Cambridge University Press, New York.

Meyer DBC (1977). The avian eye and its adaptations; in Crescitelli F (ed): *The visual system of vertebrates; handbook of sensory physiology*. Springer, New York, vol VII/5, pp. 549-612.

Nunn CL & Barton RA (2001). Comparative methods for studying primate adaptation and allometry. *Evolutionary Anthropology* 10:81-98.

Peichl L, Berhmann G, Kroger RHH (2001). For whales and seals the ocean is not blue: a visual pigment loss in marine mammals. *European Journal of Neuroscience* 13:1520–1528.

Pettigrew JD, Dreher B, Hopkins CS, McCall MJ, Brown M (1988). Peak density and distribution of ganglion cells in the retinae of microchiropteran bats: Implications for visual acuity. *Brain Behavior and Evolution* 32:39-56.

Quinn GP & Keough MJ (2002). Experimental Design and Data Analysis for Biologists. Cambridge University Press, Cambridge.

Ross CF (2004). The tarsier fovea: functionless vestige or nocturnal adaptation? In, C.F. Ross and R.F. Kay, eds., *Anthropoid Origins*: New Visions. New York: Kluwer Academic/ Plenum Publishers. pp. 477-537.

Schiviz AN, Ruf T, Kuebber-Heiss A, Schubert C, Ahnelt PK (2008). Retinal cone topography of Artiodactyl mammals: Influence of body height and habitat. *Journal of Comparative Neurology* 507:1336-1350.

StatSoft, Inc. (2011). Electronic Statistics Textbook. Tulsa, OK: StatSoft. WEB: http://www.statsoft.com/textbook/

Stone J (1981). The Wholemount Handbook. A guide to the preparation and analysis of retinal wholemounts. Maitland Publications Pty. Ltd.

Temple S, Hart NS, Marshall NJ, Collin SP (2010). A spitting image: specializations in archerfish eyes for vision at the interface between air and water. *Proceedings of the Royal Society of London B* 277:2607-2615.

Ullmann JFP, Moore BA, Temple SE, Fernández-Juricic E, Collin SP (2012). The retinal wholemount technique: a window to understanding the brain and behaviour. *Brain Behavior and Evolution* 79: 26-44.

Wässle H & Boycott BB (1991). Functional architecture of the mammalian retina. *Physiological Reviews* 71:447-80.

Wässle H, Grünert U, Röhrenbeck J, Boycott BB (1989). Cortical magnification factor and the ganglion cell density of the primate retina. *Nature* 341:643-646.

Wagner HJ, Frohlich E, Negishi K, Collin SP (1998). The eyes of seep-sea fish II. Functional morphology of the retina. *Progress in Retinal and Eye Research* 17:637-685.

Walls GL (1937). Significance of the foveal depression. *Archives of* Ophthalmology 18:912-919.

Walls GL (1942). The Vertebrate Eye and Its Adaptive Radiation. (Cranbrook Institute of Science, Michigan).

Whiteside TCD (1967). The head movement of walking birds. *Journal of Physiology* 188:31P-32P.

2.8 Appendices

2.8.1 Appendix 1

Table 2.4 Retinal topographic maps of vertebrates used in this study. Most of these maps are available from the retinal topographic map database: http://www.retinalmaps.com.au/ (Collin, 2008). Species are classified as terrestrial (T) or aquatic (T). Abbreviations: C, Chondrichthye; Ac, Actinopterygii; A, Amphibia; R, "Reptilia"; Av, Aves; M, Mammalia; RS, retinal specialization; F, fovea; VS, visual streak; Ar, *area*.

Class	Family	Genus	Species	Common Name	RS	Habitat	References
M	Ochotonidae	Ochotona	rufescens	Afghan pika	VS	T	Akaishi et al., 1995
M	Elephantidae	Loxodonta	africana	African elephant	VS	T	Stone & Halasz, 1989
R	Colubridae	Thamnophis	sirtalis	American garter snake	VS	T	Wong, 1989
Av	Accipitridae	Falco	sparverius	American Kestrel	F/F	T	Inzunza et al., 1991
M	Cercopithecidae	Papio	anubis	Anubis baboon	F	T	Fischer & Kirby, 1991
Ac	Synaphobranchidae	Synaphobranchus	kaupi	Arrowtooth Eel	Ar	A	Collin & Partridge, 1996
Ac	Batrachoididae	Halophryne	diemensis	Australian frogfish	VS	A	Collin & Pettigrew, 1988
Av	Tytonidae	Tyto	alba	Barn Owl	VS	T	Wathey & Pettigrew, 1989

M	Canidae	Canis	lupus f.familiaris	Beagle	VS	T	Peichl, 1992
Ac	Scopelarchidae	Scopelarchus	michaelsarsi	Bigfin pearleye	Ar	A	Collin & Partridge, 1996
Av	Cathartidae	Coragyps	atratus	Black Vulture	F	T	Inzunza et al., 1991
Ac	Pomacanthidae	Pomocanthus	semicirculatus	Blue Angelfish	Ar	A	Collin & Pettigrew, 1989
M	Galagidae	Otolemur	crassicaudatus	Brown greater galago	Ar	T	DeBruyn et al., 1980
Av	Icteridae	Molothrus	ater	Brown-headed Cowbird	F	T	Dolan & Fernández-Juricic, 2010
M	Phalangeridae	Trichosurus	vulpecula	Brush-tailed possum	VS	T	Freeman & Tancred, 1978
Av	Emberizidae	Pipilo	crissalis	California Towhee	F	T	Fernández-Juricic et al., 2011a
Av	Anatidae	Branta	canadensis	Canada Goose	VS	T	Fernández-Juricic et al., 2011b
M	Hydrochoerinae	Hydrochoerus	hydrochaeris	Capybara	VS	T	Silveira et al., 1989a
Ac	Carangidae	Carangoides	equula	Carangid Fish	VS	A	Takei & Somiya, 2002

Av	Paridae	Poecile	carolinensis	Carolina Chickadee	F	T	Moore & Fernández-Juricic, unpubl.
M	Felidae	Felis	catus	Cat	VS	T	Hughes, 1975
M	Cebidae	Cebus	apella	Cebus Monkey	F	T	Silveira et al., 1989b
R	Agamidae	Ctenophorus	nuchalis	Central netted dragon	VS	T	Wilhelm & Straznicky, 1992
Av	Accipitridae	Buteo	fuscenses australis	Chilean Eagle	F/F	T	Inzunza et al., 1991
Av	Falconidae	Milvago	chimango	Chimango Caracara	F	T	Inzunza et al., 1991
Ac	Balistidae	Balistoides	conspicillum	Clown Triggerfish	VS	A	Collin & Pettigrew, 1989
M	Dasyproctidae	Dasyprocta	aguti	Common Agouti	VS	T	Silveira et al., 1989a
Av	Cathartidae	Gymnogyps	californianus	Condor	F	T	Inzunza et al., 1991
C	Dalatiidae	Isistius	brasiliensis	Cookie Cutter Shark	Ar	A	Bozzano & Collin, 2000
Ac	Serranidae	Cephalopholis	miniatus	Coral Cod	Ar	A	Collin & Pettigrew, 1988
Ac	Serranidae	Plectropomus	leopardus	Coral Trout	Ar	A	Collin, 1989

Ac	Cyprinidae	Semotilus	atromaculatus	Creek Chub	Ar	A	Collin & Ali, 1994
Ac	Cyprinidae	Exoglossum	maxillingua	Cutlips Minnow	Ar	A	Collin and Ali, 1994
C	Somniosidae	Centroscymnus	coelolepis	Dogfish	VS	A	Bozzano, 2004
M	Sciuridae	Tamias	sibricus asiaticus	Eastern chipmunk	VS	T	Wakakuwa et al., 1985
C	Hemiscylliidae	Hemiscyllium	ocellatum	Epaulette Shark	VS	A	Bozzano & Collin, 2000
Av	Sturnidae	Sturnus	vulgaris	Eurpean Starling	F	T	Dolan & Fernández-Juricic, 2010
M	Mustelidae	Mustela		Ferret	Ar	T	Vitek et al., 1985
Ac	Lepisostedae	Lepisosteus	platyrhincus	Florida Garfish	VS	A	Collin & Northcutt, 1993
M	Otariidae	Callorhinus	ursinus	Fur Seal	Ar	A	Mass, 1992
M	Cricetidae	Mesocricetus	auratus	Golden Hamster	Ar	T	Tiao & Blakemore, 1976
Ac	Gobiidae	Zosterisessor	ophiocephalus	Grass Goby	Ar	A	Ota et al., 1999
Av	Tyrannidae	Pitangus	sulphuratus	Great Kiskadee	F/Ar	T	Coimbra et al., 2006
M	Caviidae	Cavia	porcellus	Guinea Pig	VS	T	Donascimento et al., 1991
M	Vombatidae	Lasirohinus	latiforns	Hairy-nosed wombat	VS	T	Tancred, 1981

Ac	Labridae	Choerodon	fasciata	Harlequin Tuskfish	VS/Ar	A	Collin & Pettigrew, 1988
M	Phocidae	Pagophilus	groenlandicus	Harp Seal	Ar	A	Mass & Supin, 2003
M	Muridae	Rattus	norvegicus	Hooded Rat	Ar	T	Jeffery, 1985
Av	Fringillidae	Carpodacus	mexicanus	House Finch	F	T	Dolan & Fernández-Juricic, 2010
Av	Passeridae	Passer	domesticus	House Sparrow	F	T	Dolan & Fernández-Juricic, 2010
M	Phascolarctidae	Phascolarctos	cinereus	Koala	Ar	T	Schmid et al., 1992
Ac	Platytroctidae	Platytroctes	apus	Legless searsid	F	A	Collin & Partridge, 1996
C	Carcharhinidae	Negaprion	brevirostris	Lemon Shark	VS	A	Hueter, 1991
Ac	Alepocephalidae	Conocara	macropterum	Longfin Smoothhead	F	A	Collin et al., 2000
M	Cuniculidae	Cuniculus	paca	Lowland paca	VS	T	Silveira et al., 1989a
Av	Procellariidae	Puffinus	puffinus	Manx Shearwater	VS	T	Hayes et al., 1991
Av	Columbidae	Zenaida	macroura	Mourning Dove	F	T	Dolan & Fernández-Juricic, 2010

M	Cheirogaleidae	Cheirogaleus	medius	Mouse lemur	Ar	T	Tetreault et al., 2004
M	Didelphidae	Didelphis	virginiana	North American Opossum	Ar	T	Rapaport et al., 1981
M	Aotidae	Aotus	Trivirgatus	Owl Monkey	F	T	Silveira et al., 1993
Ac	Aulostomidae	Aulostomus	chinensis	Painted Flutemouth	VS	A	Collin & Pettigrew, 1988
Av	Phasianidae	Pavo	cristatus	Peafowl	Ar	T	Hart, 2002
M	Leporidae	Oryctolagus	cuniculus	Pigmented Rabbit	VS	T	Provis, 1979
M	Macropodidae	Setonix	brachyurus	Quokka	VS	T	Beazley & Dunlop, 1983
Ac	Lethrinidae	Lethrinus	miniatus	Red-throated Emperor	VS	A	Collin & Pettigrew, 1989
Ac	Blenniidae	Istiblennius	edentulus	Rippled blenny	Ar	A	Collin, 1989
Av	Columbidae	Columba	livia	Rock Pigeon	F/Ar	T	Binggeli & Pauli, 1969
Av	Tyrannidae	Myiozetetes	cayanensis	Rusty-marginated Flycatcher	F/Ar	T	Coimbra et al., 2006
Ac	Leptochilichthyidae	Searsia	koefoedi	Searsid	F	A	Collin & Partridge, 1996
C	Rhinobatidae	Glaucostegus	typus	Shovel-nosed Ray	Ar	A	Collin, 1988

C	Scyliorhinidae	Scyliorhinus	canicula	Small spotted Dogfish	VS	A	Bozzano & Collin, 2000
Ac	Alepocephalidae	Rouleina	attrita	Softskin Smoothhead	F	A	Collin & Partridge, 1996
Ac	Sparidae	Acanthopagrus	butcheri	Southern Black Bream	Ar	A	Shand et al., 2000
M	Peramelidae	Isoodon	obesulus	Southern brown bandicoot	VS	T	Tancred, 1981
Ac	Opisthoproctidae	Opisthoproctus	grimaldii	Spookfish	Ar	A	Collin et al., 1997
M	Hyaenidae	Crocuta	crocuta	Spotted Hyena	VS	T	Calderone et al., 2003
Ac	Pomacentridae	Amblyglyphidon	curacao	Staghorn Damselfish	Ar	A	Collin & Pettigrew, 1988
Ac	Loricariidae	Pterygoplichthys	pardalis	Suckermouth armored catfish	Ar	A	Douglas et al., 2002
M	Dasyuridae	Sacrophilus	harissi	Tasmanian devil	VS	T	Tancred, 1981
M	Macropodidae	Thylogale	billiardieri	Tasmanian Wallaby	VS	T	Tancred, 1981
Ac	Stylephoridae	Stylephorus	chordates	Threadtail	Ar	A	Collin et al., 1997
M	Folivora	Bradypus	variegatus	Three-toed sloth	Ar	T	Costa et al., 1987
A	Hylidae	Litoria	moorei	Tree frog	Ar	A	Dunlop et al., 1997
M	Macropodidae	Dendrolagus	doriana	Tree Kangaroo	Ar	T	Hughes, 1975

M	Macropodidae	Macropus	fuliginosus	Western gray kangaroo	VS	T	Beazley, 1985
Av	Sittidae	Sitta	carolinensis	White-breasted Nuthatch	F	T	Moore & Fernández-Juricic, unpubl.
Av	Emberizidae	Zonotrichia	leucophrys	White-crowned Sparrow	F	T	Fernández-Juricic et al., 2011a
M	Canidae	Canis	lupus	Wolf	VS	T	Peichl, 1992

2.8.1.1 Literature Cited

Akaishi Y, Uchiyama H, Ito H, Shimizu Y. (1995). A morphological study of the retinal ganglion cells of the Afghan Pika (*Ochotona rufescens*). *Neuroscience Research* 22:1-12.

Beazley L & Dunlop S (1983). The evolution of an area centralis and visual streak in the marsupial *Setonix brachyurus*. *Journal of Comparative Neurology* 216:211-231.

Beazley L (1985). Pattern formation in the retinal ganglion cell layer and visual brain centers. *Australian and New Zealand Journal of Ophthalmology* 13:93-102.

Binggeli RL & Pauli WJ (1969). Pigeon retina: quantitative aspects of optic nerve and ganglion cell layer. *Journal of Comparative Neurology* 137:1-18.

Bozzano A & Collin SP (2000). Retinal ganglion cell topography in elasmobranches. *Brain Behavior and Evolution* 55:191-208.

Bozzano A (2004). Retinal specialisations in the dogfish *Centroscymnus coelolepis* from the mediterranean deep sea. *Scientia Marina* 68 (Supplement 3):185-195.

Calderone JB, Reese BE, Jacobs GH (2003). Topography of photoreceptors and retinal ganglion cells in the spotted hyena (*Crocuta crocuta*). *Brain Behavior and Evolution* 62:182-192.

Coimbra JP, Marceliano MLV, Andrade-da-Costa BLD, Yamada ES (2006). The retina of tyrant flycatchers: topographic organization of neuronal density and size in the ganglion cell layer of the great kiskadee *Pitangus sulphuratus* and the rusty marginated flycatcher *Myiozetetes cayanensis* (Aves: Tyrannidae). *Brain Behavior and Evolution* 68:15-25.

Collin SP (1988). The retina of the shovel-nosed ray, *Rhinobatos batillum* (Rhinobatidae): morphology and quantitative analysis of the ganglion, amacrine and bipolar cell populations. *Experimental Biology* 47:195-207.

Collin SP (1989). Topography and morphology of retinal ganglion cells in the coral trout *Plectropoma leopardus* (Serranidae) - a retrograde cobaltous-lysine study. *Journal of Comparative Neurology* 281:143- 58.

Collin SP (2008). A web-based archive for topographic maps of retinal cell distribution in vertebrates. *Clinical and Experimental Optometry* 91:85-95.

Collin SP & Pettigrew JD (1989). Quantitative comparison of the limits on visual spatial resolution set by the ganglion cell layer in twelve species of reef teleosts. *Brain Behavior and Evolution* 34:184-192.

Collin SP & Northcutt RG (1993). The visual system of the Florida garfish, Lepisosteus platyrhincus (Ginglymodi) III: Retinal ganglion cells. *Brain Behavior and Evolution* 42:295-320.

Collin SP & Ali MA (1994). Multiple areas of acute vision in two freshwater teleosts, the creek chub, *Semotilus atromaculatus* (Mitchill) and the cutlips minnow, *Exoglossum maxillingua* (Lesueur). *Canadian Journal of Zoology* 72:721-730.

Collin SP & Partridge JC (1996). Fish vision: retinal specialization in the eyes of deep-sea teleosts. *Journal of Fish Biology* 49 (Suppl A):157-174.

Collin SP & Pettigrew JD (1988). Retinal topography in reef teleosts II. Some species with prominent horizontal streaks and high-density areae. *Brain Behavior and Evolution* 31:283-295.

Collin SP, Lloyd DJ, Wagner HJ (2000). Foveate vision in deep-sea teleosts: a comparision of primary visual and olfactory inputs. *Philosophical Transactions of the Royal Society of London B* 355:1315-1320.

Collin SP, Hoskins RV, Partridge JC (1997). Tubular eyes of deep-sea fishes: a comparative study of retinal topography. *Brain Behavior and Evolution* 50:335-357.

Costa BLSA, Pessoa VF, Bousfield JD, Clarke RJ (1987). Unusual distribution of ganglion cells in the retina of the three-toed sloth (*Bradypus variegatus*). *Brazilian Journal of Medical and Biology Research* 20:741-748.

DeBruyn EJ, Wise VL, Casagrande VA (1980). The size and topographic arrangement of retinal ganglion cells in the galago. *Vision Research* 20:315-327.

Dolan T & Fernández-Juricic E (2010). Retinal ganglion cell topography of five species of ground foraging birds. *Brain Behavior and Evolution* 75:111-121.

Donascimento JLM, Donascimento RSV, Damasceno BA, Silveira LCL (1991). The neurons of the retinal ganglion-cell layer of the guinea pig: quantitative analysis of their distribution and size. *Brazilian Journal of Medical and Biological Research* 24:199-214.

Douglas RH, Collin SP, Corrigan J (2002). The eyes of suckermouth armoured catfish (Loricariidae, Subfamily Hypostomus): pupil response, lenticular longitudinal spherical aberration and retinal topography. *Journal of Experimental Biology* 205:3425-3433.

Dunlop SA, Moore SR, Beazley LD (1997). Changing patterns of vasculature in the developing amphibian retina. *Journal of Experimental Biology* 200:2479-2492.

Fernández-Juricic E, Gall MD, Dolan T, O'Rourke C, Thomas S, Lynch JR (2011a). Visual systems and vigilance behaviour of two ground-foraging avian prey species: white-crowned sparrows and California towhees. *Animal Behaviour* 81:705-713.

Fernández-Juricic E, Moore BA, Doppler M, Freeman J, Blackwell BF, Lima SL, DeVault TL (2011b). Testing the terrain hypothesis: Canada geese see their world laterally and obliquely. *Brain Behavior and Evolution* 77:147-158.

Fischer QS & Kirby MA (1991). Number and distribution of retinal ganglion-cells in anubis baboons (*Papio anubis*). *Brain Behavior and Evolution* 37:189-203.

Freeman B & Tancred E (1978). The number and distribution of ganglion cells in the retina of the brush-tailed possum, *Trichosurus vulpecula*. *The Journal of Comparative Neurology* 177:557-568.

Hart NS (2002). Vision in the Peafowl (Aves: *Pavo cristatus*). *Journal of Experimental Biology* 205:3925-3935.

Hayes B, Martin GR, Brooke MDL (1991). Novel area serving binocular vision in the retina of procellariiform seabirds. *Brain Behavior and Evolution* 37:79-84.

Hueter RE (1991). Adaptations for spatial vision in sharks. *Journal of Experimental Zoology* S5:130-141.

Hughes A (1975). A quantitative analysis of the cat retinal ganglion cell topography. *Journal of Comparative Neurology* 163:107-128.

Inzunza O, Bravo H, Smith RL, Angel M (1991). Topography and morphology of retinal ganglion cells in Falconiforms: a study on predatory and carrion eating birds. *Anatomical Record* 229:271-277.

Jeffery G (1985). The relationship between cell density and the nasotemporal division in the rat retina. *Brain Research* 347:354-357.

Mass AM (1992). Peak density, size and regional distribution of ganglion cells in the retina of the fur seal *Callorhinus ursinus. Brain Behavior and Evolution* 39:69-76.

Mass AM & Supin AY (2003). Retinal topography of the harp seal *Pagophilus Groenlandicus. Brain Behavior and Evolution* 62:212-222.

Moore BA, M Doppler, JE Young, E Fernandez-Juricic (2013). Interspecific differences in the visual system and scanning behavior in three forest passerines that form heterospecific flocks. *Journal of Comparative Physiology A* 199:263-277

Ota D, Francese M, Ferrero EA (1999). Vision in the grass goby, Zosterisessor ophiocephalus (Teleostei, Gobiidae): a morphological and behavioural study. *Italian Journal of Zoology* 66:125-139.

Peichl L (1992). Topography of ganglion cells in the dog and wolf retina. *Journal of Comparative Neurology* 324:603-620.

Provis JM (1979). The distribution and size of ganglion cells in the retina of the pigmented rabbit: a quanitative analysis. *Journal of Comparative Neurology* 185:121-138.

Rapaport DH, Wilson PD, Rowe MH (1981). The distribution of ganglion cells in the retina of the North American opossum (*Didelphis virginiana). Journal of Comparative Neurology* 199:465-480

Schmid KL, Schmid LM, Wildsoet CF, Pettigrew JD (1992). Retinal topography in the koala (*Phascolarctos cinereus*). *Brain Behavior and Evolution* 39:8-16.

Shand J, Chin SM, Harman AM, Moore S, Collin SP (2000). Variability in the location of the retinal ganglion cell area centralis is correlated with ontogenetic changes in feeding behavior in the black bream, *Acanthopagrus butcheri* (Sparidae, Teleostei). *Brain Behavior and Evolution* 55:176-190.

Silveira LCL, Picanco-Diniz CW, Oswaldo-Cruz E (1989a). Distribution and size of ganglion cells in the retina of large amazon rodents. *Visual Neuroscience* 2:221-235.

Silveira LCL, Picanco-Diniz CW, Sampaio LFS, Oswaldo-Cruz E (1989b). Retinal ganglion cell distribution in the cebus monkey: a comparison with the cortical magnification factors. *Vision Research* 29:1471-1483.

Silveira LCL, Perry VH, Yamada ES (1993). The retinal ganlgion-cell distribution and the representation of the visual field in area-17 of the owl monkey, *Aotus trivirgatus. Visual Neuroscience* 10(5):887-897.

Stone J & Halasz P (1989). Topography of the retina in the elephant Loxodonta africana. *Brain Behavior and Evolution* 34:84-95.

Takei S & Somiya H (2002). Guanine-type retinal tapetum and ganglion cell topography in the retina of a carangid fish, *Kaiwarinus equula. Proceedings of the Royal Society of London B* 269:75-82.

Tancred E (1981). The distribution and sizes of ganglion cells in the retinas of five Australian marsupials. *Journal of Comparative Neurology* 196:585-603.

Tetreault N, Hakeem A, Allman JM (2004). The distribution and size of retinal ganglion cells in *Cheirogaleus medius* and *Tarsius syrichta*: implications for the evolution of sensory systems in primates. In: C Ross & R Kay (Eds.) Anthropoid origins: new visions. Kluwer/Plenum, pp. 449-461.

Tiao YC & Blakemore C (1976). Regional specialisation in golden hamsters retina. *Journal of Comparative Neurology* 168:439-457.

Vitek DJ, Schall JD, Leventhal AG (1985). Morphology, central projections, and dendritic field orientation of retinal ganglion cells in the ferret. *Journal of Comparative Neurology* 241:1-11.

Wakakuwa K, Washida A, Fukuda Y. (1985). Distribution and soma size of ganglion cells in the retina of the eastern chipmunk (*Tamias sibiricus asiaticus*). *Vision Research* 25:877-885.

Wathey JC & Pettigrew JD (1989). Quantitive analysis of the retinal ganglion cell layer and optic nerve of the barn owl *Tyto alba. Brain Behavior and Evolution* 33:279-292.

Wilhelm M & Straznicky C (1992). The topographic organization of the retinal ganglion-cell layer of the lizard *Ctenophores nuchalis*. *Archives of Histology and Cytology* 55:251-259.

Wong ROL (1989). Morphology and distribution of neurons in the retina of the American garter snake *Thamnophis sirtalis*. *Journal of Comparative Neurology* 283:587-601.

2.8.2 Appendix 2: Criteria used to classify retinal specializations from topographic maps

Out of the three retinal specializations we focused on in this study, the fovea is the only one that may be seen as a funnel shaped mark on the wholemounted retina, although its presence should be confirmed through cross-sectional analysis showing tissue invagination. Many studies using topographic maps of the retinal ganglion cell layer have marked the presence of the fovea following visual inspection on the wholemounted retina. The other retinal specializations studied (areae, visual streaks) are more difficult to classify based on the topographic representation of variations in the density of retinal ganglion cells. Stone and Halasz (1989) emphasized that improving the classification of retinal specializations requires analysis beyond topographic maps; such as, establishing the projections of the RGCs to centers in the brain.

Many of the topographic maps published already do not have further tests to confirm the type of retinal specializations. Nevertheless, by following some criteria from the literature (Walls, 1937; Hughes, 1977; Collin, 2008), we classified the three types of retinal specializations based on features detectable by examination of retinal topographic maps. In general terms, we considered the fovea an indentation of the retina showing a funnel-shaped pit in the retinal tissue (Walls, 1937; Collin, 2008). We considered the area as a round, localized concentration of ganglion cells without a noticeable pit in the retinal tissue (Hughes, 1977). Finally, we considered the visual streak as a "bandlike area" crossing along the retina (Hughes, 1977).

In 74 out of the 95 retinal specializations (across 89 species, Appendix 1) included in this study, the authors' classification coincided with the general criteria presented above. In general, we followed the author's classification of the retinal specialization. However, in 21 cases, the authors did not specify a type of retinal specialization or their classification did not follow necessarily the criteria presented above. We explain in the following paragraphs the criteria we used to classify these cases.

1. Three-toed sloth (Costa et al., 1987: http://retinalmaps.com.au//view?tag0=157163). The authors classified this retinal specialization as both an area and a visual streak. However, we classified it as an area in our analysis. The first two isodensity lines are very circular (greater than 1,350 cells/ mm^2), with a concentric increase in RGC density up to a specific point, which follows the area definition (Hughes, 1977). The next two lower cell density isolines (bounding cell densities between 1,000-1,200 cells/ mm^2) have a tail that extends in the dorsal direction but not all the way to both sides of the retina. Furthermore, the lines representing even lower cell densities (beyond the 4th highest, less than 1000 cells/sq. mm) do not remain elongated and are more circular.

2. Ferret (Vilela et al., 2005: http://retinalmaps.com.au//view?tag0=157165). The retinal configuration is similar in principle to that of the three-toed sloth, in that the highest cell density ranges (greater than 4,500 cells/mm^2) are circular like an area, then the next lower isodenity line (between 3,500-4500 cells/ mm^2) becomes more elongated inone direction, but the lowest isodensity lines (less than 3,500 cells/ mm^2) become more circular. Therefore, we also classified this specialization as an area.

3. The topographic maps of seven species of birds (California towhee and white-crowned sparrow, Fernández-Juricic et al., 2011; European starling, brown-headed cowbird, house sparrow, house finch, and mourning dove, Dolan & Fernández-Juricic, 2010) were originally reported as having an area due to the lack of cross-sections. However, we confirmed through visual examination of their retinas that they have a funnel-shaped pit in the retinal tissue. Therefore, we classified them as all having foveae.

4. The topographic maps from seven species of birds (great kiskadee; http://retinalmaps.com.au//view?tag0=156862, and rusty-marginated flycatcher; http://retinalmaps.com.au//view?tag0=156966, Chilean eagle; http://retinalmaps.com.au//view?tag0=156965, American Kestrel (sparrow hawk); http://retinalmaps.com.au//view?tag0=156863, Coimbra et al., 2006; Chimango caracara; http://retinalmaps.com.au//view?tag0=156964, condor;

http://retinalmaps.com.au//view?tag0=156967, and black vulture; http://retinalmaps.com.au//view?tag0=156968, Inzunza et al., 1991) all possess both (a) a central fovea, and (b) either a temporal fovea or a temporal area. For the maps of the great kiskadee, rusty-marginated flycatcher, Chilean eagle, and American kestrel we coded both the central specialization (fovea in all cases) and temporal specialization (fovea in Chilean eagle and American Kestrel, area in great kiskadee and rusty-marginated flycatcher) as they were classified in the original paper. However, for the black vulture, chimango caracara, and condor, we only coded the central fovea, but not what the authors classified as a temporal area. Following the criteria listed above, what the authors classified as a temporal specialization would only be considered a slight increase in ganglion cell density and not a true area as there was not a concentric increase in ganglion cell density.

Also, each of the seven species (great kiskadee, rusty-marginated flycatcher, Chilean eagle, American kestrel, black vulture, chimango caracara, condor) was suggested in the original publications to also have a third retinal specialization: a visual streak. However, we did not assigned these species as having a visual streak because the streak-like extension is only an effect of the two other specializations being close to one another rather a distinctive bandlike area of high retinal ganglion cell density across the retina.

5. In situations in which one specialization was present inside of another specialization, we based our coding on the specialization with the largest area of high resolution in the retina, as this seems to be an important factor affecting how animals gather information behaviorally (e.g., through head movements) within their visual fields. More specifically, when there was an area inside of a visual streak (e.g. spotted hyena: http://retinalmaps.com.au//view?tag0=156861, Calderone et al., 2003; cat: http://retinalmaps.com.au//view?tag0=156958, Hughes, 1975; Tasmanian devil: http://retinalmaps.com.au//view?tag0=157080, Tancred, 1981; carangid fish, http://retinalmaps.com.au//view?tag0=157077, Takei & Somiya, 2002; clown triggerfish: http://retinalmaps.com.au//view?tag0=156888, Collin & Pettigrew, 1989; painted

flutemouth: http://retinalmaps.com.au//view?tag0=156889, Collin & Pettigrew, 1988; red-throated emperor: http://retinalmaps.com.au//view?tag0=157423, Collin & Pettigrew, 1988; barn owl: http://retinalmaps.com.au//view?tag0=156758, Wathey & Pettigrew, 1989; American garter snake: http://retinalmaps.com.au//view?tag0=157090, Wong, 1989), we counted it as a visual streak.

Additionally, two of the topographic maps included in the analysis (Carolina chickadee and white-breasted nuthatch) are currently in a manuscript to be submitted soon (Moore et al., in prep). These two species have a fovea that could be distinguished microscopically from the wholemount (see above).

2.8.2.1 Literature Cited

Calderone JB, Reese BE, Jacobs GH (2003). Topography of photoreceptors and retinal ganglion cells in the spotted hyena (Crocuta Crocuta). *Brain Behavior and Evolution* 62:182-192.

Coimbra JP, Marceliano MLV, Andrade-da-Costa BLD, Yamada ES (2006). The retina of tyrant flycatchers: Topographic organization of neuronal density and size in the ganglion cell layer of the great kiskadee *Pitangus sulphuratus* and the rusty marginated flycatcher *Myiozetetes cayanensis* (Aves: Tyrannidae). *Brain Behavior and Evolution* 68:15-25.

Collin SP (2008). A web-based archive for topographic maps of retinal cell distribution in vertebrates. *Clinical and Experimental Optometry* 91:85-95.

Collin SP & Pettigrew JD (1988). Retinal topography in reef teleosts II. Some species with prominent horizontal streaks and high-density areae. *Brain Behavior and Evolution* 31:283-295.

Collin SP & Pettigrew JD (1989). Quantitative comparison of the limits on visual spatial resolution set by the ganglion cell layer in twelve species of reef teleosts. *Brain Behavior and Evolution* 34:184-192.

Costa BLSA, Pessoa VF, Bousfield JD, Clarke RJ (1987). Unusual distribution of ganglion cells in the retina of the three-toed sloth (*Bradypus variegatus*). *Brazilian Journal of Medical and Biology Research* 20:741-748.

Dolan T & Fernández-Juricic E (2010). Retinal ganglion cell topography of five species of ground foraging birds. *Brain Behavior and Evolution* 75:111-121.

Fernández-Juricic E, Gall MD, Dolan T, O'Rourke C, Thomas S, Lynch JR (2011). Visual systems and vigilance behaviour of two ground-foraging avian prey species: white-crowned sparrows and California towhees. *Animal Behaviour* 81:705-713.

Hughes A (1975). A Quantitative Analysis of the Cat Retinal Ganglion Cell Topography. *Journal of Comparative Neurology* 163:107-128.

Hughes A (1977). The topography of vision in mammals of contrasting life style: comparative optics and retinal organization. In Crescitelli F (ed): The visual system in vertebrates. New York: Springer-Verlag, pp 615–756.

Inzunza O, Bravo H, Smith RL, Angel M (1991). Topography and morphology of retinal ganglion-cells in Falconiforms - A study on predatory and carrion-eating birds. *Anatomical Record* 229:271-277.

Moore BA, M Doppler, JE Young, E Fernandez-Juricic (2013). Interspecific differences in the visual system and scanning behavior in three forest passerines that form heterospecific flocks. *Journal of Comparative Physiology A* 199:263-277

Stone J & Halasz P (1989). Topography of the retina in the elephant *Loxodonta Africana*. *Brain Behavior and Evolution* 34:84-95.

Takei S & Somiya H (2002). Guanine-type retinal tapetum and ganglion cell topography in the retina of a carangid fish, *Kaiwarinus equula. Proceedings of the Royal Society of London B* 269:75-82.

Tancred E (1981). The distribution and sizes of ganglion cells in the retinas of five Australian marsupials. *Journal of Comparative Neurology* 196:585-603.

Vilela MCR, Mendonca JEF, Bittencourt H, Lapa RM, Alessio MLM, Costa MSMO, Guedes RCA, Silva VL, Costa BLSA da (2005). Differential vulnerability of the rat retina, suprachiasmatic nucleus and intergeniculate leaflet to malnutrition induced during brain development. *Brain Research Bulletin* 64:395-408.

Walls GL (1937). Significance of the foveal depression. *Archives of Ophthalmology* 18:912-919.

Wathey JC & Pettigrew JD (1989). Quantitive analysis of the retinal ganglion cell layer and optic nerve of the barn owl Tyto alba. *Brain Behavior and Evolution* 33:279-292.

Wong ROL (1989). Morphology and distribution of neurons in the retina of the American garter snake *Thamnophis sirtalis*. *Journal of Comparative Neurology* 283:587-601.

2.8.3 Appendix 3

Table 2.5 Classification functions from the linear and non-linear Discriminant Function Analyses (DFA) of terrestrial and aquatic vertebrates. Shown are the classification functions and their coefficients for each type of retinal specialization. RGC, retinal ganglion cell.

Terrestrial species

Linear DFA model

$S_{retinal\ specialization}$ = a + b * peak RGC density + c * lowest RGC density + d * temporal slope + e * x-coordinate position + f * y-coordinate position

	fovea	area	visual streak
Constant	-8.60137	-3.00077	-1.23475
Peak RGC density	0.00034	0.00007	0.00005
Lowest RGC density	0.00105	0.00021	0.00009
Temporal slope	-0.80339	0.33622	0.00107
x-coordinate position	1.63501	-3.31182	-2.00614
y-coordinate position	0.69617	-4.69082	-1.10894

Non-linear DFA model

$S_{retinal\ specialization}$ = a + b * peak RGC density + c * lowest RGC density + d * PCA factor representing a change in cell density in the temporal region of the retina + e * x-coordinate position + f * y-coordinate position + g * PCA factor representing a change in cell density in the dorsal region of the retina

	fovea	area	visual streak
Constant	-11.3203	-3.59522	-2.94342
Peak RGC density	0.0005	0.00024	0.00025
Lowest RGC density	0.0007	0.00013	-0.00011
PCA temporal	-1.7354	0.38003	-0.06805
x-coordinate position	1.8869	-1.79340	-0.79163
y-coordinate position	2.7918	-3.41312	0.62487
PCA dorsal	-4.0536	-2.57402	-3.63071

Aquatic species

Linear DFA model

$S_{retinal\ specialization}$ = a + b * peak RGC density + c * lowest RGC density + d * nasal slope + e * temporal slope + f * dorsal slope + g* x-coordinate position + h * y-coordinate position.

	fovea	area	visual streak
Constant	-2.38964	-2.22052	-6.41977
Peak RGC density	0.00012	-0.00004	0.00043
Lowest RGC density	0.00059	-0.00006	0.00004
Nasal slope	-2.19112	1.83658	-5.72918
Temporal slope	-0.19894	0.20869	-0.25415
Dorsal slope	0.31942	-0.20636	-1.08599
x-coordinate position	-1.25112	1.90093	-4.65734
y-coordinate position	-3.90749	0.77298	-2.29086

Non-linear DFA model

$S_{retinal\ specialization}$ = a + b * x-coordinate position + c * PCA factor representing a change in cell density in the temporal region of the retina + d * lowest RGC density + e * y-coordinate position + f * PCA factor representing a change in cell density in the dorsal region of the retina + g * peak RGC density

	fovea	area	visual streak
Constant	-5.53234	-1.98571	-2.83120
x-coordinate position	-3.25709	-0.46134	2.05150
PCA temporal	2.59056	-0.09945	0.38005
Lowest RGC density	-0.00018	0.00043	-0.00021
y-coordinate position	-0.52988	-1.97467	2.32646
PCA dorsal	-2.97284	-0.55221	-2.27568
Peak RGC density	0.00013	0.00005	0.00012

CHAPTER 3: ARE ALL VERTEBRATE RETINAS CONFIGURED THE SAME? IMPLICATIONS FOR THE EVOLUTION OF ACUTE VISION

This chapter is part of a manuscript co-authored with other researchers that will be submitted for publication soon:

Moore BA, Kamilar JM, Collin SP, Bininda-Emonds ORP, Dominy NJ, Hall MI, Heesy CP, Johnsen S, Lisney TJ, Loew ER, Moritz G, Nava SS, Warrant EF, Yopak KE, Fernandez-Juricic E. Are all vertebrate retinas configured the same? Implications for the evolution of acute vision. To be submitted for review.

3.1 Abstract

Little is known about whether there is convergent evolution in acute vision across vertebrates. We studied spatial visual resolution across the retina, using ganglion cell density profiles, of vertebrates with different types of retinal specializations: foveae, *areae* and visual streaks. We measured ganglion cell density profiles in 80 aquatic and terrestrial species while accounting for phylogenetic relatedness and body mass. We found that each retinal specialization type has shared morphological features across different taxa, particularly in terrestrial vertebrates. However, spatial visual resolution is encoded differently in retinas with foveae compared to those with *areae* or visual streaks. Vertebrates with foveae have higher peak cell densities and steeper gradients of cell density change from the retinal periphery to the center of the retinal specialization than species with *areae* or visual streaks. Contrary to our expectations, species with foveae had higher ganglion cell densities in the retinal periphery than those with *areae* or visual streaks. Our results have relevant implications for the evolution of the vertebrate visual

system. First, foveate vertebrates may invest more neural resources in processing visual information than non-foveate species. Second, foveate-species would rely more on the retinal specialization for different visual tasks than non-foveate species due to the higher localized spatial visual resolution. Overall, visual behaviors are likely to differ substantially in foveate vs. non- foveate vertebrates.

3.2 Introduction

The eye and ultimately the retina are the primary means by which the brain receives images of the surrounding world. Three-dimensional images that fall within the constraints of the two visual fields are converted in the retina to an array of visual signals, which are mapped onto the visual centers of the brain through the optic nerve (i.e., retinal ganglion cell axons) (McIlwain 1996). The retinal ganglion cells lining the inner retina act as a bottleneck of the information that travels from the photoreceptors to the brain. The relative number and spacing of ganglion cells represent an index of the spatial resolving power (e.g., spatial visual resolution or visual acuity) that each animal is able to use behaviorally (Pettigrew et al. 1988).

Within the retina, there are variations in visual performance given by variations in the density of ganglion cells (Hughes 1977, Meyer 1977). Most species possess a region (or regions) of high ganglion cell density for acute vision, called retinal specialization. These retinal specializations generally occupy a relatively small proportion of the retina and therefore sample small region of the visual field with higher spatial resolving power compared to the rest of the retina (Walls 1942, Pumphrey 1948, Lockie 1952). Therefore, animals need to move either or both their eyes and heads to gather the superior information provided by retinal specializations (Lemeignan et al. 1992; Dawkins & Woodington 2000; Dawkins 2002; Moinard et al. 2005).

The three most common types of retinal specializations in vertebrates are the fovea, *area*, and visual streak. A fovea consists of a pitted invagination of the retinal tissue with a high density of retinal sampling elements (with the exception of ganglion

cells at the very center of the fovea, which are often displaced) (Slonaker 1897, Walls 1937, Pumphrey 1948, Curcio et al. 1991, Collin & Collin 1999). An *area* is a concentric increase in photoreceptor/ganglion cell density in a specific retinal region, where the retina is often thicker due to the high numbers of retinal neurons (Kahmann 1935, Walls 1942). Finally, the visual streak consists of a (often horizontal) band of high ganglion cell density extending across the retinal meridian (Johnson 1901, Vincent 1912, Hughes 1977). These three types of retinal specializations have been found in a large range of vertebrates with significant differences in their number and position (Hughes 1977).

Most of the comparative vision studies to date have focused on describing the variation in the density of ganglion cells *within* the retinal specialization (e.g., peak cell density). However, relatively less is known about the variation in ganglion cell density *away* from the retinal specialization or the retinal periphery. This overlooked point is particularly relevant because differences in spatial resolving power between the retinal specialization and the retinal periphery may influence how much animals rely on different parts of the retina to sample visually their environment, which could lead to variation in scanning strategies (Fernández-Juricic 2012). For instance, besides using the acute vision provided by the retinal specialization, animals may also benefit by detecting stimuli through the retinal periphery at lower spatial resolution (e.g., covert attention, Bisley 2011). The lower the difference in visual resolution (and thus density of ganglion cells) between the retinal periphery and the retinal specialization, the higher the chances that animals may rely on the visual resolution provided by the retinal periphery (Fernández-Juricic et al. 2011b). This leads to some fundamental questions in visual biology that have not been addressed in a comparative context with multiple species and controlling for phylogenetic effects. First, do retinal specializations vary in their peak ganglion cell density? Second, is the variation in peak ganglion cell density between retinal specializations associated with cell density at the periphery of the retina? Third, and most importantly, is there convergent evolution in cell density across the *whole* retina in different vertebrates with different types of retinal specializations?

The goal of study was to establish whether ganglion cell density profiles (i.e., changes in cell density across the retina that reflect variations in spatial resolving power

across the visual field, Fig. 1) vary with the type of retinal specialization and whether each of these types of specializations shares a similar density profile in different vertebrate taxa. Two factors have previously precluded the investigation of these questions: the lack of a comparative dataset on the variation of retinal specializations and a method to quantify retinal cell density profiles in vertebrate taxa with different eye size and shape. However, these issues have recently been addressed. Collin (2008) has collated published topographic maps (i.e., representations of changes in the density of retinal ganglion cells across the retina) for over 300 species of vertebrates (see http://www.retinalmaps.com.au/). Additionally, Moore et al. (2012) proposed a new standardized method to quantitatively assess on published topographic maps how different parts of the retina sample visual information, which can affect how an animal interacts behaviorally with its environment (e.g. Temple et al. 2010). We measured retinal traits that are proxies of the highest and lowest levels of spatial resolving power in the retina (i.e., peak and lowest ganglion cell densities), the changes in resolving power from the retinal periphery to the center of the retinal specialization (i.e., cell density gradients), and the position of the retinal specialization using Cartesian co-ordinates. We determined for the first time general properties in the cell density profiles of the retina of vertebrates, considering both terrestrial and aquatic species, while controlling for the effects of phylogenetic relatedness.

We tested comparatively the long standing hypothesis in visual ecology that the fovea has higher spatial resolving power than other types of retinal specializations (Walls 1942, Inzunza et al. 1989, Gaffney & Hodos 2003, Ross 2004), and therefore we predicted that the fovea would have higher peak ganglion cell densities than either the *area* or the visual streak (Walls 1937, Fig. 1). However, the fovea covers a relatively more restricted area of the retina (which would lead to a relatively lower proportion of the visual field with high spatial resolving power) than the *area* or visual streak (Walls 1937). Therefore, assuming that the overall number of axons going to the visual centers is similar between different types of retinal specialization, we hypothesized a trade-off between the peak cell density within the retinal specialization and cell density in the retinal periphery (Fig. 1). We predicted that the higher peak cell density in the fovea

would be accompanied with a lower cell density in the retinal periphery; hence, a steeper rate of change in cell density extending from the retinal periphery to the center of the retinal specialization compared to the *area* or the visual streak (Fig. 1). Testing these predictions has implications for understanding of how different vertebrate species use acute vision in different habitat types (Collin 1999), how different visual sampling strategies (e.g., visual search, visual fixation) may be associated with the configuration of the retina (Wallman et al. 1994, Wallman & Pettigrew 1985, Collin & Shand 2003), and more broadly the role of this sensory modality in the evolution of visual behavior (e.g., Fernández-Juricic 2012).

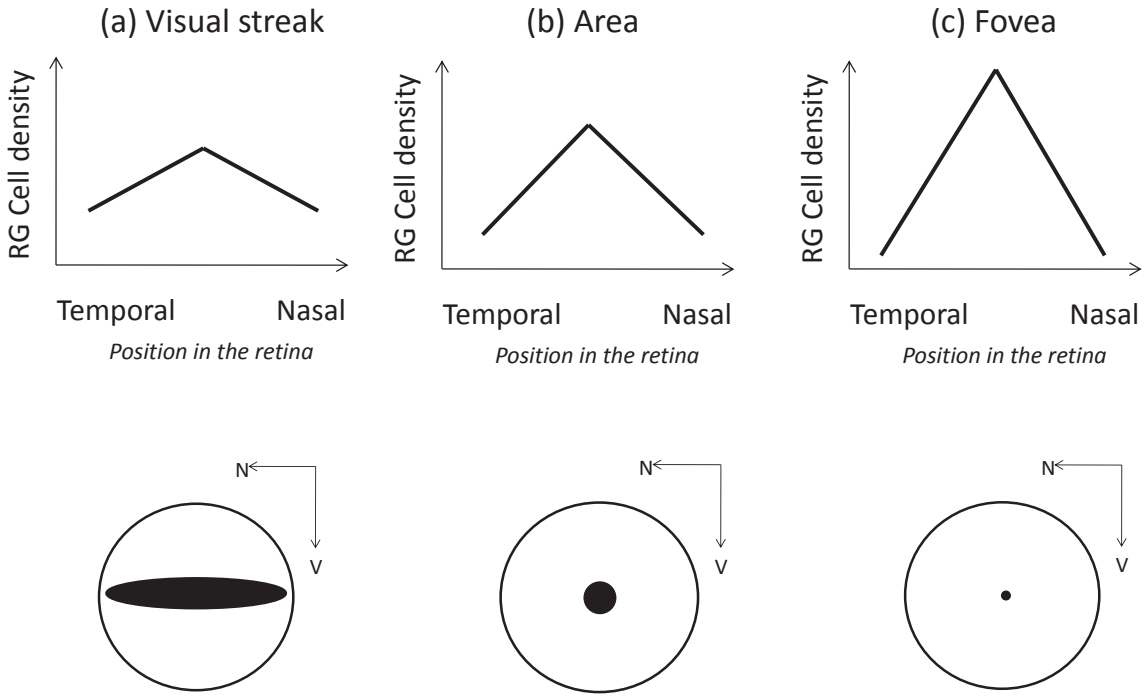

Fig 3.1 Predictions on how retinal ganglion (RG) cell density profiles would vary in different types of retinal specializations (visual streak, area, and fovea): cell density changes from the retinal periphery (shown are nasal and temporal regions) to the center of the retinal specialization (e.g., peak cell density). Also shown are schematic representations of the relative size of each type of retinal specialization.

3.3 Methods

3.3.1 General procedures

We used published topographic maps of distribution of neurons within the retinal ganglion cell layer instead of the photoreceptor layer because a higher number of studies is available across different taxa and because the ganglion cells represent the final stage of retinal processing before information is conveyed to the brain, thereby eliciting behavioral outputs pertaining to spatial resolving power (Pettigrew et al. 1988). The majority of the topographic maps for this study were downloaded from the retinal topographic map database: http://www.retinalmaps.com.au/ (Collin 2008). We included topographic maps from 80 species of vertebrates (Chondrichthyes [cartilaginous fishes], 5; Actinopterygii [ray-finned (or bony) fishes], 19; Amphibia, 1; Squamata [lizards], 2; Aves [birds], 20; Mammalia, 33; Appendix 1). In the text, we use the common names of the species, but scientific names are available in Appendix 1. Species were further classified into aquatic (part of their life cycle relying on water for foraging and/or breeding purposes, 27 species) or terrestrial (their whole life cycle occurring on land, 53 species) (Appendix 1).

In our analyses, we only included topographic maps that provided the orientation and scale of the retina and properly labeled each of the iso-density contours (Fig. 2). Based on the descriptions and topographic maps presented in the original papers and some other criteria (details in Appendix 2), we classified retinal specializations into three categories: fovea, *area*, and visual streak. When more than one map was available for a given species, we selected the one the original authors deemed as the most representative. Our statistical analyses were constrained to include a single data point per species; thus, we selected a single retinal specialization from species with reportedly more than one type of specialization on the same retina (details on the criteria used in Appendix 2), which occurred in a limited number of species (6 out of 80).

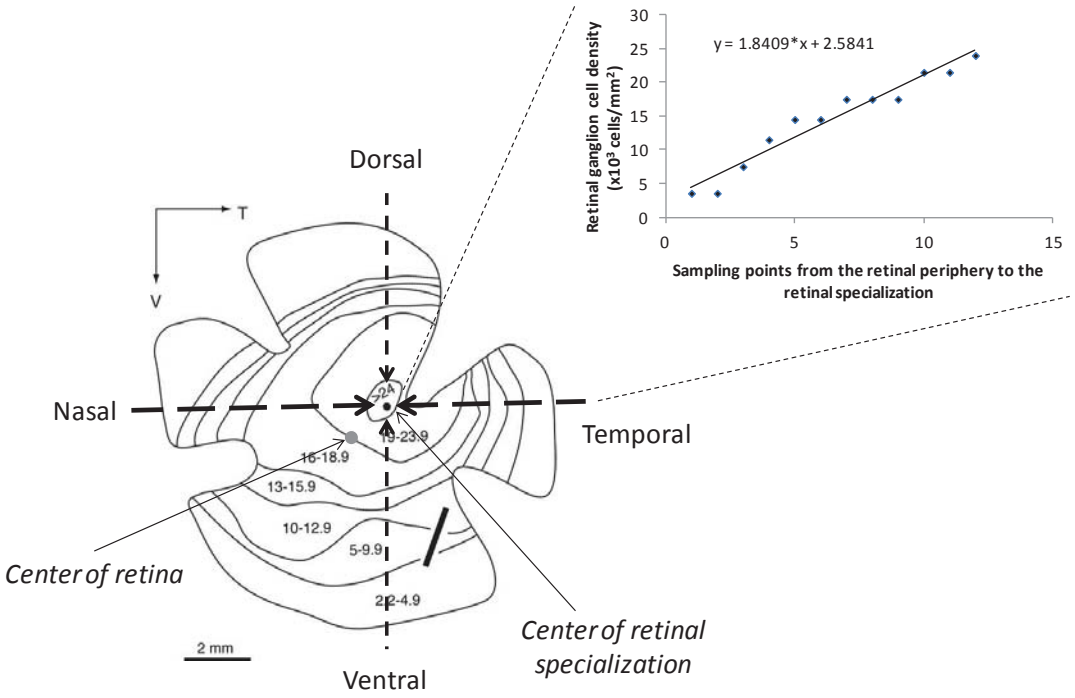

Fig 3.2 Example of a retinal topographic map showing variations in the density of ganglion cells (cells/mm^2 x 10^3) across the retina of the California towhee (*Pipilo crissalis*). Shown are the sampling vectors (nasal-temporal and dorsal-ventral) crossing the center of the retinal specialization. Insert: example of plot of the mean cell density in each of the 21 sampling points from the temporal sampling vector. We fitted a line and used its slope as the rate of change in cell density from the retinal periphery to the retinal specialization. See text and Appendix 3 for details.

We collected body mass information to control for its confounding effects (e.g., body mass can influence visual acuity through changes in eye size, Kiltie 2000). Body mass data were obtained from different sources (Dunning Jr. 2008, Jones et al. 2007, Fishbase, Youtheria). For fishes, body mass information was collected from the published studies that reported their retinal topography when available, but for eight species we had to rely on other sources (details of criteria and calculations in Appendix 3).

From the topographic maps of retinal ganglion cells (RGC) (Fig. 1), we quantified nine traits for each species: (1) peak RGC density at the retinal specialization, (2) lowest

RGC density at the retinal periphery, (3) difference between the peak and lowest RGC density, (4-7) degree of variation in RGC density from the retinal periphery to the center of the retinal specialization (RGC density gradient) in four different regions of the retina (nasal, temporal, dorsal, ventral). We also measured the (8-9) position of the retinal specialization with two coordinates because retinal specializations that are not at the retinal center may be associated with steeper/shallower changes in cell density. We did not have a-priori predictions for the position of the retinal specialization as it has been hypothesized to vary with multiple factors (diet, habitat, position of the orbits in the skull, etc.; Hughes 1977); consequently, we simply assessed whether there was any general positional pattern across the broad taxonomic range of vertebrates studied.

The detailed methods to measure these traits are discussed in Moore et al. (2012), but are summarized in Appendix 2 (see also Fig. 2).

The lowest and highest levels of spatial resolving power are often approximated by the minimum and peak retinal ganglion cell densities across the retina, respectively. We obtained this information from the original publications and the topographic maps found therein (Appendix 1), and calculated the difference in RGC density between the retinal specialization and the retinal periphery.

A gradient of RGC density also represents a gradient of change in spatial resolving power (Fernández-Juricic et al. 2011b). RGC density gradients were measured by establishing sampling transects across four main directions in the retina (nasal, temporal, dorsal, ventral) emanating from the center of each retinal specialization (Fig. 2, Appendix 2). The average RGC density was recorded at each sampling point by establishing the iso-density area each sampling point fell into (Fig. 2, Appendix 2). We plotted the RGC density values at each of the sampling points originating from the retinal specialization fitted with a linear curve (Fig. 2, Appendix 2). The slope value of this relationship was then considered as a proxy for the change in RGC density across the retina (Fig. 2). In a previous study, we found that linear, rather than non-linear, functions fit the RGC density gradient better when using species from a broad taxonomic range (Moore et al. 2012).

The position of the retinal specialization was considered the area of the visual field with highest spatial resolving power (Collin 1999), and was measured in relation to the center of the retina (Fig. 2, Appendix 2) as Cartesian coordinates: x (positive values indicate temporal, negative values indicate nasal), and y (positive values indicate dorsal, negative values indicate ventral).

3.3.2 Statistical analyses

All of our analyses were interspecific in nature. Therefore, we needed to account for the non-independence of interspecific data due to the shared evolutionary history among species (Felsenstein 1985; Nunn 2011). We used phylogenetic generalized least squares models (PGLS; Pagel 1999). These models include an additional parameter, lambda (which varies from 0 to 1), which quantifies and accounts for the amount of phylogenetic signal in the model. A lambda value of 0 indicates that the residual error in the model is completely independent of phylogeny. Conversely, a lambda value of 1 indicates that the residual error in the model varies according to a Brownian motion model of evolution, in which similarity decreases with increasing phylogenetic divergence.

We conducted all PGLS analyses using the Caper package (Orme et al 2011) in R (R Development Core Team 2010; details in Appendix 3]. First, we explored the relationships among retinal traits without considering the type of retinal specialization to identify trends in retinal configuration across vertebrate species while controlling for phylogenetic effects (Appendix 3). Second, we examined whether species with different types of retinal specializations exhibited differences in the retinal traits studied. We used a series of PGLS models using body mass and retinal specialization type (fovea, area, visual streak) as predictor variables. Retinal specialization type was treated as a categorical variable in the analysis. Body mass (log-transformed) was included as a covariate.

Before running our models, we tested the homogeneity of slopes, which is an assumption of many models that have categorical and continuous predictor variables, by conducting an additional model that included interaction effects (Quinn & Keough 2002). We found that none of our models violated the homogeneity of slopes assumption. If we

detected outliers, we removed them from the dataset and re-ran the analysis (see Appendix 3 and Results for details on the criteria used). Despite the high number of P-values obtained, we did not use a Bonferroni correction because it increases Type II errors and decreases statistical power (Nakagawa 2004).

We followed two analytical approaches to establish how the type of retinal specialization varied in the studied retinal traits. First, we used each retinal trait as a dependent variable, with the caveat that some of these traits were significantly associated (see below), and thus the results of each statistical analysis cannot be considered independent when interpreting the data. Second, we conducted a principal component analysis (PCA) including most retinal traits (peak and lowest RGC density; nasal, temporal, dorsal, ventral gradients; and x- and y-coordinate positions) to summarize them while accounting for retinal trait covariation. We did not include the difference in cell density between the retinal specialization and the retinal periphery in the PCA because we used peak and lowest RGCs to estimate it. The PC factors generated (Eigenvalues > 1) were considered independent and used as dependent variables. We report associations between PC factors and retinal traits whose loadings were > 0.70 (Statsoft, Inc. 2011).

We conducted three sets of analyses: one including all species without distinguishing between terrestrial and aquatic species, a second including only terrestrial species, and a third including only aquatic species. We ran separate analyses for terrestrial and aquatic species because these taxa occupy extremely different environments, which starkly vary in terms of the relative position of the visual stimuli, as well as the medium in which the light travels (Lythgoe 1979; Endler 1993). Additionally, retinal design has been shown to differ between some aquatic and terrestrial species (Mass & Supin 2007). A model with all species but including retinal specialization and habitat type as categorical factors did not have enough statistical power to test for interaction effects as it was an unbalanced design where some combination of factors had less than five species (e.g., aquatic species with fovea).

Finally, our comparative analyses required a phylogeny of the studied taxa, yet one did not exist. Therefore, we constructed a phylogenetic tree for our comparative analysis using data from GenBank (details in Appendix 3), presented in Fig. 3.

Fig 3.3 Maximum likelihood vertebrate phylogeny based on 25 genes obtained from GenBank. We noted the five major vertebrate groups that included at least two species. A sixth group, amphibians, is represented by the species *Litoria moorei*.

3.4 Results

3.4.1 Principal component analysis

Pooling terrestrial and aquatic species together, the PCA generated two PC factors. PC1 (Eigenvalue = 4.18, proportion of variability explained = 0.52) was positively associated with peak RGC density (0.957), and nasal (0.827), temporal (0.717), dorsal (0.874) and ventral (0.805) RGC density gradients. PC2 (Eigenvalue = 1.28, proportion of variability explained = 0.16) was positively associated with the y-coordinate position (0.875).

Considering terrestrial species only, the PCA generated two PC factors. PC1 (Eigenvalue = 5.00, proportion of variability explained = 0.63) was positively associated with the peak RGC density (0.962), and the nasal (0.952), temporal (0.914), dorsal (0.926) and ventral (0.966) RGC density gradients. PC2 (Eigenvalue = 1.15, proportion of variability explained = 0.14) was negatively associated with the y-coordinate position (-0.883).

Considering aquatic species only, the PCA generated three PC factors. PC1 (Eigenvalue = 3.92, proportion of variability explained = 0.49) was positively associated with the lowest RGC density (0.746), peak RGC density (0.964), and nasal (0.757), temporal (0.701), and dorsal (0.843) RGC density gradients. PC2 (Eigenvalue = 1.52, proportion of variability explained = 0.19) was negatively associated with the ventral gradient in RGC density (-0.757) and positively with the y-coordinate position (0.823). PC3 (Eigenvalue = 1.07, proportion of variability explained = 0.13) was negatively associated with the x-coordinate position (-0.727).

3.4.2 Relationships between retinal specialization types and retinal traits

Detailed results of all statistical models are presented in Appendix 5 (terrestrial and aquatic species pooled together, terrestrial species only, and aquatic species only). In this section, we present the models that yielded significant results ($P < 0.05$).

Pooling terrestrial and aquatic species together, we found statistically significant differences among retinal specializations in three retinal traits, accounting for phylogenetic effects and body mass (Appendix 5). Peak RGC density varied among

retinal specializations ($F_{4, 76} = 3.56$, $P = 0.013$). As predicted, species with foveae (26,103 ± 5,846 cells/mm^2) displayed significantly higher peak RGC densities compared to those with *areae* (11,840 ± 9,473 cells/mm^2) or visual streaks (8,574 ± 3,881 cells/mm^2). Lowest RGC density also varied significantly among retinal specializations ($F_{4, 76} = 3.57$, $P = 0.010$). Contrary to our expectation, species with visual streaks (1,840 ± 587 cells/mm^2) exhibited the lowest RGC densities compared to species with foveae (3,335 ± 792 cells/mm^2) or *areae* (3,211 ± 1,001 cells/mm^2). We also found a significant variation among retinal specializations when considering the difference in cell density between the retinal specialization and the retinal periphery ($F_{4, 76} = 2.66$, $P = 0.039$), with species with foveae (22,649 ± 5,774 cells/mm^2) having significantly higher values compared to species with *areae* (9,868 ± 9,357 cells/mm^2) or visual streaks (7,575 ± 3,240 cells/mm^2). The other individual retinal traits did not significantly vary among the three retinal specializations (Appendix 5). Finally, although we found a significant result in the overall model using PC1 as the dependent variable ($P = 0.04$, with one outlier removed; Appendix 5), there were no significant differences in the pair-wise comparisons between retinal specializations, with only the difference between fovea and *area* approaching statistical significance ($P = 0.08$).

Our analyses yielded other significant relationships when we examined terrestrial and aquatic species separately. For terrestrial species only, we found a significant difference in the lowest RGC density among retinal specializations ($F_{4, 48} = 17.55$, $P < 0.001$, with one outlier removed), with species with foveae having significantly higher values compared to species with *areae* or visual streaks (Fig. 4a, Appendix 5). We found similar significant differences among retinal specializations to those described above regarding the peak RGC density ($F_{4, 49} = 5.82$, $P < 0.001$, Fig. 4b, Appendix 5) and the difference in cell density from the retinal periphery to the retinal specialization ($F_{4, 49} = 18.04$, $P < 0.001$, Fig. 4c, Appendix 5), with terrestrial species with foveae having significantly higher values than those with *areae* or visual streaks. We also detected significant differences among retinal specializations in cell density gradients in the temporal ($F_{4, 48} = 5.94$, $P < 0.001$, with one outlier removed, Fig. 4d, Appendix 5), dorsal ($F_{4, 48} = 3.50$, $P = 0.013$, with one outlier removed, Fig. 4e, Appendix 5), and ventral ($F_{4,}$

$_{48}$ = 2.68, P = 0.043, with one outlier removed, Fig. 4f, Appendix 5) directions. Terrestrial species with foveae showed a steeper temporal gradient in RGC density than species with *areae* or visual streaks (Appendix 5), but this trend was non-significant for the dorsal and ventral gradients (Appendix 5). Similarly, we found a statistically significant difference in the position of the retinal specializations along the y-coordinate ($F_{4, 48}$ = 2.82, P = 0.035, with one outlier removed, Fig. 4g, Appendix 5). Terrestrial species with foveae exhibited higher values (i.e., center of retinal specialization more dorsally placed) than species with *areae* or visual streaks (Fig. 4g), although this difference was marginally non-significant (Appendix 5). Finally, we found a significant difference among retinal specializations in the PC1 for terrestrial species ($F_{4, 49}$ = 6.59, P < 0.001, Fig. 4h, Appendix 5), with species with foveae having higher values than species with *areae* or visual streaks (Appendix 5). Therefore, terrestrial species with foveae have higher peak RGC densities, and steeper nasal, temporal, dorsal and ventral RGC density gradients than non-foveate species.

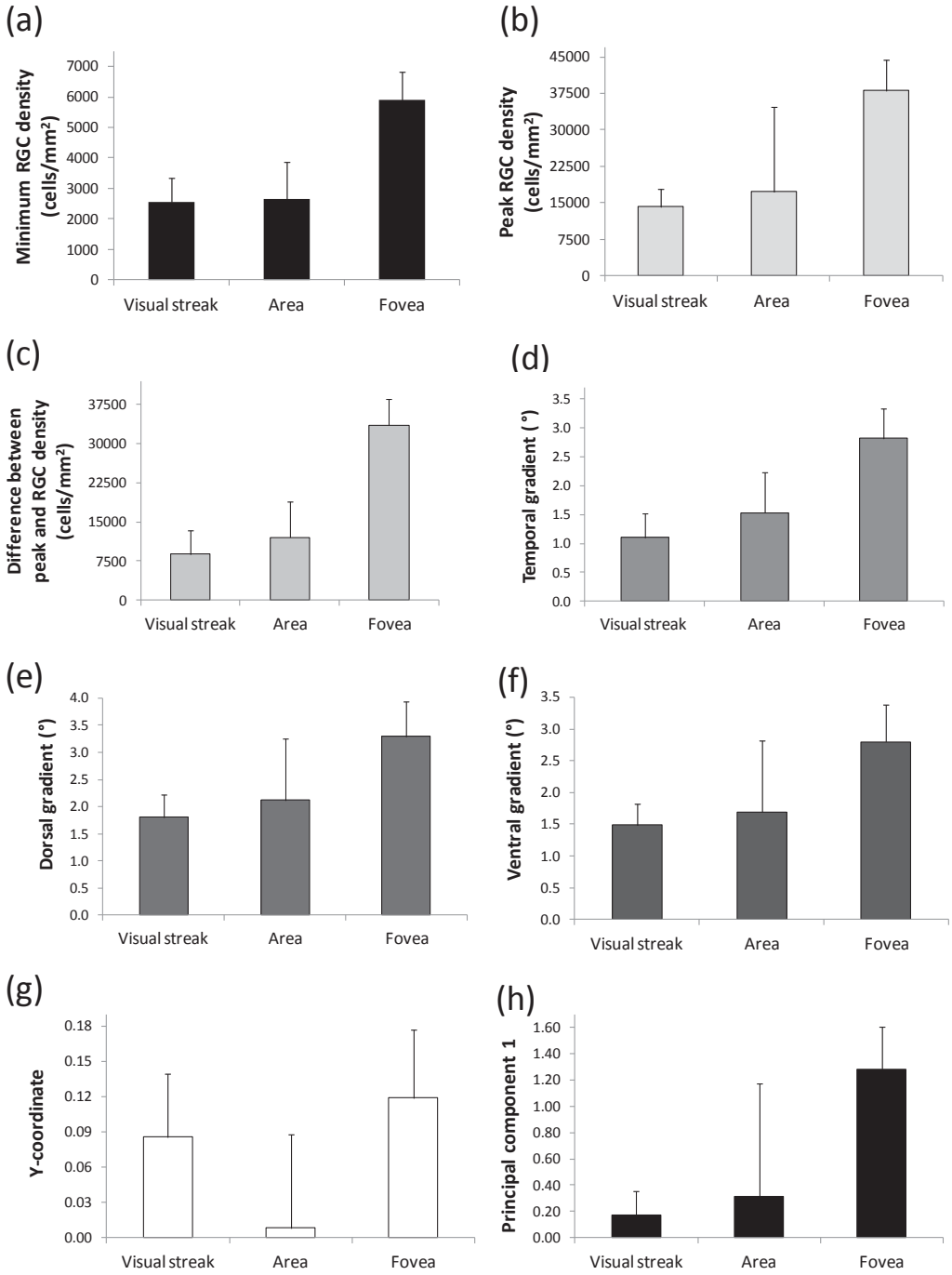

Fig 3.4 Variations in (a) minimum retinal ganglion cell (RGC) density, (b) peak RGC density, (c) difference between lowest and peak RGC density, (d) temporal cell density gradient, (e) dorsal cell density gradient, (f) ventral cell density gradient, (g) y-coordinate of the retinal specialization, and (h) principal component 1 (positively associated with peak RGC density, and nasal, temporal, dorsal, and ventral slopes) for vertebrate species. See text for details.

For aquatic species, we found only one statistically significant difference in retinal traits among retinal specializations (Appendix 5). We found that the x-coordinate position of the retinal specialization varied significantly among retinal specializations ($F_{4, 23} = 3.17$, $P = 0.033$). Aquatic species with visual streaks (0.45 ± 0.20) had significantly higher x-coordinate values (i.e., center of visual streak was more temporally located) than species with foveae (-0.42 ± 0.27) or *areae* (0.04 ± 0.28) (Appendix 5). The other retinal traits did not differ significantly among retinal specializations in aquatic species (Appendix 5).

3.5 Discussion

Studies on the spatial variation in the density of retinal ganglion cells provide important insights about how different species sample their visual fields in different visual environments (e.g., open vs. closed habitats; Collin 1999; Collin 2008). Our results reveal some general principles in the configuration of the vertebrate retina controlling for phylogenetic relatedness and body mass. We established associations between retinal traits indicating convergent evolution of acute vision in terrestrial and aquatic vertebrates. Species with higher peak ganglion cell density within the retinal specialization show a steeper gradient in cell density change between the retinal periphery and the retinal specialization in all retinal directions (nasal, temporal, dorsal, ventral) compared with species with lower peak cell densities. Additionally, terrestrial and aquatic species with higher peak ganglion cell density within the retinal specialization tend to have their retinal specialization more dorsally placed (i.e., mediating higher spatial resolving power more ventrally), which is the result of a steeper dorsal cell density gradient and a shallower ventral cell density gradient.

These shared retinal topography traits were associated with the type of retinal specialization. In general, both terrestrial and aquatic vertebrates with foveae had higher peak retinal ganglion cell densities, and thus higher localized spatial resolving power, than species with *areae* or visual streaks. Ours is the first comparative test showing

significant differences in ganglion cell density between retinal specializations across vertebrates, which supports a long standing, but untested until now, hypothesis in visual ecology (Hughes 1977; Meyer 1977; Walls 1942). Besides the effects of higher ganglion cell densities, spatial visual resolution in species with foveae is enhanced through various optical effects (Walls 1942; Pumphrey 1948; Snyder & Miller 1977, 1978; Harkness & Bennet-Clark 1978; Steenstrup & Munk 1980) resulting from the invagination of the retinal tissue.

Higher peak ganglion cell densities in the fovea occurred through steeper gradients in cell density from the retinal periphery to the retinal specialization. This led to a more pronounced difference in cell density between the retinal specialization and the retinal periphery in species with foveae than in species with *areae* or visual streaks. The implication is that foveate species would rely more on their retinal specialization for acute vision because the gradient in spatial resolution across the retina is greater and the quality of sensory information is higher at the center of the specialization compared to non-foveate species. However, the use of acute vision may be different in species with *areae* or visual streaks because (1) there is a lower difference in spatial resolving power between the retinal specialization and the retinal periphery, and (2) these specializations occupy a proportionally greater area of the retina than the fovea (Walls 1937). This could lead to differences in the neural mechanisms involved in overt vs. covert visual attention (Bisley 2011) in species with different retinal specializations, and consequently variations in their visual behavior. For instance, Canada geese (*Branta Canadensis*), which have a visual streak, have a more gradual change in cell density from the periphery to the retinal specialization (Fernández-Juricic 2011a) than California towhees (*Melozone crissalis*) and whiter-crowned sparrows (*Zonotrichia leucophrys*), which have a fovea (Fernández-Juricic 2011b). Compared to the Canada goose, towhees and sparrows move their heads at a faster rate when monitoring visually the environment (Fernández-Juricic 2011b; Fernández-Juricic 2011a), which may compensate for the smaller proportion of the visual field with high visual resolution, to enhance their ability to detect stimuli (e.g., predators) promptly.

We expected higher differences in cell density between the retinal periphery and the specialization in foveate compared to non-foveate species assuming similar overall ganglion cell densities across types of retinal specialization. However, we found a different pattern by which species with foveae have higher ganglion cell densities in the retinal periphery than species with *areae* or visual streaks. This suggests that the overall ganglion cell density (considering both the periphery and the specialization) is higher in foveate- than in non-foveate vertebrates. Thus, we predict that the number of axonal pathways for the visual inputs would be more abundant, in addition to the size of visual processing areas in the brain (i.e., retinal magnification factor) being larger, in foveate species. Although the visual projections of some vertebrates have been mapped (Schwassmann 1968; Inzunza & Bravo 1993; Leventhal et al. 1993; Letelier et al. 2004), this prediction has yet to be tested comparatively. Nevertheless, there is evidence that the representation of the fovea in the brain is enhanced (Azzopardi & Cowey 1996), and that humans who lack a fovea have a smaller region of the visual cortex dedicated to processing fine detail (Neveu et al. 2008).

The retinal configuration patterns we found appear to be mostly driven by terrestrial species, as they were mostly absent in aquatic species. This may be due to modest sample sizes of our aquatic species pool, intrinsic differences in the properties of light transmission between terrestrial and aquatic environments (Lythgoe 1979), or the retinal growth properties in aquatic species (Easter 1992). In aquatic vertebrates, however, we found a general pattern by which the center of the visual streak (which has higher visual resolution) was more temporally located (i.e., projecting towards the frontal portions of the visual field) than the center of the foveae and *areae*. This could be associated with foraging behavior. For example, the visual streak of the lateral-eyed painted flutemouth *Aulostoma chinensis* has a high density of ganglion cells in the temporal part of the retina to enhance binocular fixation of prey objects (Collin & Pettigrew 1988).

Our analytical framework uncovered some examples of convergent evolution in the configuration of the vertebrate retina, showing that, irrespective of taxa, foveae, *areae*, and visual streaks have distinct retinal configurations. Retinal specializations have

been known to have a specialized local morphology (e.g., pitted invagination of the retinal tissue); however, our results suggest that the whole retina is configured differently in terms of ganglion cell density profiles to hold each of these specializations. One of the implications is that both the degree and proportion of the visual field with localized high spatial resolving power would vary in species with different specializations. This could lead to inter-specific variations in the degree of movement of the sensory system (through eye and/or head movements) during visual search and visual fixation. Future studies should address the evolutionary transitions leading to this degree of specialization for increasing acute vision and explore the implications of these different retinal configurations for visually guided behaviors across taxa.

3.7 Literature Cited

Azzopardi P & Cowey A (1996). The overrepresentation of the fovea and adjacent retina in the striate cortex and dorsal lateral geniculate nucleus of the macaque monkey. *Neuroscience* 72:627-639.

Bisley JW (2011). The neural basis of visual attention. *Journal of Physiology* 589:49-57.

Collin SP & Collin HB (1999). The foveal photoreceptor mosaic in the pipefish, *Corythoichthyes paxtoni* (Syngnathidae, Teleostei). *Histology and Histopathol*ogy 14:369-382.

Collin SP & Shand J (2003). Retinal sampling and the visual field in fishes. In: *Sensory Processing in Aquatic Environment* (ed. by S. P. Collin & N. J. Marshall), pp. 139-169. Springer-Verlag, New York.

Collin SP & Pettigrew JD (1988). Retinal topography in reef teleosts. II: some species with prominent horizontal streaks and high-density areae. *Brain Behavior and Evolution* 31:283-295.

Collin SP (1999). Behavioural ecology and retinal cell topography. In *Adaptive Mechanisms in the Ecology of Vision* (ed. S. Archer, M.B. Djamgoz, E. Loew, J.C. Partridge, S. Vallerga), pp 509-535. Kluwer Academic Publishers, Dordrecht.

Collin SP (2008). A web-based archive for topographic maps of retinal cell distribution in vertebrates. *Australian Journal of Optometry* 91:85-95.

Curcio CA, Kimberly AA, Sloan KR, Lerea CL, Hurley JB, Klkock IB, Milam AH (1991). Distribution and morphology of human cone photoreceptors stained with anti-blue opsin. *Journal of Comparative Neurology* 312:610-624.

Dawkins MS & Woodington A (2000). Pattern recognition and active vision in chickens. *Nature* 403:652-655.

Dawkins MS (2002). What are birds looking at? Head movements and eye use in chickens. *Animal Behaviour* 63:991-998.

Dunning Jr. JB (2008). *CRC Handbook of Avian Body Masses*. Second Edition. CRC Press, Taylor & Francis Group.

Easter SS (1992). Retinal growth in foveated teleosts: nasotemporal asymmetry keeps the fovea in temporal retina. *Journal of Neuroscience* 12:2381-2392.

Endler JA (1993). The color of light in forests and its implications. *Ecological Monographs* 63:1-27.

Felsenstein J (1985). Phylogenies and the comparative method. *American Naturalist* 125:1-15

Fernández-Juricic E (2012). Sensory basis of vigilance behavior in birds: synthesis and future prospects. *Behavioral Processes* 89:143-152.

Fernández-Juricic E, Gall MD, Dolan T, O'Rourke C, Thomas S, Lynch JR (2011b). Visual systems and vigilance behaviour of two ground-foraging avian prey species: white-crowned sparrows and California towhees. *Animal Behaviour* 81:705-713

Fernández-Juricic E, Moore BA, Doppler M, Freeman J, Blackwell BF, Lima SL, DeVault TL (2011a). Testing the terrain hypothesis: Canada geese see their world laterally and obliquely. *Brain Behavior and Evolution* 77:147-158.

Fishbase, www.fishbase.org, downloaded 19 October 2011

Gaffney MF & Hodos W (2003). The visual acuity and refractive state of the American Kestrel (*Falco sparverius*). *Vision Research* 43:2053-2059.

Harkness L & Bennet-Clark HC (1978). The deep fovea as a focus indictor. *Nature* 272:814-816.

Hughes A (1977). The topography of vision in mammals of contrasting life style: comparative optics and retinal organization. In *The visual system in vertebrates* (ed. F. Crescitelli), pp 615-756. New York: Springer-Verlag.

Inzunza O & Bravo H (1993). Foveal topography in the optic-nerve and primary visual centers in Falconiforms. *Anatomical Record* 235:622-631.

Inzunza O, Bravo H, Smith RL (1989). Foveal regions of bird retinas correlate with the aster of the inner nuclear layer. *Anatomical Record* 223:342-346.

Johnson GL (1901). Contributions to the comparative anatomy of the mammalian eye chiefly based on ophthalmoscopic examination. *Philosophical Transactions of the Royal Society B* 194:1-82.

Jones MP, Pierce Jr KE, Ward D (2007). Avian vision: A review of form and function with special consideration to birds of prey. *Journal of Exotic Pet Medicine* 16:69-87.

Kahmann H (1935). Ueber das foveale Sehen der Wirbeltiere. II. Gesichtsfeld und Fovea centralis. *Sitzungsber Gesellschaft naturforschender Freunde* 361-376.

Kiltie RA (2000). Scaling of visual acuity with body size in mammals and birds. *Functional Ecology* 14:226–234.

Lemeignan M, Sansonetti A, Gioanni H (1992). Spontaneous saccades under different visual conditions in the pigeon. *NeuroReport* 3:17-20.

Letelier JC, Marı´n G, Sentis E, Tenreiro A, Fredes F, Mpodozis J (2004). The mapping of the visual field onto the dorso-lateral tectum of the pigeon (*Columba livia*) and its relations with retinal specializations. *Journal of Neuroscience Methods* 132:161–168.

Leventhal AG, Thompson KG, Liu D (1993). Retinal ganglion-cells within the foveola of new-world (*Saimiri sciureus*) and old-world (*Macaca fascicularis*) monkeys. *Journal of Comparative Neurology* 338:242-254.

Lockie JD (1952) A comparison of some aspects of the retinae of the manx shearwater, fulmar petrel and house sparrow. *The Quarterly Journal of Microscopical Science* 93:347-356.

Lythgoe JN (1979). *The Ecology of Vision*. Clarendon Press, Oxford.

Mass AM & Supin AY (2007). Adaptive features of aquatic mammals' eye. *Anatomical Record* 290:701-715.

McIlwain JT (1996). An introduction to the biology of vision. Cambridge University Press, New York.

Meyer DBC (1977). The avian eye and its adaptations. In *The visual system of vertebrates; handbook of sensory physiology* (ed. F. Crescitelli), pp 549-612. Springer, New York, vol VII/5.

Moinard C, Rutherford KMD, Statham P, Green PR (2005). Visual fixation of a landing perch by chickens. *Experimental Brian Research* 162:165-171.

Moore BA, Kamilar JM, Collin SP, Bininda-Emonds ORP, Dominy NJ, Hall MI, Heesy CP, Johnsen S, Lisney TJ, Loew ER, Moritz G, Nava SS, Warrant E, Yopak KE, Fernández-Juricic E (2012). A novel method for comparative analysis of retinal specialization traits from topographic maps. *Journal of Vision* 12:1-24.

Nakagawa S (2004). A farewell to Bonferroni: the problems of low statistical power and publication bias. *Behavioral Ecology* 15:1044-1045.

Neveu MM, Hagen EVD, Morland AB, Jeffery G (2008). The fovea regulates symmetrical development of the visual cortex. *Journal of Comparative Neurology* 506:791-800.

Nunn C (2011). *The Comparative Approach in Evolutionary Anthropology and Biology*. University of Chicago Press, Chicago.

Orme CDL, Freckleton RP, Thomas GH, Petzoldt T, Fritz SA (2011). caper: *Comparative Analyses of Phylogenetics and Evolution in R* (http://R-Forge.R-project.org/projects/caper/).

Pagel M (1999). Inferring the historical patterns of biological evolution. *Nature* 401:877–884.

Pettigrew JD, Dreher B, Hopkins CS, McCall MJ, Brown M (1988). Peak Density and Distribution of Ganglion Cells in the Retinae of Microchiropteran Bats: Implications for Visual Acuity. *Brain Behavior and Evolution* 32:39-56.

Pumphrey RJ (1948). The theory of the fovea. *Journal of Experimental Biology* 25:299-312.

Quinn G & Keough M (2002). *Experimental design and data analysis for biologists*. Cambridge: Cambridge University Press.

R Development Core Team (2010). R: *A Language and Environment for Statistical Computing*. Vienna, Austria, ISBN 3-900051-07-0, http://www.Rproject.org/.

Ross CF (2004). The tarsier fovea: functionless vestige or nocturnal adaptation? In: *Anthropoid Origins: New Visions* (ed. C.F. Ross & R.F. Kay), pp. 477-537. New York: Kluwer Academic/ Plenum Publishers.

Schwassmann HO (1968). Visual projection upon the optic tectum in foveate marine teleosts. *Vision Research* 8:1337-48.

Slonaker JR (1897). A comparative study of the area of acute vision in vertebrates. *Journal of Morphology* 13:445-494.

Snyder AW & Miller WH (1977). Photoreceptor diameter and spacing for highest resolving power. *Journal of the Optical Society of America* 67:696-698.

Snyder AW & Miller WH (1978). Telephoto lens system of falconiform eyes. *Nature* (London) 275:127-129.

StatSoft, Inc. (2011). Electronic Statistics Textbook. Tulsa, OK: StatSoft. WEB: http://www.statsoft.com/textbook/.

Steenstrup S & Munk O (1980). Optical function of the convexiclivate fovea with particular regard to notosudid deep-sea teleosts. *Optica Acta* 27:949-964.

Temple S, Hart NS, Marshall NJ, Collin SP (2010). A spitting image: specializations in archerfish eyes for vision at the interface between air and water. *Proceedings of the Royal Society B* 277:2607-2615.

Vincent SB (1912). The mammalian eye. *Journal of Animimal Behavior* 2:249-255.

Wallman J & Pettigrew JD (1985). Conjugate and disjunctive saccades in two avian species with contrasting oculomotor strategies. *Journal of Neuroscienc* 5:1418-1428.

Wallman J, Pettigrew JD, Letelier J-C (1994). The oscillatory saccades of birds: motorneuronal activity and possible functions. In *Contemporary ocular motor and vestibular research: a tribute to David A. Robinson* (ed. A.F. Fuchs, T. Brandt, V. Buttner, D. Zee), pp 480-487. Thieme Publishing, Stuttgart.

Walls GL (1937) Significance of the foveal depression. *Archives of Ophthalmology* (Chicago) 18:912-919.

Walls GL (1942). *The Vertebrate Eye and Its Adaptive Radiation*. Cranbrook Institute of Science, Michigan.

Youtheria, www.utheria.co.uk, accessed September 1, 2012

CHAPTER 4: INTERSPECIFIC DIFFERENCES IN THE VISUAL SYSTEM AND SCANNING BEHAVIOR IN THREE FOREST PASSERINES THAT FORM HETEROSPECIFIC FLOCKS

This chapter has already been published as:

Moore BA, Doppler M, Young JE, Fernandez-Juricic E (2013). Interspecific differences in the visual system and scanning behavior of three forest passerines that form heterospecific flocks. *Journal of Comparative Physiology A* 199:263-277.

4.1 Abstract

Little is known as to how visual systems and visual behaviors vary within guilds in which species share the same micro-habitat types but use different foraging tactics. We studied different dimensions of the visual system and scanning behavior of Carolina chickadees, tufted titmice, and white-breasted nuthatches, which are tree foragers that form heterospecific flocks during the winter. All species had centro-temporally located foveae that project into the frontal part of the lateral visual field. Visual acuity was the highest in nuthatches, intermediate in titmice, and the lowest in chickadees. Chickadees and titmice had relatively wide binocular fields with a high degree of eye movement right above their short bills probably to converge their eyes while searching for food. Nuthatches had narrower binocular fields with a high degree of eye movement below their bills probably to orient the fovea toward the trunk while searching for food. Chickadees and titmice had higher scanning (e.g., head movement) rates than nuthatches probably due to their wider blind areas that limit visual coverage. The visual systems of these three species seem tuned to the visual challenges posed by the different foraging and scanning strategies that facilitate the partitioning of resources within this guild.

4.2 Introduction

Birds are visually oriented animals (Schwab 2012) whose visual systems vary substantially between species in terms of the types of retinal specialization (e.g., fovea, visual streak, area; Meyer 1977; Collin 1999), the density of photoreceptors (Hart 2001), visual acuity (Kiltie 2000), the configuration of the visual fields (Martin 2007), etc. Variations in visual system configuration can also affect visual behaviors, such as scanning (Fernández-Juricic 2012). For instance, species with wider blind areas allocate more time to anti-predator vigilance to compensate for the lack of visual coverage (Guillemain et al. 2002).

This high degree of interspecific variability in the visual system has been linked to, among others, predation (Guillemain et al. 2002), foraging (Fernández-Juricic et al. 2011a), ability to feed the young (Martin 2009), and habitat type (Hart 2001). For instance, species living in closed habitats (e.g., tree foragers) have a higher density of photoreceptors associated with motion detection in areas of the retina pointing towards the ground, whereas species living in open habitats (e.g., ground foragers) have a higher density of these photoreceptors pointing towards the sky, reflecting the positions from which predators are more likely to attack (Hart 2001). Møller and Erritzøe (2010) presented evidence that birds living in open habitats have larger eyes, and thus higher overall visual acuity that might enhance the detection of predators from farther away, compared to species living in more complex habitats. Additionally, raptors living in open and closed habitats differ in the configuration of their visual fields, degree of eye movement, and scanning behavior in ways that would enhance their ability to detect prey in habitats with different degrees of visual obstruction (O'Rourke et al. 2010a, b).

However, how both the visual system and scanning behavior vary within guilds (i.e., groups of species that exploit similar resources following similar strategies; Simberloff & Dayan 1991) in which species share the same micro-habitat types but use different foraging tactics has received less attention (but see Martin & Prince 2001). Characterizing these interspecific differences may enhance our understanding of not only sensory adaptations to gather information about food and predators but also the potential

role of the sensory system in partitioning resources within guilds (Siemers and Swift 2006). The guild of passerine tree foragers inhabiting North American temperate areas is a good model system to study the degree of interspecific variability in physiological and behavioral parameters because the foraging and anti-predator behaviors of its species have been extensively studied (reviewed in Grubb and Pravasudov 1994; Mostrom, et al. 2002; Grubb and Pravasudov 2008). Our goal was to characterize key dimensions of the visual system (visual acuity, position of the fovea, visual field configuration, degree of eye movements) and scanning behavior (head movement rates) of three members of this guild: Carolina chickadees (*Poecile carolinensis*; family Paridae; hereafter, chickadees), tufted titmice (*Baeolophus bicolor*; family Paridae; hereafter, titmice), and white-breasted nuthatches (*Sitta carolinensis*; family Sittidae; hereafter, nuthatches). These species differ in the substrates they use for foraging and for protective cover.

Chickadees primarily forage on smaller tree limbs and twigs (Mostrom, et al. 2002). Titmice have a broader range of foraging substrates, including small branches, larger limbs, trunks, and the ground (Grubb and Pravasudov 1994). Finally, nuthatches forage on tree trunks and larger branches, and sometimes on the ground (Grubb and Pravasudov 2008). Because of these different foraging substrates, it can be proposed that chickadees and titmice have the visibility in their visual fields comparatively less obstructed by vegetation (e.g., tree canopy) than nuthatches (e.g., tree trunks), which can influence the probabilities of predator detection (e.g., Lima 1992). If a predator attacks, chickadees and titmice generally escape by flying towards another tree; whereas nuthatches generally escape by moving towards the opposite side of the tree trunk they were using for foraging (Lima 1993). Additionally, these three species vary in the orientation of their bodies and heads (in relation to the substrate) while foraging. Titmice and chickadees generally scan and search for food when their bodies and heads are at a steeper angle (i.e., closer to an upright position) in relation to the substrate (Grubb and Pravasudov 1994; Mostrom, et al. 2002). Nuthatches tend to scan and search for food with their bodies and heads at a shallower angle (i.e., closer to a prone position) in relation to the substrate (Grubb and Pravasudov 2008). Additionally, these three species associate during the non-breeding season to form heterospecific flocks, where chickadees

and titmice are considered nuclear species (i.e., initiate flock movements and alarm-call upon detection of predators) and nuthatches are considered satellite species (i.e., eavesdrop on social information about predators; Sullivan 1984a, b; Dolby and Grubb 1998; Dolby and Grubb 2000; Templeton and Greene 2007).

Based on the differences in their foraging and antipredator behaviors, we made predictions about inter-specific differences in their visual systems based on hypotheses on visual acuity (Kiltie 2000), position of the fovea in the retina (Collin 1999), configuration of the visual field based on the position of the orbits (Heesy 2004), and degree of movement of the fovea through eye and head movements (Fernández-Juricic 2012). First, we predicted that visual acuity would be higher in titmice and nuthatches than in chickadees because they are bigger, and body mass (and eye size) is positively related to visual acuity (Kiltie 2000). Second, based on the preferred orientation of the bill when searching for food (Grubb and Pravasudov 1994, 2008; Mostrom et al. 2002), we predicted that the fovea of titmice and chickadees would be placed centro-temporally on the retina to enable high visual resolution in the region of the binocular field directly in front of the bill, as has been found in other Passeriformes (Blackwell et al. 2009; Dolan & Fernández-Juricic 2010; Fernández-Juricic et al. 2011a). Conversely, we predicted that nuthatches would have dorso-temporal fovea projecting ventro-nasally, hence providing high resolution below the bill and towards the tree trunks as the bill is usually held at a shallow angle in relation to the foraging substrate. Third, titmouse and chickadee have slightly more frontally placed eyes (Appendix 1) than nuthatches; thus, we predicted that these two species would have wider binocular fields (see also Iwaniuk et al. 2008). Fourth, as a result of the differences in the position of the eyes in the skull (Appendix 1), we predicted that titmice and chickadees would have wider blind areas behind their heads than nuthatches. Wider blind areas would limit visual coverage in titmice and chickadees (Guillemain et al. 2002), which could increase their degree of eye movements and their rate of head movements (Fernández-Juricic et al. 2010) to scan different parts of the environment with the fovea (Fernández-Juricic 2012), depending on the visual task (i.e., converging eyes to find food, diverging eyes to detect predators, etc.).

4.3 Methods

We determined between-species differences in eye size and retinal ganglion cell density (both parameters involved in visual acuity, Pettigrew et al. 1988), position of the fovea (area with the highest visual resolution in the retina), visual field configuration (e.g., sizes of the binocular field, lateral field, and blind area), degree of eye movement, and scanning behavior (e.g., using head movement rates as proxies, Fernández-Juricic 2012).

Carolina chickadees, tufted titmice, and white-breasted nuthatches used in this study were captured in several locations in Tippecanoe County, Indiana, USA. Birds were housed indoors in cages (0.9 m x 0.7 m x 0.6 m) with 1-4 individuals per cage, and were kept on a 14:10 hour light:dark cycle at approximately 23°C with food (sunflower seeds) and water *ad libitum*, supplemented with mealworms daily. Nine chickadees, 7 titmice, and 9 nuthatches were used for visual field and degree of eye movement measurements, of which 5 individuals of each species were used for retina extraction to measure eye size, retinal ganglion cell density, and to estimate the position of the fovea. Additionally, scanning behavior (e.g., head movement rates) was measured on 11 chickadees, 17 titmice, and 14 nuthatches.

4.3.1 Eye size, ganglion cell density, and fovea position

After animals were euthanized using CO2,we removed the eyes by cutting the conjunctiva and pulling the eye out by the optic nerve with forceps. We then measured three eye size parameters with digital calipers (Neiko Tools USA, 01407A; 0.01 mm accuracy): (1) eye axial length (anterior portion of the cornea to the most posterior portion of the back of the eye), (2) corneal diameter (inner diameter of the sclerotic ossicles), and (3) eye transverse diameter (outer diameter of the eyeball from side to side). The orientation of the retina (nasal, temporal, dorsal, ventral) was maintained by tracking the position of the pecten (i.e., a pigmented and vascular structure in the avian retina; Meyer 1977) in relation to the direction of the bill (Fernández-Juricic et al. 2011c). We hemisected the eye at the ora serrata using a razor blade and removed all vitreous humor and lens fragments using forceps and spring scissors. The retina was extracted

following the wholemount technique, which is described in Ullmann et al. (2012). We used cresyl violet to stain for retinal ganglion cells, which have axons that carry the visual information from the retina to the brain through the optic nerve (McIlwain 1996). The area of the retina with the highest density of retinal ganglion cells is the fovea, and corresponds with the highest degree of visual resolution (Walls 1942; Meyer 1977).

Pictures of the retina (0.01 mm^2) were taken with a Panasonic Lumix FZ28 digital camera before and after staining to correct for tissue shrinkage. We used ImageJ (http://rsb.info.nih.gov/ij/) to measure the area of the retina before and after staining. We calculated the amount of shrinkage per picture by multiplying the area of the picture by the difference in the retinal area before and after staining (i.e., amount of shrinkage). Therefore, the correction factor for tissue shrinkage was: 0.01 + (0.01 * amount of shrinkage).

An Olympus BX51 microscope at 100x power was used to examine the retinal ganglion cell layer. Stereo Investigator (ver. 9.13; MBF Bioscience) was used to trace the perimeter of the retina with the SRS Image Series Acquire module, which uses a fractionator approach by which the program randomly and systematically places a grid onto the traced retina. We used a mean of 410 ± 2.09 grid sites per chickadee retina, 408 ± 3.76 grid sites per titmouse retina, and 407 ± 2.70 grid sites per nuthatch retina, although we could not measure cell density from all of them (see Results). A 50x50 µm counting frame was placed in the upper left hand corner of each grid site to avoid double counting, and the following parameters were estimated before counting: asf (area sampling fraction: the ratio of the area of the counting frame to the area of the grid) = 0.01751 ± 0.00054 per chickadee retina, 0.01139 ± 0.00056 per titmouse retina, and 0.01204 ± 0.00033 per nuthatch retina; tsf (thickness sampling factor: ratio of the height of the dissector to the mean measured tissue thickness) = 1 per retina, and $\sum Q^-$ (sum of the total number of retinal ganglion cells) = 14,512 ± 1,093 per chickadee retina, 14,933 ± 1,160 per titmouse retina, and 18,018 ± 1021 per nuthatch retina. On a given counting frame, we focused on the plane that would provide the highest resolution and contrast to identify the ganglion cells and obtained a photograph with an Olympus S97809 microscope camera. We captured the images using SnagIt (www.techsmith.com/Snagit),

and counted the retinal ganglion cells in each of the counting frame images with ImageJ to estimate cell density. Cell density (number of retinal ganglion cells/mm^2) was calculated by dividing the number of cells in each picture by the tissue area corrected for shrinkage of each picture.

Retinal ganglion cells were differentiated from amacrine and glial cells based on cell shape, relatively large soma size, Nissl accumulation in the cytoplasm, and staining of the nucleus (Hughes 1977; Freeman and Tancred 1978; Ehrlich 1981; Stone 1981). The soma size of ganglion cells is small and contains a darkly staining nucleus in retinal regions with higher cell density, but it shows a prominent nucleus and heterogeneous distribution of Nissl granules in perifoveal and peripheral regions of the retina. Glial cells are generally oblong, narrow and very elongated with deep Nissl accumulation, whereas amacrine cells are usually small teardrop-shaped cells with deep Nissl accumulation.

Based on the variations in the density of retinal ganglion cells across the retina, we followed Stone (1981) and Ullmann et al. (2012) in building retinal topographic maps. We plotted ganglion cell density values obtained from each counting frame onto a map of the sampling grids produced by Stereo Investigator using OpenOffice Draw (www.openoffice.org). Within a given cell density range, we created isodensity lines by hand interpolating one or more adjacent density values (Moroney and Pettigrew 1987; Wathey and Pettigrew 1989).

Visual acuity was estimated based on the averaged eye size and retinal ganglion cell density of each species, assuming that all species have similar eye shapes and eye optical properties, which is expected due to their diurnal habits (Martin 1993). Visual acuity calculations followed the sampling theorem (Hughes 1977). Eye axial length was multiplied by 0.60 (based on Hughes 1977; Martin 1993) to estimate the posterior nodal distance (PND; length between the posterior part of the eye and the anterior surface of the retina, Reymond 1985). We then obtained the retinal magnification factor (RMF), which is the linear distance on the retina that subtends 1° (Pettigrew et al. 1988), as follows: RMF = 2πPND/360. We estimated visual acuity as the highest spatial frequency that can be detected (F_n): $= \frac{RMF}{2}\sqrt{\frac{2D}{\sqrt{3}}}$; where D is the averaged retinal ganglion cell density (Williams and Coletta 1987). F_n is expressed in cycles per degree.

4.3.2 Visual field configuration and degree of eye movement

A visual field apparatus developed by Martin (1984) was used to measure the configuration of the visual field of chickadees, titmice, and nuthatches. Individuals were restrained by foam molds and straps within the apparatus with the bill placed in a fitted bill holder (preventing the head from moving) such that the head was positioned at the center of a global space in three dimensions. Each species' head was held at the angle at which it is most frequently found based on pictures and videos taken in the wild. For the chickadee and titmouse, the head was positioned such that the dorsal portion of the lower mandible was parallel to the ground, and for the nuthatch, the dorsal portion of the lower mandible was inflected in a direction 10° above parallel to the ground. The configuration of the visual field was measured using a polar coordinate system, in which the 0° elevation lay directly above the head of each species, 90° in front, and 270° behind (see Results). Thus, the 90–270° plane was defined as the horizontal plane as it is parallel to the ground.

A Keeler Professional ophthalmoscope was used to measure the retinal margins using an ophthalmoscopic reflex technique around the head to an accuracy of 0.5° (Martin 1984; Martin 2007). We then mathematically corrected each value for close viewing following Martin (1984). At some elevations, the apparatus or the animal's body blocked our view of the retinal margins, limiting our measurements from 140 to 260° around the head. We took measurements on the visual fields at every 10° elevation increments within that range.

The degree of eye movements can vary substantially between species (e.g., Martin 2007; Fernández-Juricic et al. 2008; Blackwell et al. 2009), which can change the configuration of the visual field (e.g. size of binocular and blind areas) when animals converge or diverge their eyes from their eye-resting position. Therefore, the visual fields of all three species were measured when (1) the eyes were at rest, (2) the eyes were converged, and (3) the eyes were diverged. Resting measurements were taken when the animal visibly relaxed its eyes (i.e., the animal was not tracking the observer), which happened right away or after a quick series of pursuit eye movements due to apparent fatigue of the extraocular muscles. During these eye-resting measurements, we were

careful to note that the eyes did not move by tracking the eyes and taking several measurements of the retinal margins in succession, which are the ultimate indicator of variations in retinal position. With the eyes at rest, we also measured the projection of the pecten which creates a blind spot within the dorso-frontal visual space. For converge/diverge measurements, we elicited maximum levels of eye movements by presenting objects and/or sounds around the bird's head. Therefore, the animal exhibited two types of eye movement: saccadic, when we first drew the attention of the individual to the position of the objects/sounds, and pursuit, when the individual then tracked objects/sounds. Eye movement was elicited in the direction of the elevation being measured. The degree of eye movement was measured at each 10° elevation interval from 140° below the bill to 270° behind the head. All the measurements on the degree of eye movement reported in this study consider both eyes. The degree of eye movement in a particular direction (elevation) was calculated by the difference between the maximum (converged) and minimum (diverged) values. Finally, we calculated the extent of the lateral field as [360 – (mean blind field + mean binocular field)/2] (Fernández-Juricic et al. 2008). In Fig. 4, eye movement values are presented as the averaged degree of eye movement per elevation across individuals.

4.3.3 Head movements

Recent studies have proposed that head movement rates are a good proxy of scanning behavior in birds (O'Rourke et al. 2010b; Fernández-Juricic et al. 2011a, b) because they indicate the speed with which the foveae gather high quality visual information from different parts of their surroundings (Fernández-Juricic 2012). Higher head movement rates are indicative of a faster visual sampling rate (e.g. for predators or food), which could be the result of higher perceived predation risk and higher visual obstruction in the environment (Fernández-Juricic et al. 2011c). Regular head movements (head moving along a single axis where the direction of the eye-bill tip vector follows the head movement; O'Rourke et al. 2010b) were measured when the bird was in head-up (vigilance) posture from videos recorded in the field and videos obtained from the Macaulay Library Sound and Video Catalog (http://animalbehaviorarchive.org). All

videos included in the analysis came from habitats characteristic of each of the studied species, which we evaluated based on the background vegetation.

We only used videos of individuals moving throughout the foraging substrate where head movements could be accurately measured; we did not include videos of individuals flying or videos showing inter- or intra- specific interactions (e.g., aggression) or preening events. Videos at the Macaulay Library Sound and Video Catalog listed information on the month and location the video was taken, and the observer who recorded the video. This information was used to avoid including videos from the same individual. If several videos from the same individual were available, we used the longest video.

We recorded videos in Tippecanoe County (Indiana, USA) during the 2010 and 2012 non-breeding seasons (January-March). Videos were recorded with a JVC Everio GZ-MG330-HU camcorder mostly in the mornings and early afternoons. The chances of re-sampling the same individual was reduced by keeping track of the individual recorded on a given session or by moving at least 50 m in the opposite direction of the last individual recorded. After recording a given individual, we measured ambient temperature, group size, perching height, and distance between the observer and the bird as previous studies found that these variables could influence vigilance behavior (e.g., Beauchamp 2003; Gall and Fernández-Juricic 2009; Carr and Lima 2012). Temperature was measured with a Kestrel portable weather station. Perching height was estimated by visually rotating the location of the bird in the tree onto the ground, and then measuring the ground distance with a meter tape (±0.05 m; Fernández-Juricic et al. 2006). Distance between the observer and the bird was also measured with a meter tape.

Overall, sample sizes per species were: chickadee (3, video catalog; 11, recorded by authors), titmouse (10, video catalog; 10, recorded by authors), and nuthatch (6, video catalog; 8, recorded by authors). The averaged length of all videos was 68.86 ± 12.02 secs. Head movements were recorded with JWatcher (Blumstein and Daniel, 2007). We calculated the head movement rate as changes in head position per sec while the animal was head-up (i.e., the head was above the shoulder). We did not measure the amplitude or direction of the head movements, nor did we measure head bobbing as our studied

species do not engage in this behavior. Additionally, we did not record the degree of eye movements while animals were moving their heads, because we used videos obtained in the field and we lacked the technology (e.g., eye-tracker) to obtain that information. It is likely that birds were actually moving their eyes while moving their heads (e.g., Gioanni 1988). Therefore, any interpretation we make in relation to the functional properties of eye and head movements should be taken with care due to the constraints of our measurements.

4.3.4 Statistical analysis

General linear mixed models were used to compare among species the overall and peak density of retinal ganglion cells, width of the binocular field, blind area, and pecten, and the degree of eye movements. In all these models, we included individual identity as a within-subject factor. Models on density of retinal ganglion cells included species as the between-subject factor. Models on the visual field configuration and degree of eye movement included species, elevation in the visual field, and the interaction between species and elevation as the between-subject factors. In the models on visual field configuration and degree of eye movement, we only used those elevations from which we had data on a positive (binocular area) or negative (blind area) overlap between eyes. Consequently, the means (± SE) presented did not include values from those elevations in which data were not recorded. Pair-wise comparisons (t-tests) were used to determine differences between pairs of species. General linear mixed models were run in SAS 9.2 (Cary, N.C.).

General linear models were used to establish differences among species in corneal diameter, eye transverse diameter, eye axial length, and head movement rates. Additionally, we also established the effects of potential confounding factors (flock size, temperature, perching height, distance between observer) on head movement rates with the videos we recorded using a general linear model. We excluded the Macaulay Library Sound and Video Catalog videos as they did not report any of these potential confounding factors. Tukey HSD tests were used to assess differences between pairs of

species. General linear models were run in Statistica 10 (Tulsa, OK). Throughout the text we present least squares means (±SE).

4.4 Results

4.4.1 Eye size, ganglion cell density, and fovea position

We successfully processed and counted retinal ganglion cells from 5 chickadees (3 left and 2 right eyes), 5 nuthatches (3 right and 2 left eyes), and 4 titmice (2 left and 2 right eyes). With the exception of one nuthatch retina that had a tear in its center, we were also able to determine the position of the potential fovea in each of these retinas (see below).

The differences in body mass among species (Carolina chickadee, 10 g; tufted titmouse, 21.6 g; white-breasted nuthatch, 21 g; Dunning 2008) were reflected in eye size. The three parameters related to eye size varied significantly between species: corneal diameter ($F_{2,11} = 26.09$, $P < 0.001$), transverse diameter ($F_{2,11} = 102.78$, $P < 0.001$), and axial length ($F_{2,11} = 45.82$, $P < 0.001$). Corneal diameter and eye axial length were significantly smaller in chickadees (corneal diameter, 4.13 ± 0.12 mm; axial length 5.19 ± 0.11 mm) than in titmice (corneal diameter, 5.22 ± 0.13 mm; axial length, 6.60 ± 0.13 mm) and nuthatches (corneal diameter, 5.21 ± 0.12 mm; axial length, 6.41 ± 0.11 mm; Tukey tests, $P < 0.001$), without significant differences in these traits between the latter two species (Tukey tests, $P > 0.488$). Eye transverse diameter varied significantly between species in all-pair-wise comparisons (Tukey tests, $P < 0.006$), with titmice having the highest values (8.80 ± 0.10 mm), nuthatches, intermediate values (8.27 ± 0.09 mm), and chickadees, the lowest values (6.95 ± 0.09 mm).

We quantified the density of retinal ganglion cells using 372.60 ± 6.11 grid sites per retina in the chickadee, 385.75 ± 6.83 grid sites per retina in the titmouse, and 385 ± 6.83 grid sites per retina in the nuthatch. The mean overall density of retinal ganglion cells differed significantly among species ($F_{2,10} = 66.57$, $P < 0.001$). Nuthatches (18,660 ± 239 cells/mm^2) had significantly higher ganglion cell densities than chickadees (15,467 ± 218 cells/mm^2; $t_{10} = 9.87$, $P < 0.001$) and titmice (15,189 ± 240 cells/mm^2; $t_{10} = 10.25$,

$P < 0.001$), without significant differences between the latter two species ($t_{10} = 0.86$, $P = 0.410$). The peak retinal ganglion cell density (density in the peri-foveal grid sites around the fovea) also varied significant among species ($F_{2,10} = 9.04$, $P = 0.006$). Nuthatches (35,850 ± 1,201 cells/mm^2) had significantly higher peak ganglion cell densities than titmice (31,339 ± 1,241 cells/mm^2; $t_{10} = 2.61$, $P = 0.026$) and chickadees (28,969 ± 1,102 cells/mm^2; $t_{10} = 4.22$, $P = 0.002$), without significant differences between the latter two species ($t_{10} = 1.43$, $P = 0.184$). Based on the averaged peak density of retinal ganglion cells and averaged eye size values per species, we estimated that nuthatches had the highest visual acuity of the three species (6.83 cycles/degree), followed by titmice (6.57 cycles/degree), and chickadees (4.97 cycles/degree).

The retinal ganglion cell topographic maps of the three species revealed a concentric increase in retinal ganglion cell density towards the central part of the retina (Fig. 1 shows a representative map of each species). Based on morphological features on the wholemount, we determined that each of the three species had a fovea (i.e., a pitted structure with sloping walls descending concentrically from the plane of view; black dot in each topographic map in Fig. 1) located centro-temporally from the center of the retina. However, our results differ from those of Fite and Rosenfield-Wessels (1975) who reported that white-breasted nuthatches had a fovea located ventrally from the center of the retina instead of the centro-temporal position found in our study. Although we did not perform cross-sections to determine the morphology of different retinal layers, we did not find any foveal pit in the ventral part of the nuthatch retina. We also hemisected the eye of a white-breasted nuthatch while still in the skull and confirmed the centro-temporal orientation reported here.

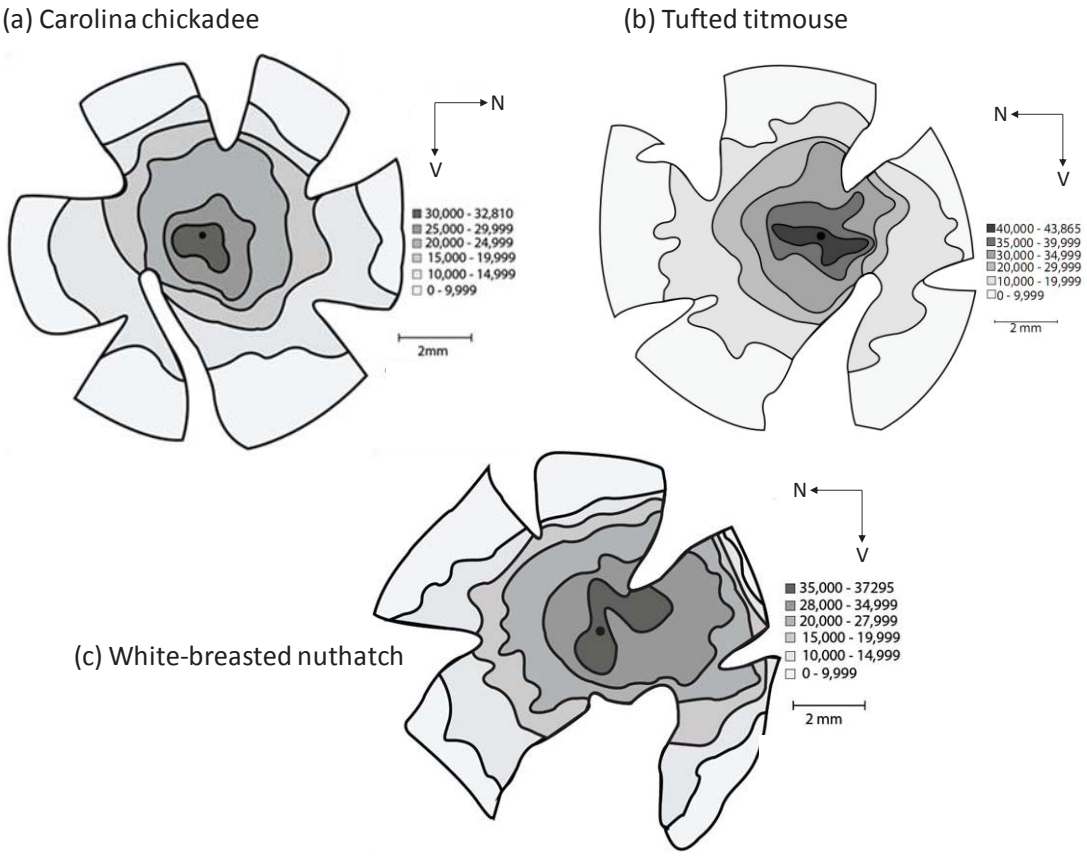

Fig 4.1 Representative examples of the retinal topographic maps of (a) Carolina chickadees, (b) tufted titmice, and (c) white-breasted nuthatches. Numbers represent ranges of retinal ganglion cell density (cell/mm^2). V, ventral; N, nasal. The presence of a potential fovea is indicated by a black dot towards the central part of the retina. These maps are based on a single individual from each species.

4.4.2 Visual fields with eyes at rest

Three-dimensional representations of the at-rest visual fields show that the three species (chickadees, titmice, nuthatches) had the projections of their bill-tips towards the binocular field (Fig. 2a-c). The bill tip of nuthatches projected towards the binocular field around the horizontal plane (90°; Fig. 2c), whereas those of chickadees and titmice projected at a slightly lower elevation (100°; Fig. 2a-b). We could not measure the total vertical extent of the binocular field as in some elevations below the bill the visual field apparatus obstructed our measurements. Consequently, our estimates of the minimum vertical extent of the binocular field were the same (130°) across species.

At elevation 90° with the eyes at rest, the width of the binocular field was similar in the titmice (53°) and chickadee (51°), but narrower in the nuthatch (37°) (Fig. 2d-f). However, in the nuthatch the bill intruded in the binocular area to the extent that it blocked our view of the retinal margins (Fig. 2f). This suggests that nuthatches could observe their bill tips (see also Martin and Coetzee 2004). Thus, the extrapolated width of the binocular field at elevation 90° with the eyes at rest was estimated as 45° for nuthatches (Fig. 2f), assuming that the retinal margin follows a circular projection (Martin and Coetzee 2004).

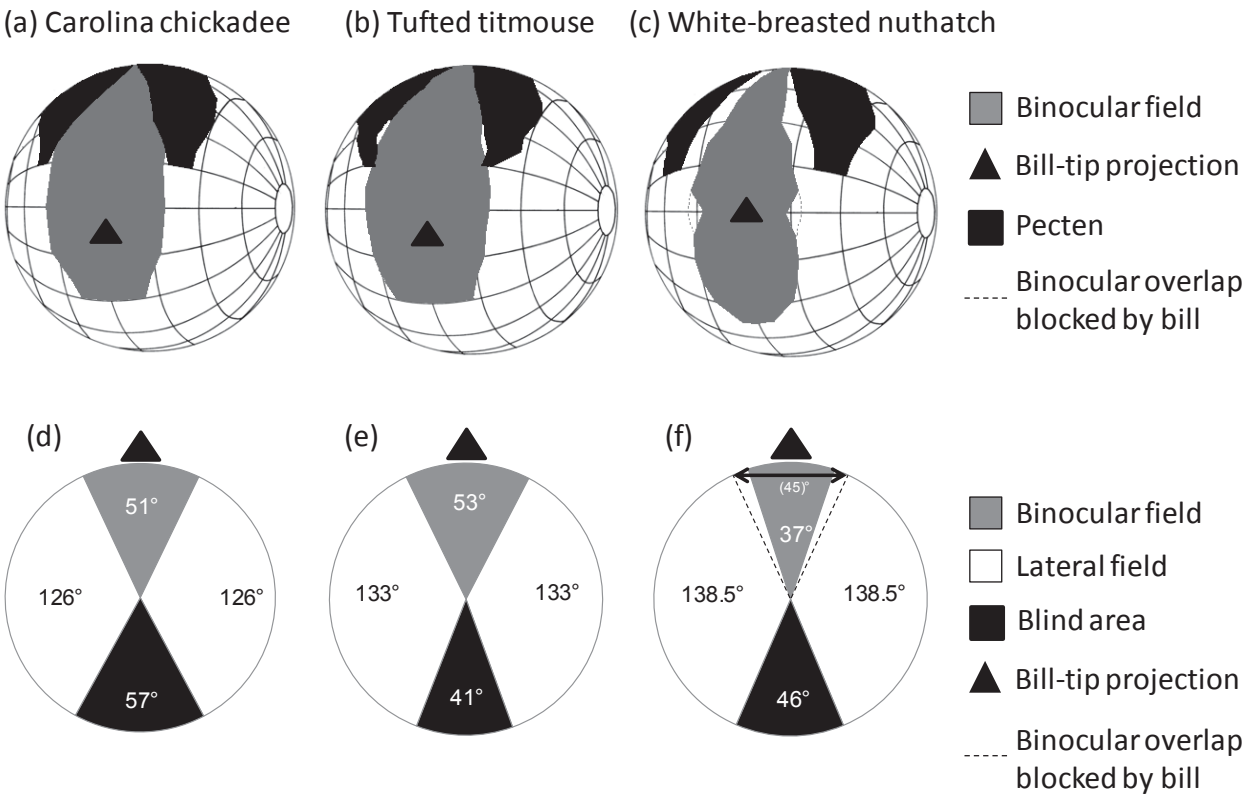

Fig 4.2 Different views of the visual field configuration with the eyes at rest of Carolina chickadees (a, d), tufted titmice (b, e), and white-breasted nuthatches (c, f). (a-c) Orthographic projection of the boundaries of the retinal fields of the two eyes, along with projection of the pectens and bill tips. A latitude and longitude coordinate system was used with the equator aligned vertically in the median sagittal plane. The head of the animal is at the center of the globe (grid is at approximately 20° intervals). (d-f) Visual field sections through the horizontal plane (90° - 270°). The dotted lines in (b, e) represent extrapolated binocular field widths assuming that the retinal margin follows a circular projection (see text for details).

Across all recorded elevations, the averaged width of the binocular field differed significantly among species ($F_{2,18} = 20.81$, $P < 0.001$). Chickadees (32.82 ± 0.78°; $t_{18} = 7.02$, $P < 0.001$) and titmice (32.70 ± 0.96°; $t_{18} = 6.06$, $P < 0.001$) had significantly wider binocular fields across the recorded elevations than nuthatches (26.38 ± 0.85°), but without significant differences between the two parid species ($t_{18} = 0.13$, $P = 0.899$; Fig. 3). Pooling all species, we found that the averaged width of the binocular field varied across elevations ($F_{16,199} = 56.12$, $P < 0.001$); however, there was no significant interaction between species and elevation ($F_{27,199} = 1.28$, $P = 0.656$; Fig. 3).

At the 270° elevation (i.e., rear of the head along the plane of the bill) with the eyes at rest, we found that the blind area was the widest in the chickadee (57°), intermediate in the nuthatch (46°), and the smallest in the titmouse (41°) (Fig. 3). Across all recorded elevations, the average width of the blind area varied significantly between species ($F_{2,18} = 8.18$, $P = 0.003$). Chickadees (32.91 ± 1.51°) had significantly wider blind areas than titmice (27.74 ± 1.81°; $t_{18} = 3.20$, $P = 0.005$) and nuthatches (27.55 ± 1.50°; $t_{18} = 3.62$, $P = 0.002$), without significant differences between the latter species ($t_{18} = 0.11$, $P = 0.913$). Pooling all species, the width of the blind area differed across elevations ($F_{17,144} = 29.12$, $P < 0.001$; Fig. 3), but without a significant interaction between species and elevation ($F_{17,144} = 0.83$, $P = 0.656$).

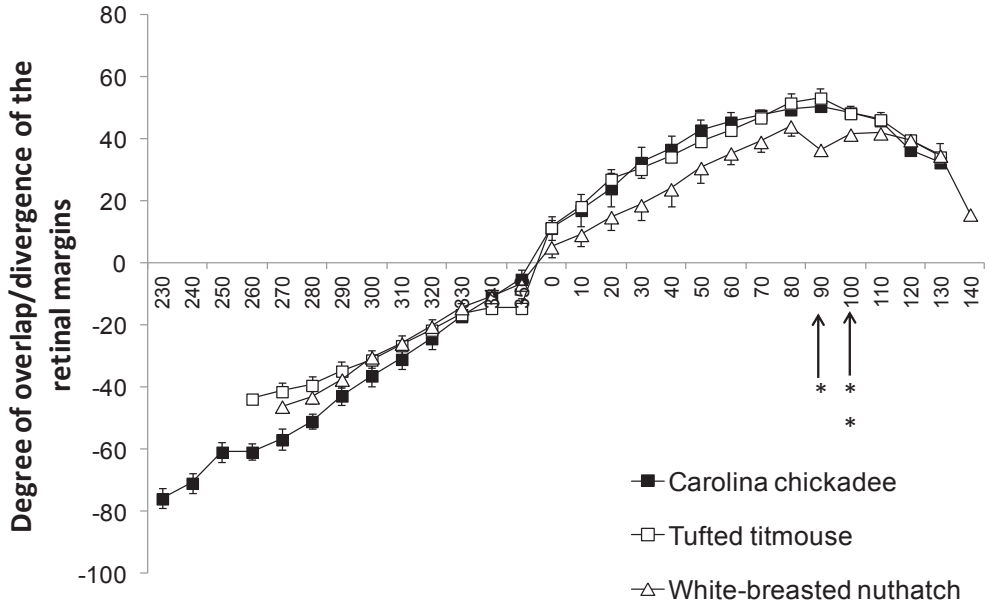

Fig 4.3 Mean (± SE) angular separation of the retinal field margins in relation to elevation around the head in the median sagittal plane of Carolina chickadees, tufted titmice, and white-breasted nuthatches. Binocular fields are indicated by positive values of overlap of the visual field margins; whereas blind areas are indicated by negative values. Orientation landmarks are at 90° (front of the head), 270° (back of the head), and 0° (above the head). Arrows indicate projection of the bill-tip (**= Carolina chickadee, tufted titmouse; * = white-breasted nuthatch).

The projection of the pecten extended vertically 70° in all species (from 0° to 70° above the bill) (Fig. 1a-c). Across elevations, the width of the pecten varied significantly among species ($F_{2,11} = 14.34$, $P < 0.001$). All pairwise differences were significant (t_{11} varied from 2.27 to 5.34, $P < 0.044$): nuthatches had the widest pecten (25.74 ± 0.82°), titmice had an intermediate sized pecten (22.95 ± 0.92°), and chickadees had the narrowest pecten (19.72 ± 0.76°). Pooling all species, the width of the pecten varied significantly across elevations ($F_{7,58} = 39.38$, $P < 0.001$), without a significant interaction between species and elevation ($F_{14,58} = 0.97$, $P = 0.489$).

4.4.3 Degree of eye movement and visual fields

Across elevations, the degree of eye movement varied among species significantly ($F_{2,21}$ = 29.35, P < 0.001; Fig. 4). Titmice (76.33 ± 1.41°) had the highest degree of eye movement, followed by chickadees (71.24 ± 1.23°), and nuthatches (61.58 ± 1.37°); with all pair-wise comparisons being significant (t_{21} varied from 2.72 to 5.25, P < 0.020). Pooling all species, the degree of eye movement varied significantly across elevations ($F_{22,221}$ = 4.79, P < 0.001; Fig. 4). Additionally, the interaction between species and elevation was significant ($F_{44,221}$ = 3.64, P < 0.001). Therefore, we ran another model to establish whether eye movement amplitude would vary above and below the bill across species. For this model, we considered up to three elevations above and below the bill (if available) without considering the elevation where the tip of the bill projected. We found significant species ($F_{2,17}$ = 11.73, P < 0.001) and elevation ($F_{1,9}$ = 36.36, P < 0.001) effects, and a significant interaction between species and elevation ($F_{2,9}$ = 45.36, P < 0.001). The degree of eye movement was higher above than below the bill in chickadees (82.90 ± 2.64° vs. 35.36 ± 3.86°, respectively) and titmice (82.20 ± 3.11° vs. 66.52 ± 4.02°, respectively; Fig. 4a-b). However, the degree of eye movement was higher below than above the bill in nuthatches (73.69 ± 4.23° vs. 58.96 ± 2.70°, respectively; Fig. 4c).

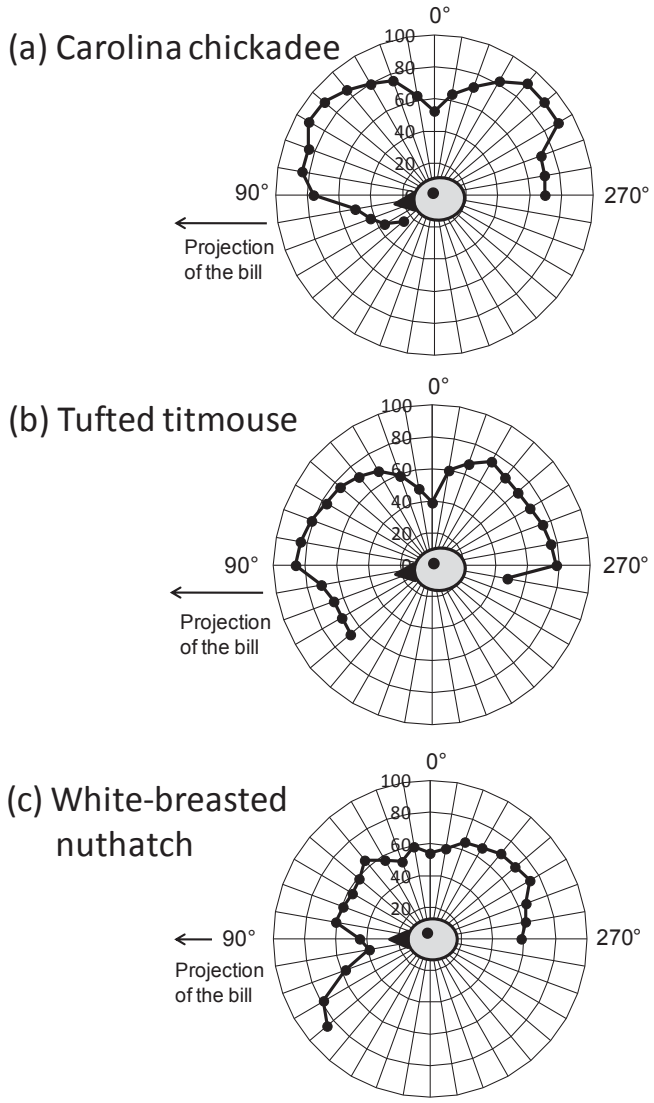

Fig 4.4 Mean degree of eye movements in relation to elevation in the median sagittal plane in (a) Carolina chickadees, (b) tufted titmice, and (c) white-breasted nuthatches. Degree of eye movement is shown in the same scale (0 – 100°) in all species while viewing the bird's head from the left side.

In the horizontal plane, eye movements modified the relative size of the binocular, lateral, and blind areas in all the species (Fig. 5). When we elicited eye convergence (see Methods), chickadees increased the binocular overlap by 49% and the blind area by 60% in relation to the eyes-at-rest position (Fig. 5a), and titmice, by 47% and 100%, respectively (Fig. 5b). The increase in the binocular field of nuthatches with the eyes converged was lower (22%) compared to the eyes-at-rest position because the bill blocked our view of the retinal margins (see above; Fig. 5c). The extrapolated width of the nuthatch binocular field with eyes converged was estimated as 55° (Fig. 5c), assuming that the retinal margin follows a circular projection (Martin and Coetzee 2004). The blind area of nuthatches with the eyes converged increased by 52% in relation to the eyes-at-rest position (Fig. 5c).

In the horizontal plane, when individuals diverged their eyes, the width of the binocular and blind areas decreased by 102% and 63%, respectively, in chickadees, and by 117% and 49%, respectively, in titmice compared to the eyes-at-rest position (Fig. 5d, e). Chickadees and titmice could actually abolish the area of binocular overlap, giving rise to a blind area of 1° and 9°, respectively, in front of the bill when the eyes diverged (Fig. 5d, e). When nuthatches diverged their eyes, the width of the binocular and blind areas decreased by 97% and 80%, respectively, in relation to the eyes-at-rest position (Fig. 5f).

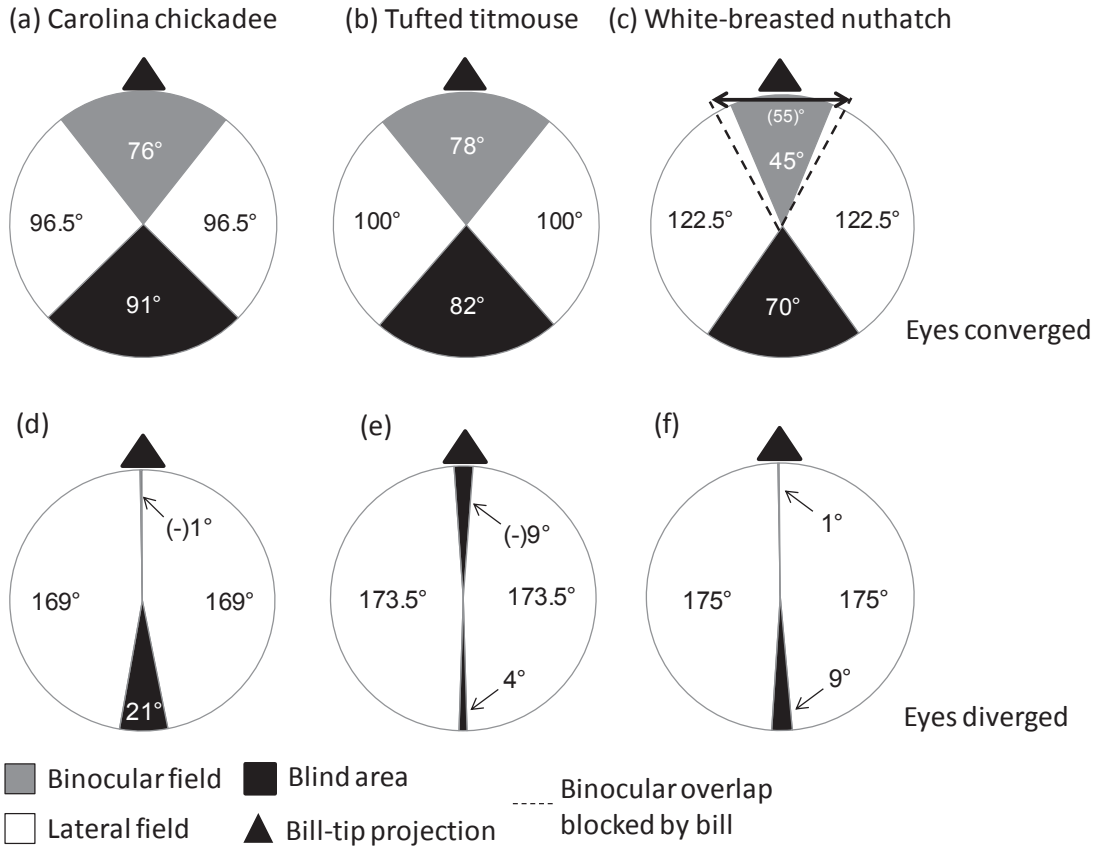

Fig 4.5 Visual field sections through the horizontal plane (90° - 270°) of (a, b) Carolina chickadees, (c, d) tufted titmice, and (e, f) white-breasted nuthatches. Charts represent the average retinal field when the eyes were converged (eyes rotated fully forward; a, c, e), which maximizes the size of the binocular and blind areas, and when the eyes were diverged (eye rotated fully backward; b, d, f), which minimizes the size of the binocular and blind areas. The dotted lines in the white-breasted nuthatch (c) chart represent the extrapolated binocular field assuming that the retinal margin follows a circular projection (see text for details)

.

4.4.4 Head movements

Head-movement rate varied significantly among species ($F_{2,45} = 24.09$, $P < 0.001$). Chickadees had the highest head movement rates (2.05 ± 0.12 events/sec), titmice had intermediate values (1.56 ± 0.10 events/sec), and nuthatches had the lowest head movement rates (0.90 ± 0.12 events/sec). All pair-wise differences between species were significant (Tukey tests, $P < 0.01$). We repeated the analysis excluding the catalog videos and including the videos we recorded to assess the effects of the potential confounding factors. None of these factors significantly influenced head movement rates (flock size, $F_{1, 22} = 3.38$, $P = 0.079$; temperature, $F_{1, 22} = 0$, $P = 1$; perch height, $F_{1, 22} = 0.69$, $P = 0.693$; distance between observer and bird, $F_{1, 22} = 0.01$, $P = 0.976$). After controlling statistically for these factors, we still found significant differences between species ($F_{2, 22} = 26.97$, $P < 0.001$) following the same patterns described above.

4.5 Discussion

Our results suggest that the visual system and scanning behavior of chickadees, titmice, and nuthatches have some similarities, but also many differences. We found support for some of our predictions (e.g., interspecific variation in visual acuity, width of the binocular fields, degree of eye movement, and head movement rates; position of the fovea in titmice and chickadees; width of the blind area in chickadees) but not for others (e.g., position of the fovea in nuthatches; width of blind areas in titmice and nuthatches). We discuss these findings in light of the foraging and anti-predator strategies of these three tree foragers.

4.5.1 Visual acuity

The inter-specific differences in visual acuity followed variations in body mass, as found previously (Kiltie 2000). Visual acuity is influenced by eye size (which is associated with body mass; Garamszegi et al. 2002; Howland et al. 2004) and retinal ganglion cell density (Pettigrew et al. 1988). The highest visual acuity of nuthatches was likely

affected by having the highest peak ganglion cell density of the three species. Titmice had intermediate values of visual acuity, followed by chickadees, which had the smallest eye size and lowest ganglion cell density. The implication is that nuthatches would be able to perceive visual stimuli (e.g., predators, conspecifics) from farther away than titmice and specially chickadees.

Contrary to our prediction, all three studied species have a single fovea, located centro-temporally in the retina, and thus projecting into the frontal side of the lateral field close to the edges of the binocular field. The peak retinal ganglion cell density around the fovea was slightly higher in these tree foragers compared to other avian ground foragers (house finch 25,256 cells/mm^2, house sparrow 23,920 cells/mm^2, brown-headed cowbird 21,665 cells/mm^2, European starling 25,317 cells/mm^2, Dolan and Fernández-Juricic 2010). This relatively higher retinal ganglion density would lead to higher localized visual resolution (given similar eye sizes). Species with a single fovea tend to have a smaller proportion of their visual fields with high visual resolution than species with other types of retinal specializations (e.g., visual streak; Walls 1937). Species with a single fovea would tend to move their eyes (hence, their foveae) around substantially to scan for predators and search visually for food. Tree foragers are expected to have visual demands that are different from those of ground foragers due to the higher complexity of their visual environments (Hughes 1977; Hart 2001; Møller and Erritzøe 2010)

4.5.2 Binocular fields

As predicted, chickadees and titmice have wider binocular fields compared to those of nuthatches (Fig. 6a, b), which may be associated with the position of the eyes in the skull (Appendix 1). Actually, the binocular widths of titmice with the eyes at rest (53°) and converged (78°) were higher than that of any previously studied bird species (Martin 1984; Martin et al. 2004; Martin et al. 2007; Fernández-Juricic et al. 2010; Fernández-Juricic et al. 2011a). Such wide binocular fields are not necessary to navigate complex environments (Martin 2009), like the closed habitats these species occupy. One possibility is that wide binocular fields may facilitate sampling the foraging substrate at relatively short distances by increasing light sensitivity and contrast discrimination

(reviewed in Heesy 2009), which would enhance the detection of food in closed habitats with relatively low ambient light levels. Another possibility is that wide binocular fields are associated with arboreal habits, potentially providing depth perception from stereoscopic cues as the animal moves through the foliage (Changizi and Shimojo 2008). However, Martin (2009) argued that stereoscopic depth perception may be absent in most bird species and that birds rely primarily upon direction of travel and time to contact cues derived from optic flow-field information. More information on the function of the binocular fields of these species should be gathered in the future to test these hypotheses.

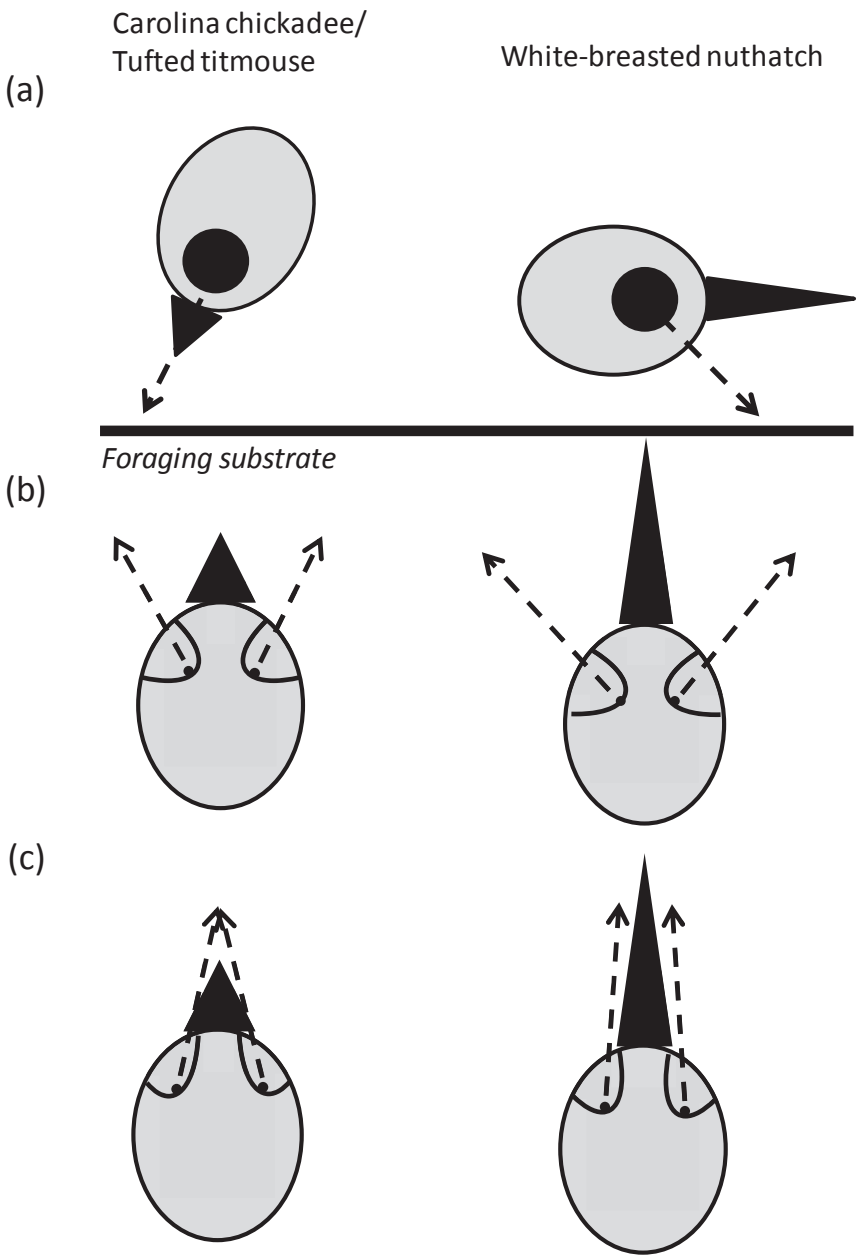

Fig 4.6 (a and b) Top-views showing the approximate projection of the fovea into the visual fields of Carolina chicakdees/tufted titmice and white-breasted nuthatches with the eyes (a) at rest and (b) converged. The more frontally-placed eyes of the chickadees/titmice would result in the fovea projecting more frontally, whereas the more laterally-placed eyes of the nuthatches would result in the fovea projecting slightly more laterally. (c) Side-view representation of the projection of the fovea of Carolina chickadees/tufted titmice and white-breasted nuthatches while seeking food, taking into account the convergence of the eyes in the direction of the foraging substrate. The arrows do not provide any reference to binocularity or the ability to visualize the bill-tip.

Previous studies have suggested that some avian species can see their bill tips (Martin 2009), which was associated with relatively wide binocular fields (e.g., American crow, Fernández-Juricic et al. 2010; New Caledonian crow, Troscianko et al. 2012). However, our results show that the nuthatch is able to see its bill-tip with a relatively narrower binocular field than that of the chickadee and titmouse. This may be explained by the nuthatch's longer bill (20.55 mm) that protrudes into the binocular field, compared to those of chickadees (7.83 mm) and titmice (10.65 mm) (Frens 2010). Visualizing the bill tip may facilitate probing for food items in trunks and branches and manipulating food items by wedging them into bark crevices (Grubb and Pravasudov 2008). Our results suggest that the ability of species to visually inspect their bills may be the result of a trade-off between the width of the binocular field and the length of the bill.

4.5.3 Eye and head movements

Our prediction of wider blind areas in species with more frontally placed eyes was met when individuals converged their eyes. However, contrary to our expectation, we found that nuthatches had wider blind areas than titmice with the eyes at rest. This difference could be attributed to eye movement amplitude. All studied species had high degrees of eye movement (with both eyes > 60° across all elevations) compared to previously studied species (Martin 1998; Martin and Coetzee 2004; Fernández-Juricic et al. 2008; Fernández-Juricic et al. 2010). However, they differed in their eye movement strategies around the bill, which may be associated with their foraging strategies.

Chickadees and titmice have slightly more frontally positioned eyes (Appendix 1) and the highest degree of eye movement occurs slightly above the plane of the bill. This may allow these two species to converge their eyes towards the bill and change the position of the foveae, which would project into the binocular field slightly above the bill when head-down searching for food at steep angles in relation to the foraging substrate (Fig. 6). Nuthatches, on the other hand, have relatively more laterally placed eyes (Appendix 1) with a high degree of eye movement mostly below the bill. This would allow nuthatches to converge their eyes and change the position of the fovea, which would project into the binocular field slightly below the bill towards the foraging

substrate when the bill is held at a shallow angle in relation to the tree trunk during food searching (Fig. 6). These morphological and sensory features may enhance the ability of these species to detect food through different foraging tactics while exploiting the same micro-habitats.

Moving the head is another strategy (besides eye movements) to move the fovea around and obtain high visual resolution information on objects of interest (Dunlap and Mowrer 1930; Friedman 1975; Fernández-Juricic 2012). Generally, quicker head movement rates should translate into more regions of the visual space that can be updated per unit time with high quality information through inspection with the foveae. The nuthatch had the lowest head movement rate of all three species. This may be the result of a lower need to scan the environment because of its higher visual acuity to detect stimuli at farther distances, smaller blind areas, and more laterally placed eyes increasing visual coverage. Conversely, chickadees and titmice had higher head movement rates, probably because they often seek food in a head-down posture with the bill oriented at steep angles in relation to the substrate, and therefore have to raise their heads frequently to monitor for potential predators. Additionally, chickadees showed higher head movement rates than titmice. Titmice have higher visual acuity and narrower blind areas than chickadees, potentially decreasing the need to scan as frequently through head movements. An alternative explanation based on Newton's second law is that it would require more force (e.g., greater energetic costs) for titmice to move their heads as often as chickadees due to their larger body mass.

4.5.4 Implications for heterospecific flocking behavior

Our results have some implications for the behavioral interactions among these species when they form heterospecific flocks during the non-breeding season. A common assumption is that satellite species eavesdrop on the alarm calls of nuclear species (Templeton and Greene 2007, Bartmess-LeVasseur et al. 2010). There is evidence in the guild of tree foragers we studied that some of its satellite species (e.g., white-breasted nuthatch, downy woodpecker *Picoides pubescens*) decrease their investment in vigilance (Sullivan 1984a, b; Dolby and Grubb 1998) and increase foraging efforts and risk-taking

behaviors (Dolby and Grubb 2000) when associated with nuclear species (tufted titmouse, Carolina chickadee). However, our results suggest that the visual system of at least one of these satellite species, the nuthatch, may enable them to have a good ability to detect predators visually from far away (i.e., higher visual acuity) and from different parts of the environment (i.e., narrower blind areas, larger lateral fields). Additionally, the auditory system of nuthatches does not have high sensitivity for the high-frequency alarm calls of chickadees and titmice (Henry and Lucas 2008). All this sensory evidence in principle challenges the idea that the nuthatch eavesdrops on the alarm calls of the titmouse and chickadee because of potential limitations of its sensory system.

One possibility is that nuthatches actually rely on social *visual* information from the nuclear species by tracking visually their foraging and anti-predator behaviors. Alternatively, nuthatches may use both sources of information (auditory and visual) depending upon their main behavioral activity. When nuthatches engage in non-foraging activities, they may rely to a greater extent on visual cues from the nuclear species. However, when foraging, they may use some vocalizations of the nuclear species as cues to engage in visual monitoring for predators. This is because foraging nuthatches tend to have a very large portion of their visual field blocked by the tree trunk as they move quickly in search of food and appear to have their visual attention focused away from the areas where predators would generally attack (Fig. 6). As a result of this compromised foraging technique, nuthatches may compensate for the reduced availability of visual information with auditory information. Future studies manipulating both visual and auditory cues separately and simultaneously could provide an opportunity to assess the attention targets of nuthatches in heterospecific flocks.

4.5.5 Conclusions

Overall, we found that chickadees, titmice, and nuthatches differ in some key components of their visual system and scanning behavior. These differences may be the result of phylogenetic relatedness (chickadees and titmice belong to the family Paridae; nuthatches to the family Sittidae) and/or specializations to the visual challenges posed by the different foraging and scanning strategies that facilitate the partitioning of resources within this guild.

4.7 Literature Cited

Bartmess-LeVasseur J, Branch CL, Browning SA, Owens JL, Freeberg TM (2010). Predator stimuli and calling behavior of Carolina chickadees (*Poecile carolinensis*), tufted titmice (*Baeolophus bicolor*), and white-breasted nuthatches (*Sitta carolinensis*). *Behavioral Ecology and Sociobiology 64*:1187-1198

Beauchamp G (2003). Group-size effects on vigilance: a search for mechanisms. *Behavioral Processes* 63:111-121

Blackwell BF, Fernández-Juricic E, Seamans TW, Dolan T (2009). Avian visual system configuration and behavioural response to object approach. *Animal Behaviour* 77:673-684

Blumstein DT, Daniel JC (2007). *Quantifying behavior the JWatcher way*. Sinauer Associates Inc, Sunderland

Carr JM, Lima SL (2012). Heat-conserving postures hinder escape: a thermoregulation–predation trade-off in wintering birds. *Behavioral Ecology* 23:434-441

Changizi MA, Shimojo S (2008). ‘‘X-ray vision’’ and the evolution of forward-facing eyes. *Journal of Theoretical Biology* 254:756–767

Collin SP (1999). Behavioural *ecology* and retinal cell topography. In: Archer S, Djamgoz MB, Loew E, Partridge JC, Vallerga S (ed) *Adaptive mechanisms in the ecology of vision.* Kluwer Academic Publishers, Dordrecht, pp 509-535

Dolan T, Fernández-Juricic E (2010). Retinal ganglion cell topography of five species of ground foraging birds. *Brain Behavior and Evolution* 75:111-121

Dolby AS, Grubb Jr. TC (1998). Benefits to satellite members in mixed species foraging groups: an experimental analysis. *Animal Behaviour* 56:501-509

Dolby AS, Grubb Jr. TC (2000). Social context affects risk taking by satellite species in a mixed-species foraging group. *Behavioral Ecology* 11:110-114

Dunlap K, Mowrer OH (1930). Head movements and eye functions of birds. *Journal of Comparative Psychology* 11:99-112

Dunning Jr. JB (2008). *CRC handbook of avian body masses*. Second edition. CRC Press, Taylor & Francis Group

Ehrlich D (1981). Regional specialization of the chick retina as revealed by the size and density of neurons in the ganglion cell layer. *Journal of Comparative Neurology* 195:643-657

Fernández-Juricic E (2012). Sensory basis of vigilance behavior in birds: synthesis and future prospects. *Behavioral Process* 89:143-152

Fernández-Juricic E, Blumstein DT, Abrica G, Manriquez L, Adams LB, Adams R, Daneshrad M, Rodriguez-Prieto I (2006). Relationships of anti-predator escape and post-escape responses with body mass and morphology: a comparative avian study. *Evolutionary Ecology Research* 8:731-752

Fernández-Juricic E, Gall MD, Dolan T, Tisdale V, Martin GR (2008). The visual fields of two ground-foraging birds, house finches and house sparrows, allow for simultaneous foraging and anti-predator vigilance. *Ibis* 150:779-787

Fernández-Juricic E, O'Rourke C, Pitlik T (2010). Visual coverage and scanning behavior in two corvid species: American crow and Western scrub jay. *Journal of Comparative Physiology A* 196:879-888

Fernández-Juricic E, Gall MD, Dolan T, O'Rourke C, Thomas S, Lynch JR (2011a). Visual systems and vigilance behaviour of two ground-foraging avian prey species: white-crowned sparrows and California towhees. *Animal Behaviour* 81:705-713

Fernández-Juricic E, Moore BA, Doppler M, Freeman J, Blackwell BF, Lima SL, DeVault TL (2011b). Testing the terrain hypothesis: Canada geese see their world laterally and obliquely. *Brain Behavior and Evolution* 77:147-158

Fernández-Juricic E, Beauchamp G, Treminio R, Hoover M (2011c). Making heads turn: association between head movements during vigilance and perceived predation risk in brown-headed cowbird flocks. *Animal Behaviour* 82:573-577

Fite KV, Rosenfield-Wessels S (1975). A comparative study of deep avian foveas. *Brain Behavior and Evolution* 12:97-115

Freeman B, Tancred E (1978). The number and distribution of ganglion cells in the retina of the brush-tailed possum, *Trichosurus vulpecula*. *Journal of Comparative Neurology* 177:557-67

Frens K (2010). Effects of food type and patch location on foraging in local birds: a field test of optimal foraging predictions. Masters thesis, University of Michigan. http://deepblue.lib.umich.edu/handle/2027.42/69156

Friedman MB (1975). How birds use their eyes. In: Wright P, Caryl P, Vowles DM (ed) *Neural and endocrine aspects of behavior in birds*, Elsevier, Amsterdam, pp. 182-204

Gall MD, Fernández-Juricic E (2009). Effects of physical and visual access to prey on patch selection and food search effort in a sit-and-wait predator, the Black Phoebe. *Condor* 111:150-158

Garamszegi LZ, Møller AP, Erritzøe J (2002). Coevolving avian eye size and brain size in relation to prey capture and nocturnality. *Proceeding of the Royal Society of London B* 269:961-967

Gioanni H (1988). Stabilizing gaze reflexes in the pigeon (*Columba livia*). I. Horizontal and vertical optokinetic eye (OKN) and head (OCR) reflexes. *Experimental Brain Research* 69:567–582

Grubb Jr. TC, Pravasudov VV (1994). Tufted Titmouse (*Baeolophus bicolor*). In: Poole A (ed) *The birds of North America* online, Cornell Lab of Ornithology, Ithaca. doi: 10.2173/bna.86

Grubb Jr. TC, Pravasudov VV (2008). White-breasted Nuthatch (*Sitta carolinensis*). In: Poole A (ed) *The birds of North America* online, Cornell Lab of Ornithology, Ithaca. doi: 10.2173/bna.54

Guillemain M, Martin GR, Fritz H (2002). Feeding methods, visual fields and vigilance in dabbling ducks (Anatidae). *Functional Ecology* 16:522-529

Hart NS (2001). Variations in cone photoreceptor abundance and the visual ecology of birds. *Journal of Comparative Physiology A* 187:685-698

Heesy CP (2004). On the relationship between orbit orientation and binocular visual field overlap in mammals. *Anatomical Record* 281A:1104-1110

Heesy CP (2009). Seeing in stereo: The ecology and evolution of primate binocular vision and stereopsis. *Evolutionary Anthropology* 18:21-35

Henry KS, Lucas JR (2008). Coevolution of auditory sensitivity and temporal resolution with acoustic signal space in three songbirds. *Animal Behaviour* 76:1659-1671

Howland HC, Merola S, Basarab JR (2004). The allometry and scaling of the size of vertebrate eyes. *Vision Research* 44:2043–2065

Hughes A (1977). The topography of vision in mammals of contrasting life style: comparative optics and retinal organization. In: Crescitelli F (ed) *The visual system in vertebrates*, Springer-Verlag, New York, pp. 615–756

Iwaniuk AN, Heesy CP, Hall MI, Wylie DR (2008). Relative Wulst volume is correlated with orbit orientation and binocular visual field in birds. *Journal of Comparative Physiology A* 194:267-282

Kiltie RA (2000). Scaling of visual acuity with body size in mammals and birds. *Functional Ecology* 14:226–234

Lima SL (1992). Vigilance and foraging substrate: anti-predatory considerations in a non-standard environment. *Behavioral Ecology and Sociobiology* 30:283-289

Lima SL (1993). Ecological and evolutionary perspectives on escape from predatory attack: a survey of North American birds. *Wilson Bulletin* 105:1-47

Martin GR (1984). The visual fields of the tawny owl, *Strix aluco L*. *Vision Research* 24:1739–1751

Martin GR (1993). Producing the image. In: Zeigler HP, Bischof H-J (ed) *Vision, brain and behaviour in birds*. MIT press, Massachusetts, pp 5–24

Martin GR (1998). Eye structure and amphibious foraging in albatrosses. *Proceedings of the Royal Society of London B* 265:665-671

Martin GR (2007). Visual fields and their functions in birds. *Journal of Ornithology* 148:S547-S562

Martin GR (2009). What is binocular vision for? A birds' eye view. *Journal of Vision* 9:1-19

Martin GR, Prince PA (2001). Visual fields and foraging in Procellariiform seabirds: sensory aspects of dietary segregation. *Brain Behavior and Evolution* 57: 33-38

Martin GR, Coetzee HC (2004). Visual fields in hornbills: precision-grasping and sunshades. *Ibis* 146:18-26

Martin GR, Rojas LM, Figueroa YMR, McNeil R (2004). Binocular vision and nocturnal activity in oilbirds (*Steatornis caripensis*) and Pauraques (*Nyctidromus albicollis*); Caprimulgiformes. *Ornitologia Neotropical 15*(Suppl):233-242

Martin GR, Jarrett N, Williams M (2007). Visual fields in blue ducks *Hymenolaimus malacorhynchos* and pink-eared ducks *Malacorhynchus membranaceus*: visual and tactil foraging. *Ibis* 149:112-120

McIlwain JT (1996). *An introduction to the biology of vision*. Cambridge University Press, New York

Meyer DBC (1977). The avian eye and its adaptations. In: Crescitelli F (ed) *The visual system of vertebrates; handbook of sensory physiology* Springer, New York. pp 549-612

Møller AP, Erritzøe J (2010). Flight distance and eye size in birds. *Ethology* 116:458-465

Moroney MK, Pettigrew JD (1987). Some observations on the visual optics of kingfishers (Aves, Coraciformes, Alcedinidae). *Journal of Comparative Physiology A* 160:137-149

Mostrom AM, Curry RL, Lohr B (2002). Carolina Chickadee (*Poecile carolinensis*). In: Poole A (ed) *The birds of North America* online, Cornell Lab of Ornithology, Ithaca. doi: 10.2173/bna.636

O'Rourke CT, Hall MI, Pitlik T, Fernández-Juricic E (2010a). Hawk eyes I: diurnal raptors differ in visual fields and degree of eye movement. *PLoS ONE* 5:e12802

O'Rourke CT, Pitlik T, Hoover M, Fernández-Juricic E (2010b). Hawk eyes II: diurnal raptors differ in head movement strategies when scanning from perches. *PLoS ONE* 5:e12169

Pettigrew JD, Dreher B, Hopkins CS, Mccall MJ, Brown M (1988). Peak density and distribution of ganglion-cells in the retinae of Microchiropteran bats - implications for visual-acuity. *Brain Behavior and Evolution* 32:39-56

Reymond L (1985). Spatial visual acuity of the eagle, Aquila audax: a behavioural, optical and anatomical investigation. *Vision Research* 25:1477-1491

Schwab IR (2012). *Evolution's witness. How eyes evolved*. Oxford University Press, Oxford

Siemers BM, Swift SM (2006). Differences in sensory ecology contribute to resource partitioning in the bats *Myotis bechsteinii* and *Myotis nattereri* (Chiroptera: Vespertilionidae). *Behavioral Ecology and Sociobiology* 59:373-380

Simberloff D, Dayan T (1991). The guild concept and the structure of ecological communities. *Annual Review of Ecololgy, Evolution, and Systematics* 22:115-143

Stone J (1981). *The wholemount handbook. A guide to the preparation and analysis of retinal wholemounts*. Maitland Publishing, Sydney

Sullivan KA (1984a). Information exploitation by downy woodpeckers in mixed-species flocks. *Behavior* 91:294-311

Sullivan KA (1984b). The advantages of social foraging in downy woodpeckers. *Animal Behaviour* 32:16-22

Templeton CN, Greene E (2007). Nuthatches eavesdrop on variations in heterospecific chickadee mobbing alarm calls. *Proceedings of the National Academy of Science* 104:5479-5482

Troscianko J, von Bayern AM, Chappell J, Rutz C, Martin GR (2012). Extreme binocular vision and a straight bill facilitate tool use in New Caledonian crows. *Nature Communications* 3:1110

Ullmann JFP, Moore BA, Temple SE, Fernández-Juricic E, Collin SP (2012). The retinal wholemount technique: a window to understanding the brain and behaviour. *Brain Behavior and Evolution* 79:26-44

Walls GL (1937). Significance of the foveal depression. *Archives of Ophthalmology* 18: 912-919

Walls GL (1942). *The vertebrate eye and its adaptive radiation*. Cranbrook Institute of Science, Michigan

Wathey JC, Pettigrew JD (1989). Quantitative analysis of the retinal ganglion cell layer and optic nerve of the Barn Owl *Tyto alba*. *Brain Behavior and Evolution* 33:279-292

Williams DR, Coletta NJ (1987). Cone spacing and the visual resolution limit. *Journal o the Optical Society of America A* 4:1514-1523

4.8 Appendices

4.8.1 Appendix 1

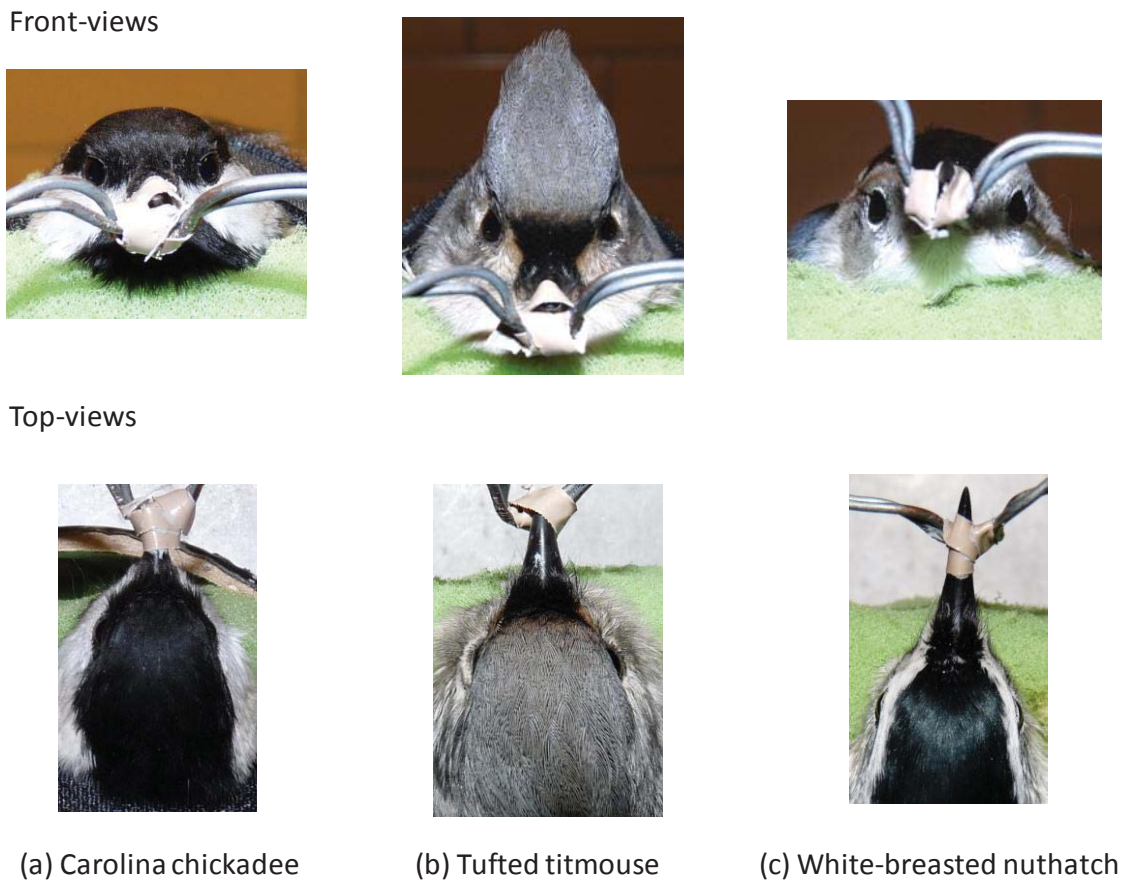

Fig 4.7 Eye positioning in the skull of (a) Carolina chickadees, (b) tufted titmice, and (c) white-breasted nuthatches. Chickadees and titmice have their orbits positioned slightly more towards the bill than nuthatches.

CHAPTER 5: MULTIDIMENSIONAL VISION IN AVIAN PASSIVE PREY FORAGERS: MAXIMIZING BINOCULAR VISION WITH FRONTO-LATERAL VISUAL ACUITY

This chapter is part of a manuscript co-authored with other researchers that is in the peer-review process at the moment:

Moore BA, Pita D, Tyrrell LP, Fernandez-Juricic E. Multidimensional vision in avian passive prey foragers: maximizing binocular vision with fronto-lateral visual acuity. In press at *Journal of Experimental Biology*.

5.1 Abstract

Avian species vary in their visual system configuration, which has been linked to variation in behavior. Previous studies on sensory system variation often compared single visual traits between 2-3 distantly related species. However, birds use different visual dimensions that cannot be maximized simultaneously to meet different perceptual demands, potentially leading to trade-offs between visual traits. This is the first study on the degree of inter-specific variation in multiple visual traits related to foraging and anti-predator behaviors in nine species of closely related emberizid sparrows, controlling for phylogenetic effects. Sparrows have a single retinal center of acute vision projecting fronto-laterally, whose orientation relative to the binocular field may shorten gathering visual information from the foraging substrate. Different species maximize binocular vision, even seeing their bill tips, which may enhance the detection of prey (e.g., seeds, insects) and facilitate food handling. Contrary to previous work, we found that species

with more visual coverage had higher visual acuity, which may compensate for larger blind spots above the center of acute vision, enhancing predator detection. Finally, species with a steeper change in cell density across the retina have more eye movement amplitude likely to sample more quickly the surroundings with acute vision. Overall, the visual configuration of these passive prey foragers is substantially different from previously studied avian groups (e.g., sit-and-wait and tactile foragers).

5.2 Introduction

The question of how birds see their world has been the subject of considerable attention mostly because the properties of the avian visual system are different from that of humans (e.g., wider color space, high temporal visual resolution, etc.; Cuthill 2006). Understanding how birds gather different types of information from the environment can help us explain multiple behaviors that have been studied over decades (Birkhead 2012). This is relevant because birds have often been used as model systems to address fundamental questions in evolutionary ecology (Birkhead et al. 2014).

Interestingly, the avian visual system varies considerably between species in terms of visual acuity (Kiltie 2000), type and position of the areas of acute vision (e.g., Meyer 1977; Hughes 1977; Moore et al. 2012), visual field configuration (Martin 2007), etc. This inter-specific variability has generally been studied from a unidimensional perspective (i.e., variation in the size of the binocular field *or* visual acuity *or* placement of orbits). However, this approach does not take into account the complexity of the visual information demands birds face, sometimes simultaneously, using different visual sensory dimensions; for instance, visual acuity to detect predators and binocular vision to guide the bill towards food (Martin 2014). By studying different visual dimensions, particularly in closely related species, we can begin to understand the steps involved in the evolutionary divergence of the avian visual system (Martin 2012) as well as the sensory basis of resource partitioning within ecological niches (Martin and Prince 2001; Siemers and Swift 2006; Safi and Siemers 2010).

Probably the most widely known visual system in birds is that of active prey foragers, including diurnal raptors (Reymond 1985; Inzunza et al. 1991; O'Rourke et al. 2010a) and flycatchers (Coimbra et al. 2006, 2009; Gall and Fernández-Juricic 2010), which often employ sit-and-wait foraging tactics. Avian active prey foragers generally have retinae with two centers of acute vision: one projects into the lateral visual field to detect prey at far distances, while the other projects into the binocular field to grab prey at close distances (Tucker 2000). Sit-and-wait foragers also tend to have relatively high visual acuity, wide blind areas, and low degree of eye movement (Jones et al. 2007; O'Rourke et al. 2010a).

However, the visual system of passive prey foragers, which both detect and grab prey items at close distances (i.e., ground and tree foragers), has received considerably less attention (but see Fernández-Juricic et al. 2008; Dolan and Fernández-Juricic 2010; Moore et al. 2013). This is puzzling because many of these species belong to speciose groups of extant birds (e.g., Passeriformes) and have a large diversity in morphology, diet, and behavior (Ricklefs 2012), which is expected to be mirrored in their visuals systems to enhance visual performance in different habitat types (Boughman 2002; Seehausen 2008; Dalton et al. 2010).

Passive prey avian foragers appear to share some visual traits (Fernández-Juricic et al. 2008; Dolan and Fernández-Juricic 2010; Moore et al. 2013): (a) a single retinal center of acute vision (i.e., fovea) projecting into the lateral field, (b) relatively wide binocular fields, (c) the bill projecting towards (but not intruding into) the binocular field, (d) a large degree of convergent and divergent eye movements that allows manipulation of the size of the binocular field and blind area, and (e) the presence of a pecten, a pigmented vascular structure that supplies nutrients to the avian retina but reduces visual coverage because its projection generates a blind spot right above the fovea (Meyer 1977; van den Hout and Martin 2011). Despite the studies conducted so far on passive prey foragers, it is challenging to make generalizations for two main reasons (reviewed in Martin 2014). First, studies have often included species that are phylogenetically very distant; hence, functional interpretations on the visual system configuration are confounded by phylogenetic variation in morphology and behavior. Second, many studies

looking at between-species variation in visual traits include too few species (generally 2-3) and fail to control for phylogenetic effects.

In this study, we assessed the degree of inter-specific variation in several key visual dimensions related to foraging and anti-predator behaviors and tested specific predictions about their co-variation in species belonging to the Emberizidae family. Emberizid sparrows forage close to the ground on seeds during the winter and insects during the breeding season, and escape to vegetative cover when attacked by aerial and ground predators (Elphick et al. 2001). The overreaching hypothesis behind our predictions (see below) is that different visual dimensions cannot be maximized simultaneously to meet different perceptual demands (Martin 2014). Consequently, ours is the first study considering multiple visual dimensions from a quantitative perspective and testing for trade-offs in avian visual configuration.

Our study is divided in three parts. First, we established the degree of inter-specific variability in the four visual dimensions in seven species of closely related emberizids: American tree sparrow *Spizella arborea*, chipping sparrow *Spizella passerine*, dark-eyed junco *Junco hyemalis*, Eastern towhee *Pipilo erythrophthalmus*, field sparrow *Spizella pusilla*, song sparrow *Melospiza melodia*, and white-throated sparrow *Zonotrichia albicollis* (Appendix 1). We studied (a) eye size and retinal ganglion cell density (i.e., cells that transfer information from the retina to the visual centers of the brain) as proxies of visual acuity, (b) ganglion cell density profiles across the retina as proxies of the position of the center of acute vision and its projection into the visual field, which is usually associated with visual attention (Bisley 2011), (c) visual field configuration as a proxy of visual coverage around the head (i.e., size of the binocular and lateral fields, and blind area), and (d) degree of eye movement as a proxy of the extent to which the area of acute vision can be moved around the visual space for scanning purposes. Additionally, we measured bill size (length, width, depth) to assess its influence on the configuration of the visual field. Second, we described quantitatively the multidimensional visual space of these emberizid species including these seven species along with two others already described in the literature (California towhee *Pipilo crissalis* and white-crowned sparrow *Zonotrichia leucophrys*; Fernández-Juricic et al.

2011; Appendix 1). Establishing how these species distribute themselves across different visual dimensions simultaneously can help us understand associations between different visual traits. Third, we tested the following specific predictions, considering all nine emberizid species and controlling for their degree of phylogenetic relatedness, about relationships between these visual dimensions in the context of foraging and anti-predator behaviors.

5.2.1 Binocular field width and bill size.

Martin (2009) proposed that binocular vision in birds is mostly associated with controlling bill direction and time of contact with targets. Therefore, species that guide their bills to explore the substrate and glean food items are expected to have relatively wider binocular fields (Martin 2014). In Passeriformes, the bill usually projects towards the binocular field (e.g., Tyrrell et al. 2013; Baumhardt et al. 2014). The implication is that larger bills can block areas of binocular overlap leaving them covered only by monocular vision (i.e., the visual field of a single eye; Moore et al. 2013). If keeping a certain degree of binocular coverage around the bill is relevant for detecting and capturing food, we predicted that species with larger bills would have wider binocular fields to compensate for the loss of binocular vision.

5.2.2 Pecten size, binocular field width, and degree of eye movement.

The size of the pecten and the binocular field width varies substantially between species (e.g., Meyer 1977; Fernández-Juricic et al. 2010; Moore et al. 2013). Given that the pecten projects towards the edges of the binocular field (example in Fig. 3), larger pectens could constrain the space available for binocular vision. This would lead to a negative relationship between the size of the projection of the pecten and the binocular field width with the eyes at rest. If emberizid sparrows need to maximize the size of the binocular field for foraging purposes, one strategy is to converge their eyes when looking for and gleaning food to enhance binocular vision. Therefore, we predicted that species with larger pectens would have higher degrees of eye movement, compared to those with smaller pectens, to compensate for narrower binocular fields with the eyes at rest.

5.2.3 *Blind spots and eye size.*

High levels of ambient light can decrease visual performance (i.e., reduce image contrast) due to an excess of light in the eye chamber (i.e., glare effects; Koch 1989). Species with larger eyes can be more prone to glare effects because of larger optical apertures leading to a greater influx of sunlight (Martin and Katzir 2000). Positioning the sun image in a blind spot would reduce glare effects, which leads to two alternative solutions for species with larger eyes: larger blind areas (Martin and Katzir 2000) and/or larger pectens (Fernández-Juricic and Tran 2007; van den Hout and Martin 2011). We then predicted a positive association between eye size and pecten size as well as eye size and blind area width.

5.2.4 Visual coverage and visual acuity.

One of the implications of the predicted positive association between eye size and blind area width is that visual acuity (i.e., a positive function of eye size and ganglion cell density; Pettigrew et al. 1988) and visual coverage (i.e., the inverse of blind area; Martin 2014) may be related. Additionally, species with lower visual acuity have been proposed to compensate for the limitations of detecting predators from far distances by having more laterally placed eyes to enhance the chances of detection from a wider area around their heads (Hughes 1977). Therefore, we predicted species with lower visual acuity to have higher visual coverage.

5.2.5 Retinal configuration and degree of eye movements.

The density of ganglion cells (and thus visual acuity) varies across the vertebrate retina (Collin 1999), generally being higher close to center of acute vision than the retinal periphery in many Passeriformes (e.g., Moore et al. 2013; Tyrrell et al. 2013). Species with lower ganglion cell density, hence lower acuity, in the retinal periphery compared to the retinal center have been proposed to rely more on the high visual acuity provided by the center of acute vision (Dolan and Fernández-Juricic 2010). This would increase the need for higher degree of eye movement to move the center of acute vision around to sample the visual environment with high visual resolution (Fernández-Juricic et al. 2011).

Consequently, we predicted that species with a more pronounced difference in cell density across the retina would have a higher degree of eye movement.

5.3 Methods

All sparrows used in this study were captured in Tippecanoe County, Indiana, USA. All birds were captured in accordance to protocol #09-018, approved by the Purdue Animal Care and Use Committee. Handling and experimental procedures were also approved by the same committee. Birds were housed indoors with 1-3 individuals of the same species per (0.9 m x 0.7 m x 0.6 m) cage, and kept on a 14:10 hour light:dark cycle at approximately 23°C. Animals were provided food (millet) and water *ad libitum*. We used 8 American tree sparrows, 5 Chipping sparrows, 13 dark-eyed juncos, 3 Eastern towhees, 7 field sparrows, 9 song sparrows, and 11 white-throated sparrows for visual field and degree of eye movement measurements, of which 3-5 individuals from each species were used for retinal tissue collection.

5.3.1 Eye size, retinal ganglion cell density, and visual acuity

Immediately after euthanasia, we removed the eyes and measured eye axial length to enable approximation of visual acuity. Axial length was measured from the most axial, anterior portion of the cornea to the posterior eye (axially) using digital calipers (0.01 mm accuracy). We then hemisected the eye at the *ora serrata*, and removed all vitreous humor using forceps and spring scissors. Orientation of the eye was maintained throughout by the position of the pecten (Meyer 1977) in relation to the bill. We extracted the retina, wholemounted it, and then stained with cresyl violet for the ganglion cell visualization following the wholemount technique described in detail in Ullman et al. (2012). A thorough description of our methods to process the retinal tissue has been recently published in Baumhardt et al. (2014). We chose to stain ganglion cells because they have been proposed to be the information bottlenecks from the retina to the visual

centers of the brain (Collin 1999), and therefore have an important role in visual acuity (McIlwain 1996).

We used an Olympus BX51 microscope to examine the retina. Using Stereo Investigator (ver. 9.13; MBF Bioscience), we first traced the perimeter of the retina with the SRS Image Series Acquire module. This module randomly and systematically formulates a grid by use of a fractionator approach, which can then be placed onto the traced retina. We used on average between 407 and 413 grid sites per species (see Appendix 2), although we were able to count ganglion cells on fewer sites (between 357 and 398 per species (Appendix 2) because some counting frames were outside of the retina, some retinal spots were out of focus or had tears. Each grid site contained a counting frame in the upper left hand corner that was 50x50 µm. The following parameters were then estimated: asf (the ratio of the area of the counting frame to the area of the grid), $\sum Q^-$ (sum of the total number of retinal ganglion cells counted), and the total number of ganglion cells in the retina (Appendix 2). At each counting frame, we focused at 1000x total power on the plane that provided the highest resolution and contrast to enable identification of ganglion cells. We then took a photograph of the focused counting frame with an Olympus S97809 microscope camera. Each photograph was captured and saved using SnagIt (www.techsmith.com/Snagit). We counted the retinal ganglion cells in each of the images using ImageJ (http://imagej.nih.gov/ij/).

We differentiated retinal ganglion cells from amacrine and glial cells following a set of criteria established in previous studies: cell shape, soma size, Nissl accumulation, and staining characteristics of the nucleus (following Hughes 1977; Freeman and Tancred 1978; Ehrlich 1981; Stone 1981; Mitkus et al. 2014). The soma size of ganglion cells tends to vary depending on the location in the retina and type of ganglion cells, but they consistently have heterogeneously distributed Nissl granules more densely located around the cytoplasmic periphery, and a prominent, darkly staining nucleus. On the other hand, the soma of glial cells is generally narrow and elongated with a less intensely stained nucleus that often contains multiple nucleoli. Amacrine cells are smaller than ganglion cells, are distinctly teardrop-shaped and contain Nissl accumulation that is primarily located close to the nucleus but may extend into the cytoplasmic tail. We differentiated

retinal ganglion cells from all other cell types throughout the entire retina, however nearly every cell within the high ganglion cell density regions was counted because the non-ganglion cell population declines below 1% of the total cell count (Ehrlich, 1981). We discuss this approach to differentiating ganglion cells in detail in Baumhardt et al. (2014).

To correct for shrinkage of the retina during processing, we photographed the retina with a Panasonic Lumix FZ28 digital camera before and after the staining procedure, with an image area of 0.01 mm^2. ImageJ was then used to measure the area of the retina before and after staining. Shrinkage was calculated as a relative difference between pre- and post-staining procedures [Picture area * (Retinal area pre-staining – Retinal area post-staining)].

We built topographical representations of the cell densities across the retina (i.e. retinal topographic maps) following Stone (1981) and Ullmann et al. (2012). Ganglion cell density values obtained from each counting frame were then entered into a blank map showing the retinal outline and the sampling grid. We then created isodensity lines by hand, separating grid boxes into different cell density ranges (Moroney and Pettigrew 1987; Wathey and Pettigrew 1989). The final topographic maps were developed using Adobe Illustrator CS5.

We assumed similar eye shapes and optical properties across species (Martin 1993) because all our study species are diurnal (Appendix 1). We then used the sampling theorem to obtain a morphological estimate of spatial resolving power (i.e., a proxy of visual acuity or visual resolution) using eye size and retinal ganglion cell density (Hughes 1977). First, we multiplied eye axial length by 0.60 (following Hughes 1977; Martin 1993) as an estimate of posterior nodal distance (PND; length from the posterior nodal point of the eye to the photoreceptor layer; Vakkur et al. 1963). We then calculated the retinal magnification factor (RMF, the linear distance on the retina subtending 1° of visual space; Pettigrew et al. 1988) by using the following equation: RMF = 2πPND/360. We then estimated spatial resolving power (in cycles per degree) to be the highest spatial frequency that can be detected (F_n): $= \frac{RMF}{2}\sqrt{\frac{2D}{\sqrt{3}}}$; where D is the averaged retinal ganglion cell density throughout the retina (Williams and Coletta 1987). The distance at

which an object occupies the same angle of retinal space as one cycle at the threshold of visual acuity can be considered the theoretical maximum distance that an animal could detect that object under optimal ambient light conditions. We calculated the distance (*d*) at which each sparrow species could detect objects the size of a Cooper's hawk wingspan and sharp-shinned hawk wingspan using: $d = \frac{r}{\tan\frac{\alpha}{2}}$, where *r* is the radius of the object, and α is the inverse of visual acuity.

5.3.2 Cell density profile and position of the center of acute vision

Following a new method introduced by Moore et al. (2012), we quantified the position of the center of acute vision and the changes in the ganglion cell density from the periphery to the center of acute vision (slope) along the nasal, temporal, dorsal, and ventral retinal axes for each species based on the retinal ganglion cell topographic maps (see Fig. 1). Variations in ganglion cell density across the retina provide an estimate of how visual acuity changes between the retinal periphery and the center of acute vision (i.e., the higher cell density, the higher the acuity or visual resolution).

We measured the position of the center of acute vision following a Cartesian coordinate system in relation to the center of the retina, where positive x-values indicate nasal and negative x-values indicate temporal, and positive y-values indicate dorsal and negative y-values indicate ventral (details in Moore et al. 2012). Ganglion cell density gradients were measured by establishing sampling transects across the nasal, temporal, dorsal, and ventral retinal axes, centered on the center of acute vision (see Moore et al. 2012). The average density of retinal ganglion cells was recorded at each sampling point by establishing which cell density range each sampling point fell into. These sampling points were then plotted linearly and fit with a trend line from which the slope was calculated for use as an approximation for the change in RGC density from the retinal periphery to the center of acute vision (Moore et al. 2012).

To determine the angular projection of the center of acute vision into visual space, we converted the Cartesian coordinates into angular coordinates by multiplying the Cartesian value by the half width of the visual field of a single eye. We then aligned the center of the retina with the center of the single eye visual field and expressed the center

of acute vision projection as the angular offset from standard positions in the x- (line perpendicular to the beak axis) and y- (parallel to the ground) dimensions. This method assumes that identically sized retinal regions project identical angles of visual space, as has been considered in birds (Holden et al. 1987).

5.3.3 Visual field configuration and degree of eye movement

To measure the configuration of the visual field, we used a visual field apparatus developed by Martin (1984). Following methods described in detail in Moore et al. (2013) and Martin (2014), birds were placed in the visual field apparatus with their heads held stationary. The visual fields were measured using a polar coordinate system, such that the 90–270° plane was the horizontal plane (i.e. parallel to the ground); the 0° elevation lay directly above the head of each species, 90° in front, and 270° behind (see Results). We measured the retinal boundaries at every 10° elevation around the head (± 0.5°), which was then mathematically corrected for close viewing following Martin (1984). We measured as many elevations around the subject as possible unless our view was blocked by its body or the apparatus. Overlapping retinal projections from both eyes at a given elevation represent the binocular field, whereas the lack of any retinal projection into an area represents the blind area. Using these two values, we calculated the size of the lateral fields as: [360 – (mean blind field + mean binocular field)/2] (Fernández-Juricic et al. 2008). With the eyes at rest, we also measured the size of the blind spot in the dorso-frontal part of the visual field caused by the projection of the pecten.

We measured the visual field configuration not only when the eyes were at rest, but also when (1) the eyes were converged, and (2) the eyes were diverged. The degree of eye movement of a given elevation in space was calculated as: (Converged value – Diverged value). Binocular field, blind area, and the lateral fields were calculated in the same manner as explained before for converged and diverged eye positions.

5.3.4 Bill dimensions

Bill dimensions were measured on specimens at the Field Museum, Chicago, IL and at Purdue University Department of Forestry and Natural Resources, West Lafayette, IN. We measured bill length (posterior nostril to tip of the bill), bill width (horizontal thickness at the anterior edge of the nostrils), and bill depth (vertical thickness at the anterior edge of the nostrils) following Willson (1971). Measurements were taken on 10 American tree sparrows, 16 chipping sparrows, 19 dark-eyed juncos, 24 Eastern towhees, 9 field sparrows, 6 song sparrows, 6 white-throated sparrows, 9 California towhees, and 11 white-crowned sparrows.

5.3.5 Statistical analysis

We first established the degree of between-species variability on the seven sparrow species whose visual traits are described for the first time here. For these analyses, we decided not to run post-hoc pair-wise comparisons to minimize increasing the probability of committing Type I error due to the higher number of P estimates. Additionally, associations between visual traits across species were assessed in the last part of the Results. We ran general linear models with Statistica 10 (Tulsa, OK) to determine between-species differences in bill length, width, and depth, eye axial length, the x- and y-coordinates reflecting the position of the center of acute vision, and the slopes of cell density change from the retinal periphery to the center of acute vision. We also ran a Principal Component Analysis to combine the three bill measurements into a single component reflecting overall bill size. After comparing eye axial length between species, we ran another general linear model considering the residuals of the regression between ($\log_{10}$) axial length and ($\log_{10}$) body mass to ascertain the variation in eye size relative to body mass between species.

We ran general linear mixed models in SAS 9.2 (Cary, N.C.) to determine between-species differences in overall (i.e., whole retina) and highest (i.e., around center of acute vision) ganglion cell density, width of the binocular field, blind area, and pecten, and the degree of eye movements. Individual identity was included as a within-subject factor and species and elevation as the between-subject factors in all these models.

Reported means only consisted of elevations around the head from which we were able to record either a positive of negative overlap between the eyes (see above). Throughout, we present least square means ± SE.

We modeled the visual space of the nine emberizid sparrows (seven from this study and two from Fernández-Juricic et al. 2011) using a PCCA (Principal Components and Classification Analysis, Statsoft 2013). The PCCA considered different visual traits, derived common dimensions to classify those traits that are uncorrelated to each other, and mapped the relative position of each species into the space bounded by these common dimensions. We used a single value (least squares means of a given visual trait) per species as we did not have information for every single studied trait on every studied individual. We selected dimensions with Eigenvalues > 1. For this exploratory analysis, we considered visual field traits that would reflect overall visual coverage (e.g., binocular field width across all recorded elevations) instead of specific elevations. In the next section, we tested specific predictions that were relevant for specific elevations (i.e., binocular field with at the plane of the bill due to its relevance for foraging). We included the following traits: binocular field width across all recorded elevations, blind area width across all recorded elevations, pecten width across all recorded elevations, eye axial length, highest ganglion cell density (i.e., around center of acute vision), and average slope of change in ganglion cell density from retinal periphery to the center of acute vision across all retinal axes (nasal, temporal, dorsal, and ventral).

In testing the specific predictions laid out in the Introduction, we established associations between different visual traits using a single value (i.e., least squares mean) for each species. We ran general linear models with these raw species data (i.e., species means without phylogenetic relatedness corrections). However, we also accounted for the shared evolutionary history of these species by using phylogenetic generalized least squares models (PGLS, Pagel 1999; Nunn 2011). PGLS models calculate using a maximum likelihood procedure the parameter lambda (λ), which estimates the amount of phylogenetic signal in the model: $\lambda = 0$ indicates that the residual error is completely independent of phylogeny, whereas $\lambda = 1$ indicates that the residual error varies according

to a Brownian motion model of evolution (i.e., trait similarity is lower with increasing phylogenetic distance).

We conducted all PGLS analyses using the Caper package (Orme et al. 2011) in R (R Development Core Team 2010). We corroborated that our results met the model assumptions by visually inspecting the distribution of residuals and the fitted vs. the residual values. We also checked for outliers (samples with values > 3 or < -3, Yang and Su 2009) but did not detect any. For the PGLS analyses, we used a tree (Appendix 3) based on the phylogenetic relationships of emberizid sparrows described in Carson and Spicer (2003).

To test for the relationship between binocular field width and bill size, we used the width of the binocular field at the plane of the bill (90°) with the eyes at rest and with the eyes converged as this is the elevation generally involved in food searching. Bill size was the PCA factor that included bill length, width, and depth (see Results). We tested for the relationships between binocular field and pecten size by using the binocular field values at the plane of the bill (90°) with the eyes at rest and pecten width across all elevations. The hypothesis behind this prediction assumes that species with wide binocular fields with the eyes at rest would also have wide binocular fields with the eyes converged, which we also tested using binocular field values at the plane of the bill (90°). To test the relationship between degree of eye movement and pecten width, we used values across all recorded elevations as the presence of the pecten blind spot can influence eye movement across the whole visual field. To test the relationship between blind area and eye size, and pecten width and eye size, we used the width of the blind area across all recorded elevations with the eyes at rest, the width of the pecten across all recorded elevations, and the (log) eye axial length as a proxy of eye size. To test the relationship between visual coverage and visual acuity, we calculated the width of the cyclopean field (combination of binocular and lateral fields) with the eyes at rest by subtracting the total amount of blind area from 360. We used the elevation around the plane of the bill for the cyclopean field because measurements from in front of the head and behind the head of a given plane must be present (e.g. 90 and 270 degree) to calculate the cyclopean field, and only at the given elevations could both be calculated

for every species. To test for the relationship between retinal configuration and degree of eye movements, we used the mean slope of the change in cell density between the retinal periphery and the center of acute vision (considering all directions: nasal, temporal, dorsal, ventral) and the average degree of eye movement across all elevations.

5.4 Results

Overall, we found a large degree of interspecific variation in most of the visual traits studied. We first provide a quantitative account of this variability in the seven species of emberizid sparrows studied for the first time here (Table 1). We then present the modeled visual space of these seven species along with two other emberizid sparrows studied before (Fernández-Juricic et al. 2011). Finally, we establish the associations between different visual traits including all nine species.

Table 5.1 Least squares means of different visual traits of seven emberizid sparrows. See text for details. Abbreviations: RGCs, retinal ganglion cells.

	American tree sparrow	chipping sparrow	dark-eyed junco	Eastern towhee	field sparrow	song sparrow	white-throated sparrow
Axial length (mm)	6.08 ± 0.07	5.37 ± 0.08	6.23 ± 0.07	7.59 ± 0.11	5.63 ± 0.07	6.53 ± 0.07	7.06 ± 0.08
X- coordinate	-0.082 ± 0.040	-0.231 ± 0.040	-0.143 ± 0.035	-0.118 ± 0.049	-0.116 ± 0.035	-0.154 ± 0.040	-0.245 ± 0.049
X- coordinate 95% confidence intervals	-0.168 – 0.005	-0.317 – -0.145	-0.218 – -0.068	-0.223 – -0.012	-0.191 – -0.042	-0.240 – -0.068	-0.350 – -0.139
Y-coordinate	0.100 ± 0.051	0.069 ± 0.051	0.107 ± 0.044	0.106 ± 0.062	0.134 ± 0.044	-0.002 ± 0.051	0.148 ± 0.062
Y- coordinate 95% confidence intervals	-0.009 – 0.209	-0.040 – 0.179	0.013 – 0.202	-0.028 – 0.240	0.039 – 0.228	-0.111 – 0.108	0.014 – 0.282
Nasal slope	3.693 ± 0.368	3.890 ± 0.450	2.458 ± 0.319	3.065 ± 0.450	4.327 ± 0.368	2.727 ± 0.368	3.130 ± 0.450
Temporal slope	5.227 ± 0.542	5.505 ± 0.664	3.095 ± 0.469	5.590 ± 0.664	4.973 ± 0.542	4.313 ± 0.542	6.365 ± 0.664
Dorsal slope	6.770 ± 0.556	6.040 ± 0.681	3.805 ± 0.481	4.240 ± 0.681	6.780 ± 0.556	3.930 ± 0.556	5.645 ± 0.681
Ventral slope	4.477 ± 0.382	5.050 ± 0.468	3.538 ± 0.331	4.465 ± 0.468	4.477 ± 0.382	3.660 ± 0.382	3.550 ± 0.468
Overall RGC density (cells/mm2)	23,423 ± 297	22,570 ± 321	18,098 ± 296	17,882 ± 443	19,801 ± 283	18,338 ± 288	19,094 ± 322
Highest RGC density (cells/mms2)	42,319 ± 1,361	47,920 ± 1,522	34,938 ± 1,361	38,188 ± 2,152	41,765 ± 1,361	37,046 ± 1,361	37,557 ± 1,522
Visual acuity (cycles/degree)	7.03	6.62	6.55	8.35	6.45	7.07	7.70
Binocular field across elevations (degrees)	24.64 ± 0.72	24.03 ± 0.78	24.55 ± 0.56	23.41 ± 0.87	25.27 ± 0.65	24.50 ± 0.55	26.42 ± 0.51
Blind area across elevations (degrees)	20.38 ± 1.10	26.73 ± 1.03	17.30 ± 0.89	24.39 ± 1.73	27.13 ± 0.99	21.19 ± 0.97	16.77 ± 0.97
Eye movement across elevations (degrees)	21.81 ± 0.53	31.44 ± 0.59	32.95 ± 0.39	35.26 ± 0.55	35.94 ± 0.51	32.80 ± 0.41	30.81 ± 0.34
Pecten width across elevations (degrees)	14.55 ± 0.96	19.63 ± 0.93	24.46 ± 0.73	26.96 ± 1.38	23.78 ± 0.76	24.25 ± 0.74	22.69 ± 0.73
Maximum distance to resolve Cooper's hawks (m)	306	288	285	364	281	308	335
Maximum distance to resolve sharp-shinned hawks	199	188	186	237	183	201	218

5.4.1 Eye size, retinal ganglion cell density, and visual acuity

Eye axial length varied significantly among species ($F_{6, 43} = 79.40$, $P < 0.001$), from 5.37 mm (chipping sparrow) to 7.59 mm (Eastern towhee; Table 1). Pooling all species, the relationship between ($\log_{10}$) axial length and ($\log_{10}$) body mass was significant ($F_{1, 46} = 129.29$, $P < 0.001$, Adjusted $R^2 = 0.74$). The residuals of this relationship (i.e., eye axial length relative to body mass) differed significantly among species ($F_{6, 41} = 5.59$, $P < 0.001$). Three species showed smaller eyes relative to their body mass: chipping sparrow, -0.0209 ± 0.0072; American tree sparrow, -0.0113 ± 0.0062; and dark-eyed junco, -0.0109 ± 0.0058. Four species showed larger eyes relative to their body mass: white-throated sparrow, 0.0223 ± 0.0079; song sparrow, 0.0194 ± 0.0062; field sparrow, 0.0051 ± 0.0058; and Eastern towhee, 0.0004 ± 0.0102.

The mean overall density of retinal ganglion cells differed significantly among species ($F_{6,23} = 51.97$, $P < 0.001$), from 23,423 cells/mm2 (American tree sparrow) to 17,882 cells/mm2 (Eastern towhee; Table 1). The highest ganglion cell density (in the quadrats around the center of acute vision) also varied significantly among species ($F_{6,23} = 8.91$, $P < 0.001$), from 34,938 cells/mm2 (dark-eyed junco) to 47,920 cells/mm2 (chipping sparrow; Table 1).

Based on the averaged eye axial length and highest density of ganglion cells, we found that visual acuity varied by about 25% among emberizid sparrows (Table 1). Based on their visual acuities, we estimated the maximum distances at which each emberizid species would be able to resolve two of their most common predators under optimal ambient light conditions (Table 1). For the Cooper's hawk, the maximum distance varied from 281 to 364 m, and for the Sharp-shinned Hawk, from 183 to 237 m (Table 1).

5.4.2 Retinal configuration

Fig. 1 shows a representative topographic map of the distribution of ganglion cells for each of the studied species. These maps show a concentric increase in ganglion cell density from the periphery to an approximate central location in the retina (black dots in Fig. 1). Based on morphological features on the wholemount (i.e., small circular area devoid of retinal ganglion cells at the very center, but surrounded by the highest ganglion

cell density), we determined that all the studied species appear to have a single fovea per retina. To corroborate this, we adjusted the microscope focus (400x magnification), and observed changes in the surface of the retinal tissue that suggested a potential invagination characteristic of a fovea. Based on tissue availability, we also did cross-sections for some of the studied species (song sparrow, dark-eyed junco, field sparrow), and confirmed that the morphological characteristics observed on the wholemounted tissue corresponded to a fovea (photographs available upon request).

Based on the x-coordinates of the fovea position of all species (Table 1), the single fovea was generally located slightly off the center towards the temporal side of the retina (Fig. 1), but we did not find significant differences among species ($F_{6, 14} = 2.01$, $P = 0.133$; Table 1). Based on the negative upper and lower bound 95% confidence intervals of the fovea x-coordinates (Table 1), the temporal displacement of the fovea was prevalent in chipping sparrows, dark-eyed juncos, Eastern towhees, field sparrows, song sparrows, and white-throated sparrows. However, the 95% confidence intervals of the fovea x-coordinate of American tree sparrows included positive values, which suggests than in this species the temporal placement of the fovea cannot be discriminated from a central placement.

Based on the y-coordinates of the fovea position (Table 1), we found some, non-significant ($F_{6, 14} = 0.91$, $P = 0.516$), level of inter-specific variability in the location of the fovea in the dorso-ventral axis. Based on the positive upper and lower bound 95% confidence intervals of the fovea y-coordinates (Table 1), dark-eyed juncos, field sparrows, and white-throated sparrows appeared to have their foveae displaced dorsally in relation to the center of the retina (Fig. 1). However, the positive upper and negative lower bound 95% confidence intervals of the fovea y-coordinate of American tree sparrows, chipping sparrows, Eastern towhees, and song sparrows (Table 1) suggest that the dorsal or ventral placement of the fovea cannot be discriminated from a central placement.

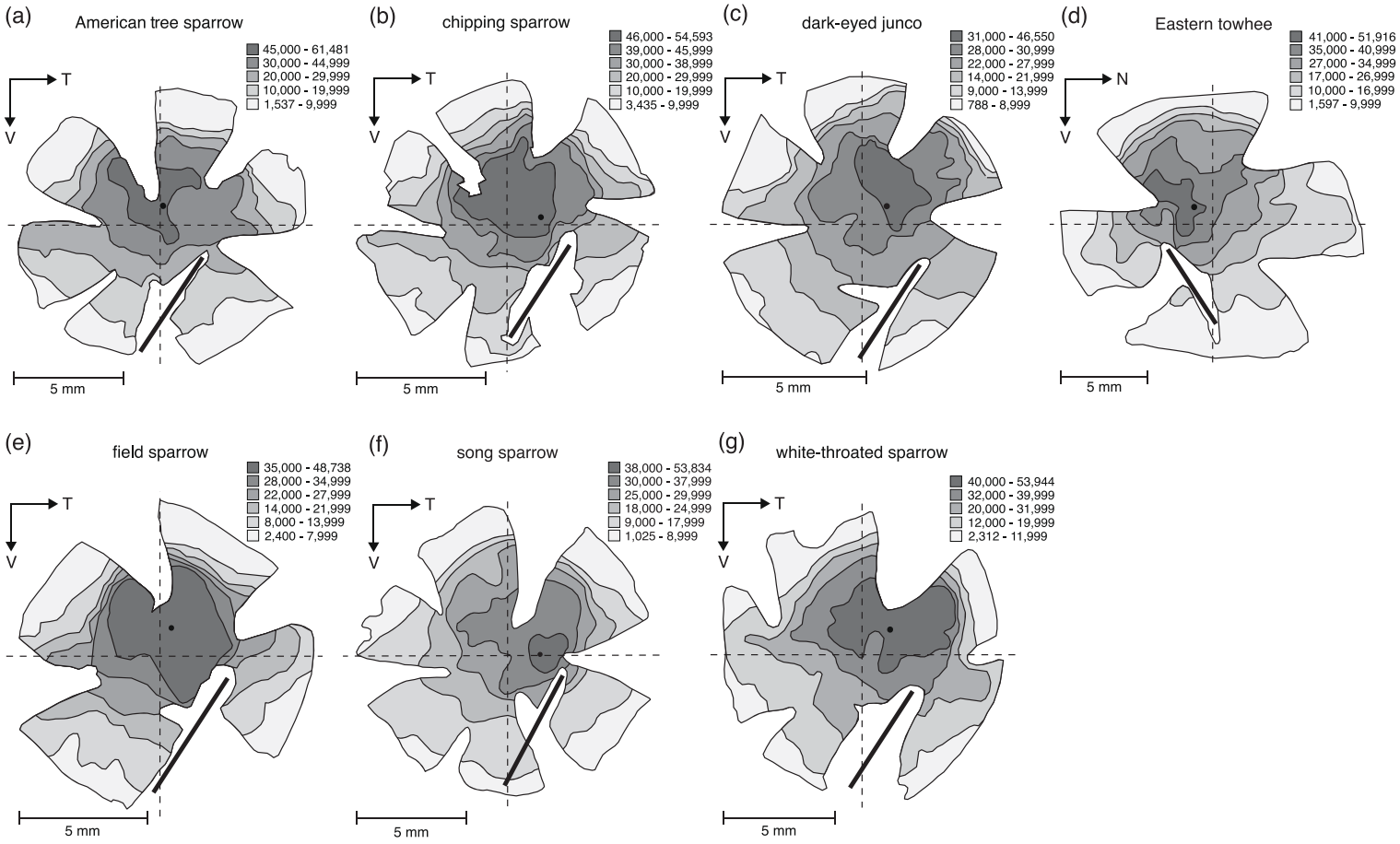

Fig 5.1 Example topographic maps of retinal ganglion cell densities of (a) American tree sparrows, (b) chipping sparrows, (c) dark-eyed juncos, (d) Eastern towhees, (e) field sparrows, (f) song sparrows, and (g) white-throated sparrows. Numbers represent ranges of cell densities in cells/mm^2. The dashed lines represent the nasal-temporal and dorsal-ventral axes, with the intersection of the two axes indicating the center of the retina. The fovea is indicated by the black dot in each map and the pecten is indicated by the thick black bar. All maps are of left eyes except for (d). V = ventral, T = temporal, N = nasal.

Overall, American tree sparrows have an approximately central fovea; dark-eyed juncos, field sparrows, and white-throated sparrows have a dorso-temporal fovea, and chipping sparrows, Eastern towhees, and song sparrows a centro-temporal fovea. Under the assumptions explained in the Methods, we estimated the approximate projection of the fovea from top and side views using the averaged values of the x- and y- coordinates (Fig. 2). In general, based on the 95% confidence intervals, the fovea projects fronto-laterally in all species (Fig. 2). From a side view, the fovea tends to project below the bill in dark-eyed juncos, field sparrows, and white-throated sparrows, but in the other species the foveal projection appears as straight-ahead (Fig. 2).

We found significant variation among species in the nasal ($F_{6, 12} = 3.41$, $P = 0.033$), temporal ($F_{6, 12} = 3.80$, $P = 0.023$), and dorsal ($F_{6, 12} = 5.60$, $P = 0.006$) slopes of ganglion cell density change between the retinal periphery and the fovea. In general, dark-eyed juncos and song sparrows had the lowest values in the three slopes, suggesting a shallow change in ganglion cell density (and hence spatial visual resolution) across the retina (Table 1). We did not find significant differences among species in the ventral slope values ($F_{6, 12} = 2.04$, $P = 0.137$).

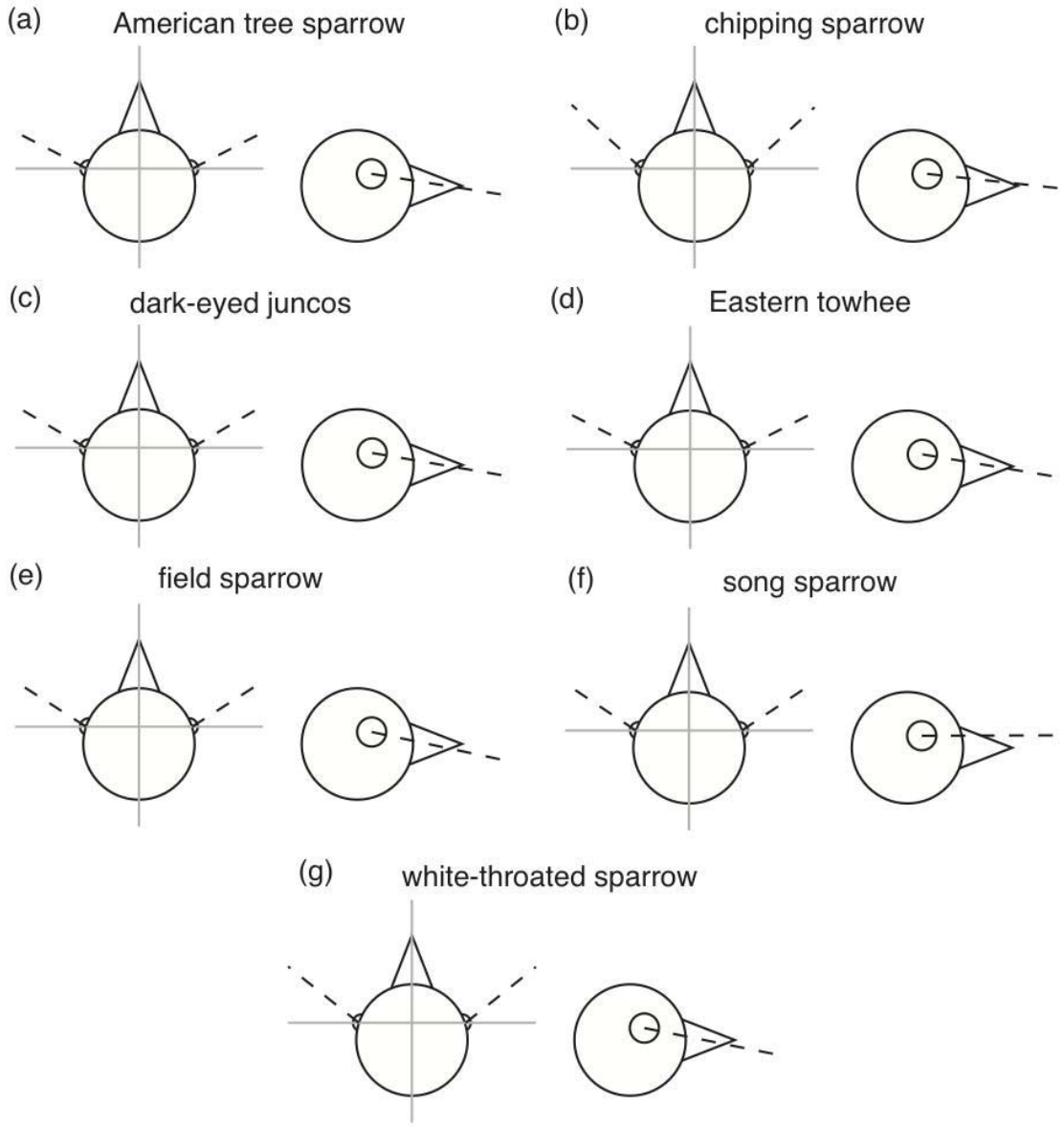

Fig 5.2 Schematic top- and side-view representations of the approximate angular projections of the foveae into the visual field (dashed-dotted lines; see assumptions in Methods) for (a) American tree sparrows, (b) chipping sparrows, (c) dark-eyed juncos, (d) Eastern towhees, (e) field sparrows, (f) song sparrows, and (g) white-throated sparrows. The triangle represents the beak, the vertical dashed line represents the axis passing through the center of the beak, and the horizontal dashed line represents the axis passing through the posterior nodal point of both eyes.

5.4.3 Visual field configuration and degree of eye movement

At the horizontal plane with the eyes at rest, the width of the binocular field varied by 11° among species (from 33° in the Eastern towhee to 44° in the chipping sparrow, Appendix 4-A1). Considering all recorded elevations, we found significant differences in the width of the binocular field among species (species, $F_{6,49} = 3.41$, $P = 0.007$; elevation, $F_{19,665} = 133.62$, $P < 0.001$, Fig. 3, Appendix 4-A2), with white-throated sparrows having the highest values (Table 1). At the horizontal plane with the eyes at rest, the width of the blind area varied by 15° among species (from 31° in the dark-eyed junco to 46° in the field sparrow, Appendix 4-A1). Taking into account all recorded elevations, the width of the blind area differed significantly among species (species, $F_{6,43} = 24.53$, $P < 0.001$; elevation, $F_{10,322} = 61.55$, $P < 0.001$; Appendix 4-A2), from 17° in the white-throated sparrow to 27° in the field sparrow (Table 1).

Considering all recorded elevations, we found significant differences in the degree of eye movement among species (species, $F_{6,43} = 24.53$, $P < 0.001$; elevation, $F_{10,322} = 61.55$, $P < 0.001$; Appendix 4-A3), from 22° in the American tree sparrow to 36° in the field sparrow (Table 1). The differential ability to move the eyes changed the configuration of the visual fields of each of the species when the eyes were either converged or diverged. When the eyes converged, the width of the binocular field increased substantially, varying from 53° in the American tree sparrow to 69° in the Eastern towhee along the horizontal plane (Appendix 4-A4). In all species but one (American tree sparrow) individuals converged their eyes to the degree that they could see their bill tips, but only in the converged position (Appendix 4-A5). When the eyes diverged, visual coverage increased in all species due to a reduction in the width of the blind area, which varied along the horizontal plane from 1° in the chipping and field sparrows to 18° in the American tree sparrow.

Finally, the width of the projection of the pecten (i.e., blind spot in the upper and frontal part of the visual field) across all measured elevations with the eyes at rest varied significantly between species ($F_{6,36} = 18.01$, $P < 0.001$; elevation, $F_{7,228} = 60.68$, $P < 0.001$, Fig. 3), from 15° in the American tree sparrow to 27° in the Eastern towhee (Table 1).

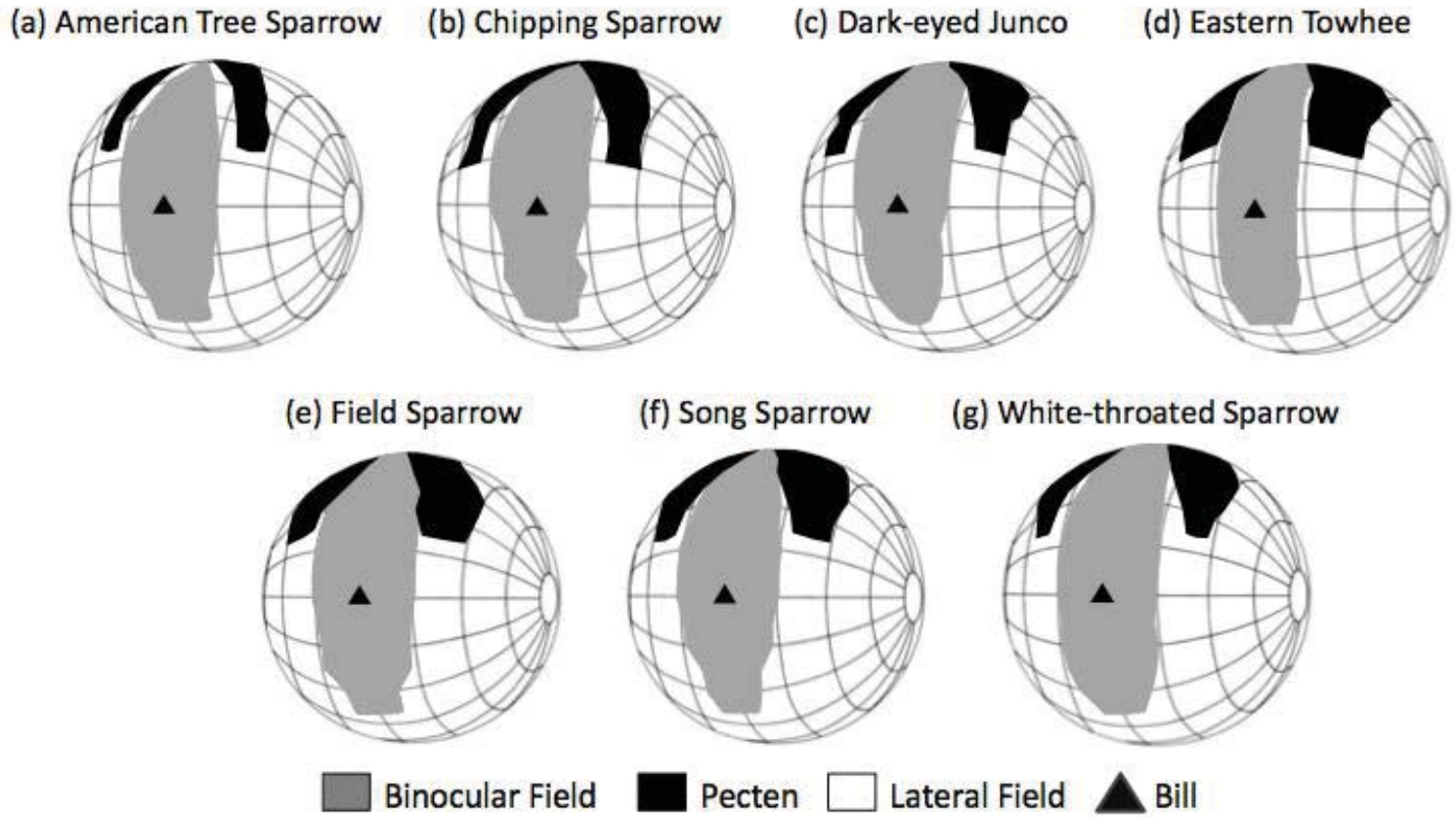

Fig 5.3 Orthographic projection of the boundaries of the two retinal fields around the head of an animal while the eyes are in a resting position for (a) American tree sparrows, (b) chipping sparrows, (c) dark-eyed juncos, (d) Eastern towhees, (e) field sparrows, (f) song sparrows, and (g) white-throated sparrows. Values are averaged across all individuals measured per species. A latitude and longitude coordinate system was used with the head of the animal at the center of the globe. The grid is set at 20° intervals, and the equator aligned vertically in the median sagittal plane (the horizontal plane, 90° - 270°). The projections of the pecten produce a blind spot in the upper, frontal field. The projection of the bill tips are presented for orientation purposes.

5.4.4 Visual space of emberizid sparrows

We included in the PCCA the following visual traits: binocular field across all recorded elevations with eyes at rest, blind area across all recorded elevations with eyes at rest, width of the pecten across all recorded elevations, eye axial length, highest retinal ganglion cell (RGC) density, and average slope of change in RGC density from the retinal periphery to the fovea. The PCCA identified two factors with eigenvalues higher than 1: factor 1 accounted for 57.63% of the variation, whereas factor 2, for 20.11%. Table 2 shows the correlations between the visual variables and factors 1 and 2 (see also Fig 4a). Factor 1 was bounded by eye axial length and the width of the binocular field (positive values) and by the highest RGC density and the slope of change in RGC density across the retina (negative values; Fig. 4a). Factor 2 was bounded by pecten width (positive values) and the width of the blind area and the binocular field (negative values; Fig. 4a). California towhees and white-crowned sparrows grouped together as species with wide binocular fields (Fig. 4b). Eastern towhees, dark-eyed juncos, song sparrows, and white-crowned sparrows grouped together as species with wide pectens (Fig. 4b). Finally, field sparrows, chipping sparrows, and American tree sparrows grouped together as species with wide blind areas, high RGC densities, and steep slopes of RGC density change across the retina (Fig. 4b).

Table 5.2 Results from the Principal Component Classification Analysis (PCCA) to establish the visual space of emberizid sparrows. (a) Correlations between six visual variables and the two factors identified by the PCCA with eigenvalues > 1. (b) Case contributions (based on correlations) of each species to factors 1 and 2. See also Fig. 4.

(a)

Visual variables	Factor 1	Factor 2
Binocular field across elevations (at rest)	0.88	-0.36
Blind area across elevations (at rest)	-0.48	-0.39
Pecten with across elevations (at rest)	-0.26	0.87
Eye axial length	0.77	0.41
Highest RGC density	-0.98	0.00
Mean slope of variation in ganglion cell density from retinal periphery to fovea	-0.90	-0.05

(b)

Species	Factor 1	Factor 2
American tree sparrow (AMTS)	3.30	18.57
California towhee (CATW)	36.46	0.03
Chipping sparrow (CHSP)	19.67	12.76
Dark-eyed junco (DEJU)	0.05	11.56
Eastern towhee (EATW)	1.89	24.24
Field sparrow (FISP)	12.05	1.50
Song sparrow (SOSP)	0.35	6.05
White-crowned sparrow (WCSP)	26.12	18.99
White-throated sparrow (WTSP)	0.10	6.30

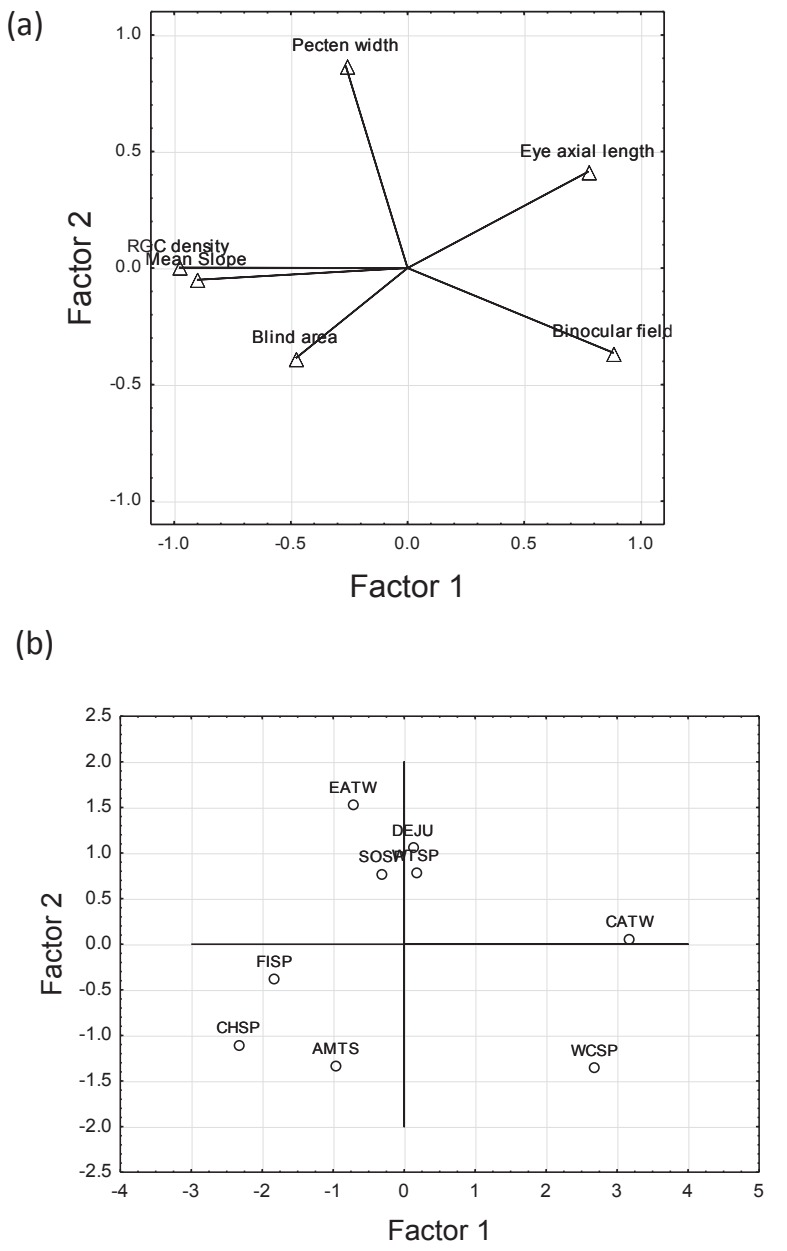

Fig 5.4 Modeled visual space (Principal Component Classification Analysis) of emberizid sparrows based on six visual traits: binocular field at rest across elevations (binocular field), blind area at rest across elevations (blind area), pecten width at rest across elevations (pecten width), eye axial length, highest retinal ganglion cell density (RCG density), and mean slope of variation in ganglion cell density from retinal periphery to fovea in the nasal, temporal, dorsal and ventral retinal directions (Mean slope). (a) Alignment of visual variables along the two factors identified by the PCCA. (b) Positioning of the nine emberizid sparrows along the visual space defined by factors 1 and 2. Species abbreviations are the same as those in Table 2.

5.4.5 Bill size

Bill length ($F_{8,101} = 157.58$, $P < 0.001$), width ($F_{8,101} = 61.85$, $P < 0.001$), and depth ($F_{8,101} = 112.87$, $P < 0.001$) varied significantly among the nine species of emberizid sparrows (Appendix 5). Using these three variables, our PCA produced a single factor (hereafter, bill size; Eigenvalue = 2.92) that accounted for 97.41% of the variability in the data. Bill length (factor score = - 0.990), bill depth (factor score = - 0.988), and bill width (factor score = - 0.983) were negatively correlated with PC1 so that smaller values indicated larger bills. Overall, bill size increased in the following order: chipping sparrow, field sparrow, dark-eyed junco, American tree sparrow, white-crowned sparrow, white-throated sparrow, song sparrow, Eastern towhee, and California towhee (Appendix 5). Bill size was significantly correlated with body mass ($r = -0.91$, $P < 0.001$), such that larger species had larger bills.

5.4.6 Binocular field width and bill size

Using raw species data, we found that there was no significant association between the bill size and the width of the binocular field with the eyes at rest ($F_{1,7} = 0.26$, $P = 0.627$, $R^2 = 0.04$) and with the eyes converged ($F_{1,7} = 0.92$, $P = 0.369$, $R^2 = 0.12$) at the plane of the bill. We found similar non-significant results when controlling for phylogenetic effects: width of the binocular field with the eyes at rest vs. bill size ($F_{2,7} = 0.95$, $P = 0.432$, $R^2 = 0.12$, coefficient 1.34 ± 1.37, $\lambda = 0$), and width of the binocular field with the eyes converged vs. bill size ($F_{2,7} = 0.23$, $P = 0.793$, $R^2 = 0.03$, coefficient 1.58 ± 3.23, $\lambda = 0$).

5.4.7 Pecten size, binocular field width, and degree of eye movement

As predicted, we found a negative association between pecten size across all elevations and binocular field width with the eyes at rest at the plane of the bill using raw species data ($F_{1,7} = 6.90$, $P = 0.034$, $R^2 = 0.49$) as well as controlling for phylogenetic effects ($F_{2,7} = 7.34$, $P = 0.019$, $R^2 = 0.51$, coefficient -0.70 ± 0.26, $\lambda = 0$). Thus, species with wider pecten projections tended to have narrower binocular fields (Fig. 5a). This prediction assumes a negative association between the width of the binocular field with the eyes at

rest and the width of the binocular field with the eyes converged at the plane of the bill, which was significant using raw species data ($F_{1,7} = 9.42$, $P = 0.018$, $R^2 = 0.57$) as well as controlling for phylogenetic effects ($F_{2,7} = 9.76$, $P = 0.009$, $R^2 = 0.58$, coefficient -1.71 ± 0.55, $\lambda = 0$). Overall, species with wider binocular fields with the eyes at rest tended to converge their eyes less into the binocular field (Fig. 5b).

We also found support for the second prediction: a significant and positive association between the width of the pecten across all elevations and the degree of eye movement across all elevations using raw species data ($F_{1,7} = 2.89$, $P = 0.023$, $R^2 = 0.54$) and controlling for phylogenetic effects ($F_{2,7} = 9.09$, $P = 0.011$, $R^2 = 0.56$, coefficient 1.89 ± 0.63, $\lambda = 0$). Thus, species with wider pectens tended to move their eyes more (Fig. 5c).

5.4.8 Blind spots and eye size

Using raw species data, we found no significant association between the width of the blind area across all elevations with the eyes at rest and (log10) eye axial length ($F_{1,7} = 1.95$, $P = 0.205$, $R^2 = 0.21$). We obtained a similar non-significant result controlling for the effects of phylogeny ($F_{2,7} = 1.89$, $P = 0.219$, $R^2 = 0.21$, coefficient -29.45 ± 21.38, $\lambda = 0$). Similarly, the width of the pecten across all elevations was not significantly associated with (log10) eye axial length, using raw species data ($F_{1,7} = 0.07$, $P = 0.797$, $R^2 = 0.01$) and controlling for phylogenetic effects ($F_{2,7} = 0.06$, $P = 0.945$, $R^2 = 0.01$, coefficient 5.72 ± 23.96, $\lambda = 0$).

5.4.9 Visual coverage and visual acuity

Using raw species data, we found no significant relationship between visual acuity and the width of the cyclopean field (i.e., lateral plus binocular fields) at the horizontal plane with the eyes at rest ($F_{1,7} = 2.53$, $P = 0.156$, $R^2 = 0.27$). A similar non-significant result was found controlling for the effects of phylogeny ($F_{2,7} = 2.50$, $P = 0.151$, $R^2 = 0.26$, coefficient 2.93 ± 1.85, $\lambda = 0.73$). We decided to further assess this relationship but considering each component of the cyclopean field separately (binocular and lateral fields) due to the significant interspecific differences found above in the width of the binocular field.

Using the raw species data, visual acuity was significantly and negatively associated with the width of the binocular field at the horizontal plane with the eyes at rest ($F_{1,7} = 9.51$, $P = 0.018$, $R^2 = 0.56$). We found a similar significant and negative relationship when accounting for phylogenetic effects ($F_{2,7} = 8.95$, $P = 0.012$, $R^2 = 0.56$, coefficient -3.53 ± 1.18, $\lambda = 0$). Additionally, visual acuity was significantly and positively associated with width of the lateral field at the horizontal plane with the eyes at rest using raw species data ($F_{1,7} = 7.41$, $P = 0.030$, $R^2 = 0.51$) and phylogenetically controlled data ($F_{2,7} = 6.82$, $P = 0.023$, $R^2 = 0.49$, coefficient 3.43 ± 1.32, $\lambda = 0$). Overall, species with higher visual acuity tended to have narrower binocular fields (Fig. 5d), but wider lateral areas (Fig. 5e).

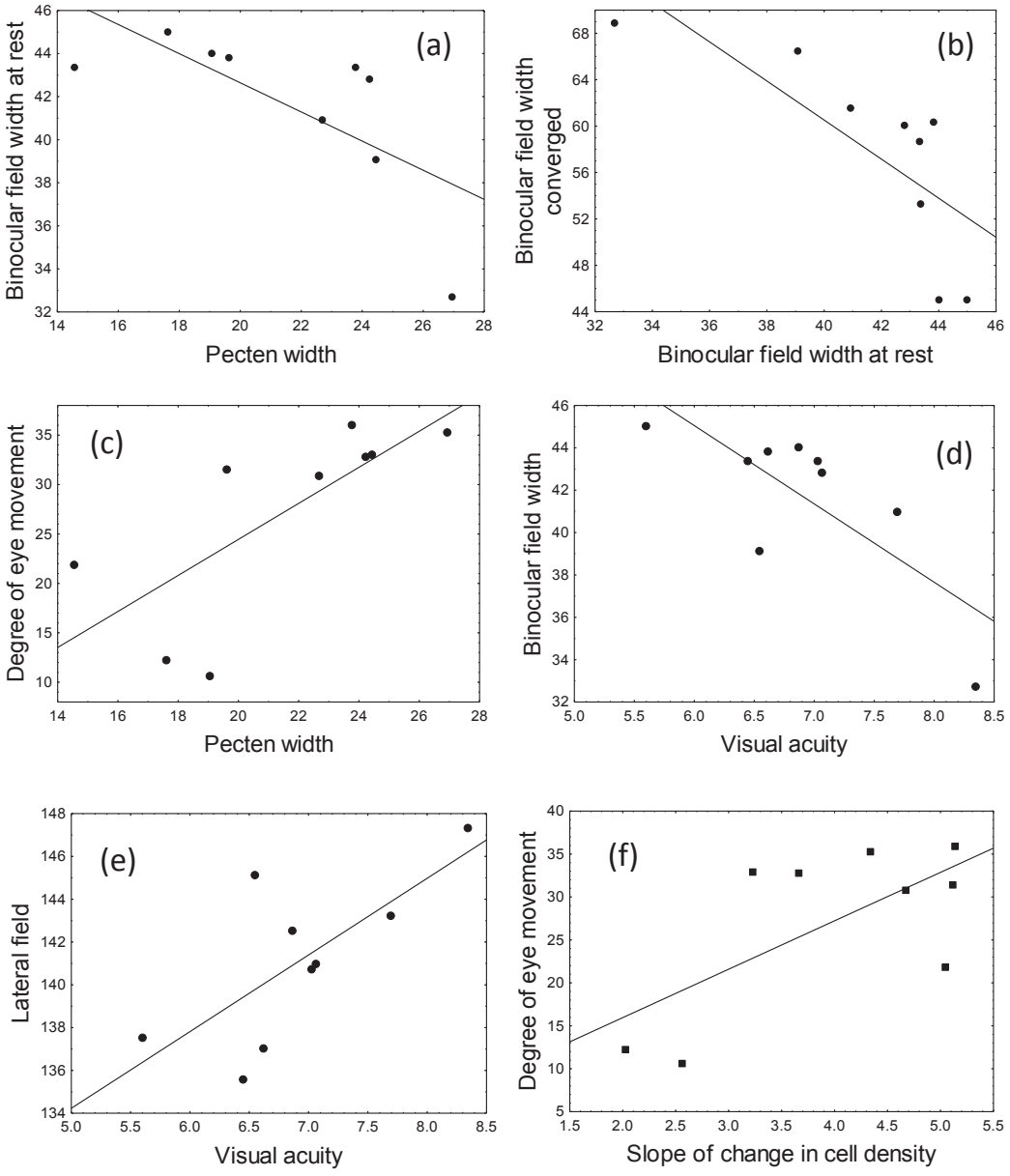

Fig 5.5 Scatterplots showing the relationships (raw species data) between different visual traits in nine emberizid sparrows: (a) binocular field width at the horizontal plane with eyes at rest (°) vs. pecten width across elevations (°); (b) binocular field width (°) at the horizontal plane with the eyes converged vs. binocular field width at the horizontal plane with eyes at rest (°); (c) degree of eye movement across elevations (°) vs. pecten width across elevations (°); (d) binocular field width at the horizontal plane with eyes at rest (°) vs. visual acuity (cycles/degree); (e) lateral field width at the horizontal plane with eyes at rest (°) vs. visual acuity (cycles/degree); and degree of eye movement across elevations (°) vs. averaged slope of change in cell density across the retina (considering the temporal, frontal, ventral, dorsal retinal areas).

5.4.10 Retinal configuration and degree of eye movements

Using the raw species data, we found that the mean slope of the change in RGC density from the retinal periphery to the fovea was positively associated with the degree of eye movements across all elevations ($F_{1,7} = 5.77$, $P = 0.047$, $R^2 = 0.45$; Fig. 5f). Controlling for phylogenetic effects, we found a similar significant relationship ($F_{2,7} = 6.48$, $P = 0.026$, $R^2 = 0.48$, coefficient 5.75 ± 2.26, $\lambda = 0$). Therefore, species with steeper cell density profiles tended to have a larger degree of eye movements.

5.5 Discussion

In general terms, emberizid sparrows show some convergence in some visual traits identified previously in other Passeriformes that detect and consume their prey at close distances: (a) a single retinal center of acute vision (fovea) on each eye with fronto-lateral projection into the lateral field, (b) a relatively wide binocular visual field, (c) a bill projecting towards the binocular field with the eyes at rest, and (d) a relatively large degree of eye movement. However, our results also show that emberizid sparrows have an interesting visual field specialization: when they converge their eyes to widen their binocular fields, the bills of most of the studied species intrude into the area of binocular overlap. Functionally, this means that these sparrows would be able to see their bill tips. This is contrary to the binocular field configuration proposed for birds with ballistic pecking towards seeds (Martin 2014), like these emberizid sparrows during the winter. The implication is that sparrows have the ability to modify their visual field configuration through eye movements to visually inspect the prey items held between their mandibles. This is characteristic of a few bird species that use their bills for precision-gasping (e.g., European starlings *Sturnus vulgaris*, Martin 1986; white-breasted nuthatches *Sitta carolinensis*, Moore et al. 2013; Eastern meadowlark *Sterna magna*, Tyrrell et al. 2013). For emberizid sparrows, visualizing the bill tip may come particularly relevant during the breeding season, when their diet shifts strongly towards catching insects, hence identifying prey (type, size, etc.) may optimize their parental investment. This finding

emphasizes the functional relevance (and flexibility) of the Passeriform binocular field for foraging purposes.

Interestingly, we found a relatively large degree of inter-specific variability in several visual traits in emberizid sparrows despite being closely related phylogenetically (Carson and Spicer 2003). The nine species diverged along two main axes in the modeled visual space (Fig. 4): one considering eye size, binocular field width, and ganglion cell density, and the other considering the widths of the pecten and the blind area. This suggests that the visual sensory inputs of emberizid sparrows differ in key dimensions linked to visual perception (e.g., visual acuity, binocular vision, visual coverage, variation in visual resolution across the visual field, etc.). Associating between-specific variation in visual traits with that in behavior could be challenging given the overlap in foraging and anti-predator strategies between the studied species (Appendix 1), although we can highlight some patterns. Species that had the highest visual acuity (relative to body mass) most commonly preyed upon flying insects (Eastern towhee, white-throated sparrow, and American tree sparrow; Appendix 1). Capture of swiftly moving prey is associated with higher visual resolution (Garamszegi *et al.* 2002). On the other hand, the emberizid sparrows with the lowest visual acuity (relative to body mass) do not generally pursue flying prey (dark-eyed junco, field sparrow, chipping sparrow, Appendix 1). Additionally, species with relatively higher visual acuity (towhees and song sparrows) tend to be more territorial compared to species with relatively lower acuity, which tend to flock more (field sparrows, dark-eyed juncos; Goodson et al. 2012). The implication is that the emberizid sparrows with lower visual acuity, and thus lower probabilities of detecting predators from far away (Tisdale and Fernández-Juricic 2009) may reduce perceived predation risk by joining groups, hence benefiting from dilution and collective detection effects (Krause and Ruxton 2002).

Our study provided the opportunity to identify for the first time associations between different visual sensory dimensions in birds, which can help explain how these emberizid sparrows solve specific perceptual tasks related to seeking food and detecting predators. This is relevant because some species may be more constrained than others in some sensory inputs (e.g., lower visual acuity, lower degree of visual coverage, etc.),

which could influence their decision-making in different ecological contexts (Fernández-Juricic et al. 2004).

The size of the pecten varied significantly between species. Sparrows with larger pectens could be constrained in terms of visual coverage due to the larger blind spot within the visual field (above the fovea). Furthermore, the size of the pecten may limit the spatial extent of binocular vision: species with larger pectens have narrower binocular fields with the eyes at rest. Our findings suggest that this sensory challenge may be solved by moving the eyes: species with larger pectens have a larger degree of eye movement that allows them to converge their eyes and widen their binocular fields. On the other end of the continuum, species with narrower pectens have wider binocular fields with the eyes at rest and a lower degree of eye movement, probably because of the lower need to converge their eyes. Consequently, maintaining a relatively large degree of binocular vision (between approximately 45° and 65°) may have important functional consequences for emberizid sparrows in terms of finding and manipulating food items.

Most of the studied species have temporally placed centers of acute vision (i.e., foveae) that project into the lateral fields near the edges with the binocular field (but not intruding into the binocular field itself with the eyes at rest). From a foraging perspective, this visual configuration would allow emberizid sparrows to explore the substrate using (a) binocular vision (subtended by the peripheral areas of the retina) when the bill is perpendicular to the substrate, and (b) the centers of acute vision with the eyes converged when moving the bill just a few degrees to the sides (Fig. 6). Combining the inputs of the wide binocular field with those of the foveae within a limited range of head movements could actually shorten the processing time of the three visual inputs, ultimately enhancing food detection and handling. This is in contrast to species with relatively narrower binocular fields and with centrally placed centers of acute vision (hence projecting more laterally; zebra finch, Bischof 1988), which would need a wider range of head movements to visually explore the foraging substrate (i.e., from bill pointing directly to the substrate to bill pointing almost laterally to align the fovea with the substrate; Fig. 6). Furthermore, by diverging their eyes while head-down, emberizid sparrows could project the centers of acute vision more laterally, thereby increasing the chances of detecting

potential threats (e.g., conspecifics trying to displace individuals from a foraging patch, predators, etc.) at farther distances given the higher visual acuity provided by the fovea.

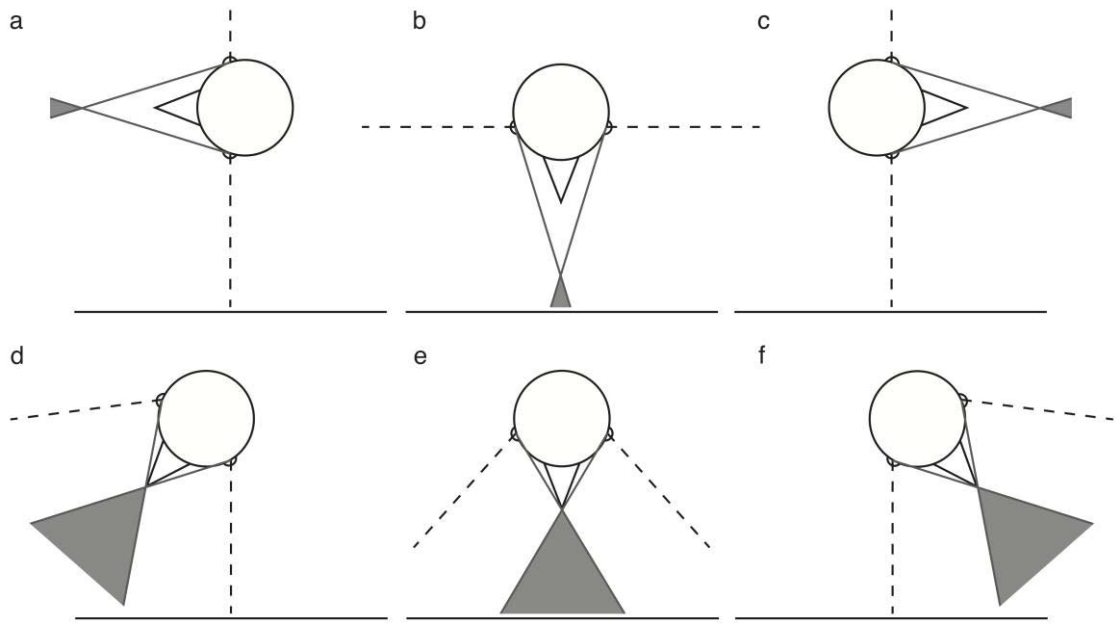

Fig 5.6 A hypothetical bird with a narrow binocular field and laterally projecting fovea inspecting a foraging substrate with the (a) left fovea, (b) binocular field, and (c) right fovea. A white-throated sparrow inspecting the foraging substrate with its eyes in a converged position with (d) left fovea, (e) binocular field, and (f) right fovea. The hypothetical bird must rotate its head 90º to switch from viewing with the fovea to the binocular field (a to b), and a total of 180º to switch from one fovea to the other (a to c). The white-throated sparrow, on the other hand, must only rotate its head 40º to switch between the fovea and the binocular field (d to e), and 80º to switch between foveae. Dotted lines represent the projections of the foveae from the right and left eyes. The shaded region represents the binocular field and the solid line at the bottom of the figure represents the foraging substrate.

Emberizid sparrows may then maximize visual sampling at close distances to the substrate with a wide binocular field and closely spaced centers of acute vision. Although the perception benefits of using the foveae are clear (e.g., higher quality visual information), the contribution of the binocular field is still unclear given that it is subtended by areas of the retina with lower density of ganglion cells and photoreceptors (Martin 2009, 2014). One possibility is that the summation of the right and left visual inputs enhances contrast discrimination when the bill is perpendicular to the substrate (Heesy 2009), which could increase the ability of individual to resolve food items from the background. Another possibility is that the binocular overlap improves the ability to guide spatially and temporally the bill into the substrate to increase the precision to grab a food item (Martin 2009). Irrespective of the mechanism, we speculate that when head-down foraging, emberizid sparrows may have to juggle their visual attention among three visual inputs (binocular field, right fovea, left fovea). How this is accomplished is a matter of acute interest for future research given the visual and behavioral differences between sparrows that detect prey at close distances and other Passeriformes that detect prey at far distances while in perches (e.g., flycatchers, Gall and Fernández-Juricic 2009, Coimbra et al. 2006, 2009).

Along a different visual axis, we found that emberizid sparrows with narrower binocular fields with the eyes at rest also have higher visual acuity and wider lateral visual fields. This is contrary to the idea accepted in the vertebrate literature that species with relatively lower visual acuity should have wider visual coverage (Hughes 1977). One possibility is that higher acuity and wider lateral visual coverage may compensate for the wider blind spots in the visual field (i.e., pectens) of these species (see above). Additionally, visual acuity is positively associated with body mass in birds (Kiltie 2000). Given their body mass range, larger emberizid sparrows may be subject to higher predation rates from aerial predators (e.g., Gotmark and Post 1996; Roth et al. 2006), and thus may benefit from enhanced predator detection from farther away and from wider areas of visual coverage around their heads. However, the larger species (Eastern towhee, California towhee, and white-throated sparrow) tend to forage in more covered or dense habitats (Appendix 1), which would help hide them from aerial attacks. Alternatively,

this combination of visual traits (narrower binocular fields, wider lateral fields, higher acuity) may be related to temporarily exploiting some resources that smaller sparrows (i.e., lower visual acuity) may not use, such a swiftly flying insects, as suggested above.

A large degree of eye movement appears to be a common characteristic of Passeriformes (e.g., Fernández-Juricic et al. 2008). We found that at least part of the variation in eye movement in emberizid sparrows may be accounted for by the configuration of the retina. Cell density profiles provide a proxy of the variation in visual resolution across the retina (hence, across the visual field). In general, ganglion cell density is the highest around the fovea and decreases towards the retinal periphery (Fig. 1). Yet this decrease in cell density could be more or less pronounced, leading to a higher or lower, respectively, difference in cell density between the fovea and the retinal periphery (Moore et al. 2012). Our results provide the first empirical evidence, controlling for phylogenetic effects, that species with greater difference in cell density between the fovea and retinal periphery (i.e., higher slopes) have a greater degree of eye movement. Species with higher cell density difference have been hypothesized to rely more on the center of acute vision for gathering high quality information due to the relatively lower levels of visual resolution elsewhere in the retina (Dolan and Fernández-Juricic 2010), which would lead to a greater need to move the eyes to get snapshots of high visual resolution from different parts of the visual environment (Fernández-Juricic et al. 2011). Species with lower cell density difference may have a proportionally greater area of the retina with high visual resolution, and thus the need for eye movement may be reduced (Fernández-Juricic et al. 2011). Future research should determine if the covariation between retinal configuration and eye movement could affect the prevalence of different types of visual attention mechanisms, such as overt (centered around the fovea) and covert (centered in the retinal periphery) attention (Bisley 2011).

We also found that some proposed associations between visual traits were not as strong in emberizid sparrows as in non-Passeriformes. For example, we did not find the relationship between eye size and blind area width predicted by the glare hypothesis (Martin and Katzir 2000). This could be related to our low sample size (i.e., nine species). Alternatively, the eye size range of emberizid sparrows may not be as strongly affected

by imaging the sun as those species with much larger eyes (Martin 2014), which generally exhibit sunshade structures like eye lashes (Martin and Coetzee 2004). This is not to say that glare does not affect relatively small species (e.g., Fernández-Juricic et al. 2012), but emberizid sparrow may use behavioral strategies to minimize these effects, such as avoiding sunlit patches, decreasing head-up vigilance bouts, and aligning the pecten with the sun (Fernández-Juricic and Tran 2007; van den Hout and Martin 2011).

5.6 Conclusions

Based on our findings as well as previous studies (Fernández-Juricic et al. 2011), the retina of Passeriformes have several specializations to enhance visual resolution at the local level (fovea), which co-vary with the visual field configuration and eye movement. For emberizid sparrows, the highlights of their visual system consist of a single fovea projecting into the lateral field close to the edges of the binocular field, a wide binocular field (with eyes at rest or converged), eye convergence to see prey items held in the bill, and a pecten that may constrain visual coverage above the fovea. Emberizid sparrows vary in several visual traits, but they exhibit strategies to change visual configurations (mostly through eye movements) that would maximize food detection and food handling at close distances from the foraging substrate as well as gather quickly high quality information around their heads to detect threats (e.g., predators). This visual configuration is considerably different from those reported previously in other groups of birds, such as sit-and-wait foragers (two centers of acute vision, high visual acuity, narrow binocular fields, wide blind areas, low eye movement amplitude; Coimbra et al. 2006, 2009; Jones et al. 2007; O'Rourke et al. 2010a, b) and tactile foragers (low visual acuity, narrow binocular fields, bill does not project into binocular field; Martin 1994, Martin et al., 2007). Consequently, we propose that the visual system of avian passive prey foragers, particularly in Passeriformes, evolved to meet multiple sensory demands for foraging and predator detection purposes, particularly because their small eye sizes could limit their overall visual acuity compared to larger species.

5.8 Literature Cited

Baumhardt PE, Moore BA, Doppler M, and Fernández-Juricic E (2014). Do American goldfinches see their world like passive prey foragers? A study on visual fields, retinal topography, and sensitivity of photoreceptors. *Brain Behavior and Evolution* 83:181-198.

Birkhead T (2012). *Bird sense: what it's like to be a bird*. Bloomsbury, London.

Birkhead T, Wimpenny J, Montgomerie B (2014). *Ten thousand birds: ornithology since Darwin.* Princeton University Press, Princeton.

Bischof H-J (1988). The visual field and visually guided behavior in the zebra finch (Taeniopygia guttata). *Journal of Comparative Physiology A* 163:329-337.

Bisley JW (2011). The neural basis of visual attention. *The Journal of Physiology* 589:49–57.

Boughman JW (2002). How sensory drive can promote speciation. *Trends in Ecology and Evolution* 17:571-577.

Carson RJ & Spicer GS (2003). A phylogenetic analysis of the emberizid sparrows based on three mitochondrial genes. *Molecular Phylogenetics and Evolution* 29:43-57.

Coimbra JP, Trevia N, Marcelliano MLV, Andrade-da-Costa BLD, Picanco-Diniz CW, Yamada ES (2009). Number and distribution of neurons in the retinal ganglion cell layer in relation to foraging behaviors of tyrant flycatchers. *The Journal of Comparitive Neurology* 514:66-73.

Coimbra JP, Marceliano MLV, Andrade-da-Costa BLD, Yamada ES (2006). The retina of tyrant flycatchers: topographic organization of neuronal density and size in the ganglion cell layer of the great kiskadee *Pitangus sulphuratus* and the rusty marginated flycatcher *Myiozetetes cayanensis* (Aves: Tyrannidae). *Brain Behavior and Evolution* 68:15-25.

Collin SP (1999). Behavioural ecology and retinal cell topography. Pages 509-535 *in* S. Archer, M.B. Djamgoz, E. Loew, J.C. Partridge and S. Vallerga, ed. *Adaptive Mechanisms in the Ecology of Vision*. Kluwer Academic Publishers, Dordrecht.

Cuthill IC (2006). Color perception. In G.E. Hill, and K.J. McGraw, ed. *Bird coloration: mechanisms and measurements.* Harvard University Press, Cambridge.

Dalton BE, Cronin TW, Marshal NJ, Carleton KL (2010). The fish eye view: Are cichlids conspicuous? *Journal of Experimental Biology* 213:2243-55.

Dolan T & Fernández-Juricic E (2010). Retinal ganglion cell topography of five species of ground foraging birds. *Brain Behavior and Evolution* 75:111-121.

Ehrlich D (1981). Regional specialization of the chick retina as revealed by the size and density of neurons in the ganglion cell layer. *The Journal of Comparative Neurology* 195:643-657.

Elphick C, Dunning Jr JB, Sibley DA (2001). *The Sibley guide to bird life and behavior*. National Audubon Society, Alfred A. Knopf, New York.

Fernández-Juricic E, Moore BA, Doppler M, Freeman J, Blackwell BF, Lima SL, DeVault TL (2011b). Testing the terrain hypothesis: Canada geese see their world laterally and obliquely. *Brain Behavior and Evolution* 77:147-158.

Fernández-Juricic E, Erichsen JT, Kacelnik A (2004). Visual perception and social foraging in birds. *Trends in Ecology and Evolution* 19:25-31.

Fernández-Juricic E, Gall MD, Dolan T, Tisdale V, Martin GR (2008). The visual fields of two ground foraging birds, House finches and house sparrows, allow for simultaneous foraging and anti-predator vigilance. *Ibis* 150:779-787.

Fernández-Juricic E, O'Rourke CT, Pitlik T (2010). Visual coverage and scanning behavior in two corvid species: American crow and Western scrub jay. *Journal of Comparative Physiology A* 196:879-888.

Fernández-Juricic E, Gall MD, Dolan T, O'Rourke C, Thomas S, Lynch JR (2011). Visual systems and vigilance behaviour of two ground-foraging avian prey species: white-crowned sparrows and California towhees. *Animal Behaviour* 81:705-713.

Fernández-Juricic E, Deisher M, Stark AC, Randolet J (2012). Predator detection is limited in microhabitats with high light intensity: an experiment with brown-headed cowbirds. *Ethology* 188:341-350.

Fernández-Juricic E & Tran E (2007). Changes in vigilance and foraging behaviour with light intensity and their effects on food intake and predator detection in house finches. *Animal Behaviour* 74:1381-1390.

Freeman B & Tancred E (1978). The number and distribution of ganglion cells in the retina of the brush-tailed possum, *Trichosurus vulpecula. The Journal of Comparative Neurology* 177:557-67.

Garamszegi LZ, Møller AP, Erritzoe J (2002). Coevolving avian eye size and brain size in relation to prey capture and nocturnality. *Proceedings of the Royal Society of London B: Biological Sciences* 269:961-967.

Gall MD & Fernández-Juricic E (2010). Visual fields, eye movements, and scanning behavior of a sit-and-wait predator, the Black Phoebe (*Sayornis nigricans). Journal of Comparative Physiology A* 196:15-22.

Goodson JL, Wilson LC, Schrock SE (2012). To flock or fight: Neurochemical signatures of divergent life histories in sparrows. *Proceedings of the National Academy of Sciences of the United States of America* 109:10685-10692.

Gotmark F & Post P (1996). Prey selection by sparrowhawks, Accipiter nisus: relative predation risk for breeding passerine birds in relation to their size, ecology and behaviour. *Philosophical Transactions of the Royal Society of London B: Biological Sciences* 351:1559-1577.

Heesy CP (2009). Seeing in stereo: The ecology and evolution of primate binocular vision and stereopsis. *Evolutionary Anthropology* 18:21-35.

Holden AL, Hayes BP, Fitzke FW (1987). Retinal magnification factor at the ora terminalis: a structural study of human and animal eyes. *Vision Research* 27:1229–1235.

Hughes A (1977). The topography of vision in mammals of contrasting life style: comparative optics and retinal organization. Pages 615-756 *in* F. Crescitelli, ed. *The visual system in vertebrates*. Springer-Verlag, New York.

Inzunza O, Bravo H, Smith RL, Angel M (1991). Topography and morphology of retinal ganglion-cells in Falconiforms: A study on predatory and carrion-eating birds. *Anatomical Record* 229:271-277.

Jones MP, Pierce Jr KE, Ward D (2007). Avian vision: a review of form and function with special consideration to birds of prey. *Journal of Exotic Pet Medicine* 16:69-87.

Kiltie RA (2000). Scaling of *visual acuity* with body size in mammals and birds. *Functional Ecology* 14:226–234.

Koch DD (1989). Glare and contrast sensitivity testing in cataract patients. *Journal of Cataract and Refractive Surgery* 15:158-164.

Krause J & Ruxton GD (2002). Living in Groups. Oxford University Press, Oxford.

Martin GR (1986). The eye of a passeriform bird, the European starling (*Sturnus vulgaris*): eye movement amplitude, visual fields and schematic optics. *Journal of Comparative Physiology* 159:545-547.

Martin GR (1984). The visual fields of the tawny owl, Strix aluco L. *Vision Research* 24:1739–1751.

Martin GR (1993). Producing the image. Pages 5-24 *in* H.P. Zeigler, and H-J. Bischof, ed. *Vision, brain and behaviour in birds*. MIT press, Massachusetts.

Martin GR (1994). Visual fields in woodcocks *Scolopax rusticola* (Scolopacidae: Charadriiformes). *Journal of Comparative Physiology A* 174:787-793.

Martin GR (2007). Visual fields and their functions in birds. *Journal of Ornithology* 148:S547-S562.

Martin GR (2012). Through bird's eyes: insights into avian sensory ecology. *Journal of Ornithology* 153(Suppl. 1): S23-S48.

Martin GR (2014). The subtlety of simple eyes: the tuning of visual fields to perceptual challenges in birds. *Philosophical Transactions of the Royal Society of London B: Biological Sciences* 369:20130040.

Martin GR & Prince PA (2001). Visual fields and foraging in procellariform seabirds: sensory aspects of dietary segregation. *Brain Behavior and Evolution* 57:33-38.

Martin GR (2009). What is binocular vision for? A birds' eye view. *Journal of Vision* 9:1-19.

Martin GR Coetzee HC (2004). Visual fields in hornbills: precision-grasping and sunshades. *Ibis* 146:18-26.

Martin GR & Katzir G (2000). Sun shades and eye size in birds. *Brain Behavior and Evolution* 56:340-344.

Martin GR, Jarrett N, Williams M (2007). Visual fields in blue ducks *Hymenolaimus malacorhynchos* and pink-eared ducks *Malacorhynchus membranaceus*: visual and tactile foraging. *Ibis* 149:112–120.

McIlwain JT (1996). *An introduction to the biology of vision*. Cambridge University Press, New York.

Meyer DBC (1977). The avian eye and its adaptations. Pages 549-612 *in* F. Crescitelli, ed. *The visual system of vertebrates; handbook of sensory physiology*. Springer, New York.

Mitkus M, Chaib S, Lind O, Kelber A (2014). Retinal ganglion cell topography and spatial resolution of two parrot species: budgerigar (*Melopsittacus undulatus*) and Bourke's parrot (*Neopsephotus bourkii*). *Journal of Comparative Physiology A* 200:371–384.

Moore BA, Kamilar JM, Collin SP, Bininda-Emonds ORP, Dominy NJ, Hall MI, Heesy CP, Johnsen S, Lisney TJ, Loew ER, Moritz G, Nava SS, Warrant E, Yopak KE, Fernández-Juricic E (2012). A novel method for comparative analysis of retinal specialization traits from topographic maps. *Journal of Vision* 12:1-24.

Moore BA, Doppler M, Young JE, Fernández-Juricic E (2013). Interspecific differences in the visual system and scanning behavior of three forest passerines that form heterospecific flocks. *Journal of Comparative Physiology A* 199:263-277.

Moroney MK & Pettigrew JD (1987). Some observations on the visual optics of kingfishers (Aves, Coraciformes, Alcedinidae). *Journal of Comparative Physiology A* 160:137-149.

Nunn C (2011). *The Comparative Approach in Evolutionary Anthropology and Biology*. University of Chicago Press, Chicago.

O'Rourke CT, Hall MI, Pitlik T, Fernández-Juricic E (2010a). Hawk eyes I: diurnal raptors differ in visual fields and degree of eye movement. *PLoS ONE* 5:e12802

O'Rourke CT, Pitlik T, Hoover M, Fernández-Juricic E (2010b). Hawk eyes II: diurnal raptors differ in head movement strategies when scanning from perches. *PLoS ONE* 5:e12169

Orme CDL, Freckleton RP, Thomas GH, Petzoldt T, Fritz SA (2011). caper: *Comparative Analyses of Phylogenetics and Evolution in R* (http://R-Forge.R-project.org/projects/caper/).

Pagel M (1999). Inferring the historical patterns of biological evolution. *Nature* 401:877–884.

Pettigrew JD, Dreher B, Hopkins CS, Mccall MJ, Brown M (1988). Peak density and distribution of ganglion-cells in the retinae of Microchiropteran bats - implications for visual-acuity. *Brain Behavior and Evolution* 32:39-56.

Reymond L (1985). Spatial visual acuity of the eagle, Aquila audax: a behavioural, optical and anatomical investigation. *Vision Research* 25:1477-1491.

Ricklefs RE (2012). Species richness and morphological diversity of passerine birds. *Proceedings of the National Academy of Sciences* 109:14482–14487.

Roth III TC, Lima SL, Vetter WE (2006). Determinants of predation risk in small wintering birds: the hawk's perspective. *Behavioral Ecology and Sociobiology* 60:195-204.

Safi K & Siemers BM (2010). Implications of sensory ecology for species coexistence: biased perception links predator diversity to prey size distribution. *Evolutionary Ecology* 24:703-713.

Seehausen O, Yerai Y, Magalhaes IS, Carleton KL, Mrosso HDJ, Miyagi R, Sluijs IVD, Schneider MV, Maan ME, Tachida H, Imai H, Okada N (2008). Speciation through sensory drive in cichlid fish. *Nature* 455:620-626.

Siemers BM & Swift SM (2006). Differences in sensory ecology contribute to resource partitioning in the bats *Myotis bechsteinii* and *Myotis nattereri* (Chiroptera: Vespertilionidae). *Behavioral Ecology and Sociobiology* 59:373-380.

StatSoft, Inc. 2013. *Electronic Statistics Textbook*. Tulsa, OK: StatSoft. WEB: http://www.statsoft.com/textbook/.

Stone J (1981). *The wholemount handbook. A guide to the preparation and analysis of retinal wholemounts*. Maitland Publishing, Sydney

Tyrrell LP, Moore BA, Loftis C, Fernández-Juricic E (2013). Looking above the prairie: localized and upward acute vision in a representative grassland bird. *Scientific Reports* 3:3231.

Tucker VA (2000). The deep fovea, sideways vision and spiral flight paths in raptors. *Journal of Experimental Biology* 203:3745-3754.

Tisdale V & Fernández-Juricic E (2009). Vigilance and predator detection vary between avian species with different visual acuity and coverage. *Behavioral Ecology* 20:936-945.

Ullmann JFP, Moore BA, Temple S, Fernández-Juricic E, Collin SP (2011). The retinal wholemount technique: a window to understanding the brain and behavior. *Brain Behavior and Evolution* 79:26-44.

Vakkur GJ, Bishop PO, Kozak W (1963). Visual optics in the cat, including posterior nodal distance and retinal landmarks. *Vision Research* 3:289-314.

Van der Hourt PJ & Martin GR (2011). Extreme head-tilting in shore birds: predator detection and sun-avoidance. *Wader Study Group Bulletin* 118:18-21.

Wathey JC & Pettigrew JD (1989). Quantitative analysis of the retinal ganglion cell layer and optic nerve of the Barn Owl *Tyto alba*. *Brain Behavior and Evolution* 33:279-292

Williams DR & Coletta NJ (1987). Cone spacing and the visual resolution limit. *Journal of the Optical Society of America A* 4:1514-1523

Willson MF (1971). Seed selection in some North American finches. *Condor* 73:415-229.

Yan X & Su XG (2009). *Linear regression analysis: theory and computing.* World Scientific Publishing, London.

5.9 Appendices

5.9.1 Appendix 1

Table 5.3 Habitat use, foraging methods, main food types, and usual predators of the nine emberizid sparrows used in this study.

Species	Habitat	Foraging methods	Food Type	Predators	Reference
American Tree Sparrow	Forest edge, open scrubby grasslands	Scratching, hopping, gleaning, darting, pecking	Seeds, berries, insects	Hawks, owls	Naugler 1993
California Towhee	Forest edge, scrubby, dense vegetation	Pecking, scratching, gleaning	Seeds more than other vegetable matter, some insects	Hawks, owls, ground predators	Benedict et al. 2011
Chipping Sparrow	Open grassy, forest edges, human landscapes	Scratching, pecking, hopping, running, by wing	Seeds, grasses, some insects, invertebrates	Hawks, owls, mammalian ground predators	Middleton 1998
Dark-eyed Junco	Forest edge, harvested fields, parks	Gleaning, pecking, scratching, hopping	Seeds and arthropods	Hawks, owls, jays, ground predators	Nolan et al. 2002
Eastern Towhee	Forest edge, dense shrubs	Double scratching, pecking, hovering, gleaning, hawking, aerial pursuit	Seeds, fruits, many invertebrates	Hawks	Greenlaw 1996
Field Sparrow	Fields, woodland openings, forest edges	Pecking, perching, pouncing	Primarily grass seeds, some insects	Hawks	Carey et al. 2008
Song Sparrow	Forest edge, scrubby fields	Double scratching, hawking, aerial capture, pecking	Seeds, fruits, invertebrates	Hawks, owls, mammalian ground predators	Arcese et al. 2002
White-crowned sparrow	Forest edge to tundra, grassy	Hawks from perch, scratching, pecking	Seeds, fruits, plants, insects	Hawks, owls, ground predators	Chilton et al. 1995
White-throated sparrow	Edge, forests, dense shrubs	Double scratching, pouncing, gleaning, aerial capture, pecking	Seeds, fruits, many insects	Hawks, owls, mammalian ground predators	Falls & Kopachena 2010

5.9.1.1 Literature Cited

Arcese P, Sogge MK, Marr AB, Patten MA (2002). Song Sparrow (*Melospiza melodia*), The *Birds of North America* Online (A. Poole, Ed.). Ithaca: Cornell Lab of Ornithology; Retrieved from the *Birds of North America* Online: http://bna.birds.cornell.edu/bna/species/704 doi:10.2173/bna.704

Benedict L, Kunzmann MR, Elliso K, Purcell KL, Johnson RR, Haight LT (2011). California Towhee (*Melozone crissalis*), The *Birds of North America* Online (A. Poole, Ed.). Ithaca: Cornell Lab of Ornithology; Retrieved from the *Birds of North America* Online: http://bna.birds.cornell.edu/bna/species/632 doi:10.2173/bna.632

Carey M, Carey M, Burhans DE, Nelson DA (2008). Field Sparrow (*Spizella pusilla*), The *Birds of North America* Online (A. Poole, Ed.). Ithaca: Cornell Lab of Ornithology; Retrieved from the *Birds of North America* Online: http://bna.birds.cornell.edu/bna/species/103 doi:10.2173/bna.103

Chilton G, Baker MC, Barrentine CD, Cunningham MA (1995). White-crowned Sparrow (*Zonotrichia leucophrys*), The *Birds of North America* Online (A. Poole, Ed.). Ithaca: Cornell Lab of Ornithology; Retrieved from the *Birds of North America* Online: http://bna.birds.cornell.edu/bna/species/183 doi:10.2173/bna.183

Falls JB & Kopachena JG (2010). White-throated Sparrow (*Zonotrichia albicollis*), The *Birds of North America* Online (A. Poole, Ed.). Ithaca: Cornell Lab of Ornithology; Retrieved from the *Birds of North America* Online: http://bna.birds.cornell.edu/bna/species/128 doi:10.2173/bna.128

Greenlaw JS (1996). Eastern Towhee (*Pipilo erythrophthalmus*), The *Birds of North America* Online (A. Poole, Ed.). Ithaca: Cornell Lab of Ornithology; Retrieved from the *Birds of North America* Online: http://bna.birds.cornell.edu/bna/species/262 doi:10.2173/bna.262

Middleton AL (1998). Chipping Sparrow (Spizella passerina), The *Birds of North America* Online (A. Poole, Ed.). Ithaca: Cornell Lab of Ornithology; Retrieved from the *Birds of North America* Online: http://bna.birds.cornell.edu/bna/species/334 doi:10.2173/bna.334

Naugler CT (1993). American Tree Sparrow (Spizella arborea), The *Birds of North America* Online (A. Poole, Ed.). Ithaca: Cornell Lab of Ornithology; Retrieved from the *Birds of North America* Online: http://bna.birds.cornell.edu/bna/species/037 doi:10.2173/bna.37

Nolan Jr V, Ketterson ED, Cristol DA, Rogers CM, Clotfelter ED, Titus RC, Schoech SJ Snajdr E (2002). Dark-eyed Junco (*Junco hyemalis*), The *Birds of North America* Online (A. Poole, Ed.). Ithaca: Cornell Lab of Ornithology; Retrieved from the *Birds of North America* Online: http://bna.birds.cornell.edu/bna/species/716 doi:10.2173/bna.716

5.9.2 Appendix 2

Table 5.4 Average number of grid sites deployed and eventually counted per retina, average asf (the ratio of the area of the counting frame to the area of the grid), average $\sum Q^-$ (sum of the total number of retinal ganglion cells counted), and average estimated total number of ganglion cells in the retina.

Species	# grid sites laid out	# grid sites counted	asf	$\sum Q^-$	Total RGCs
American tree sparrow	409.60 ± 2.84	378 ± 6	0.01247 ± 0.00379	22854.47 ± 1179.79	1841750.57 ± 120425.95
Chipping sparrow	410.75 ± 2.87	379 ± 9	0.01576 ± 0.00054	22292.99 ± 1615.64	1409253.08 ± 54827.08
Dark-eyed junco	406.80 ± 3.71	357 ± 11	0.01216 ± 0.00024	16492.90 ± 1292.92	1359735.79 ± 112505.59
Eastern towhee	413.00 ± 0.00	398 ± 7	0.00673 ± 0.00026	18353.67 ± 106.00	2732432.00 ± 90908.16
Field sparrow	407.20 ± 4.24	390 ± 6	0.01491 ± 0.00065	20284.00 ± 1092.44	1362862.54 ± 57873.74
Song sparrow	406.80 ± 1.24	377 ± 7	0.01082 ± 0.00038	17758.40 ± 809.07	1645727.81 ± 78272.79
White-throated sparrow	409.00 ± 3.34	376 ± 9	0.01133 ± 0.00052	19188.50 ± 697.35	1705752.48 ± 109274.70

5.9.3 Appendix 3

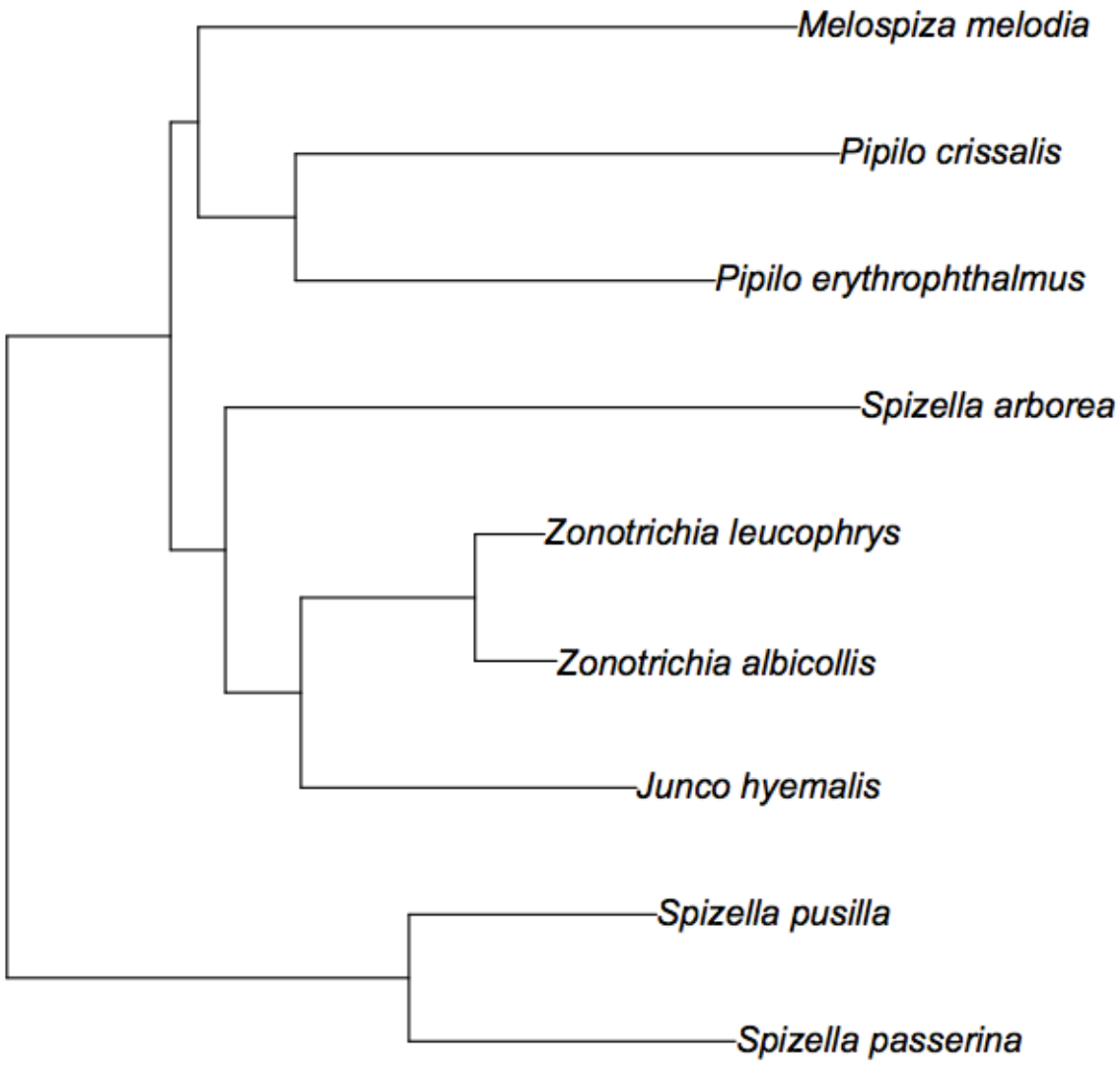

Fig 5.7 Phylogenetic Tree of all nine Emberizid species studied. The tree was modified from Carson & Spicer (2003).

5.9.4 Appendix 4: This appendix shows the interspecific variability in the following parameters: visual field configuration with the eyes at rest in the horizontal plane (Fig. A1), the degree of angular separation of the retinal field margins (Fig. A2), degree of eye movement around the head (Fig. A3), configuration of the visual field with the eyes converged in the horizontal plane (Fig. A4), and 3-dimensional representations of the visual fields with the eyes converged (Fig. A5).

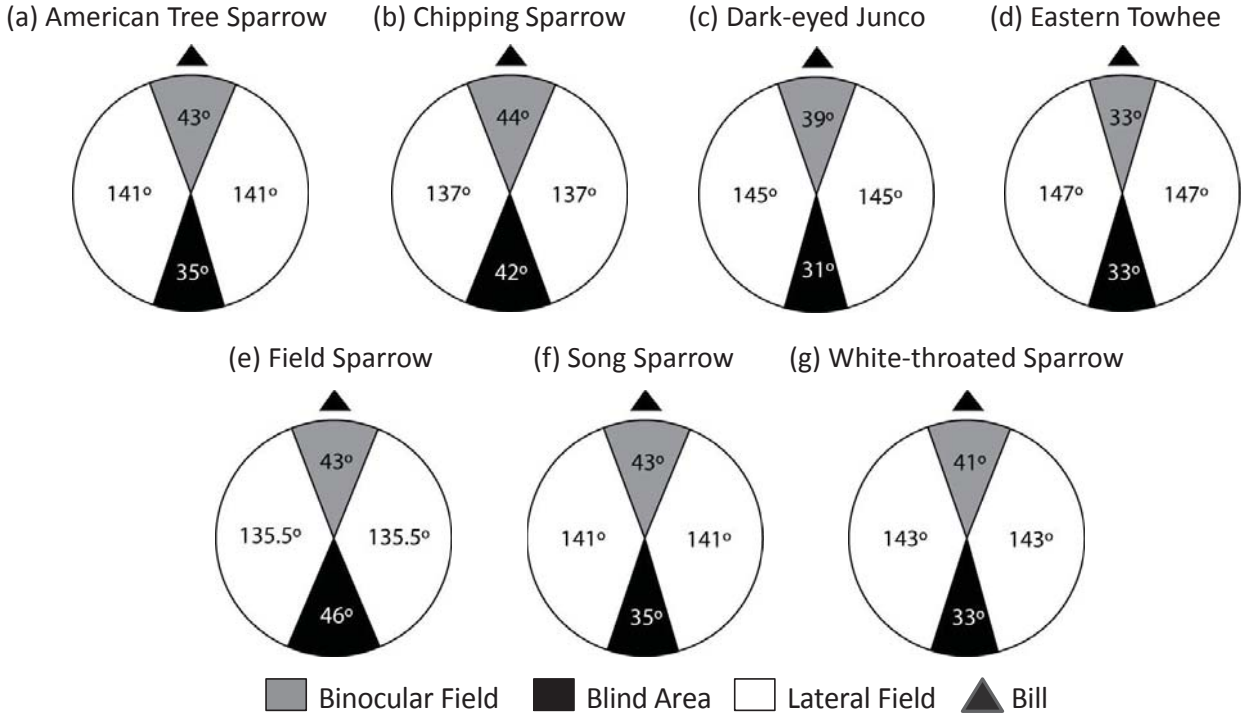

Fig A1/5.8 Configuration of the visual field in the horizontal plane (90° - 270°) while the eyes are at rest in the (a) American tree sparrow, (b) chipping sparrow, (c) dark-eyed junco, (d) Eastern towhee, (e) field sparrow, (f) song sparrow, and (g) white-throated sparrow. Shown are the size of the binocular field, lateral field, and blind area, along with the projection of the bill. Values are averaged across all individuals measured per species.

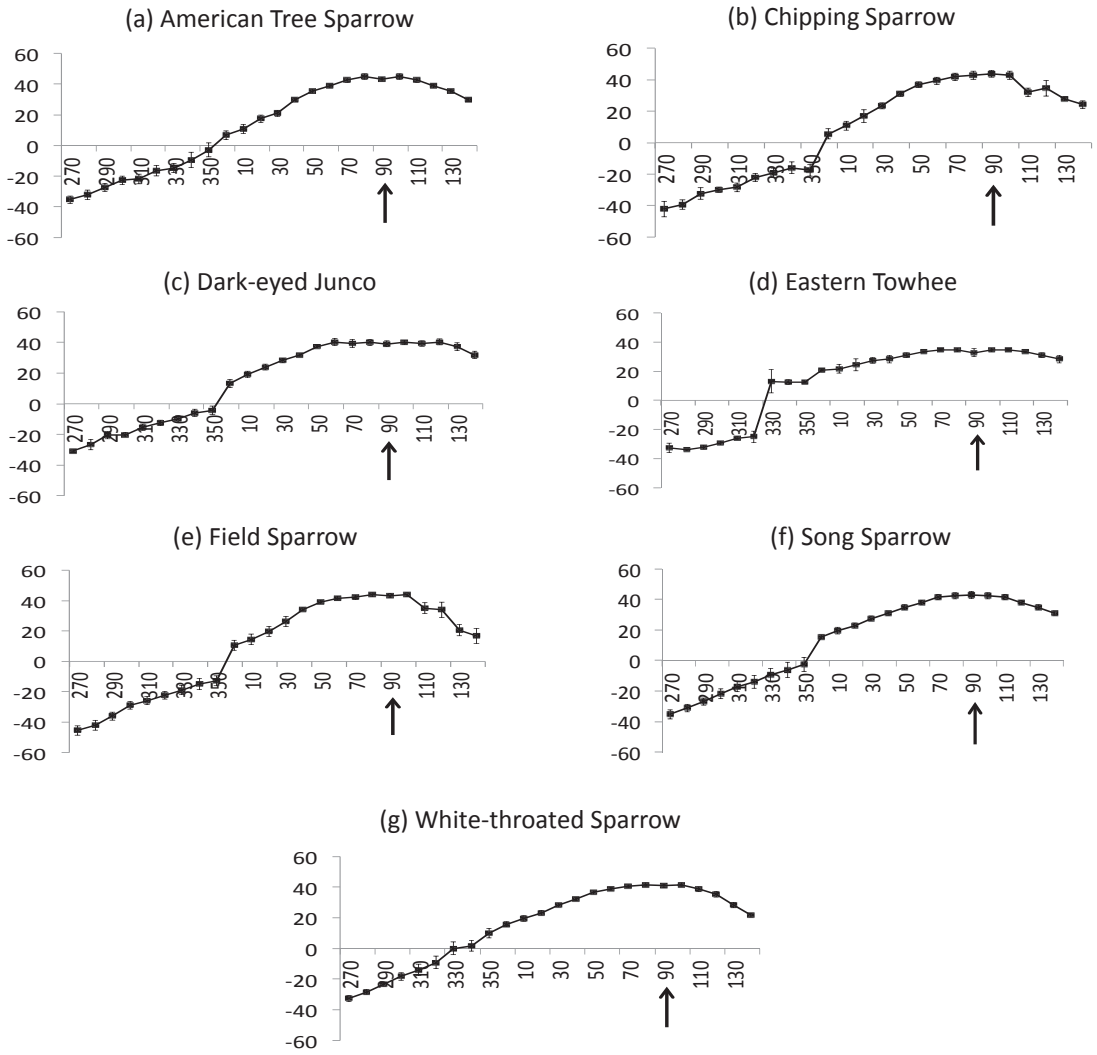

Fig A2/5.9 Median-sagittal angular separation of the retinal field margins per 10° of elevation around the head of (a) American tree sparrows, (b) chipping sparrows, (c) dark-eyed juncos, (d) Eastern towhees, (e) field sparrows, (f) song sparrows, and (g) white-throated sparrows. Positive values represent binocular field overlap, whereas negative values represent blind areas. Values are averaged across all individuals measured per species. The front of the head is at 90°, back of the head is at 270°, and above the head is at 0° (above the head). Arrows indicate projection of the bill-tip in relation to the ground (all horizontally placed at 90°).

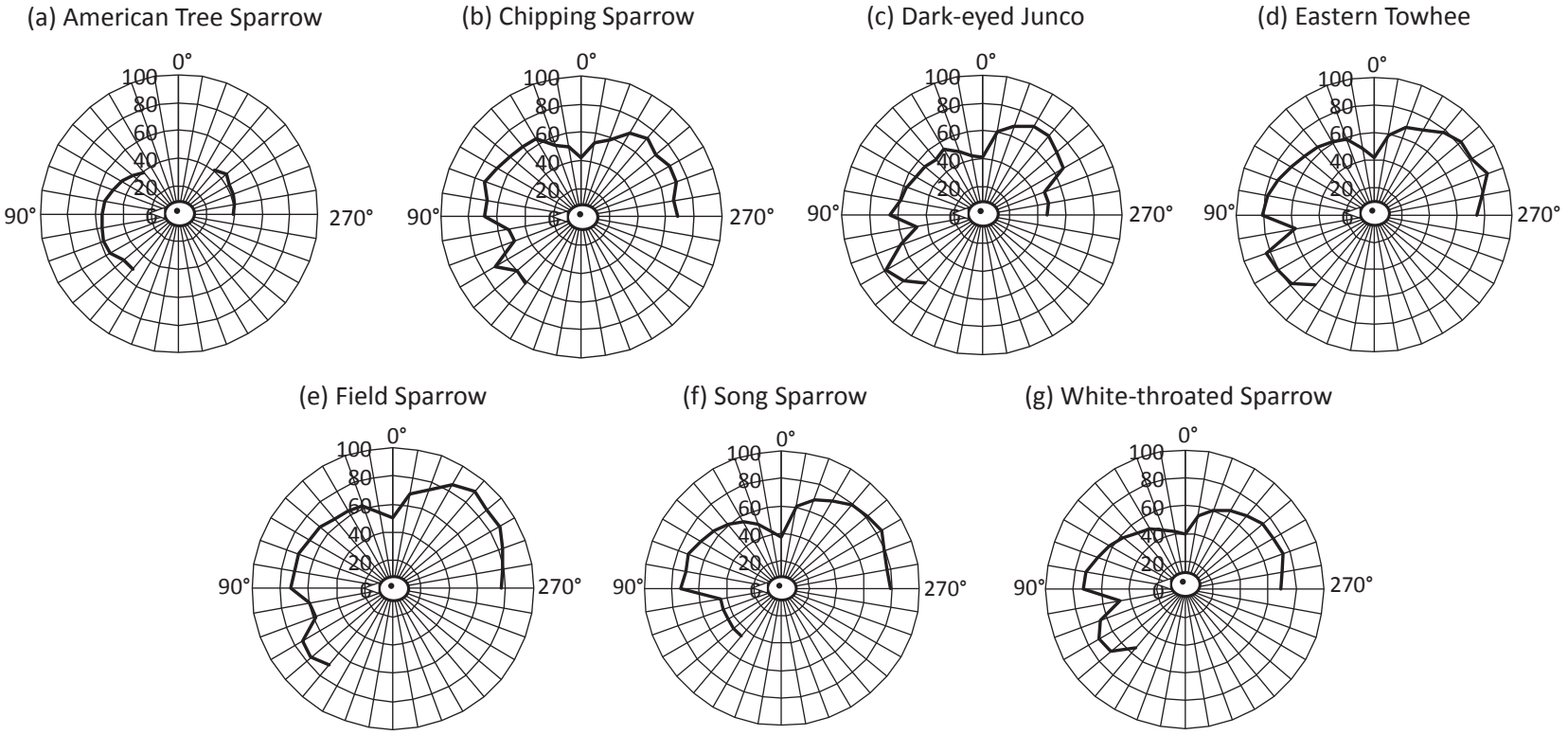

Fig A3/5.10 Degree of eye movements in the direction of each elevation of (a) American tree sparrows, (b) chipping sparrows, (c) dark-eyed juncos, (d) Eastern towhees, (e) field sparrows, (f) song sparrows, and (g) white-throated sparrows. Eye movements are shown in the medial sagittal plan from the left side of the bird's head. Values are averaged across all individuals measured per species. Some values are not shown for the American Tree Sparrow because we were not successful at measuring eye movements above its head.

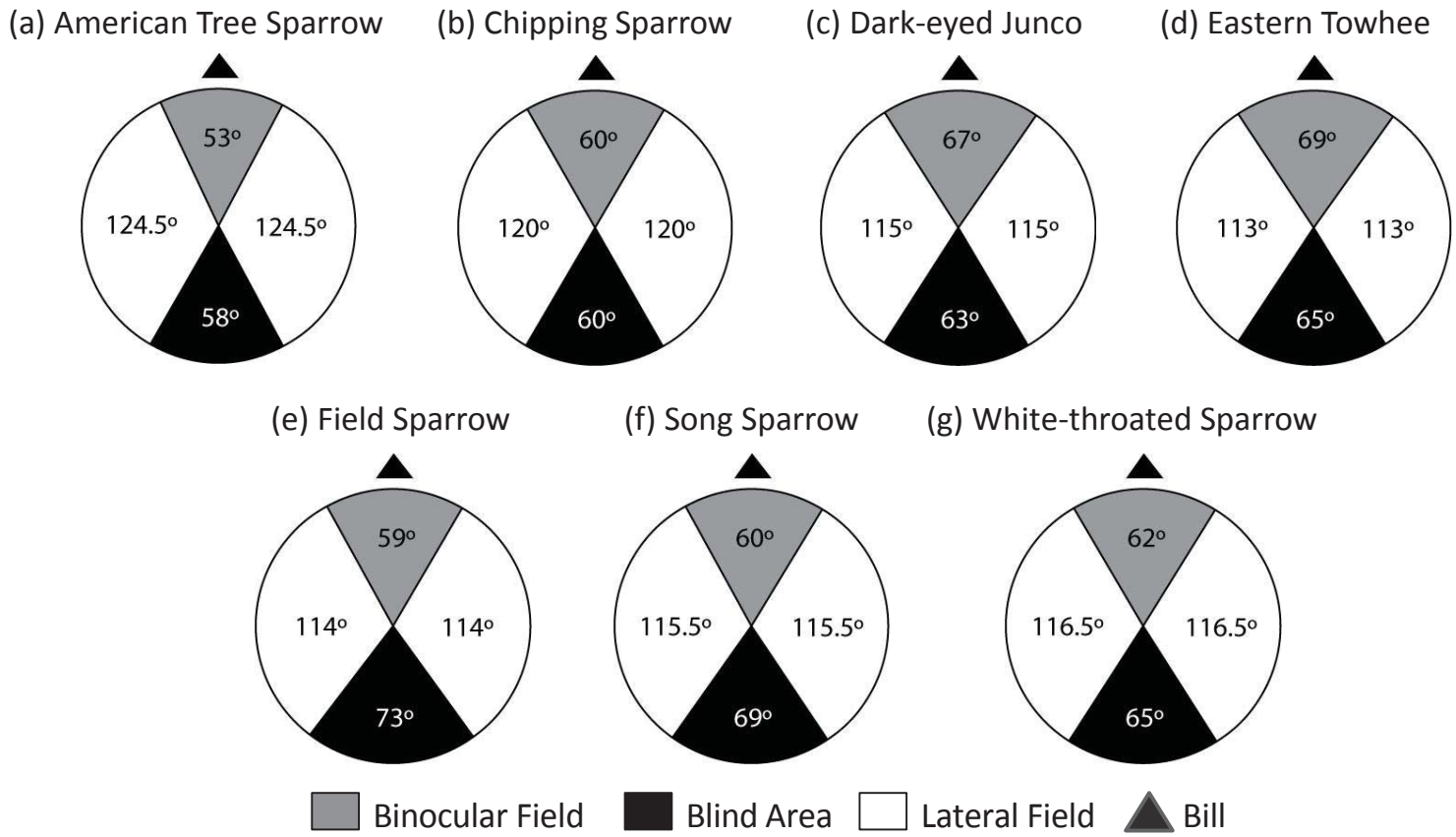

Fig A4/5.11 The configuration of the visual field in the horizontal plane (90° - 270°) while the eyes are converged maximally forward (e.g., rotated forward) in (a) American tree sparrows, (b) chipping sparrows, (c) dark-eyed juncos, (d) Eastern towhees, (e) field sparrows, (f) song sparrows, and (g) white-throated sparrows. Shown are the size of the binocular field, lateral field, and blind area, along with the projection of the bill. Values are averaged across all individuals measured per species.

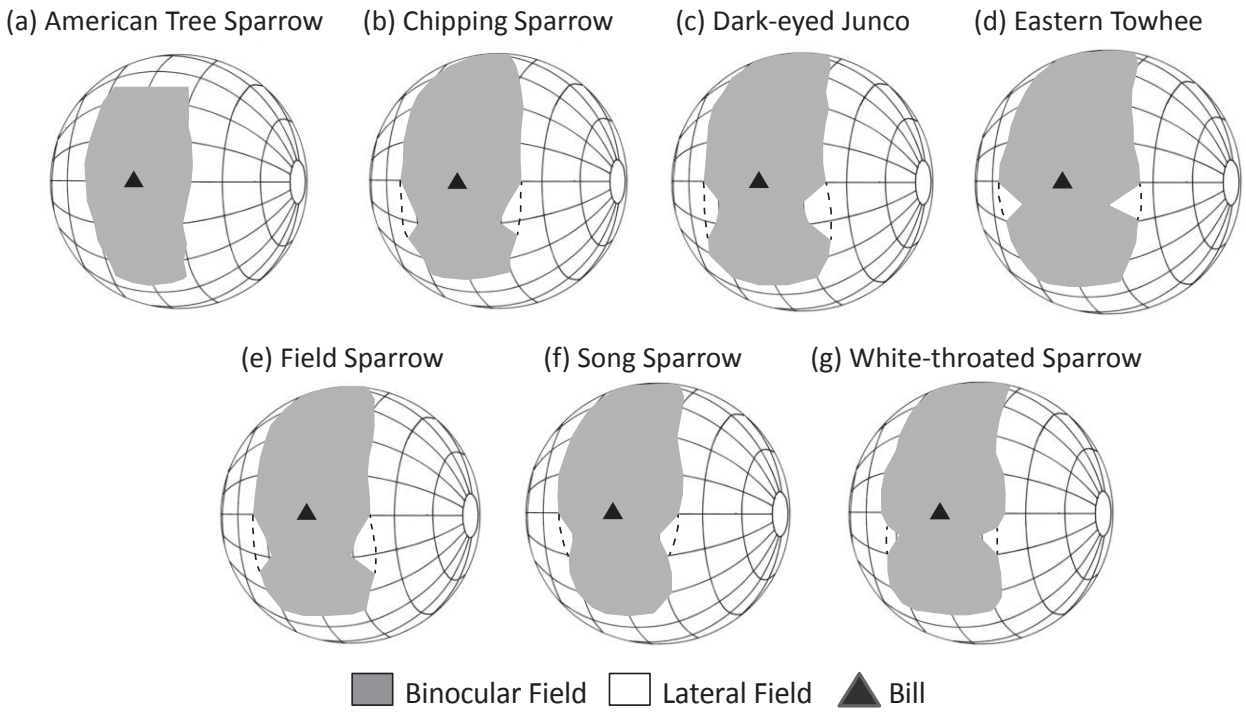

Fig A5/5.12 Orthographic projection of the boundaries of the retinal fields of the two eyes around the head while the eyes are converged maximally forward for (a) American tree sparrows, (b) chipping sparrows, (c) dark-eyed juncos, (d) Eastern towhees, (e) field sparrows, (f) song sparrows, and (g) white-throated sparrows. Values are averaged across all individuals measured per species. The eyes are converged in the direction of the elevation being measured, so the figures do not represent the visual field at any particular given moment but rather the value of maximal convergence in the direction of each elevation. A latitude and longitude coordinate system was used with the head of the animal at the center of the globe. The grid is set at 20° intervals, the equator aligned vertically in the median sagittal plane (the horizontal plane, 90° - 270°). The projection of the bill tips are presented for orientation purposes. The dotted lines represent the extrapolated binocular field assuming that the retinal margin follows a circular projection, suggesting that the individuals could see their bill tips. Some values are not shown for the American Tree Sparrow because we were not successful at measuring eye movements above its head.

5.9.5 Appendix 5

Table 5.5 Bill size measurements (length, width, depth, in mm) of nine sparrows belonging to the Emberizidae Family. See main text for details on specimens and measurement methods.

	length mean	length SE	width mean	width SE	depth mean	depth SE
American tree sparrow	8.75	0.14	4.77	0.09	5.83	0.11
California towhee	12.04	0.14	6.17	0.10	7.70	0.12
chipping sparrow	7.81	0.11	4.03	0.07	4.81	0.09
dark-eyed junco	9.35	0.10	4.55	0.07	5.66	0.08
Eastern towhee	11.42	0.09	5.44	0.06	7.59	0.07
field sparrow	7.58	0.14	4.00	0.10	5.04	0.12
song sparrow	10.72	0.18	5.28	0.12	6.52	0.15
white-crowned sparrow	9.63	0.13	4.96	0.09	6.28	0.11
white-throated sparrow	10.22	0.18	4.85	0.12	6.52	0.15

CHAPTER 6: VISUAL SYSTEM CONFIGURATION IS ASSOCIATED WITH VISUAL INFORMATION GATHERING BEHAVIORS IN BIRDS

This chapter is part of a manuscript co-authored with other researchers that will be submitted soon:

Moore BA, Pita D, Tyrrell LP, Bininda-Emonds ORP, Fernandez-Juricic E. Visual system configuration is associated with information gathering behaviors in birds. To be submitted.

6.1 Abstract

The ability to change the field of view, i.e. scan, is an important aspect of gathering visual information, yet little is known about how visual scanning behaviors in birds are influenced by the configuration of their visual system. Previous studies have often suggested associations between few visual parameters and visual behaviors in a small number of bird species, without empirical testing. However, given the variation in the avian visual system even amongst closely related species, examining empirically the relationship between visual traits and visual behaviors in a large number of species will better provide evidence of a relationship between vision and it's actions.This is the first comparative study explicitly testing the relationship between multiple visual traits and visual behaviors controlling for phylogenetic effects. We characterized key visual dimensions and visual behaviors of 29 species of birds across 14 families, and tested specific hypotheses/predictions about variation in scanning strategies in species with different visual systems. We found that the size of the binocular field, blind area, and change in retinal ganglion cell density across the retina was positively associated with either/or the degree of eye movements or the head movement rate. We also suggest a

potential continuum between the need for binocular vision in a foraging context and for having small blind areas to increase the field of view from which to detect predators. Overall, our findings suggest that there is indeed a relationship between scanning behavior and how the avian visual system is configured.

6.2 Introduction

Animals gather visual information by moving their eyes and heads for two main reasons. First, most animals do not have 360° visual coverage around their heads (Martin 2007). Second, the vertebrate retina has certain regions (i.e., retinal specializations) that provide higher quality information (e.g., high spatial visual resolution or visual acuity) than the rest of the retina due to variations in the density of photoreceptors (Collin 1999). Consequently, moving heads and eyes around provides a way to obtain snapshots of high-resolution visual information. Furthermore, the retinal specialization has been associated with the center of visual attention (Bisley 2011); thus, eye and head movements can be a proxy of how animals allocate their attention while scanning (Fernández-Juricic 2012).

However, little is known about how the configuration of the visual system (e.g., visual fields, eye size, variations in cell density across the retina) could influence eye and head movement behaviors. This is particularly relevant in species with laterally placed eyes, like birds, because their retinal specializations tend to project laterally (see previous chapters) rather than into the binocular field. Therefore, to perform different tasks that are visually dependent or demanding (e.g. visual search and visual fixation, birds are expected to move their eyes and heads in different patterns based on their visual configuration (Meyer 1977, Martin 2007, Moore et al. 2013). For instance, visual fixation in birds has been proposed to be different from that of humans in that birds expose an object of interest to retinal specializations in each eye in rapid succession (Dawkins 2002), leading to an increase in head movement rate and amplitude.

Our goal was to assess at the comparative level the relationship between visual traits and behaviors indicative of visual information gathering, and to test some specific

predictions about the variation in scanning strategies in species with different visual systems (see Predictions section). We studied the size of the binocular field and blind area as indicators of visual coverage, which is the volume of viewable visual space at any given point in time. We also studied eye size and variation in ganglion cell density across the retina as indicators of ,overall visual acuity and changes in localized visual acuity, respectively.. The idea of overall visual acuity considers the ability of the whole eye to resolve stimuli at a given distance, whereas localized visual acuity is the potential of the retinal specialization to provide the highest visual resolution in a single spot within the retina (Fernandez-Juricic 2012). However, since retinal ganglion cells heterogeneously populate the retina, visual and that heterogenosity has been show to vary across species (Moore et al. 2012) visual acuity could vary in a more or less pronounced manner from the retinal periphery to the retinal specialization. Overall, variation in these different visual traits are expected to influence scanning behavior (Fernandez-Juricic 2012). At the behavioral level, we measured the degree of eye movement (i.e., amplitude of eye movement in a given direction) and head movement rate (i.e., number of times the head changes position per unit time). From a physiological perspective, eye and head movements are driven by very different mechanisms (Land & Tatler 2009). However, from a functional perspective, we assumed that eye and head movements are used for similar reasons: to scan the visual space for information given the limits imposed by the blind area (i.e., lack of 360° visual coverage). To test this assumption, we first assessed whether species with a high degree of eye movement also showed high head movement rates.

We used 29 species of North American birds across 14 families (Table 1). This database includes a large number of Passeriformes, as well as species from the orders Anseriformes and Columbiformes. Our database is characterized by the measurement of the aforementioned traits following standardized techniques across different species (see Methods), which minimizes the effect of between-species differences due to different methodological approaches.

Table 6.1 Source of avian species used in this study

Family	Genus Species	Common Name	Reference
Anatidae	Branta Canadensis	Canada goose	Fernandez-Juricic et al. 2011b; Unpublished data
Cardinalidae	Cardinalis cardinalis	Northern Cardinal	Unpublished data
Cardinalidae	Passerina cyanea	Indigo bunting	Unpublished data
Columbidae	Zenaida macroura	Mourning Dove	Blackwell et al. 2009; Dolan & Fernandez-Juricic 2010; Unpublished data
Corvidae	Cyanocitta cristata	Blue Jay	Unpublished data
Emberizidae	Junco hyemalis	Dark-eyed Junco	Moore et al. 2014 in review, a
Emberizidae	Melospiza melodia	Song Sparrow	Moore et al. 2014 in review, a
Emberizidae	Pipilo crissalis	California Towhee	Fernandez-Juricic et al. 2011a
Emberizidae	Pipilo crythrophthalmus	Eastern Towhee	Moore et al. 2014 in review, a
Emberizidae	Spizella arborea	American tree sparrow	Moore et al. 2014 in review, a
Emberizidae	Spizella passerina	Chipping sparrow	Moore et al. 2014 in review, a
Emberizidae	Spizella pusilla	Field sparrow	Moore et al. 2014 in review, a
Emberizidae	Zonotrichia albicollis	White-throated sparrow	Moore et al. 2014 in review, a
Emberizidae	Zonotrichia leucophrys	White-crowned sparrow	Fernandez-Juricic et al. 2011a
Fringillidae	Carduelis tristis	American goldfinch	Baumhardt et al. 2014
Fringillidae	Carpodacus mexicanus	House finch	Fernandez-Juricic et al. 2008; Dolan & Fernandez-Juricic 2010
Icteridae	Agelaius phoeniceus	Red-winged	Unpublished data

		blackbird	
Icteridae	Molothrus ater	Brown-headed cowbird	Blackwell et al. 2009; Dolan & Fernandez-Juricic 2010; Unpublished data
Icteridae	Quiscalus quiscula	Common grackle	Unpublished data
Icteridae	Sturnella magna	Eastern meadowlark	Tyrrell et al. 2013
Mimidae	Dumetella carolinensis	Gray catbird	Unpublished data
Mimidae	Toxostoma rufum	Brown thrasher	Unpublished data
Paridae	Baeolophus bicolor	Tufted titmouse	Moore et al. 2013
Paridae	Poecile atricapilla	Carolina chickadee	Moore et al. 2013
Passeridae	Passer domesticus	House sparrow	Fernandez-Juricic et al. 2008; Dolan & Fernandez-Juricic 2010
Sittidae	Sitta carolinensis	White-breasted nuthatch	Moore et al. 2013
Sturnidae	Sturnus vulgaris	European starling	Dolan & Fernandez-Juricic 2010; Unpublished data
Troglodytidae	Troglodytes aedon	House wren	Unpublished data
Turdidae	Turdus migratorius	American robin	Unpublished data

6.2.1 Predictions

6.2.1.1 Binocularity

The size of the binocular field is primarily a function of foraging needs (Martin & Katzir 1999) due to such factors as visualization of the bill tip (Martin 2009, Troscianko et al. 2012, Moore et al. 2013), increasing contrast discrimination of short-field sampling of the foraging medium (Heesy 2009), and enhancing depth perception through stereoscopic cues in complex habitats (Changizi & Shimojo 2008). Given the importance of the binocular field in foraging, and evidence of wide interspecific variation in binocular field sizes (Martin 2009), we hypothesized that species whose food search relies mostly on the visualization of the frontal field (as opposed to the lateral fields) would benefit from

wider binocular fields. Assuming foraging behaviors have a direct effect of eye and head movments, and that binocularity is important for foraging in these species, we predicted that species with wider binocular fields would tend to have lower degree of eye movement or slower head movement rates to detect objects of interest with their binocular field during visual information gathering bouts compared to species with narrower binocular fields

6.2.1.2 Blind area

The blind area limits the space at the rear of the head from which animals can visualize approaching predators; hence limiting visual coverage (Martin 1984, Guiellemain et al. 2002). With a larger blind area (decreased total visual coverage), animals would need increased scanning of the environment to sample areas not visible around their heads. Therefore, we predicted that species with larger blind areas would have higher degrees of eye movements and higher head movement rates to increase visual coverage around their head.

6.2.1.3 Overall and localized visual acuity

Visual acuity can have important implications for antipredator behavior, because species with higher overall visual acuity (i.e. average visual acuity across the entire eye) would be better able to *detect* objects (e.g., predators) from farther away than species with lower overall visual acuity. We used eye axial length as a proxy for overall visual acuity as it has the largest effect on the calculation of visual acuity (see Methods for formulas). We predicted that species with larger eye axial length (i.e., higher overall visual acuity) would have a lower degree of eye movement and head movement rate because at a given distance they can better resolve objects (Fernández-Juricic 2012). Species with smaller eye axial length (i.e., lower overall visual acuity) are expected to have higher degree of eye movement and head movement rate to update the status of their visual surroundings more quickly and enhance their ability to detect threats (Fernández-Juricic 2012).

Additionally, we considered localized visual acuity using the highest density of retinal ganglion cells, which generally peak within the retinal specialization (Moore et al.

2012). Species with a higher peak of retinal ganglion cells have been suggested to have deeper foveae (Fernández-Juricic 2012). The *deeper* the fovea is, the *narrower the width* of the foveal pit (Fite & Rosenfield-Wessels 1975), which would lead to a smaller area of the visual field with the highest visual resolution. We then predicted that species with higher localized visual resolution would have higher degree of eye movement and head movement rate (due to the smaller high visual acuity area) to obtain the maximum amount of high quality information per unit time to detect potential threats in visual space.

6.2.1.4 Retinal configuration

Retinal ganglion cells transfer the information from the retina to the visual centers of the brain (Collin 1999). The density of ganglion cells is not homogenous across the retina (Meyer 1977), with areas with higher cell density (i.e., close to the retinal specialization) providing higher visual acuity than the areas with lower ganglion cell density (i.e., close to the retinal periphery). Interestingly, the rate of change in cell density from the periphery to the specialization varies between species (Fernández-Juricic et al. 2011a), which Dolan & Fernández-Juricic (2010) hypothesized could have implications for visual behavior. More specifically, species in which the rate of change in cell density is more pronounced across the retina would need to rely more on the retinal specialization to gather high quality information, leading to a greater need to move the retinal specialization through eye and/or head movements. Therefore, we predicted that the scanning behaviors (degree of eye movement and the head movement rate) would increase in species with a larger gradient in ganglion cell density across the retina than those with less pronounced gradient.

6.3 Methods

All species in this study with unpublished data were captured in Tippecanoe County, Indiana, USA (Table 2). The Purdue Animal Care and Use Committee (protocol# 09-018) approved all procedures. Permits for capture of all birds were obtained from Indiana Department of Natural Resources and US Fish and Wildlife Service.

6.3.1 Eye size, retinal ganglion cell density, and visual acuity

After euthanasia by CO2, the eyes were removed and axial length was measured with calipers (0.01 mm accuracy). We then hemisected each eye at the ora serrata, removed vitreous humor using forceps and spring scissors, then placed the eyecup in 4% paraformaldehyde. After fixation, we processed the retina following the procedures in Ullman et al. (2012) and Moore et al. (2013). Ganglion cells were stained with cresyl violet as they are the terminal retinal cell sending information towards the brain (McIlwain 1996). A higher density of ganglion cells within a retinal specialization represents increased signal to the brain and therefore higher visual resolution (Walls 1942; Meyer 1977), thus it is important to characterize their distribution across the retina.

To characterize the retina, we used an Olympus BX51 microscope at 1000x and an Olympus S97809 camera to capture images at 410 sites across each retina using Stereo Investigator (MBF Bioscience, Williston, Vermont). Ganglion cells were then counted to estimate density (cells/sq.mm) in 50mm x 50mm counting frames in each of the 410 sites. Other cell types within the ganglion cell layer (e.g. amacrine, glial cells, etc.) were selectively excluded from our counts by differential identification (Ehrlich 1981; Freeman & Tancred 1978; Rahman et al. 2006; Stone 1981). After differentiation, ganglion cells in each counting frame were counted in ImageJ. In order to develop a visual respresentation of the ganglion cell distribution across the retina, topographic maps were constructed as described in Ullmann et al. (2012). We also characterized the location of the retinal specialization using a Cartesian coordinate system, as well as the degree of specialization both following Moore et al. (2012).

In all species a fovea was recognizable on a wholemount using microscopy. If a fovea of a particular species was rather inconspicuous, we performed histological cross sections on one eye to confirm the presence of a fovea by evidence of a structural pitting in the retinal tissue. Eyes were fixed in Bouin's solution for 24-28 hours, and were then washed with 70% ethanol. We then embedded the retinal tissue in paraffin and sectioned the embedded tissue with a Thermo Scientific Shandon Finesse ME microtome (Waltham, Massachusetts). All sections were then stained with haemotoxylin/eosin.

We considered both overall and localized (peak) visual acuity. Eye axial length was used as a proxy for overall visual acuity as visual acuity scales linearly with eye size (Kirschfeld 1976, Kiltie 2000). Localized visual acuity was determined by using peak retinal ganglion cell density as it is related to the highest spatial resolving power within the retinal specialization (Moore et al., 2012).

6.3.2 Visual field configuration and degree of eye movement

The visual field configuration was recorded following Martin (1984) and Moore et al. (2013), using a visual field apparatus and an ophthalmoscopic reflex technique. Individuals heads were centered within the apparatus as if in the center of a sphere, where elevation 0 was directly above the head, 90 was in front of the head, and 270 was directly behind the head. The retinal field was then examined with a Keeler Professional ophthalmoscope every 10 degrees from below the bill (140) to behind the head (270). The degrees of eye movement were also measured every 10 degrees as a proxy for scanning behavior (Fernandez-Juricic 2012, Moore et al. 2013) with the animal converging and diverging maximally towards that direction of the specific elevation being measured. We also calculated the percent of the visual field above and including the horizontal plane (from the bill at 90 degrees to the back of the head at 270 degrees) of both the binocular coverage and blind area. This enables us to determine how much of a species' visual field is occupied by binocular vision or is not visualized at all, and it enables us to detect changes across the entire visual field when the animal moves its eyes. Also in some species, the bill protruded into the binocular field in front of the head at some elevations. Therefore, we calculated the extrapolated width of the binocular field at

these points, or the width considering a circumferential extension of the binocular field measurements as if the bill was not intruding and blocking visibility. This is a more accurate representation of the degree of eye movement as it is the actual degree the animal is moving its eyes.

In a few species, measurements above the head were not recorded in a consistent manner with the rest of the species in our dataset (American tree sparrow, brown thrasher, brown-headed cowbird, California towhee, Canada goose, house finch, house sparrow, mourning dove, and white-crowned sparrow). Also, the eyes at rest measurements were not taken for the mourning dove. Therefore, the visual parameters of these species that were not measured consistently with the rest of the species were excluded from any calculations or analyses.

6.3.3 Statistical analysis

We conducted phylogenetic generalized least squares models (PGLS, Pagel, 1999; Nunn, 2011) to account for the effects of shared evolutionary history of these species. We used a phylogenetic tree developed by Olaf Bininda-Emonds with data from GenBank (www.ncbi.nlm.nih.gov/genbank/). We ran the PGLS analyses using the Caper package (Orme et al., 2011) in R (R Development Core Team, 2010). Each species was represented by a single data point (mean values across individuals) in our dataset.

6.4 Results

We found a significant positive relationship between degree of eye movement and head movement rate ($F_{2, 19} = 4.92$, $P = 0.018$, $R^2 = 0.21$; Fig. 1), such that species that tended to diverge and converge their eyes to a larger extent also moved their heads at a faster rate.

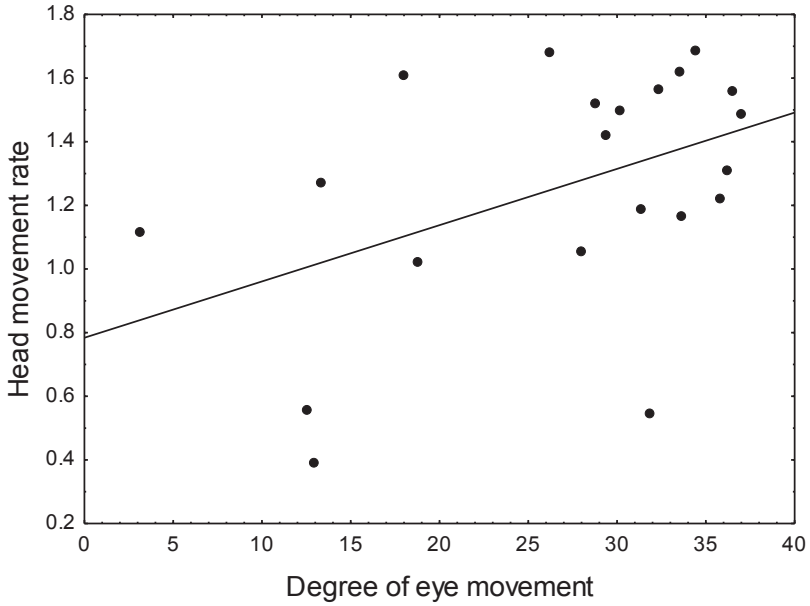

Fig 6.1 Relationship between head movement rate (events per s) and degree of eye movement (°) in 29 bird species.

6.4.1 Binocularity

We found positive significant relationships between binocularity and eye and head movement behaviors. Species with wider binocular fields also showed higher head movement rates ($F_{2, 27} = 11.29$, $P < 0.001$, $R^2 = 0.29$; Fig. 2a) and greater degrees of eye movement ($F_{2, 19} = 4.98$, $P = 0.018$, $R^2 = 0.21$; Fig. 2b).

6.4.2 Blind area

The size of the blind area was significantly associated with eye and head movement behaviors. Overall, species with wider blind areas tended to have higher head movement rate ($F_{2, 27} = 8.06$, $P = 0.002$, $R^2 = 0.23$; Fig. 2c) as well as greater degree of eye movement ($F_{2, 19} = 13.73$, $P < 0.001$, $R^2 = 0.42$; Fig. 2d).

6.4.4 Visual acuity

We ran models including proxies of both overall visual acuity (eye axial length) and localized visual acuity (peak retinal ganglion cell density). Both models yielded significant results: head movement rate ($F_{3, 26} = 13.04$, $P < 0.001$, $R^2 = 0.50$) and degree of eye movement ($F_{3, 18} = 7.13$, $P = 0.002$, $R^2 = 0.44$). Eye axial length was significantly associated with head movement rate ($t = -4.95$, $P < 0.001$) and the degree of eye movement ($t = -3.13$, $P = 0.006$). Species with higher overall visual acuity showed lower head movement rates (Fig. 3a) and degree of eye movement (Fig. 3b) than those with lower acuity. Peak retinal ganglion cell density was not significantly associated with either head movement rate ($t = -0.67$, $P = 0.504$) or degree of eye movement ($t = 1.69$, $P = 0.109$).

6.4.5 Retinal configuration

The change in ganglion cell density across the retina was significantly associated with the degree of eye movement ($F_{2, 19} = 4.87$, $P = 0.019$, $R^2 = 0.20$) but not with head movement rate ($F_{2, 27} = 1.83$, $P = 0.179$, $R^2 = 0.06$). Species with steeper changes in ganglion cell density across the retina showed a higher degree of eye movement than species with shallower slopes (Fig. 3a).

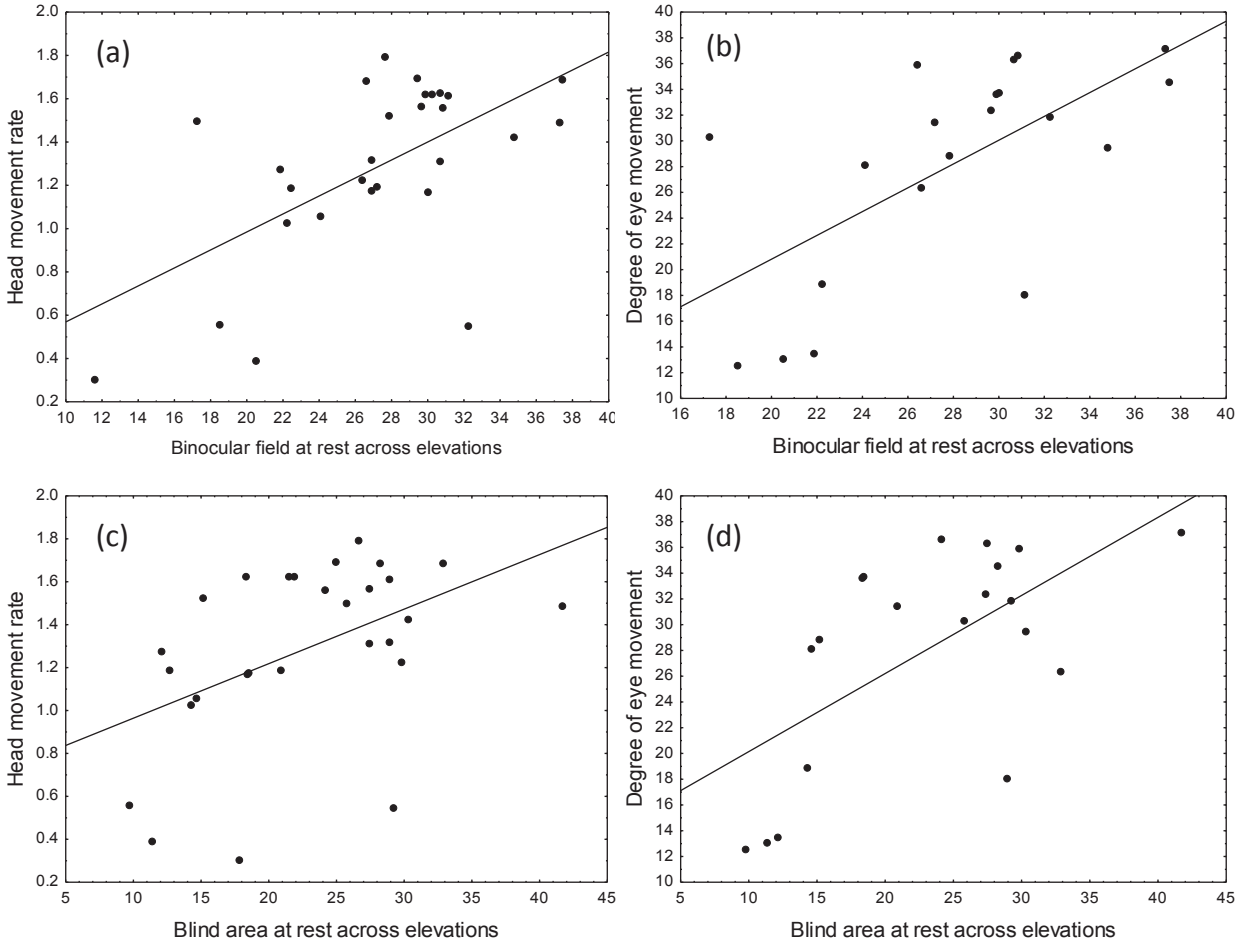

Fig 6.2 Scatterplots showing the relationships between: binocular field width (°) across all elevation with the eyes at rest and (a) head movement rate (events/s) and (b) degree of eye movement; width of the blind area (°) across all elevation with the eyes at rest and (c) head movement rate (events/s) and (d) degree of eye movement area (°).

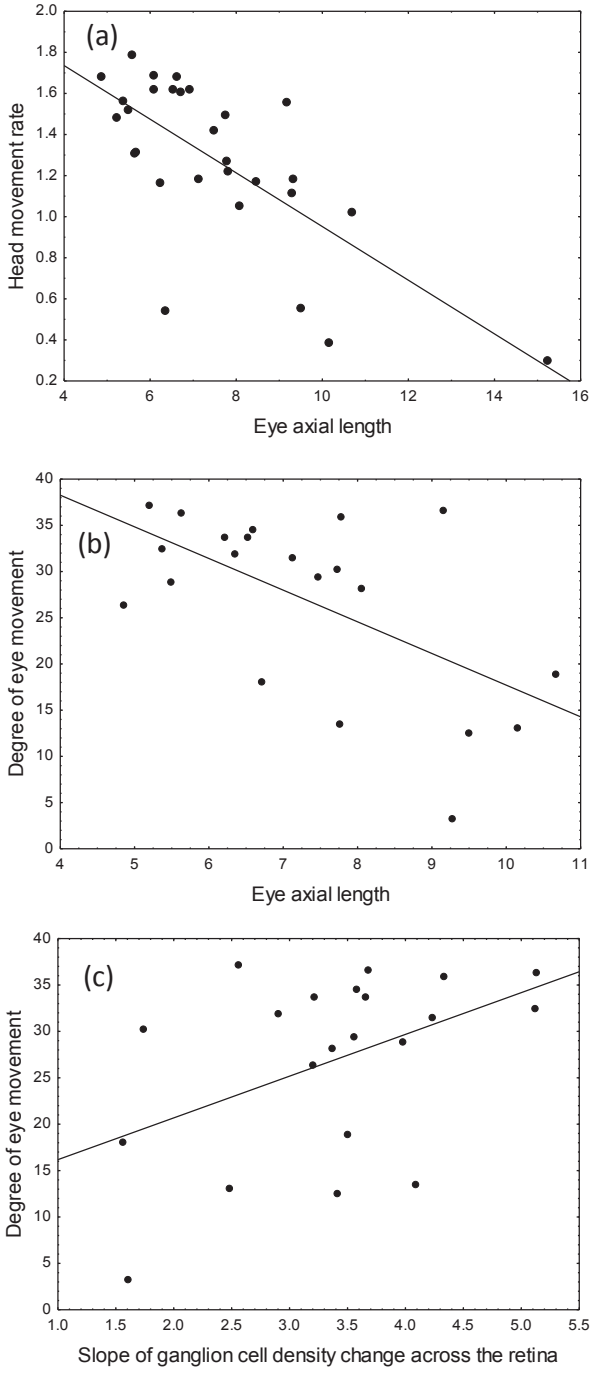

Fig 6.3 Scatterplots showing the relationships between: eye axial length (mm) and (a) head movement rate (events/s) and (b) degree of eye movement (°), and (c slope of change in ganglion cell density from the retinal specialization to the periphery of the retina and degree of eye movement (°).

6.5 Discussion

Overall, we found across bird families that variation in different components of the visual system were associated with information gathering behaviors. The nature of our comparative analysis prevents us from making conclusions about the causality of these associations (e.g., physiology affecting behavior or the other way around), but this is the first empirical evidence supporting them.

Contrary to our prediction, we found that bird species with wider binocular fields tended to have a greater degree of eye movement as well as higher head movement rates. Given that in birds the retinal specializations do not project into the binocular field, but outside of it (see previous chapters), it is possible that wider binocular fields would lead to a more pronounced divergence of the axes of the projection of the retinal specializations. Consequently, species with wider binocular fields would require a greater degree of eye movement or faster head movements to expose their retinal specializations to objects of interest during visual information gathering bouts (e.g., sideways head movements, Dawkins 2002).

Our findings also show that species with wider blind areas tended to have greater degree of eye movement as well as head movement rates. As visual coverage decreases, birds seem to compensate for this limitation by moving their eyes more but also by covering more of the visual space with more frequent head movements (Martin et al. 2007; Fernandez-Juricic et al., 2010; Fernandez-Juricic, 2012). This could allow animals to visualize with their retinal specialization the portions of the visual space beyond the restrictions given by their visual field configuration. Future studies should assess whether these opposing sensory strategies (large visual coverage with low movement of the retinal specialization vs. narrow visual coverage with high movement of the retinal specialization) could have any bearing on the ability of individuals to detect predators.

The relationships we found for scanning behavior and both the size of the binocular field and the blind area suggests that there may be a continuum between the need for binocular vision for foraging and having small blind areas to increase the field of view from which to detect predators. Since binocular vision in birds seems to be

primarily involved with foraging needs, such as controlling the position of the tip of the bill (Martin 2009, Martin et al. 2012), and small blind areas at the rear of the head is beneficial for predator detection, the continuum between the need for more prominent need for binocular foraging demands and the need for early detection of predators with wider visual coverage (smaller blind area). As an animal values more what is happening towards the front of their head (e.g. foraging behavior and having larger binocular fields), they may be able to sacrifice vision towards the rear (e.g. larger blind areas and less predator detection). On the other hand, some species may not require much binocular vision. For example, filter feeders (e.g. ducks, Guillemain et al. 2002, Martin et al. 2007) do not need to visualize the bill tip during foraging, and thus have narrow binocular fields where the bill is not visualized et al. 2011). Therefore, they may be able to allocate more effort towards predator detection, as they tend to have much wider total visual coverage due to smaller blind areas (Martin et al. 2007).

Bird species with lower overall visual acuity (small eye size) also show higher head moment rates and greater degrees of eye movement. Therefore, species with lower overall acuity tend to update visual information by moving their heads and eyes at a faster rate and to a greater amount respectively. This may be a compensatory strategy to increase the chances of detecting a predator nearby that can be challenging to detect far away due to their visual acuity constraints (Fernandez-Juricic 2012). Alternatively, this finding may be linked to temporal visual resolution. A recent study (Healey et al. 2013) found that smaller sized vertebrates tend to have higher temporal visual resolution (i.e. able to detect light flicker at a higher frequency, suggestive of a higher rate of visual temporal processing). In birds, smaller species have lower visual acuity (Kiltie 2000). Consequently, if species with lower visual acuity also have higher temporal visual resolution, we would expect higher head movement rates and greater degrees of eye movements to update visual information moreso than species with lower temporal visual resolution. Furthermore, we found no significant association between peak retinal ganglion cell density and either head movement rate or the degree of eye movement. This may be because the area of peak ganglion cell density (i.e. retinal specialization) may be used more for visual tracking or visualization of an identified or located object rather than

visual scanning (Bloch et al., 1984; Maldonado et al., 1988; Fernandez-Juricic, 2012).

Finally, we found that species with a more pronounced change in ganglion cell density from the retinal periphery to the retinal specialization have higher degrees of eye movement. As the ganglion cell distribution across the retina becomes more heterogenous across the retina (i.e., greater change in density up to the retinal specialization), the functional role of the retinal specialization to provide high quality information can be considered more relevant. As a result, there is a greater dependence on this retinal specialization for visualizing objects with high acuity, as the cell density (hence acuity) in the rest of the retina is more similar and may not be sufficient to reach an acceptable level of visual performance. The implication is that species with greater difference in ganglion cell density may have a greater need to reposition the retinal specialization around the visual field to sample with high acuity at high rates.

This is the largest study to date to demonstrate the relationship between visual traits and information gathering behaviors in birds. Our findings suggest that some components of anti-predator behavior (e.g., scanning) are influenced by how the avian visual system is configured. This is relevant because the predictions of many models on anti-predator behavior implicitly assume little variation in the sensory system of prey. Consequently, incorporating some of the inter-specific variability in the prey visual system may help develop more realistic predictions on variation in anti-predator behavior (Fernández-Juricic et al. 2004). Also, studying the visual systems of predatory species in a similar manner would enable more realistic predictions to be made regarding prey-seeking and detecting behavior.

6.6 Literature Cited

Baumhardt PE, Moore BA, Doppler M, Fernandez-Juricic E (2014). Do American goldfinches see their world like passive prey foragers? A study on visual fields, retinal topography, and sensitivity of photoreceptors. *Brain Behavior and Evolution* 83:181-198.

Bisley JW (2011). The neural basis of visual attention. *Journal of Physiology* 589:49-57.

Blackwell BF, E Fernandez-Juricic, TW Seamans, T Dolan (2009). Avian visual system configuration and behavioural response to object approach. *Animal Behaviour* 77:673-684.

Bloch S, Rivaud S, Martinoya C (1984). Comparing frontal and lateral viewing in the pigeon III. Different patterns of eye movements for binocular and monocular fixation. *Behavioral Brain Research* 13:173-182.

Changizi MA & Shimojo S (2008). A functional explanation for the effects of visual exposure on preference. *Perception* 37:1510-1519.

Collin SP (1999). Behavioural ecology and retinal cell topography. In: Archer S, Djamgoz MB, Loew E, Partridge JC, Vallerga S (ed) Adaptive mechanisms in the ecology of vision. Kluwer Academic Publishers, Dordrecht, pp 509-535.

Dawkins MS (2002). What are birds looking at? Head movements and eye use in chickens. *Animal Behaviour* 63:991-998.

Demery ZP, Chappell J, Martin GR (2011). Vision, touch and object manipulation in Senegal parrots *Poicephalus senegalus*. *Proceedings of the Royal Society of London B* 278:3687-3693.

Dolan T & Fernández-Juricic E (2010). Retinal ganglion cell topography of five species of ground foraging birds. *Brain Behavior and Evolution* 75:111-121.

Ehrlich D (1981). Regional specialization of the chick retina as revealed by the size and density of neurons in the ganglion cell layer. *Journal of Comparative Neurology* 195:643–657.

Fernandez-Juricic E, Erichsen JT, Kacelnik A (2004). Visual perception and social foraging in birds. *Trends in Ecology and Evolution* 19:25-31.

Fernandez-Juricic E, MD Gall, T Dolan, V Tisdale, GR Martin (2008). The visual fields of two ground-foraging birds, House Finches and House Sparrows, allow for simultaneous foraging and anti-predator vigilance. *Ibis* 150:779-787.

Fernández-Juricic E, O'Rourke C, Pitlik T (2010). Visual coverage and scanning behavior in two corvid species: American crow and Western scrub jay. *Journal of Comparative Physiology A* 196:879-888.

Fernández-Juricic E (2012). Sensory basis of vigilance behavior in birds: synthesis and future prospects. *Behavioral Processes* 89:143-152.

Fernández-Juricic E, Gall MD, Dolan T, O'Rourke C, Thomas S, Lynch JR (2011a). Visual systems and vigilance behaviour of two ground-foraging avian prey species: white-crowned sparrows and California towhees. *Animal Behaviour* 81:705-713.

Fernández-Juricic E, Moore BA, Doppler M, Freeman J, Blackwell BF, Lima SL, DeVault, TL (2011b). Testing the terrain hypothesis: Canada geese see their world laterally and obliquely. *Brain Behavior and Evolution* 77:147-158.

Fite KV & Rosenfield-Wessels S (1975). A comparative study of deep avian foveas. *Brain Behavior and Evolution* 12:97-115

Freeman B & Tancred E (1978). The number and distribution of ganglion cells in the retina of the brush-tailed possum, Trichosurus vulpecula. *Journal of Comparative Neurology* 177:557–567

Guillemain M, Martin GR, Fritz H (2002). Feeding methods, visual fields and vigilance in dabbling ducks (Anatidae). *Functional Ecology* 16:522-529

Healy K, McNally L, Ruxton GD, Cooper N, Jackson AL (2013). Metabolic rate and body size are linked with perception of temporal information. *Animal Behaviour* 86:685-696.

Heesy CP (2009). Seeing in stereo: The ecology and evolution of primate binocular vision and stereopsis. *Evolutionary Anthropology* 18:21-35

Kiltie RA (2000). Scaling of visual acuity with body size in mammal and birds. *Functional Ecology* 14:226-234.

Kirschfeld K (1976). The resolution of lens and compound eyes. *Neural Principles in Vision* (eds. F Zettler & R. Weiler), Springer-Verlag, Berlin, pp. 354-370.

Land MF & Tatler BW (2009). *Looking and acting: vision and eye movements in natural behaviour.* Oxford University Press, Oxford.

Maldonado PE, Maturana H, Varela FJ (1988). Frontal and lateral visual systems in birds. Frontal and lateral gaze. *Brain Behavior and Evolution* 32:57-62.

Martin GR (1984). The visual fields of the tawny owl, *Strix aluco L*. *Vision Research* 24:1739–1751

Martin GR (2007). Visual fields and their functions in birds. *Journal of Ornithology* 148:S547–S562.

Martin GR (2009). What is binocular vision for? A birds' eye view. *Journal of Vision* 9:1–19.

Martin GR, Jarrett N, Williams M (2007). Visual fields in blue ducks *Hymenolaimus malacorhynchos* and pink-eared ducks *Malacorhynchus membranaceus*: visual and tactil foraging. *Ibis* 149:112-120.

Martin GR & Katzir G (1999): Visual field in Short-toed eagles *Circaetus gallicus* and the function of binocularity in birds. *Brain Behavior and Evolution* 53:55-66.

Martin GR, Portugal SJ, Murn CP (2012). Visual fields, foraging and collision vulnerability in Gyps vultures. *Ibis* 154:626-631.

McIlwain JT (1996). *An introduction to the biology of vision*. Cambridge University Press, New York.

Meyer DBC (1977). The avian eye and its adaptations. In: Crescitelli F (ed) *The visual system of vertebrates; handbook of sensory physiology* Springer, New York. pp 549-612

Moore BA, Kamilar JM, Collin SP, Bininda-Emonds ORP, Dominy NJ, Hall MI, Heesy CP, Johnsen S, Lisney TJ, Loew ER, Moritz G, Nava SS, Warrant E, Yopak KE, Fernández-Juricic E (2012). A novel method for comparative analysis of retinal specialization traits from topographic maps. *Journal of Vision* 12:1-24.

Moore BA, M Doppler, JE Young, E Fernandez-Juricic (2013). Interspecific differences in the visual system and scanning behavior in three forest passerines that form heterospecific flocks. *Journal of Comparative Physiology A* 199:263-277

Moore BA, Tyrrell L, Pita D, Fernandez-Juricic E (2014). Vision in Emberizid sparrow: more than meets the eye. In review,*Journal of Experimental Biology*

Nunn C (2011). *The Comparative Approach in Evolutionary Anthropology and Biology*. University of Chicago Press, Chicago.

Orme CDL, Freckleton RP, Thomas GH, Petzoldt T, Fritz SA (2011). caper: *Comparative Analyses of Phylogenetics and Evolution in R* (http://R-Forge.R-project.org/projects/caper/).

Pagel M (1999). Inferring the historical patterns of biological evolution. *Nature* **401**, 877–884.

R Development Core Team (2010). R: *A Language and Environment for Statistical Computing*. Vienna, Austria, ISBN 3-900051-07-0, http://www.Rproject.org/.

Rahman ML, Aoyama M, Sugita S (2006). Number, distribution and size of retinal ganglion cells in the jungle crow (*Corvus macrorhynchos*). *Anatomical Science International* 86:252-259

Stone J (1981). *The Wholemount Handbook. A Guide to the preparation and Analysis of Retinal Wholemounts*. Maitland, Sydney.

Troscianko J, Bayern AMPV, Chappell J, Rutz C, Martin GR (2012) Extreme binocular vision and a straight bill facilitate tool use in New Caledonian crows. *Nature Communications* 3:1110.

Tyrrell LP, Moore BA, Loftis C, Fernandez-Juricic E (2013). Looking above the prairie: localized and upward acute vision in a native grassland bird. *Scientific Reports* 3:3231.

Ullmann JFP, Moore BA, Temple SE, Fernández-Juricic E, Collin SP (2012). The retinal wholemount technique: a window to understanding the brain and behaviour. *Brain Behavior and Evolution* 79:26-44

Walls GL (1942). *The vertebrate eye and its adaptive radiation*. Cranbrook Institute of Science, Michigan

CHAPTER 7: DISCUSSION AND FUTURE DIRECTIONS

7.1 The Current View on Visual Ecology.

The past few years have brought about a lot of insight into the field of visual ecology. We have learned more about how variations in visual field configuration can affect primarily non-locomotive behaviors (Martin 2011, 2012, 2014) and how retinal organization may play a role in behavior (Fernandez-Juricic, 2012; Moore et al. 2012). Our vast database of visual information has grown as well, for example adding new species into our knowledge pool of retinal topography (giraffe, Coimbra et al. 2012b; snakes, Hart et al. 2012; penguins, Coimbra et al. 2012a; owls, Lisney et al. 2012a), and visual fields (Ibises and spoonbills, Martin & Portugal 2011; Senegal parrots, Demery et al. 2011; crows, Troscianko et al. 2012; Vultures, Martin et al. 2012). We have discovered some sensory systems in recent studies to be spectacular and surprising. Species with surprisingly high degrees of binocularity in different parts of the visual field have been found (tufted titmouse, Carolina chickadee, and white-breasted nuthatch, Moore et al. 2013), as well as the only Passeriform with a fovea that projects below the horizontal meridian (Eastern meadowlark, Tyrrell et al. 2013).

The work provided in this dissertation has also contributed to our understanding of visual ecology. Chapter 2 provides a novel standardized way to harvest from the vast number of retinal topographic maps (Moore et al. 2012). Until now we have not had the ability to perform comparative analyses on retinal organization and have relied solely on qualitative descriptions. Using this method, in chapter 3 I provided an analytical framework that uncovered some examples of convergent evolution as to how the vertebrate retina is configured (Moore et al. in review, b). In so doing I showed that retinas of different species are distinct not only by their retinal specializations, but that

the retinal ganglion cell profile of the entire retina is different and can be distinguished using the new method. This provided evidence that could help understand differences between species in tasks such as visual search and visual fixation.

In chapters 4-6, analyses of the visual traits of different groups of species led to some interesting findings. In studying three species of forest passerines that form heterospecific flocks, I found in chapter 4 that their visual field configuration was dramatically changed by eye movements, and differed between species in a way that provided a specific advantage to meet foraging needs. I also found evidence challenging the common assumption that satellite species may rely on the enhanced visual ability of nuclear species.

Chapter 5 was the first analysis of multiple components of the visual system that was able to control for phylogenetic effects, and was performed on nine closely related species from the Emberizidae family. I characterized the visual system of each species, and also for the first time mapped their visual space. This provided evidence suggesting that these closely related species may have different ways of perceiving visually their world, despite being phylogenetically very close. I also tested a number of specific predictions regarding various components of the visual system and visual behaviors. I found that species with larger intraocular organs that generate a blind spot in the visual field (i.e. pecten) have greater degrees of eye movement, which likely aids in quickly scanning areas of the visual field that have some degree of visual obstruction.

Finally, I examined the visual systems of a large group of 29 North American species across 14 families, testing some specific predictions regarding the interplay between different visual parameters and visual behavior. Through this I was able to show the how visual traits are related to each other and to behavior in different species. Overall it seems as though some components of anti-predatory behavior (e.g. scanning) are influenced by how the avian visual system is configured. This is the largest study demonstrating the relationship between visual traits and information gathering in birds, the results may help us develop more realistic predictions on variation in anti-predator behavior (Fernandez-Juricic et al. 2004).

Species with larger eyes have different visual orientations than species with

smaller eyes. Larger eyed species had wider visual coverage for detecting predators, and smaller binocular fields to aid in foraging. Their retina was more homogenous and therefore, combined with the large size of the eye, accounted for higher spatial resolution across the visual field. As a result, they showed a lower need to scan the environment since they had higher total coverage and higher acuity across that field of view. Smaller eyed species, however, tended to have larger binocular fields for foraging and less visual coverage for detecting predators. They also had more specialized retinae, with higher peak ganglion cell density that differ more from the periphery than in larger eyed species. In order to position the high acuity area within space, and in an attempt to make up for lower total visual coverage, the smaller species had greater degrees of eye movements to scan the environment (Moore et al. in review, c).

Overall it appears as though some visual behaviors may be dependent on multiple visual traits. Our past tendency in visual ecology to present the visual information of a single visual trait is incomplete, and rather than trying to associate a single trait with complex visual behaviors, we will be better served by following the approach presented here and examining the interaction between multiple traits to understand the co-evolution of visual traits with behavior. By following this comparative and multi-trait approach, we will expand our understanding of how vertebrates perceive and interact with their environment.

7.2 Future Directions

Future studies should explore the interplay between different sensory modalities (e.g., hearing and vision). We have determined some interesting relationships between different sensory systems by extrapolating information from different studies (e.g. vision and hearing in forest passerines, Henry & Lucas 2008, Moore et al. 2013; vision and olfaction in vultures, Inzunza et al. 1991, Martin et al. 2012, Smith & Paselk 1986). There are already some comparative databases in which some species have both visual and auditory traits measured: house finch (Fernandez-Juriric et al. 2008, Gall et al. 2012), white-crowned sparrow (Fernandez-Juricic et al. 2011, Gall et al. 2012), brown-headed cowbird

(Blackwell et al. 2009, Gall et al. 2012), and Carolina chickadee (Freeberg & Lucas 2011, Moore et al. 2013) are a few examples. Collecting more information on species with either sensory modality would enhance these comparative data and provide an opportunity for testing hypotheses about trade-offs between different sensory modalities (American tree sparrow). Additionally, if future studies would manipulate multiple sensory systems at once, they may provide opportunities to assess how animals use different sensory modalities for specific tasks (e.g., mating, Ronald et al. 2012).

More work is needed in regards to the function of different retinal specializations and as well as how they evolved in species inhabiting environments with different visual challenges. There have been many hypotheses put forth for the function of different retinal specializations, by far the most being for the fovea (e.g. reduction in chromatic aberration, Rodieck 1973; increased acuity by optical aberration beyond what neural sampling can achieve, Rossi & Roorda, 2010; magnification of the light image, Walls 1942, Snyder & Miller 1978; attenuation of angular displacement for movement detection, Pumphrey 1948). However, most of the hypotheses accounting for the function of retinal specializations remain untested. We may consider testing these specializations from a behavioral perspective (e.g. using eye tracking as discussed below, or designing empirical behavioral tests), or via physiological (e.g. specific cell properties within these specializations and their central projections, as each cell type is associated with specific functions, Field & Chichilnisky 2007, Pushchin & Karetin 2009), developmental (e.g. fovea knock-out studies to compare visual behaviors, Marmor et al. 2008), or optical (e.g. optical coherence tomography, Tanna et al. 2010) methods.

One method by which we can study the fovea is characterizing its dimensions across species. Currently, a computer program is under construction that will enable automated characterization of specific foveal dimensions (e.g. depth, width, and slope of the fovea pit) of both foveal cross-sections and optical coherence tomographic images (Moore et al. unpublished data). By relating the dimensions of the fovea to other visual parameters and to visual behaviors, we hope to uncover the potential use that different foveal shapes may be associated with.

Another method by which to study the fovea, as well as other retinal specializations and organizations, is eye-tracking technology (Yorzinski et al. 2013). Eye-tracking uses computer technology and a set of cameras to enable you to visualize on a computer screen what the animal tracks with its region of acute vision, giving us a tool to begin linking the physiologic aspects of retinal morphology to behavior, and in-so-doing enabling us to begin answering general questions about how birds use their eyes and what they use them for. From a comparative approach, it will enable us to answer fundamental questions about the interplay between phylogeny and ecology, linking physiology to the ecological parameters that birds experience (Tyrrell et al. in review).

7.3 Literature Cited

Blackwell BF, Fernandez-Juricic E, Seamans TW, Dolan T (2009). Avian visual system configuration and behavioural response to object approach. *Animal Behaviour* 77:673-684.

Coimbra JP, Hart NS, Collin SP, Manger PR (2012b). Scene from above: retinal ganglion cell topography and spatial resolving power in the giraffe (Giraffa camelopardalis). *Journal of Comparative Neurology* 521:2042-2057.

Coimbra JP, Nolan PM, Collin SP, Hart NS (2012a). Retinal ganglion cell topography and spatial resolving power in penguins. *Brain Behavior and Evolution* 80:254-268.

Collin SP (2010). Evolution and ecology of retinal photoreception in early vertebrates. *Brain Behavior and Evolution* 75:174-185.

Curcio CA, Sloan KR, Meyers D (1989). Computer methods for sampling, reconstruction, display and analysis of retinal whole mounts. *Vision Research* 29:529-540.

Demery ZP, Chappell J, Martin GR (2011). Vision, touch and object manipulation in Senegal parrots *Poicephalus senegalus*. *Proceedings of the Royal Society of London B* 278:3687-3693.

Fernandez-Juricic E, Gall MD, Dolan T, Tisdale V, Martin GR (2008). The visual fields of two ground foraging birds, House finches and house sparrows, allow for simultaneous foraging and anti-predator vigilance. *IBIS* 150:779-787.

Fernandez-Juricic E, Gall MD, Dolan T, O'Rourke C, Thomas S, Lynch JR (2011). Visual systems and vigilance behavior of two ground-foraging avian prey species: white-crowned sparrows and California towhees. *Animal Behaviour* 81: 705-713.

Fernandez-Juricic E (2012). Sensory basis of vigilance behavior in birds: Synthesis and future prospects. *Behavioural Processes* 89:143-152.

Field GD & Chichilnisky EJ (2007). Information processing in the primate retina: Circuitry and Coding. *Annual Review of Neuroscience* 30:1-30.

Freeberg TM & Lucas JR (2011). Information theoretical approaches to chick-a-dee calls of Carolina chickadees (Poecile carolinensis). *Journal of Comparative Psychology* 126:68-81.

Gall MD, Henry KS, Lucas JR (2012). Two measures of temporal resolution in brown-headed cowbirds (*Molothrus ater*). *Journal of Comparative Physiology* 198:61-68.

Gall MD, Brierley LE, Lucas JR (2012). The sender-receiver matching hypothesis: support from the peripheral coding of acoustic features in songbirds. *Journal of Experimental Biology* 215:3742-3751.

Hart NS, Coimbra JP, Collin SP, Westhoff G (2012). Photoreceptor types, visual pigments, and topographic specializations in the retinas of hydrophiid sea snakes. *Journal of Comparative Neurology* 520:1246-1261.

Henry KS & Lucas JR (2008). Coevolution of auditory sensitivity and temporal resolution with acoustic signal space in three songbirds. *Animal Behaviour* 76:1659-1671.

Inzunza O, H Bravo, RL Smith, M Angel (1991). Topography and morphology of retinal ganglion cells in *Falconiformes*: A study on predatory and carrion-eating birds. *The Anatomical Record* 229:271-277.

Lisney TJ, Iwaniuk AN, Bandet MV, Wylie DR (2012b). Eye shape and retinal topography in owls (Aves: Strigiformes). *Brain Behavior and Evolution* 79:218-236.

Lisney TJ, Theiss SM, Collin SP, Hart NS (2012a). Vision in elasmobranches and their relative: 21st century advances. *Journal of Fish Biology* 5:2024-2054.

Marmor MF, SS Choi, RJ Zawadzki, JS Werner (2008). Visual insignificance of the foveal pit. *Archives of Ophthalmology* 126:907-913.

Martin GR (2012). Through birds' eyes: insights into avian sensory ecology. *Journal of Ornithology* 153 (Suppl 1):S23-S48.

Martin GR (2014). The subtlety of simple eyes: the tuning of visual fields to perceptual challenges in birds. *Philosophical Transactions of the Royal Society B* 369:20130040.

Martin GR, Portugal SJ, Murn CP (2012). Visual fields, foraging and collision vulnerability in Gyps vultures. *Ibis* 154:626-631.

Martin GR & Portugal SJ (2011). Differences in foraging ecology determine variation in visual field in ibises and spoonbills (*Threskiornithidae*). *Ibis* 153:662-671.

Martin GR (2011). Understanding bird collisions with man- made objects: a sensory ecology approach. *Ibis* 153:239-254.

Moore BA, Kamilar JM, Collin SP, Bininda-Emonds ORP, Dominy NJ, Hall MI, Heesy CP, Johnsen S, Lisney TJ, Loew ER, Moritz G, Nava SS, Warrant E, Yopak KE, Fernández-Juricic E (2012). A novel method for comparative analysis of retinal specialization traits from topographic maps. *Journal of Vision* 12:1-24.

Moore BA, Kamilar JM, Collin SP, Bininda-Emonds ORP, Dominy NJ, Hall MI, Heesy CP, Johnson S, Lisney TJ, Loew ER, Moritz G, Nava SS, Warrant E, Yopak KE, Fernandez-Juricic E. Are all vertebrate retinas configured the same? Implications for the evolution of acute vision. In review, b

Moore BA, M Doppler, JE Young, E Fernandez-Juricic (2013). Interspecific differences in the visual system and scanning behavior in three forest passerines that form heterospecific flocks. *Journal of Comparative Physiology A* 199:263-277.

Moore BA, Tyrrell L, Pita D, Fernandez-Juricic E. Vision in 29 species of North American birds: a comparative approach. In review, c

Moore BA, Tyrrell L, Pita D, Fernandez-Juricic E. Vision in Emberizid sparrow: more than meets the eye. In review, a.

Pumphrey RJ (1948). The Theory of the Fovea. *Journal of Experimental Biology* 25:299-312.

Pushchin II, Karetin YA (2009): Retinal Ganglion Cells in the Eastern Newt *Notophthalmus viridescens*: Topography, Morphology, and Diversity. *Journal of Comparative Neurology* 516:533–552.

Rodieck RW (1973). *The Vertebrate Retina: Principles of Structure and Function*. San Francisco, W. H. Freeman.

Ronald KL, Fernandez-Juricic E, Lucas JR (2012). Taking the sensory approach: how individual differences in sensory perception can influence mate choice. *Animal Behaviour* 84(100):1283-1294.

Rossi EA & A Roorda (2010). The relationship between visual resolution and cone spacing in the human fovea. *Nature Neuroscience* 13:156-157.

Schieber NL, Collin SP, Har NS (2012). Comparative retinal anatomy in four species of elasmobranch. *Journal of Morphology* 273:423-440.

Smith SA & Paselk RA (1986). Olfactory sensitivity of the turkey vulture (Cathartes aura) to three carrion-associated odorants. *The Auk* 103:586-592.

Snyder AW & Miller WH (1978). Telephoto lens system of falconiform eyes. *Nature* (London) 275:127-129.

Sterratt DC, Lyngholm D, Willshaw DJ, Thompson ID (2013). Standard anatomical and visual space for the mouse retina: computational reconstruction and transformation of flattened retinae with the Retistruct Package. *PLOS Computational Biology* 9: e1002921

Tanna H, Dubis AM, Ayub N, Tait DM, Rha J, Stepien KE, Carroll J (2010). Retinal imaging using commercial broadband optical coherence tomography. *British Journal of Ophthalmology* 94:374-376.

Troscianko J, Bayern AMPV, Chappell J, Rutz C, Martin GR (2012). Extreme binocular vision and a straight bill facilitate tool use in New Caledonian crows. *Nature Communications* 3:1110.

Tyrrell LP, Moore BA, Loftis C, Fernandez-Juricic E (2013). Looking above the prairie: localized and upward acute vision in a native grassland bird. *Scientific Reports* 3:3231.

Tyrrell LP, Butler SR, Yorzinski J, Fernandez-Juricic E. A system for binocular eye-tracking and gaze projection in small birds. *In prep*.

Walls GL (1942). *The Vertebrate Eye and Its Adaptive Radiation*. Cranbrook Institute of Science, Michigan.

Yorzinski JL, Patricelli GL, Babcock JS, Pearson JM, Platt ML (2013). Through their eyes: selective attention in peahens during courtship. *Journal of Experimental Biology* 216:3035-3046.

VITA

VITA

Bret Alan Moore

AWARDS

- The Society of Phi Zeta, Omicron Chapter, Honor Society of Veterinary Medicine, Inducted Spring 2014
- William W. Carlton Aptitude in Veterinary Pathology Award, Purdue University College of Veterinary Medicine
- 2014 – Semester Dean's List Spring 2014
- 2013 - Semester Dean's List, Fall 2013
- 2013 - Semester Dean's List, Spring 2013
- 2012 - Semester Dean's List, Fall 2012
- 2012 - Veterinary Scholars Fellowship
- 2012 - Semester Dean's List, Spring 2012
- 2011 - Semester Dean's List, Fall 2011
- 2010 - NESCENT Graduate Fellowship, Duke University
- 2010 - Ross Graduate Fellowship, Purdue University
- 2009 - Quantitative Physiology Scholarship Program, Purdue University

ABSTRACTS

- Ayed Mamdouh Allawzi, Eve Nicole Grelle, Mary Ellen Teclaw, **Bret Moore**, Esteban Fernandez-Juricic, Nancy Pelaez. 2010. Isometric force of isolated extraocular muscles of wild cowbirds. Experimental Biology Meeting, Anaheim, CA.

- **Bret Moore,** Megan Doppler, Joe Freeman, Kathie Kapernaros, Bradley F. Blackwell, Esteban Fernandez-Juricic. 2010. Geese see the world laterally and transversally: implications for vigilance. Animal Behavior Society Meeting, Williamsburg, VA.
- Ayed Mamdouh Allawzi, Eve Grelle, **Bret Moore**, Esteban Fernández-Juricic, Nancy Pelaez. 2011. Contractile properties of the lateral rectus in starlings and house sparrows using supramaximal electrical stimulation. Experimental Biology Meeting
- Megan Doppler, **Bret Moore**, Jordan Young, Taylor Curry, Esteban Fernandez-Juricic. It's all about eye movement: Different visual and foraging strategies of the chickadee and nuthatch. Sigma Xi Foundation, Purdue University, February 2011.
- Megan Doppler, **Bret Moore**, Jordan Young, Esteban Fernandez-Juricic. Visual fields and eye movements of titmice and chickadees. Animal Behavior Conference, Indiana University, April 2011.
- Megan Doppler, Patrice Baumhardt, **Bret A. Moore**, Jacquelyn Randolet, Esteban Fernandez-Juricic. Color vision in Canada geese: an 'oblique' violet-sensitive system. Animal Behavior Society Conference, Indiana University, July 2011.
- Diana Pita, **Bret A. Moore**, Esteban Fernandez-Juricic. Visual fields and foraging techniques in Blue Jays and Red-winged Blackbirds. Animal Behavior Society Conference, Indiana University, July 2011.
- Diana Pita, **Bret A. Moore**, Esteban Fernandez-Juricic. How do small birds see? Visual field configuration and eye movements in closely related sparrows. Indiana Academy of Science Conference, Purdue University, April 2012.
- Jordan E. Young, Megan Doppler, **Bret A. Moore**, Esteban Fernandez-Juricic. Visual resolution within the retina of ground and tree avian foragers to different degrees: ecological implications. Indiana Academy of Science Conference, Purdue University, March 2012.
- **Bret A. Moore**, Megan Doppler, Esteban Fernandez-Juricic. Interspecific differences in the visual system and scanning behavior of three forest passerines that form heterospecific flocks. Merial-NIH Conference, Colorado State University, August 2012.

- Diana Pita, **Bret A. Moore**, Luke Tyrrell, Esteban Fernandez-Juricic. How do small birds see? Relationships in binocularity and bill morphology in closely related sparrows. Purdue University, April 2013.

PUBLICATIONS

- Baumhardt PE, **Moore BA**, Doppler M, Fernandez-Juricic E (2014). Do American goldfinches see their world like passive prey foragers? A study on visual fields, retinal topography, and sensitivity of photoreceptors. *Brain, Behavior and Evolution* 83:181-198.
- Gutierrez-Ibanez C, Iwaniuk AN, **Moore BA**, Fernandez-Juricic E, Corfield JR, Krilow JM, Kolominsky J, Wylie DR (2014). Mosaic and concerted evolution in the visual system of birds. *PLOS ONE* 9(3):e90102
- Tyrrell LP, **Moore BA**, Loftis C, Fernandez-Juricic E (2013): Looking above the prairie: localized and upward acute vision in a native grassland bird. Scientific Reports 3:3231.
- **Moore BA**, M Doppler, JE Young, E Fernandez-Juricic (2013): Interspecific differences in the visual system and scanning behavior in three forest passerines that form heterospecific flocks. J Comp Physiol A 199:263-277.
  Selected for Journal of Comparative Physiology A: Celebrating 90 Years (1924-2014) Anniversary edition.
- **Moore BA**, Kamilar JM, Collin SP, Bininda-Emonds ORP, Dominy NJ, Hall MI, Heesy CP, Johnsen S, Lisney TJ, Loew ER, Moritz G, Nava SS, Warrant EF, Yopak KE, Fernandez-Juricic E (2012). A novel method for comparative analysis of retinal specialization traits from topographic maps. *Journal of Vision* 12(12):1-24.
- **Moore BA,** Baumhardt P, Doppler M, Randolet J, Blackwell BF, DeVault TL, Loew ER, Fernández-Juricic E (2012). Oblique color vision in an open-habitat bird: spectral sensitivity, photoreceptor distribution, and behavioral implications. *Journal of Experimental Biology* 215:3442-3452.
  Media Coverage: http://jeb.biologists.org/content/215/19/iii.full

- Ullmann JFP, **Moore BA**, Temple S, Fernandez-Juricic E, Collin SP (2011). The retinal wholemount technique: a window to understanding the brain and behavior. *Brain, Behavior and Evolution* 79(1):26-44.
  Editor's Choice Award, December 5, 2011
- Fernandez-Juricic E, **Moore BA**, Doppler M, Freeman J, Blackwell BF, Lima SL, DeVault TL (2011). Testing the terrain hypothesis: Canada geese see their world laterally and obliquely. *Brain, Behavior and Evolution* 77:147-158.

MANUSCRIPTS IN PRESS

- **Moore BA**, Pita D, Tyrrell LP, Fernandez-Juricic E. Multidimensional vision in avian passive prey foragers: maximizing binocular vision with fronto-lateral visual acuity. *Journal of Experimental Biology*.

MANUSCRIPTS IN REVIEW

- Moore BA, Tyrrell L, Pita D, Fernandez-Juricic E. Vision in Emberizid sparrow: more than meets the eye. In review, a.
- Moore BA, Kamilar JM, Collin SP, Bininda-Emonds ORP, Dominy NJ, Hall MI, Heesy CP, Johnson S, Lisney TJ, Loew ER, Moritz G, Nava SS, Warrant E, Yopak KE, Fernandez-Juricic E. Are all vertebrate retinas configured the same? Implications for the evolution of acute vision. In review, b
- Moore BA, Tyrrell L, Pita D, Fernandez-Juricic E. Vision in 29 species of North American birds: a comparative approach. In review, c

MANUSCRIPTS IN PREPARATION

- **Moore BA,** Yu I, Benes B, Fernandez-Juricic E. A new model for comparative fovea analysis. To be submitted 2015.

- **Moore BA**, Ronald K, Lucas J, Fernandez-Juricic E. Prey detection in the American Robin: Which sensory modality prevails? To be submitted to 2015.
- **Moore BA**, Kamilar JM, Collin SP, Bininda-Emonds ORP, Dominy NJ, Hall MI, Heesy CP, Johnsen S, Lisney TJ, Loew ER, Moritz G, Nava SS, Warrant EF, Yopak KE, Fernandez-Juricic E. Functional implications of retinal specializations: going back to behavior. To be submitted 2015.
- **Moore BA**, Tyrrell LP & Fernandez-Juricic E. What makes a fovea special? A comparative analysis on retinal fovea of 20 avian species. To be submitted 2015.

COLLABORATIVE STUDIES UNDER WAY

- Prey detection in the American Robin: Which sensory modality prevails? With Dr. Jeff Lucas (Purdue University).
- A comparison of binocular overlap and orbit convergence in Brown-headed cowbirds. With Dr. Christopher Heesey and Margaret Hall (Midwestern University, AZ).
- Comparative study of binocular visual brain centers (Wulst, optic tectum), orbit convergence, and the degree of binocularity in 20 Passeriformes. With Dr. Jeremy Corfield and Dr. Andrew Iwaniuk (Canada), and Dr. Christopher Heesey and Dr. Margaret Hall (Midwestern University, AZ).
- Characterization and modeling of the fovea with computer graphics. With Dr. Bedrich Benes (Purdue University, IN)
- Study of the visual system of zebrafish, visual fields. (Princeton University).
- Study of the visual systems of tropical manakins. Dr. Lainy Day (University of Mississippi, MS).
- Comparative vertebrate vision. Richard R. Dubielzig and Leandro Textiera (University of Madison Wisconsin, COPLOW – Comparative Ocular Pathology Lab of Wisconsin, WI
- Lizard (*Sceloporus spp*) color vision, signals, and social communication. Dr. Diana K. Hews (Indiana State University, Department of Biology, IN)

- ❖ Comparative exotic animal vision. Angela Lennox (Avian and Exotic Animal Clinic of Indianapolis, IN)
- ❖ Interosseus Orbital Processes in camelids and bats for evidence of phylogenetic relatedness. Dr. Fabiano Montiani-Ferreira (Universidade Ferderal do Parana, Department of Veterinary Medicine, Curitiba, Parana, Brazil).
- ❖ Hummingbird vision and its role in flight dynamics. Dr. Doug Altshuler (University of British Columbia, Canada).

LEADERSHIP AND EXTRACURRICULARS

- ❖ 2011-2014 Veterinary Student Resource Center
  - *President, Pathology Tutor 2013-2014*
  - *Parasitology Tutor 2012-2013*
  - *Histology Tutor 2011-2013*

- ❖ 2012-2014 Veterinary Purdue Student Supplies Association
  - *President*

- ❖ 2011-2015 College of Veterinary Medicine, Class of 2015
  - *President*

- ❖ 2012-2014 Student Chapter of the American College of Veterinary Internal Medicine
  - *Vice President*

- ❖ 2013-2014 Student Chapter of the American College of Veterinary Pathology
  - *President*

TEACHING EXPERIENCE

TEACHING

- Grupo Fowler, Foz de Iguazu, Itaipu Bionacional. For University of Curitiba, Setor de Ciencias Agrarias, Medicina Veterinaria – Parana, Curitiba, Brazil
  "Visual Field Wet Lab" – November 2014
- VCS 820 – Applications and Integrations I
  Group Instructor (substitute) for freshman small group case-based course – Spring 2014
- VCS 840 – Applications and Integrations III
  Group Instructor (substitute) for sophomore small group case-based course – Spring 2014
- VCS 830 – Applications and Integrations II
  Group Instructor (substitute) for freshman small group case-based course – Fall 2013
- VCS 840 – Applications and Integrations IV
  Group Instructor (substitute) for sophomore small group case-based course – Fall 2013

GUEST LECTURES AND PULIC TALKS

- Grupo Fowler, Foz de Iguazu, Itaipu Bionacional. For University of Curitiba, Setor de Ciencias Agrarias, Medicine Veterinaria, Parana, Curitiba, Brazil.
  "The retinal wholemount, comparative topography, and the peculiar fovea" – November 2014
  "Visual fields, visual ecology, and why…" – November 2014
- Avian and Exotic Animal Clinic of Indianapolis, Dr. Angela Lennox
  "Comparative vision of domestic and wild animals" – April 2014
- 2013 Purdue University (Course: BIOL 442 - Senior Laboratory in Anatomy and Physiology) – West Lafayette, Indiana, US.
- "An introduction to the visual system: form, function, and design". - April 2013.
- "How to approach diseases of the CNS: gross pathology, histopathology, and forming differential diagnoses" - April 2013.
- 2010 Whiteland Community High School (Course: Honors Anatomy and Physiology) – Whiteland, Indiana, USA "College: A guide to survival AND success"

PRESENTATIONS

RESEARCH SEMINARS

- Purdue University, Department of Biological Sciences – West Lafayette, Indiana, USA
  "A multidimensional approach to comparative avian visual systems" – August 2014
- Purdue University, Department of Biological Sciences – West Lafayette, Indiana, USA, May 2012.
  "The role of the avian visual system in scanning behavior: a comparative approach" – May 2012
- Purdue University, Department of Biological Sciences – EcoLunch: Ecology Seminar Series West Lafayette, Indiana, USA, March 2011
  "Functional implications of retinal specializations: Going back to behavior" – March 2011
- Duke University, NESCent.
  "Functional hypotheses of retinal specializations" – July 2011
- Purdue University, Department of Biological Sciences – EcoLunch: Ecology Seminar Series West Lafayette, Indiana, USA, November 2010.
  "Testing the terrain hypothesis: Canada geese see their world laterally and obliquely" – November 2010

SCIENTIFIC MEETINGS

- COPS (Comparative Ocular Pathology Society) Conference – Colorado State University School of Veterinary Medicine, Fort Collins, Colorado, USA.
  "The retinal wholemount, comparative topography, and the peculiar fovea" – September 2014
- Moore BA, Doppler M, Fernandez-Juricic E 2011: It's all about eye movement: different visual and foraging strategies of chickadees and nuthatches. April 2011, Animal Behavior Society, Bloomington , Indiana, USA

UNDERGRADUATE MENTORING

- 2013 Melanie Meyer – Purdue University
- 2012-2014 Alexandra Osbourne – Purdue University
- 2012-2013 Ryan Cross – Purdue University, Senior Honors Thesis
- 2012-2013 Haley Jost – Purdue University
- 2012-2013 Brad Abplanalp – Purdue University
- 2012 Lily Liang – Purdue University
- 2012 Kimble Slonaker – Purdue University
- 2012 Emily Chen – Purdue University
- 2012 -2014 Amanda Mark – Purdue University
- 2011-2013 Jen Hanchar – Purdue University
- 2011-2013 Diana Pita – Purdue University, Senior Honors Thesis
- 2011-2012 Steven Ison – Purdue University
- 2011-2012 Skyler King – Purdue University
- 2011-2012 Erica Wayne – Purdue University
- 2011 Tony Fleming – Purdue University
- 2011 Sailun You – Purdue University
- 2011 Jon Gritzer – Purdue University
- 2011 Jihyun Han – Purdue University
- 2011 Christina Carey – Purdue University
- 2011 Brianna Burry – Purdue University
- 2011 Becky Czaja – Purdue University
- 2011 Andy Schwend – Purdue University
- 2011 -2013 Amanda Elmore – Purdue University, Senior Honors Thesis
- 2010-2012 Jordan Young – Purdue University
- 2010-2011 Melissa Hoover – Purdue University
- 2010-2011 Megan Doppler – Purdue University
- 2010-2011 Marci Deisher – Purdue University
- 2010-2011 Jacquelyn Lynch – Purdue University

- 2010 Kathie Kapernaros – Purdue University
- 2010-2011 Pete Perno – Purdue University

REVIEWER

- Animal Cognition
- PLOS ONE